

The Institute of Paper Chemistry

Appleton, Wisconsin

Doctor's Dissertation

**Correlation of Certain Morphological
and Hydrodynamic Aspects of
Loblolly Pine Bleached Kraft Pulp**

Anthony P. Binotto

January, 1977

CORRELATION OF CERTAIN MORPHOLOGICAL
AND HYDRODYNAMIC ASPECTS OF
LOBLOLLY PINE BLEACHED KRAFT PULP

A thesis submitted by

Anthony P. Binotto

B.S. 1970, The Pennsylvania State University

M.S. 1972, The Pennsylvania State University

in partial fulfillment of the requirements
of The Institute of Paper Chemistry
for the degree of Doctor of Philosophy
from Lawrence University,
Appleton, Wisconsin

Publication Rights Reserved by
The Institute of Paper Chemistry

January, 1977

I am extremely appreciative for the secretarial and technical skills of my wife, Barbara, for whom this undertaking has resulted in many years of struggling with little more than basic necessities. Without her help, encouragement, and patience, I would not have made it through these trying times.

TABLE OF CONTENTS

	Page
ABSTRACT	1
INTRODUCTION	3
Objective	4
Review of Pertinent Literature Concerning Morphological Aspects of Pulp Fibers	4
Wall Fraction Variation	5
Fiber Length Variation	7
Review of Pertinent Literature Concerning Hydrodynamic Evaluation of Pulps	9
Wet Mat Compressibility	10
Specific Filtration Resistance	18
Specific Surface and Specific Volume	20
EXPERIMENTAL PROCEDURES	24
Isolation of Fiber Populations	24
Raw Materials	24
Preparation of Pulp	24
Earlywood and Latewood Separation	26
Fiber Length Separation	29
Fiber Analysis	29
Hydrodynamic Measurements	30
Wet Mat Compressibility	30
Constant Rate Filtration	32
Permeation	32
RESULTS AND DISCUSSION	34
Measured and Calculated Morphological Properties	34
Fiber Separation and Dimensions	34
Number of Fibers per Gram	44
Calculated Moments of Inertia	45

	Page
Calculated Surface and Volume to Mass Ratios	48
Fiber Morphology and Wet Mat Compressibility	50
Compressibility Constants \underline{M} and \underline{N}	50
Compressibility	55
Wet Mat Density	56
Correlation of \underline{M} and Fiber Dimensions	59
Mathematical Procedure for Determination of Derivatives from Curves of Experimental Data	66
Least Squares Solution of $\underline{y} = \underline{b}_0 + \underline{b}_1 \underline{x}^{\underline{m}} + \underline{b}_2 \underline{x}^{\underline{n}}$	66
Computer Program	70
Fiber Morphology and Specific Filtration Resistance	71
Average Specific Filtration Resistance	71
Local Specific Filtration Resistance	74
Feasibility of Determining \underline{S}_W and \underline{v} as Functions of Pressure	81
Refinement of Calculation Procedures	82
Analysis of Assumption in Determining \underline{S}_W and \underline{v} as Functions of Pressure	83
Fiber Morphology and Average Specific Surface and Volume	84
Average Specific Surface	87
Average Specific Volume	88
CONCLUSIONS	91
IMPLICATIONS OF RESULTS	93
SUGGESTIONS FOR FUTURE WORK	95
LIST OF SYMBOLS	96
ACKNOWLEDGMENTS	99
LITERATURE CITED	100
APPENDIX I. ORIGINAL MAT DENSITY DATA	103
APPENDIX II. THREE-DIMENSIONAL PLOTTING PROGRAM	108

	Page
APPENDIX III. COMPUTER PROGRAM USED TO CALCULATE AN EQUATION OF THE FORM $y = b_0 + b_1 x^m + b_2 x^n$	109
APPENDIX IV. TWO-DIMENSIONAL PLOTTING PROGRAM	111
APPENDIX V. COMPUTER PROGRAM FOR THE ANALYSIS OF CONSTANT RATE FILTRATION DATA	112
APPENDIX VI. OUTPUT FROM PROGRAM CRFILT USING AVERAGED PRESSURE VS. TIME DATA FROM CONSTANT RATE FILTRATION, AND AVERAGED COMPRESSIBILITY DATA	119
APPENDIX VII. HISTORICAL PROGRAM AND OUTPUT FOR CALCULATION OF $\langle S_w \rangle$ AND $\langle v \rangle$ AS FUNCTIONS OF PRESSURE FROM FILTRATION RESISTANCE AND COMPRESSIBILITY DATA	131
APPENDIX VIII. HISTORICAL PROGRAM AND OUTPUT FOR CALCULATION OF S_w AND v AS FUNCTIONS OF PRESSURE FROM MULTIPLE PRESSURE TAP PERMEATION	150
APPENDIX IX. ANALYSIS OF INHERENT ASSUMPTION IN DETERMINING S_w AND v AS FUNCTIONS OF PRESSURE SIMULTANEOUSLY	171

ABSTRACT

Unbeaten, bleached loblolly pine kraft pulp is separated into fiber populations characterized by differences in wall-fraction and mean fiber length, \bar{L}_F . Briefly, the procedure first involves separation of the bleached pulp into predominantly earlywood and latewood fiber fractions (low and high wall-fractions, respectively) using a Jacquelin apparatus. These fractions are next subdivided into fiber populations according to mean fiber length using a Bauer-McNett classifier. Variation in mean fiber length within the set of earlywood and latewood fiber populations correlates with wall thickness and fiber diameter in a manner similar to that within a tree. Static compressibility data show the relationship between mat density, \bar{c} , and pressure, \bar{P}_F , follows $\bar{c} = \bar{M} \frac{\bar{P}_F^{\bar{N}}}{\bar{L}_F}$ for \bar{P}_F of about 10 to 150 cm H₂O. In this expression the compressibility constant \bar{N} is found to equal 0.373 for earlywood and latewood fiber populations and the compressibility constant \bar{M} correlates with fiber length for all fiber fractions. Compressibility, $d\bar{c}/d\bar{P}_F$, is greatest for shortest earlywood fibers and least for longest latewood fibers. \bar{M} is linearly related to $(1/\bar{I}_F)^{1/3}$, where \bar{I}_F represents the moment of inertia for a flattened fiber model, in agreement with the simple compressibility model originally developed by Wilder. The linearity of the relationship supports bending as the dominant mechanism in compressibility of wood pulp, and suggests that the wood pulp fiber is essentially flattened prior to bending. Since \bar{I}_F is defined as $2/3 \bar{W}\bar{T}^3 \bar{d}_F$, where $\bar{W}\bar{T}$ is wall thickness and \bar{d}_F fiber diameter, it appears that the wood pulp fiber dimensions influencing compressibility are primarily wall thickness and to a lesser degree fiber diameter. Trends in \bar{M} with changes in mean fiber length of earlywood and latewood fibers tend to follow previously reported changes in dynamic modulus of earlywood and latewood in successive growth rings, and also in elastic moduli and fibril angle. Average specific filtration resistance, $\langle \bar{R} \rangle$, obtained from constant rate filtration data at a given pressure drop, $\Delta \bar{P}_F$, in the range 10 to 90 cm H₂O also correlates

with wall fraction and fiber length. Percentage change in $\langle \underline{R} \rangle$ is about comparable to those trends observed for \underline{c} ; however, change in $\langle \underline{R} \rangle$ with \underline{L}_f is much greater. Smallest earlywood fibers have highest $\langle \underline{R} \rangle$ values and these increase most with increase in $\Delta \underline{P}_f$ compared with other fiber fractions. At constant mat density, $\underline{c} = 0.100$ g/cc, $\langle \underline{R} \rangle / \Delta \underline{P}_f$ has a sixfold change arising from fiber morphological variation. Local specific filtration resistance, \underline{R} , is calculated from pressure vs. time data obtained from constant rate filtration using a newly developed statistical procedure for determining derivatives. Changes in \underline{R} with fiber wall fraction and length are similar to those found for $\langle \underline{R} \rangle$, but \underline{R} values were much higher and increased significantly more with pressure. The square of average hydrodynamic specific surface, $\langle \underline{S}_w \rangle^2$, is proportional to $\langle \underline{R} \rangle$, and this relationship is comparatively insensitive to changes in \underline{c} and average specific volume, $\langle \underline{v} \rangle$. Calculated geometric specific surface is closest to $\langle \underline{S}_w \rangle$ for latewood with greatest fiber length, probably because these fibers most closely approximate circular fibers. The swollen volume calculated from filtration and compressibility data is considerably less than that of a cylindrical model, indicating fiber collapse under fluid drag forces. The ratio of the two corresponding volumes is almost 3 for earlywood and about 1.6 for latewood. Data for $\langle \underline{v} \rangle$ also indicate immobilized water varies from 1.04 to 1.97 cc/g with morphological changes. Apparently most of this water is within the fibers and not elsewhere.

INTRODUCTION

Interest in the genetic and silvicultural improvement of wood fiber properties has been increasing for many years, especially with respect to the correlation of fiber improvements with the dry sheet properties of pulp. Changes in sheet properties have been related to changes in morphological factors such as cell wall thickness, length, and width (1-3). A comprehensive study on the relationship between fiber morphology and kraft paper properties for loblolly pine was also used as part of the basis for Tappi committee activities concerned with the aim of assigning economic values to specific methods of altering wood and fiber properties (4). From such studies and activities it is apparent that there is significantly more known about the relationships between fiber morphology and products than is known about morphology and processes.

One process related area in which the role of wood fiber morphology is unclear concerns the hydrodynamic (water related) properties of pulp; specifically wet mat compressibility, filtration resistance, average specific surface, and average specific volume. Previous work has related these hydrodynamic properties to the structure of model fibers; i.e., the effects of glass or synthetic fiber dimensions and shape on compression and resistance to flow of fluids through fiber mats have been reported (5-8). On the basis of such studies it is to be expected that correlations would exist between wet mat compressibility and resistance to fluid flow, as reviewed by Han (9), and certain aspects of wood fiber morphology. One aspect is that thick-walled latewood fibers with relatively high wall fraction and thin-walled earlywood fibers with relatively low wall fraction would vary significantly in the compressibility of their wet mats. The latewood fibers, which have thicker cell walls and greater axial elastic moduli (10-14), might be expected to compress less readily into flattened cross sections and bend to a lesser degree, thereby providing lower wet mat density and less resistance

to fluid flow. Another correlative aspect would be variation in fiber length (9). Short fibers which also have smaller diameters might be expected to pack tighter than long fibers and give mats of higher density. In addition to the dimensional aspects of wood fibers it is also necessary to take into account degree of delignification since this also relates to mat compressibility and flow of fluids through fiber mats (15,16).

In the past these hydrodynamic properties were of interest primarily in understanding paper machine processes such as drainage. Recently, however, technological developments in the area of displacement washing and bleaching have made use of wet mat compressibility and filtration resistance data in the design and operation of equipment (17). Correlation of variations in gross fiber morphology, such as wall fraction and fiber length, to these hydrodynamic properties should aid in equipment design and development of efficient operating conditions.

OBJECTIVE

The aim of this study is to obtain correlations between the aforementioned hydrodynamic pulp properties and wood fiber morphological variation, including wall fraction and fiber length, using unbeaten bleached loblolly pine kraft pulp.

REVIEW OF PERTINENT LITERATURE CONCERNING MORPHOLOGICAL ASPECTS OF PULP FIBERS

Studies involving model systems of synthetic fibers (5-9) have demonstrated the relative importance of fiber characteristics such as fiber cross-sectional shape and length in influencing the hydrodynamic properties of pulp slurries. Unfortunately, the pulp and paper industry does not work with "ideal" fiber systems. Wood, the principle raw material of the industry, is morphologically complex. The length of fibers varies within a given tree, and wood produced in temperate climates contains cells of greatly varying wall thickness. The

largest difference, however, between wood fibers and the solid synthetic fibers previously used in model studies is that wood fibers contain a lumen.

WALL FRACTION VARIATION

Collapse of the lumens of wet wood pulp fibers under pressure increases fiber conformability by altering the cross-sectional shape of the fiber. At relatively low pressures fibers can collapse to varying degrees, and the degree of collapse appears dependent upon the fiber wall fraction (percentage of the fiber radius that consists of fiber wall).

For a softwood pulp major differences in wall fraction naturally occur between thin-walled earlywood fibers which have lower wall fraction and thick-walled latewood fibers. Earlywood fibers collapse at significantly lower compressive stress than latewood fibers, and a comparison of the apparent transverse elastic moduli (compressive modulus of the fiber wall) of wet earlywood and latewood spruce kraft pulp fibers also revealed earlywood modulus to be significantly lower (14).

In order to study the effects of these differences between earlywood and latewood wall fraction, the two fiber populations must be separated.

Usually the separation of large amounts of earlywood and latewood fiber for laboratory investigation is a difficult process. Conventional separation is achieved by splitting growth rings with a knife. Although the degree of separation using this technique is excellent, the job is tedious and the time required often prohibitive. Thus, large scale investigations are often impractical.

A mechanical method of fiber classification, which proposedly utilizes the modulus differences between earlywood and latewood pulp fibers, was discovered

by Jacquelin (18) and has been successfully used at the Institute (19,20). Briefly, Jacquelin's procedure involves the slow rotating agitation of a pulp slurry in an inclined cylindrical container as shown in the schematic of Fig. 1. The rotating agitation causes the thick-walled latewood fibers to felt into flocs while the more flexible thin-walled earlywood fibers remain in the field fraction. Each fraction can then be isolated, redispersed, and reagitated to increase the degree of separation.

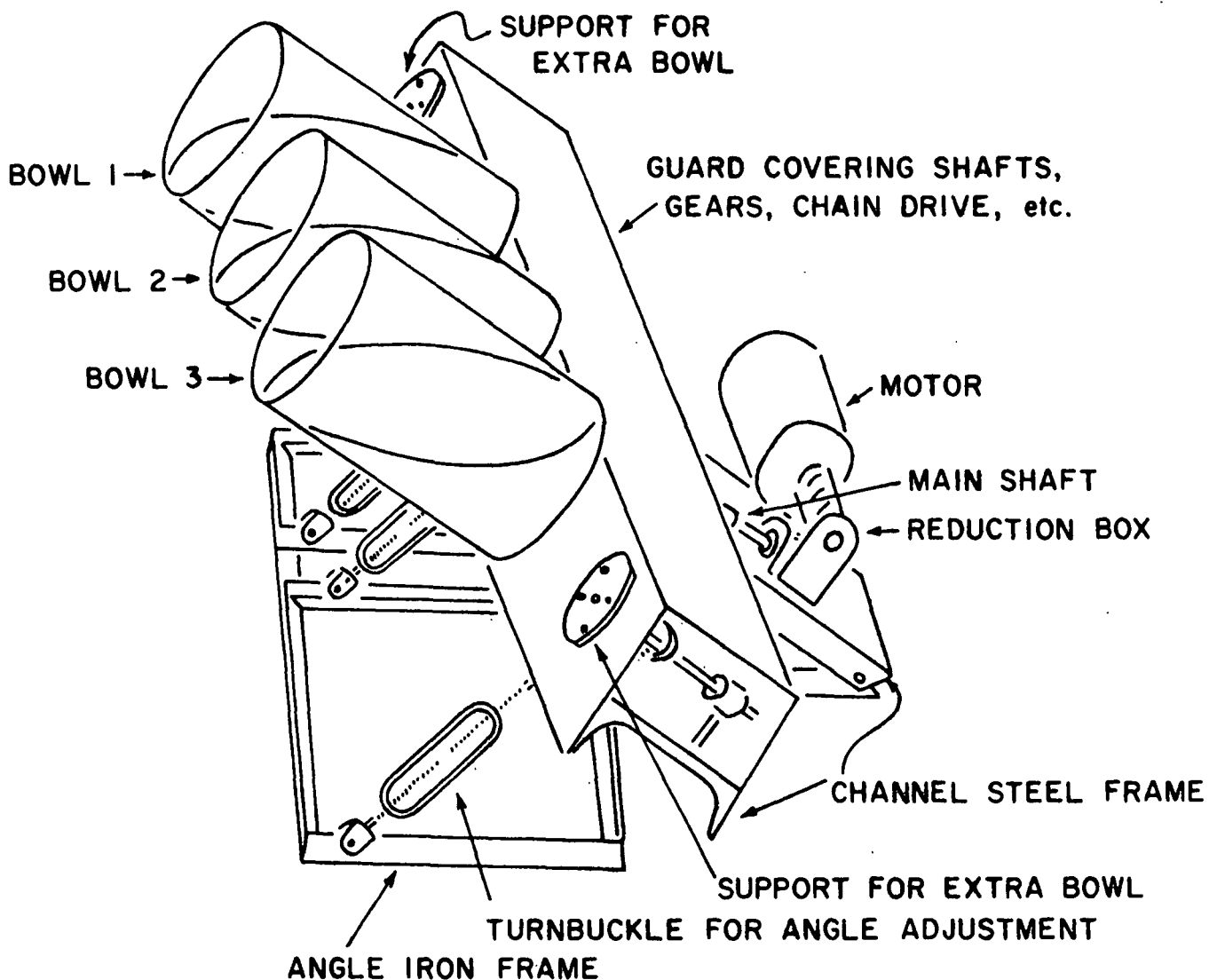


Figure 1. Schematic of Jacquelin Apparatus

FIBER LENGTH VARIATION

Fiber length distributions for unbleached loblolly pine earlywood and latewood fibers have been compiled and show for a range of specific gravities that earlywood and latewood mean fiber length increases with increasing distance from the pith. Thus, juvenile wood is composed of shorter fibers than mature wood. This trend is generally true for all conifer species, and is exemplified by the data in Fig. 2.

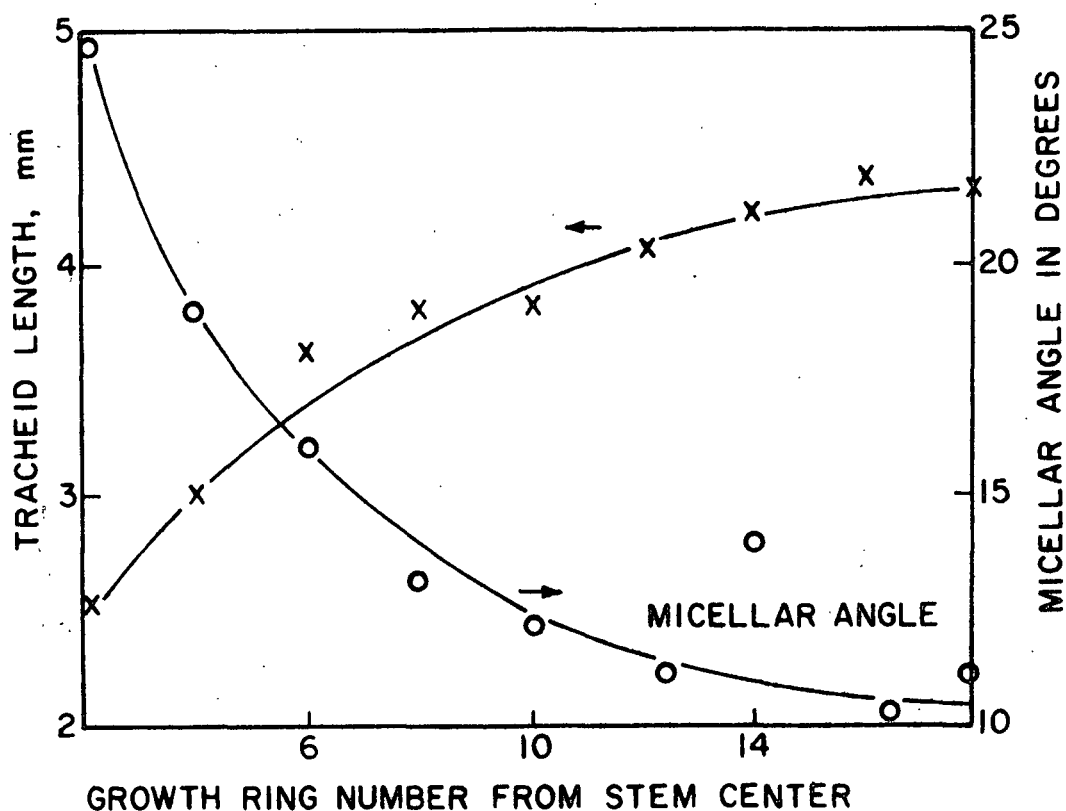


Figure 2. Variation in Tracheid Length and S_2 Fibril Angle in Successive Growth Rings of *Pinus radiata* (21)

Latewood fibers for a given growth ring and specific gravity are longer than earlywood, but within a given tree the range of earlywood and latewood fiber lengths overlaps (22). Therefore, a single tree produces earlywood and latewood fibers of the same length; however, the respective fibers may not occur within the same growth ring.

Unlike synthetic fibers, the lengths of unbroken wood pulp fibers are related to other fiber dimensions (22,23). As the average length of a wood pulp fiber increases:

1. average fiber diameter increases,
2. average wall-thickness increases, and
3. S_2 fibril angle decreases.

The decrease in S_2 fibril angle, θ , with increasing fiber length, L_f , shown in Fig. 2 can be described by Equation (1),

$$L_f = a + b \cot \theta \quad (1)$$

where a and b are constants. This relationship is important since the S_2 layer comprises the majority of the cell wall, and decreasing the fibril angle increases the apparent axial modulus of elasticity of the wall material (13,23,24).

The strong correlation of fiber length to these properties is a result of the growing process of the tree. Fibers near the pith are influenced by a rapidly growing apical meristem. They are generally short, narrow, thin-walled, and have high S_2 fibril angles. These fibers are called juvenile wood. As distance from the pith increases, the influence of the apical meristem decreases and an increase in the girth of the vascular cambium occurs (permitting the diameter of the tree to increase with age). In order for the girth of the cambium to increase, the cells composing the cambium (called fusiform initials which through repeated division give rise to a radially directed row of fibers) increase in number and alter their shape by increasing tangential diameter and length (23). Fibers in turn become longer, wider, thicker walled, contain higher wall fractions, and have lower S_2 fibril angles and subsequently higher modulus values with increasing age of the tree (23-25). The change from juvenile wood to mature wood is a gradual one and varies from tree to tree; however, wood is

generally considered mature when the ratio of earlywood to latewood is approximately equal. This occurs after about 10-years growth, i.e., distances greater than 10 growth rings from the pith (22,23).

The isolation of fiber populations of corresponding length can be achieved through a second mechanical process -- Bauer-McNett classification. This fiber length separation is based on the statistical probability that fibers of a certain length will be retained by a given size screen during agitation and controlled water flow.

REVIEW OF PERTINENT LITERATURE CONCERNING HYDRODYNAMIC EVALUATION OF PULPS

The flow of water through pulp fiber mats is of great importance since it is involved in both pulp washing and sheet formation. Technically, washing and sheet formation may be described by a process of filtration and/or permeation. Filtration generally refers to the retention of fibers on a screen (mat formation), whereas permeation describes the flow of water through a previously formed mat.

These flow processes may be quantified using mathematical expressions based on the well known empirical relationship, the Darcy equation (described below). In the pulp and paper industry, evaluations of this type are generally referred to as hydrodynamic evaluations.

A detailed review of the development of the field of hydrodynamics with respect to the pulp and paper industry has been presented by Han (26,27). For the sake of clarity, however, the development of the equations used to calculate wet mat compressibility, filtration resistance, specific surface, and specific volume is presented below.

WET MAT COMPRESSIBILITY

The wet mat compressibility of a wood pulp mat is generally defined by the correlation of wet mat density to static load. Compressibility data is obtained for first compression using the equipment shown in Fig. 3 in conjunction with the procedure developed by Ingmanson and Andrews (29) as presented in the Experimental section. Briefly, a fiber slurry is poured into the cylinder, agitated, and allowed to settle. The porous piston is placed on top of the mat and loaded with brass weights at equally spaced time intervals. Mat thickness (and subsequently mat density) is measured as a function of pressure with the dial micrometer.

The empirical correlation between wet mat density and static load used by Campbell (30) for kraft and groundwood pulps has repeatedly been shown to apply to other pulps for the pressure range of 10 to 100 g/cm² (26,27,31,32) and appears applicable up to pressures of 10⁴ g/cm² (9). The empirical correlation which was modified by Ingmanson (31) is of the form:

$$c = c_0 + M P_f^N \quad (2)$$

where c_0 is the mat density at zero stress which is usually about 0.02 to 0.04 g/cm³, c is defined as the wet mat density at a pressure P_f , and M and N are empirical constants. The equation is the result of the linearity of a log-log plot of c vs. P_f .

In an attempt to define the physical significance of the compressibility constants M and N in Equation (2), Wilder (33) formulated a simplified mathematical model to describe the compressibility of a synthetic fiber mat. Wilder's model was refined by Han (9), resulting in a more realistic though still oversimplified description of compressibility. Development of this refined model with discussion

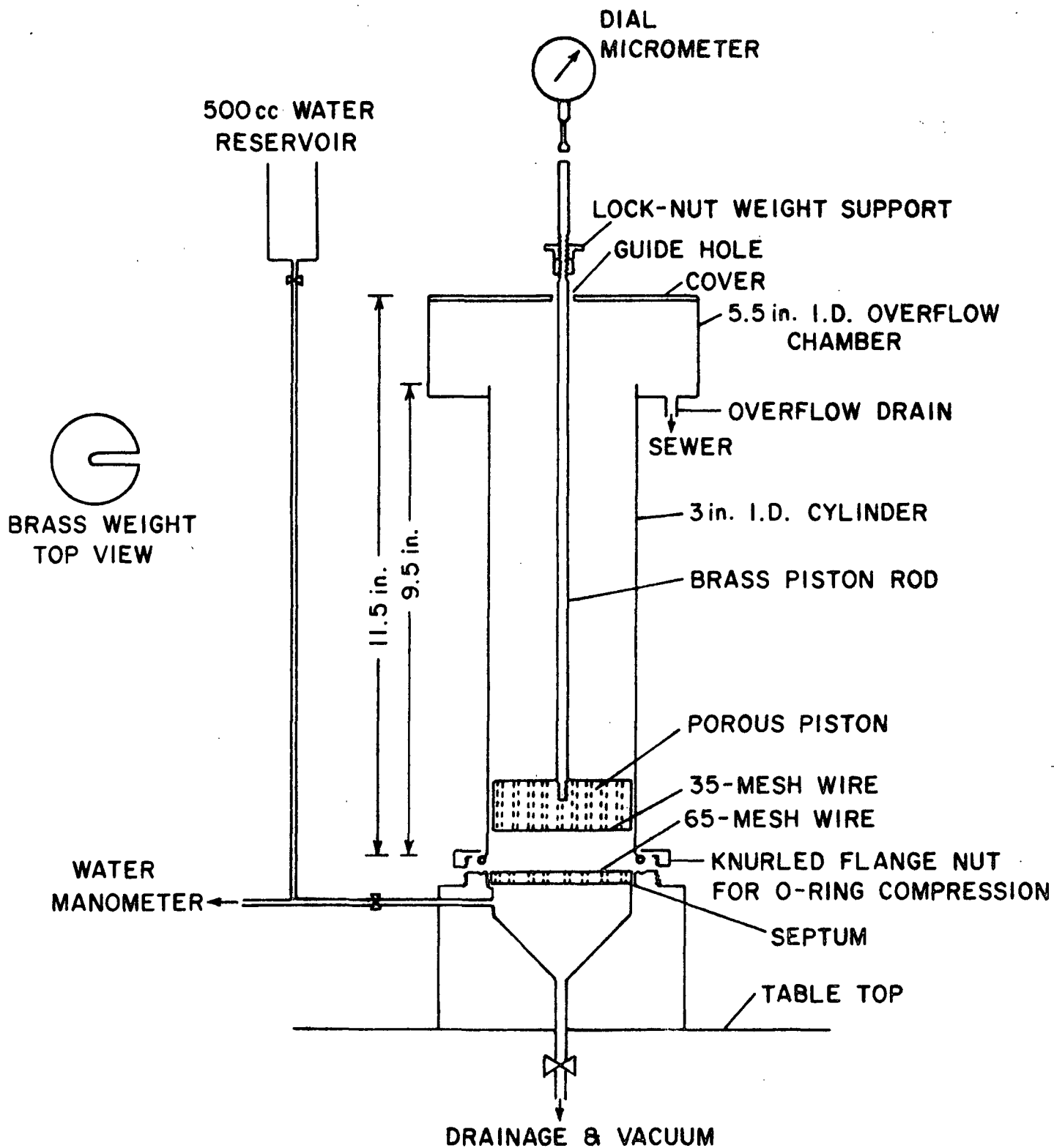


Figure 3. Compressibility Apparatus (28)

of the applicability of the necessary assumptions to wood pulp fiber mats is presented below.

The model is based on the statistical arrangement of fibers in a bed such that the fiber to fiber contact points are alternately arranged above and below a given fiber, as in Fig. 4. The structure of the mat is assumed to consist of horizontal layers (all fibers oriented in the x-y plane), and each layer supports the applied load equally. End effects are neglected.

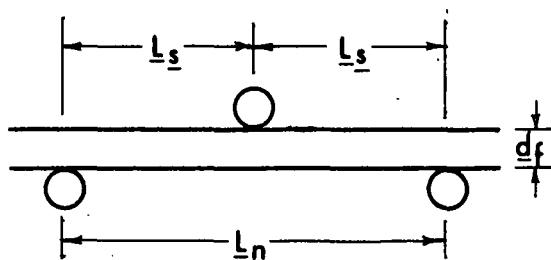


Figure 4. Alternate Arrangement of Fiber to Fiber Contacts

At any state of compaction there is a constant distance between fiber to fiber contacts called the segment length, L_s . Applying the Onagi-Sassaguri equation (62) to the unstressed structure, the initial segment length, $L_{s,o}$, is related to the initial solid fraction by the following equation,

$$\frac{c_o}{\rho_f} = \frac{\pi^3}{16} \frac{d_f}{L_{s,o}} \quad (3)$$

where ρ_f is the fiber density. The segment length is assumed to be statistically the same everywhere in the mat and is constant for a specific level of applied stress.

The initial mat density in a mat of unit area consisting of n similar layers would be:

$$c_o = \frac{W}{L_o} = \frac{(\pi d_f^2/4) N_f L_f \rho_f}{n d_f} \quad (4)$$

where \underline{W} is the mass of the fibers, $\underline{L_o}$ is the initial mat thickness and $\underline{N_f}$ is the number of fibers per unit area.

Upon compacting a structural element, no deformation is assumed to occur at the contact points (an assumption necessary to facilitate solution of the resulting mathematical equations). Therefore, increase in mat density with increase in pressure is due to an increase in the number of contacts brought about by fiber bending. Increasing the number of contacts decreases $\underline{L_s}$; this may be related to mat density using the simplest solution of the Onagi-Sassaguri theory:

$$\frac{c}{c_o} = \frac{L_{s,o}}{L_s} \quad (5)$$

The number of contacts per layer, $\underline{n_c}$, adjacent to two other layers is:

$$n_c = \frac{N_f L_f}{2L_s n} \quad (6)$$

If the elastic deformation of the fibers is small, the deformation may be assumed to be governed by the equations of beam deflection. This enables the deflection, δ , of the fibers in the z-direction to be described by:

$$\delta = \frac{L_n^3 P_n}{K_n E I} \quad (7)$$

where $\underline{L_n}$ is the free span between two supports (Fig. 4), $\underline{P_n}$ is the magnitude of the total load, \underline{E} is the elastic modulus of the fibers, \underline{I} is the second moment of the fiber cross-sectional area or moment of inertia. The product \underline{EI} represents the flexural rigidity of the fibers, and $\underline{K_n}$ is a parameter dependent upon load distributions. The subscript \underline{n} refers to the number of spans.

An infinitesimal load uniformly applied to the top of the mat is uniformly transmitted through the mat via the interfiber contact points. The incremental force sustained by each contact in the layer is $\frac{dP_f}{n_c}$. This force causes the fibers to bend, when the simple beam theory described by Equation (7) is applied, the reduction in thickness is:

$$-\frac{dL}{n} = \frac{L_n^3}{K_n E I} \frac{dP_f}{n_c} \quad (8)$$

where:

$$L = W'/c \quad (9)$$

From Fig. 4, L_n is twice L_s , and from Equation (4), $n = W/(c_o d_f)$. This information plus Equation (9) substituted into Equation (8) yields:

$$-\frac{d(W'/c)}{W'/(c_o d_f)} = \frac{(2L_s)^3}{K_n E I} \frac{dP_f}{n_c} \quad (10)$$

which reduces to:

$$\frac{dc}{c^2} = \frac{(2L_s)^3}{K_n E I c_o d_f} \frac{dP_f}{n_c} \quad (11)$$

From Equations (5) and (3):

$$L_s = L_{s,o} \frac{c_o}{c} = \frac{\pi^3 \rho_f d_f}{16 c} \quad (12)$$

Substituting Equations (4) and (12) into Equation (6) yields:

$$n_c = \frac{32 c_o c}{\pi^4 \rho_f^2 d_f^2} \quad (13)$$

The final differential equation is obtained by combining Equations (11), (12), and (13):

$$c^2 \, dc = \frac{\pi^{13} \rho_f^5 d_f^4}{4^7 K_n E I c_o^2} dP_f \quad (14)$$

For a wood pulp fiber system K_n , d_f , and I are functions of P_f . Resolution of Equation (14), therefore, leads to Equation (15) which has little practical value since the integral cannot be evaluated.

$$c^3 - c_o^3 = \frac{3\pi^{13} \rho_f^5 d_f^4}{4^7 E c_o^2} \int_0^{P_f} \frac{d_f^4}{K_n I} dP_f \quad (15)$$

However, for synthetic fiber systems in which the fibers do not appreciably deform under pressure, d_f and I are essentially constant with respect to changes in P_f . Furthermore, K_n has been shown to be a strong function of P_f (6) such that,

$$K_n = \alpha (P_f/E)^\beta \quad (16)$$

where α and β are constants. With these contentions, Equation (15) reduces to:

$$c^3 - c_o^3 = \frac{3\pi^{13} \rho_f^5 d_f^4}{4^7 \alpha (1-\beta) c_o^2 I E^{1-\beta}} P_f^{1-\beta} \quad (17)$$

Lacking understanding of the mechanism in Equation (16), the possibility of $\pm\beta$ may be assumed; and when $c_o \ll c$, Equation (17) becomes:

$$c = \left[\frac{3\pi^{13} \rho_f^5 d_f^4}{4^7 \alpha (1\pm\beta) c_o^2 I E^{1\pm\beta}} \right]^{1/3} P_f^{(1\pm\beta)/3} = M P_f^N \quad (18)$$

Although Equation (18) is only an approximate description of the complex system of compressibility, it correlates well with experimental data, thereby giving at least a qualitative indication how the compressibility constant M is complexly related to the physical properties of the fibers comprising the mat. Through development of this model, N appears to be significantly less dependent on these properties.

From Equation (18) it is apparent that the most important factors influencing wet mat density are fiber dimensions and pressure. Wilder (33) in a study of compression, creep, and creep recovery showed that time was also an important factor, with initial changes in mat density primarily due to the resistance of the mat to the flow of water as pressure is applied very rapidly. Equation (18), therefore, applies primarily to relatively long periods of loading (several minutes) where the mat has, for practical purposes, reached an equilibrium.

The effects of fiber dimensions on compressibility were also studied by Jones (5) and Elias (6).

Jones (5) in a thesis on compression recovery response studied the compressibility effects of fiber length, diameter, and modulus of elasticity (M.O.E.). Using glass, Nylon, and Dacron fibers he was able to show that changes in wet mat compression response are independent of synthetic fiber diameter, and that mat compressibility at constant pressure increases with decreasing fiber length and M.O.E. Southern pine summerwood pulp fibers were shown to have a similar length vs. compressibility relationship; however, fiber M.O.E. was not measured.

Although the data compiled for the synthetic fibers was extensive, data compiled for the wood pulp was minimal. Specifically, Jones' study incompletely examined the effect of wood pulp fiber dimensions on compressibility.

Elias (6) further examined the factors relating to the mechanism of compressibility of fibrous mats by developing equipment and techniques which allowed individual fibers in the interior of thick glass fiber mats to be visually observed while the mat was subject to compression. By observing the arrangement and configuration of fibers within the mats, he was able to show how the internal structure of the mat was influenced by fiber dimensions and how the fibers respond to compression. As previously shown by Jones (5), fiber

length was a critical fiber dimension in the glass system used by Elias. Beds of longer fibers compressed more readily, i.e., showed a greater change in solids fraction for a given increase in applied stress, than beds containing fibers of shorter length. By observing the distance between fiber contacts (segment length) this phenomenon could be explained. Elias found that segment length was proportional to fiber length; the mean number of fibers touching a given fiber per millimeter of fiber length decreased as the fiber length increased. This increase in segment length allows fibers to bend more readily, thereby making the mat more easily compressed.

In wood pulp fiber systems the process parameters of cooking and beating have also been shown to be important factors influencing wet mat compressibility. Gren (15) has shown that the compressibility constant, \underline{N} , of fiber beds decreased slightly with increasing kappa number. If the assumption is made that wood pulp fiber stiffness decreases with lignin content, it may be noted that the compressibility of a pulp mat (like synthetic fibers) also increases with decreasing stiffness.

Hans (9) has shown that wet mat density at a given applied stress increases with increase in time of Valley beating. The effect of beating on fibers is difficult to analyze, but Valley beating generally decreases mean fiber length, and on this basis would be expected to influence compressibility. This contention is supported by observation that ball milling does not appear to affect compressibility constants \underline{M} and \underline{N} .

For the above discussion, it may be hypothesized that the respective wet mat density of earlywood and latewood at a given applied stress would decrease with increasing fiber length; and that the slope of a plot of wet mat density vs. pressure should increase more rapidly with pressure for thin-walled earlywood fibers than for thick-walled latewood fibers.

SPECIFIC FILTRATION RESISTANCE

Specific filtration resistance is a reliable index of drainage, and, therefore, an important property of the pulp slurry (31); and like wet mat compressibility, constant rate filtration data from which specific filtration resistance is calculated, is relatively easy to obtain.

The equipment used is schematically shown in Fig. 5. Briefly, a dilute suspension of fibers, from an agitated holding tank, flows into the filtration tube, and the fibers are retained on a septum (wire screen). The water is pumped out of the tube through a rotameter at a constant rate, thus the name constant rate filtration. As the mat gets thicker, the pressure drop increases and is recorded with time on an electronic recorder.

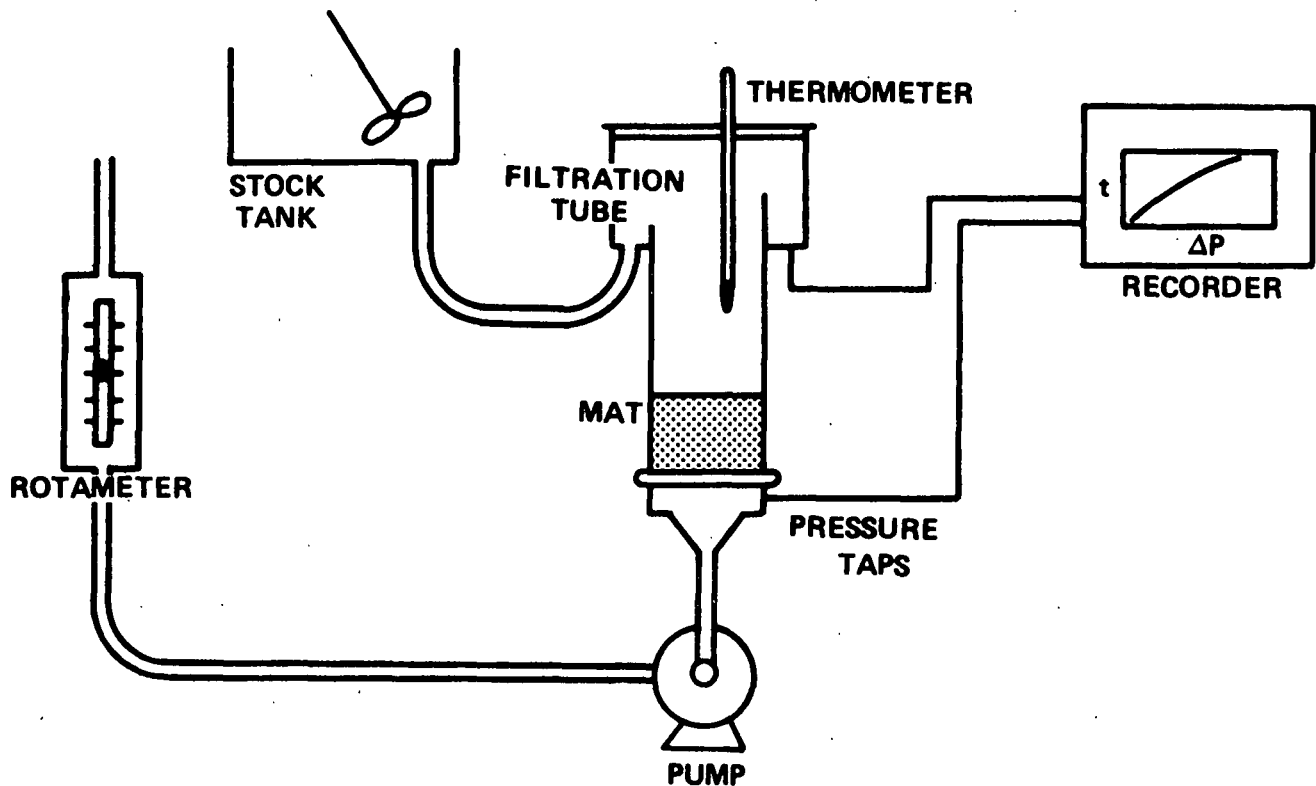


Figure 5. Filtration Apparatus

The equation from which specific filtration resistance, R , is calculated is based on the differential form of the Darcy equation (31,32,34,35),

$$-\frac{d\Delta P_f}{dz} = \frac{1}{K} \frac{q\mu}{A} \quad (19)$$

where q is the volumetric flow rate of a noncompressible fluid of viscosity, μ , through a fiber bed of cross-sectional area, A , and thickness, dz , which develops a frictional pressure drop, $d\Delta P_f$. The negative sign indicates flow in the downward (negative z) direction.

The permeability coefficient, K , is related to the specific filtration resistance, R , by the following expression:

$$K = \frac{1}{R(dW/dz)} = \frac{1}{Rc} \quad (20)$$

where W is the mass of fibers per unit area of mat; therefore dW/dz represents a local mat density, c .

W can also be expressed in terms of the filtration time, t , and stock consistency, C .

$$W = \frac{q}{A} \int_0^t C dt \quad (21)$$

Systematic substitution of Equations (20) and (21) into Equation (19) results in an equation describing the local specific filtration resistance,

$$R = \frac{A^2}{q^2 \mu C} \frac{d\Delta P_f}{dt} = B \frac{d\Delta P_f}{dt} \quad (22)$$

where B is a constant for a given filtration. The R described by Equation (22) applies to a small but measurable section of the forming mat immediately above the retaining screen.

For a relatively dilute slurry, C may be assumed independent of t . Integration of Equation (22) will then yield an equation describing the average specific filtration resistance, $\langle R \rangle$, for the whole mat,

$$\langle R \rangle = B \frac{\Delta P_f}{t} \quad (23)$$

Problems in obtaining accurate values for $d\Delta P_f/dt$ have necessitated use of Equation (23) for calculation of filtration resistance values (26). Recently, these problems have been resolved through development of an accurate numerical procedure for differentiation (described in a later section).

The major factors influencing specific filtration resistance are pressure and fiber dimensions. It may be observed from Equations (22) and (23) that filtration resistance increases with $d\Delta P_f/dt$ and $\Delta P_f/t$ and, therefore, pressure and time are important parameters in the filtration analysis. Further mathematical resolution of filtration resistance into its component parts (described below) reveals that fiber specific surface and mat porosity are also important factors. Filtration resistance increases with the square of specific surface, and decreases with increasing porosity.

SPECIFIC SURFACE AND SPECIFIC VOLUME

The most successful mathematical relationship to describe the creeping permeation of an incompressible porous bed as a function of certain physical properties of the material composing the bed is, again, the Darcy equation [Equation (19)]. The Darcy proportionality factor, K , is not only related to the filtration resistance but is dependent on the structure of the porous medium.

This dependence of K on the physical properties of the porous medium was found by Kozeny (36) to be a function of the porosity, ϵ , and the specific

surface per unit volume, $\frac{S}{V}$. Kozeny's relationship was expanded by Carman (37) resulting in the Kozeny-Carman equation.

$$K = \frac{\epsilon^3}{k S_V^2 (1-\epsilon)^2} \quad (24)$$

The Kozeny factor, k , in Equation (24) was unfortunately found not to be a constant as originally believed, but also dependent on the porosity at porosities greater than about 0.8.

In a study of air flow through fibrous materials, Davies (38) obtained an empirical correlation to describe the dependence of k on ϵ . Later, Ingmanson, et al. (39) discovered that k was also dependent on fiber orientation. Since mats formed during papermaking processes usually have fibers oriented with their axis perpendicular to flow, the empirical correlation developed by Davies was slightly modified to Equation (25) for solid circular cylindrical fibers.

$$k = \frac{k_1 \epsilon^3}{(1-\epsilon)^{1/2}} \left[1 + k_2 (1-\epsilon)^3 \right] \quad (25)$$

where $k_1 = 3.5$ and $k_2 = 57$.

Substitution of Equation (20) into the modified Darcy equation used to describe filtration resistance [Equation (22)] yields an expression relating the constant rate filtration terms, B and $d\Delta P_f/dt$, to K .

$$d\Delta P_f/dt = (BcK)^{-1} \quad (26)$$

Substitution of Equation (25) into Equation (24) yields an expression for K in terms of ϵ and $\frac{S}{V}$. By definition, $\epsilon = 1 - \frac{V_c}{V}$ and $\frac{S}{V} = \frac{S_w}{V}$, where $\frac{V}{V}$ is the specific volume (volume denied to flow) and $\frac{S_w}{V}$ is the specific surface per gram of fiber (surface to mass ratio). Incorporation of these substitutions into Equation (26) results in:

$$\frac{d\Delta P_f}{dt} = \frac{k_1 S_W^2 c^{1/2}}{B v^{1/2}} \left[1 + k_2 v^3 c^3 \right] \quad (27)$$

Equation (27) can be solved for \underline{v} and \underline{S}_W from constant rate filtration data and compressibility data with the aid of additional information describing the pressure relationship of either \underline{S}_W or \underline{v} .

Alternatively, Equation (27) may be integrated and rectified (rearranged to the form of a linear equation) with the assumptions that \underline{v} and \underline{S}_W remain constant with respect to the integration, and the average mat density, \underline{c}_{avg} , is of the form (40)

$$\underline{c}_{avg} = (1-N/2)^2 \Delta P_f^N = (1-N/2)^2 c \quad (28)$$

This integration results in Equation (29) which can be solved for $\langle \underline{v} \rangle$ and $\langle \underline{S}_W \rangle$ (average values of \underline{v} and \underline{S}_W) through linear interpretation of a plot of $\Delta P_f / (\underline{c}^{1/2} t)$ vs. \underline{c}^3 .

$$\frac{\Delta P_f}{\underline{c}^{1/2} t} = \frac{3.5(1-N/2)\langle \underline{S}_W \rangle^2}{B \langle \underline{v} \rangle^{1/2}} \left[1 + 57 \langle \underline{v} \rangle^3 (1-N/2)^6 \underline{c}^3 \right] \quad (29)$$

Linear interpretation of Equation (29) and other forms of the modified Darcy equation (31) has been the accepted procedure for determining $\langle \underline{v} \rangle$ and $\langle \underline{S}_W \rangle$ at the Institute. The development of this procedure has enabled clarification of the relative effects of beating (29) and cooking (15,16) on the hydrodynamic properties of pulps as well as contributed to the basic understanding of water removal from fiber mats (31). Equation (29) appears to be in widespread use throughout the paper industry and currently represents the best available method of determining $\langle \underline{S}_W \rangle$ and $\langle \underline{v} \rangle$.

Alternative procedures for the hydrodynamic evaluation of specific surface and swollen volume as functions of pressure have been presented (41,42). These procedures, however, involve an invalid assumption. The procedures and assumption are discussed in the section on Feasibility of Determining \underline{S}_w and \underline{v} as Functions of Pressure.

EXPERIMENTAL PROCEDURES

ISOLATION OF FIBER POPULATIONS

A two way fiber classification scheme was developed; it is capable of separating a large amount of wood pulp fiber into earlywood and latewood fiber populations of varying length. A bleached southern pine kraft pulp was first separated into earlywood and latewood fiber populations with a Jacquelin apparatus. The earlywood and latewood populations were then subdivided into smaller populations of varying fiber length distribution using a Bauer-McNett classifier. The resulting fiber populations were morphologically homogeneous, making them a desirable raw material for hydrodynamic evaluation.

RAW MATERIAL

A 27-year old medium dense loblolly pine was obtained from a natural even-aged stand in Union Camp's experimental forest in Effingham County, Georgia. The tree was 9.1 inches dbh (diameter at breast height), 81-feet high, and cut into 16 5-foot bolts.

The bottom 5 bolts were longitudinally cut (on a sawmill circular saw) into three sections as shown in Fig. 6 in order to increase the relative percentage of juvenile wood in the sample.

The three sections of each 5-foot bolt were then further divided (by sawing with an 8-inch circular saw) as shown in Fig. 7.

PREPARATION OF PULP

The chips obtained from the rail portion of the fifth 5-foot bolt were used in a preliminary cooking investigation to determine applicability of selected cooking conditions (3).

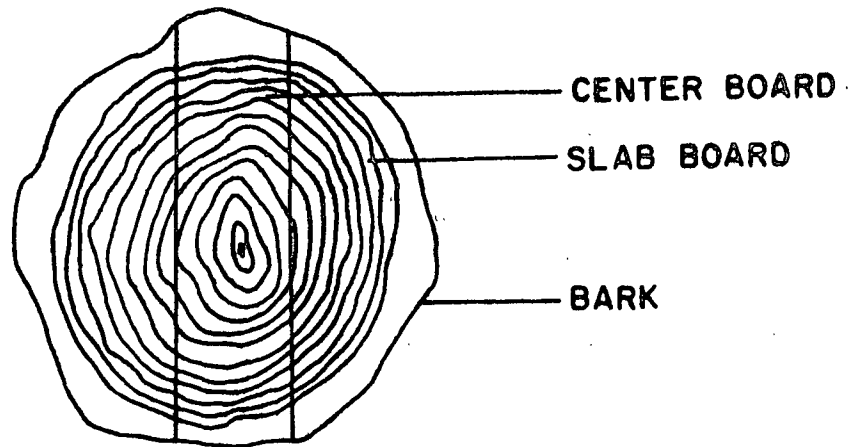


Figure 6. Cross Section of 5-Foot Loblolly Pine Bolt Depicting First Sawing Pattern

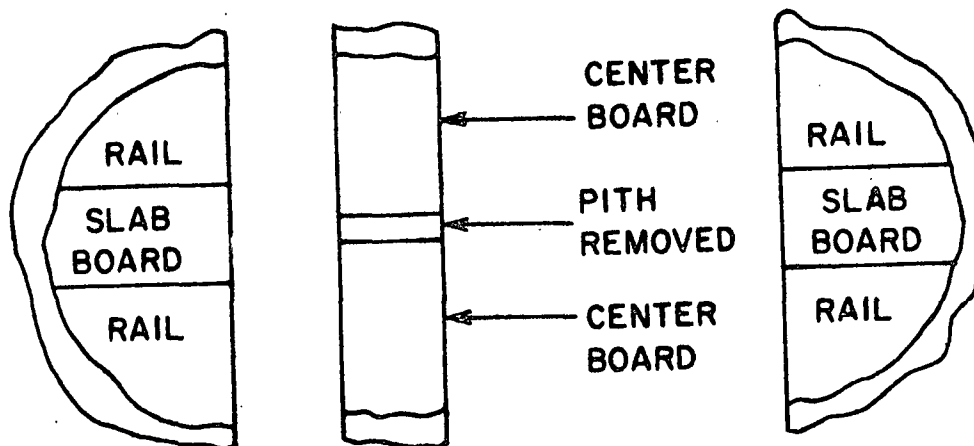


Figure 7. Cross Section of 5-Foot Loblolly Pine Bolt Depicting Second Sawing Pattern

Four conventional kraft cooks were then performed in a batch digester, each using 900 g (o.d. basis) of chips selected from the center and slab boards. After cooking, the chips were washed and disintegrated with hot then cold water in a pulp washer, and dewatered without fines retention in a laundry centrifuge. The resulting pulp was screened on a 0.009-inch slot pulsating screen and screened yield determined. A representative sample of the screened pulp was

removed and kappa number determined according to TAPPI Standard Method T 236 m-60. A summary of the pulping data is presented in Table I.

TABLE I
PULPING DATA

Active alkali (as Na ₂ O)	= 20.6%
Sulfidity (as Na ₂ O)	= 25.0%
Liquor to wood ratio	= 4.0:1 ml/g
Maximum temperature	= 170°C
Time to maximum temperature	= 1.5 hr
Total cooking time	= 4.0 hr
pH at end of cook	= 12.9
Yield	= 46%
Screened rejects	= negligible
Kappa number of screened pulp	= 19.8

For reasons previously discussed, bleaching was necessary. A CEDED bleaching sequence based on prior experience (IPC unpublished work) was employed. The bleaching conditions are given in Table II.

EARLYWOOD AND LATEWOOD SEPARATION

The bleached pulp was first separated into earlywood and latewood fiber populations using the method originally developed by Jacquelin (18).

An electric stirrer was used to gently disintegrate 100 g (o.d. basis) of the bleached kraft pulp with 10 liters of distilled water. The pulp slurry (1.0% consistency) was poured into one bowl of the Jacquelin apparatus (schematically shown in Fig. 1) and rotated for 12 hours at 36 rpm. The rotating agitation

causes the thick-walled latewood fibers to felt into balls while the more flexible thin-walled earlywood fibers remain in the field fraction. The resulting floc and field fractions were then isolated as follows.

TABLE II
BLEACHING CONDITIONS

First Stage - Chlorination

Chlorine, %	6.0
Consistency, %	3.1
Temperature, °C	25
Time, min	60
Residual Cl ₂ , % of applied	16.2
pH	1.8

Second Stage - Alkaline Extraction

NaOH, %	2.5
Consistency, %	10
Temperature, °C	60
Time, min	60
pH	11.3
Permanganate number	6.0

Third Stage - Chlorine Dioxide

ClO ₂ , %	1.0
Consistency, %	10
Temperature, °C	70
Time, min	165
Residual ClO ₂ , %	2.9

Fourth Stage - Alkaline Extraction

NaOH, %	1.8
Consistency, %	10
Temperature, °C	60
Time, min	60
pH	11.4

Fifth Stage - Chlorine Dioxide

ClO ₂ , %	0.6
Consistency, %	10
Temperature, °C	70
Time, min	240
pH	4.6

Standard brightness as received = 89.4%

Yield = 97%

Three hundred grams of previously rotated pulp (3 bowls of 100 g each represent 1 run) were poured into a stainless steel tank containing 300 liters of filtered tap water at 3-5°C. The flocs readily sank to the bottom, but with gentle agitation the field fibers remained suspended and could be siphoned onto a muslin-covered wash box. The tank was refilled with cold water and the siphoning repeated until the amount of field fibers in suspension were depleted to the point of negligible recovery. The tank was again refilled and the temperature raised above 15°C. With the addition of heat, the solubility of air in the water decreased and small bubbles were formed. These bubbles became trapped in the flocs and carried them to the surface. Without agitation, the field fibers remained at the bottom of the tank. The floc fibers were easily skimmed from the water surface, leaving the remaining field fibers to be siphoned onto the wash box.

The isolated floc fraction was washed to remove adhering field fibers using the following method developed by Chang (43).

One liter of fiber flocs was poured into a 4-liter stainless steel beaker which had been drilled with 2.5 mm diameter holes at about 1-cm spacing. Raising and lowering the beaker in a large tank of filtered tap water diluted the free fibers and caused them to flow outward through the holes, which were too small for the flocs. The flocs were removed from the perforated beaker when the amount of free fibers being removed became negligible. After all of the flocs had been washed, the free fibers were siphoned onto a muslin-covered wash box and added to the field fraction.

Each fraction was then redispersed and reagitated to increase the degree of separation.

This procedure enabled separation of 30 g (o.d. basis) of pulp into early-wood and latewood fiber populations each day.

FIBER LENGTH SEPARATION

A Bauer-McNett classifier was used to separate floc and field pulp fractions into fiber populations of varying length. The screen sizes (10, 20, and 65 mesh) were experimentally determined to yield an optimum amount of fiber retained (weight basis) as well as to maximize differences in mean fiber length. An unidentified equipment change, detected by percent retained data, resulted in two groups of on-65 mesh fibers for latewood. The separation, based on TAPPI Standard Method T 233 su-64 was as follows.

Ten grams (o.d. basis) of the respective pulp fraction were briefly agitated (approximately 5 seconds) in a British disintegrator with 2 liters of water. The resultant pulp slurry was then added to the first tank of the Bauer-McNett classifier and classified for 15.0 minutes. Water temperature was 3-5°C. After classification, the separated fibers were flushed from their respective screens onto muslin-covered wash boxes. This method permits 30 g of pulp to be separated each hour.

FIBER ANALYSIS

Standard 1.6 g handsheets wet pressed to 50 psig for 15.0 minutes made from representative floc and field fractions were used to monitor the degree of latewood-earlywood separation. Representative sections of the handsheets were coated with a 60:40 mixture of Au/Pd and viewed with a JSM-U3 scanning electron microscope to obtain a qualitative indication of the degree of separation. No attempt was made to quantify the degree of separation by fiber counting.

Fiber lengths were determined on samples of not less than 1000 fibers with The Institute of Paper Chemistry semiautomatic fiber length recorder according to the method of Illvessalo-Pfaffli and Alfthan (44).

Fiber width and cell wall thickness were measured at 210X with a filar micrometer on samples of not less than 100 fibers. Fibers were wet mounted on glass slides in a mixture of water and glycerin and covered lightly with a cover glass to insure that fibers, particularly earlywood, were not flattened.

The number of fibers per gram was determined by directly weighing air dry samples of 100-300 fibers on a quartz balance accurate to 0.5×10^{-6} g and compensating for moisture content.

Percentage whole fibers were determined by counting the number of whole and broken fibers in representative samples of not less than 200 fibers of pulp fractions. The fibers were mounted on glass slides in mineral oil and viewed at 35X.

HYDRODYNAMIC MEASUREMENTS

The hydrodynamic properties of the isolated fiber populations were measured according to the procedures of wet mat compressibility, constant rate filtration, and multiple pressure tap permeation.

WET MAT COMPRESSIBILITY

Apparent wet mat density as a function of pressure was determined for each isolated pulp fraction with the equipment and procedure developed by Ingmanson and Andrews (29).

A schematic of the equipment is shown in Fig. 3. Prior to each run, the micrometer was zeroed with the piston placed in the empty cylinder. The piston was then removed and the septum flooded with water from the reservoir. A representative sample of a pulp fraction slurried in a British disintegrator at about 0.5% consistency was poured into the tube, stirred thoroughly with a glass stirring

rod, and allowed to settle until the fiber level was below that of the overflow level. The piston and cover were inserted, and the piston was gently lowered by hand until it rested on the loosely formed fiber mat, at which point it was released and the foot of the dial micrometer was placed on top of the piston rod. The mass of the piston and piston arm corrected for the buoyancy force of the water formed the first weight.

Fifteen minutes after the micrometer was positioned, the micrometer was read to obtain the mat thickness. A brass weight similar to the one shown in Fig. 3 was placed on the weight support and after 15 minutes the micrometer was read again. This procedure was repeated with five additional weights of increasing mass.

After the seventh micrometer reading was recorded the water was drained out of the tube, piston and cover removed, and the cylinder assembly detached from the septum. The pad was quantitatively removed from the septum, placed in a tared weighing bottle, dried overnight at 105°C in a forced air oven, and weighed.

Apparent wet mat density, \underline{c} , was calculated as a function of pressure from the pad weight, \underline{W} , cross-sectional area of the tube, \underline{A} , and measured pad thicknesses, \underline{L} , at various pressures using the following equation:

$$c = \frac{W}{AL} \quad (30)$$

An identical procedure was used in a second compressibility apparatus. The mass and water displacement of the new piston head and shaft, however, was greater than that of the original equipment, and although the same brass weights were used, actual compacting pressures differed slightly. Pad thickness was measured with a cathetometer.

CONSTANT RATE FILTRATION

The filtration resistance of the separated fiber populations was quantified with the aid of a research model constant rate filtration apparatus schematically shown in Fig. 4 using the procedure developed by Ingmanson and Whitney (31).

Deaerated pulp at about 0.01% consistency was agitated in the feed tank and permitted to flow through the flow control valve into the filtration tube. In the filtration tube the pulp slurry was maintained at a constant head while the pulp fibers were collected by filtration on the septum. A constant filtration rate was monitored with the rotameter and was maintained by varying the speed of the gear pump. During the run a plot of time (t , seconds) vs. pressure drop (P_f , cm H₂O) was recorded with a strip chart recorder.

The information obtained from the experiment was used with Equations (22) and (23) to respectively obtain local and average specific filtration resistance values as a function of pressure for the samples.

PERMEATION

A multiple pressure tap permeation procedure was adapted from the experimental techniques developed by Chang and Han (45). A schematic of the equipment is shown in Fig. 8.

Deaerated pulp was placed into the feed tank and diluted with filtered, freshly distilled water to approximately 0.01% consistency. A thick mat was formed by slow filtration (1 cm/sec flow rate) and conditioned at 60.0 cm H₂O overall pressure drop for 30 minutes by permeation with filtered, freshly distilled water. The permeation was then stopped and the mat allowed to expand freely for 15 minutes. The process was repeated until the mat thickness at 60.0 cm H₂O remained the same (approximately 5-7 cycles). At this point, the

pressure was measured at different levels in the mat with a pressure transducer indicator.

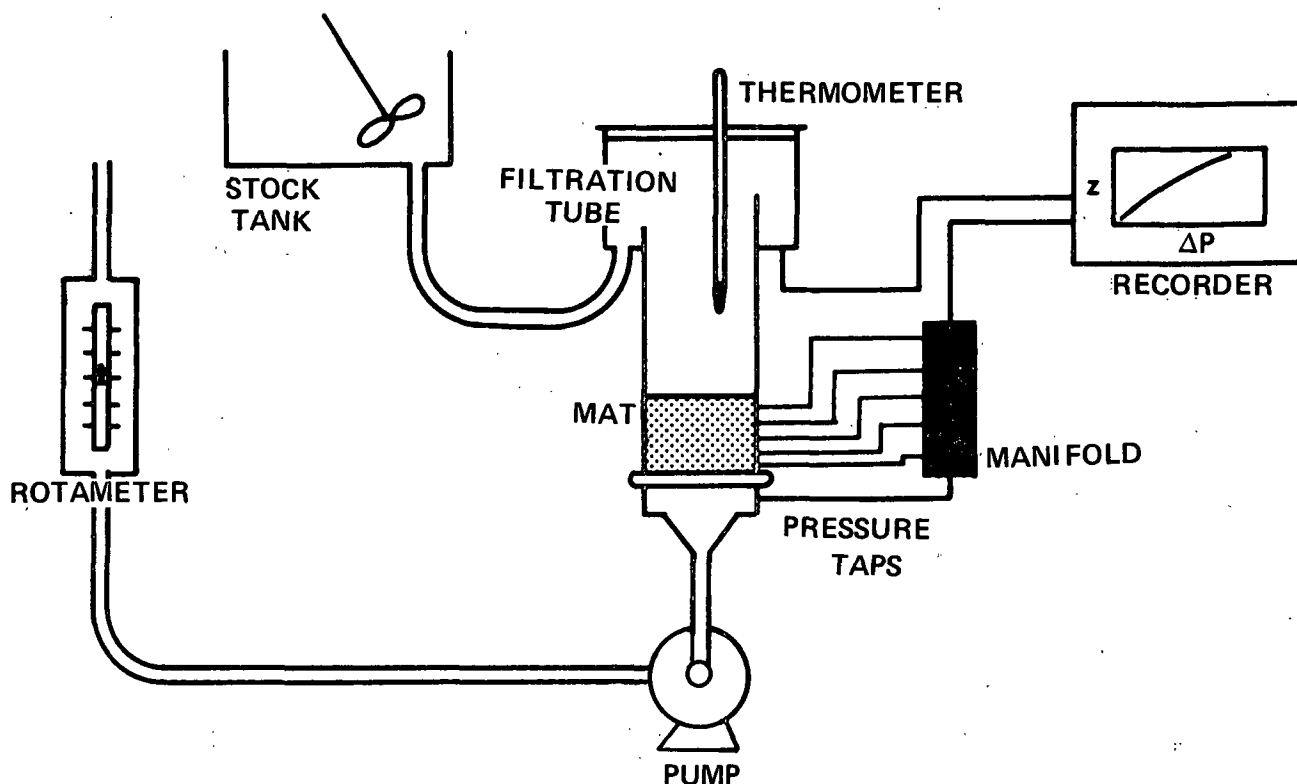


Figure 8. Permeation Apparatus

Latewood and whole pulp fiber populations with fiber lengths greater than 2.7 mm would not develop sufficient fluid drag forces to attain 60.0 cm H₂O overall pressure drop without the formation of mats of excessive thickness or permeation velocities which exceeded the limits of laminar flow. To decrease the porosity (and thus increase fluid drag force) a permeable piston with a static load was applied to these fiber mats.

After permeation the mat was permitted to expand freely for 45 minutes. A permeable piston was then placed on top of the mat, and the mat density determined as a function of static load. From this point the compressibility procedure was identical to that described earlier except a cathetometer instead of a dial micrometer was used to measure mat thickness.

RESULTS AND DISCUSSION

MEASURED AND CALCULATED MORPHOLOGICAL PROPERTIES

FIBER SEPARATION AND DIMENSIONS

The two way fiber classification scheme developed for this work and presented in the Experimental Procedures section resulted in a series of earlywood and latewood fiber populations of varying length.

Figure 9 is a comparison of scanning electron micrographs of handsheets composed of field and floc fractions of bleached loblolly pine after two separations with the Jacquelin apparatus. The micrographs show the field fraction is composed of predominantly earlywood fibers which easily collapse into flat "ribbons," thus forming relatively dense mats with few openings for water to pass through. In contrast, the floc fraction is composed of predominantly latewood fibers which form mats of high porosity.

Jacquelin (18) attributed this morphological separation to relative fiber stiffness. Observations made during this study suggest there is a critical degree of relative stiffness required to achieve morphological separation. Unbleached fibers yielded field and floc fractions which contained no apparent morphological separation. Only after additional lignin had been removed through bleaching did separation into earlywood and latewood occur.

Table III summarizes the results of the Jacquelin separation and also shows the degree of variability encountered in the system. An attempt was made to compare the variability obtained during this study with that obtained by Jacquelin (18,46-48); however, data of this type does not appear available in the general literature. Apparently, this study represents one of the first attempts to statistically quantify separation data.

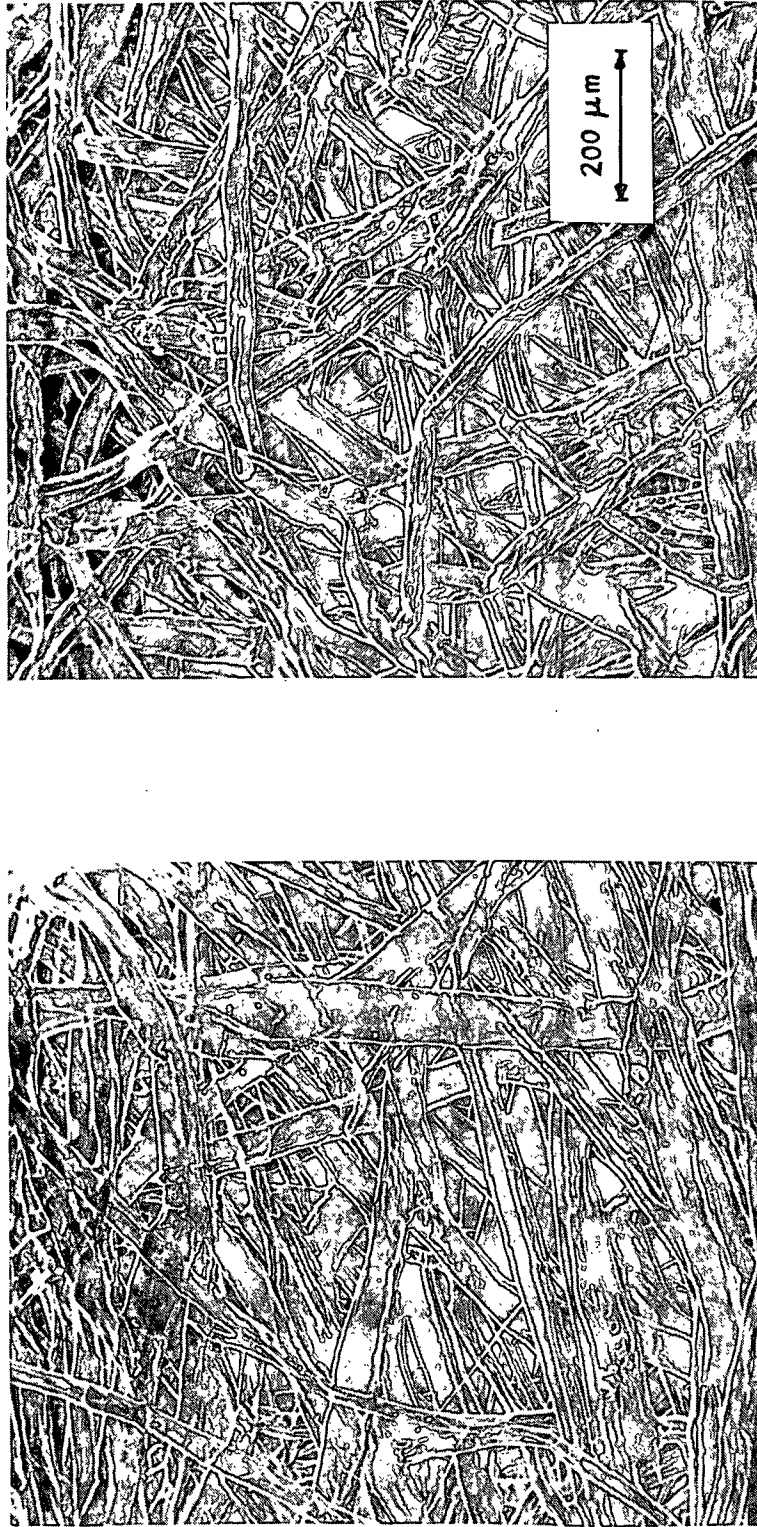


Figure 9. Scanning Electron Micrographs of Handsheets Composed of Field (Left) and Floc
Fractions of Bleached Loblolly Pine After Two Separations
by the Jacquelin Apparatus

TABLE III
QUANTITATIVE RESULTS OF JACQUELIN SEPARATION

Pulp Fraction	Quantity Separated, g	Relative Percent
First Separation		
Floc	9,340.4	57.7 ± 3.0 ^a
Field	<u>6,844.0</u>	<u>42.3 ± 3.0</u>
Total	16,184.4	100.0%
Second Separation ^b		
Floc→floc	4,418.5	38.1 ± 3.1
Floc→field ^c	2,471.2	21.1 ± 3.0
Field→floc ^d	2,716.5	17.1 ± 2.1
Field→field	<u>3,990.8</u>	<u>25.2 ± 2.1</u>
Total	13,597.0	101.5%

^a95% Confidence limits.

^bQuantity separated and relative percentages are not proportional since isolation of floc-floc fractions was terminated after a sufficient quantity had been separated.

^cField fibers resulting from floc fraction.

^dFloc fibers resulting from field fraction.

The table shows that significantly higher percentages of fiber were retained in the floc and floc-floc fractions. This result is in qualitative agreement with the unusually high amounts of latewood fiber observed from the cross sections of the unprocessed logs.

The quantitative results of the Bauer-McNett separation are given in Table IV, along with the mean fiber length, \bar{L}_f , of each population. In addition, the variability of results is reported.

TABLE IV

QUANTITATIVE RESULTS OF BAUER-McNETT CLASSIFICATION

Water Temperature = 3-5°C (Normal Winter Temperature)

Pulp Fraction	Screen Size	Amount Retained, g	Percent Retained	Mean Fiber Length, \bar{L}_f , mm
Field-field (400 separations)	10 mesh	1592.9	39.9 ± 2.5 ^a	3.94 ± 0.04 ^a
	20 mesh	1412.1	35.4 ± 2.4	3.05 ± 0.03
	65 mesh	586.1	14.7 ± 0.9	1.63 ± 0.02
	Fines ^b	399.7	10.0 ± 1.4	
Floc-floc (450 separations)	10 mesh	1558.6	35.3 ± 3.5	4.13 ± 0.06
	20 mesh	1256.5	28.4 ± 9.0	2.98 ± 0.03
	65 mesh(I)	1028.0	23.3	2.07 ± 0.04
	65 mesh(II)	385.5	8.7	1.74 ± 0.03
	Fines ^b	197.9	4.5 ± 2.0	
Whole pulp (150 separations)	10 mesh	531.7	36.3 ± 0.7	3.88 ± 0.03
	20 mesh	607.1	41.4 ± 2.4	2.76 ± 0.04
	65 mesh	300.3	20.5 ± 1.9	1.49 ± 0.01
	Fines ^b	25.9	1.8 ± 3.9	

^aArithmetic mean ± 95% confidence limits.

^bDetermined by difference.

Fines loss for field-field was found to be significantly higher than for other fractions. This higher loss was anticipated since ray cells and other parenchymal tissue fragments would concentrate in this fraction.

The \bar{L}_f values for fibers retained on 10, 20, and 65 mesh screens are significantly different as graphically depicted on the histograms of Fig. 10-12. The histograms also show that the lengths of the fibers retained on the various mesh screens follow an approximately normal distribution function, thus supporting the choice to use arithmetic means in Table IV to describe mean fiber length. In addition, the histograms reveal that fibers retained on the 65 mesh screen

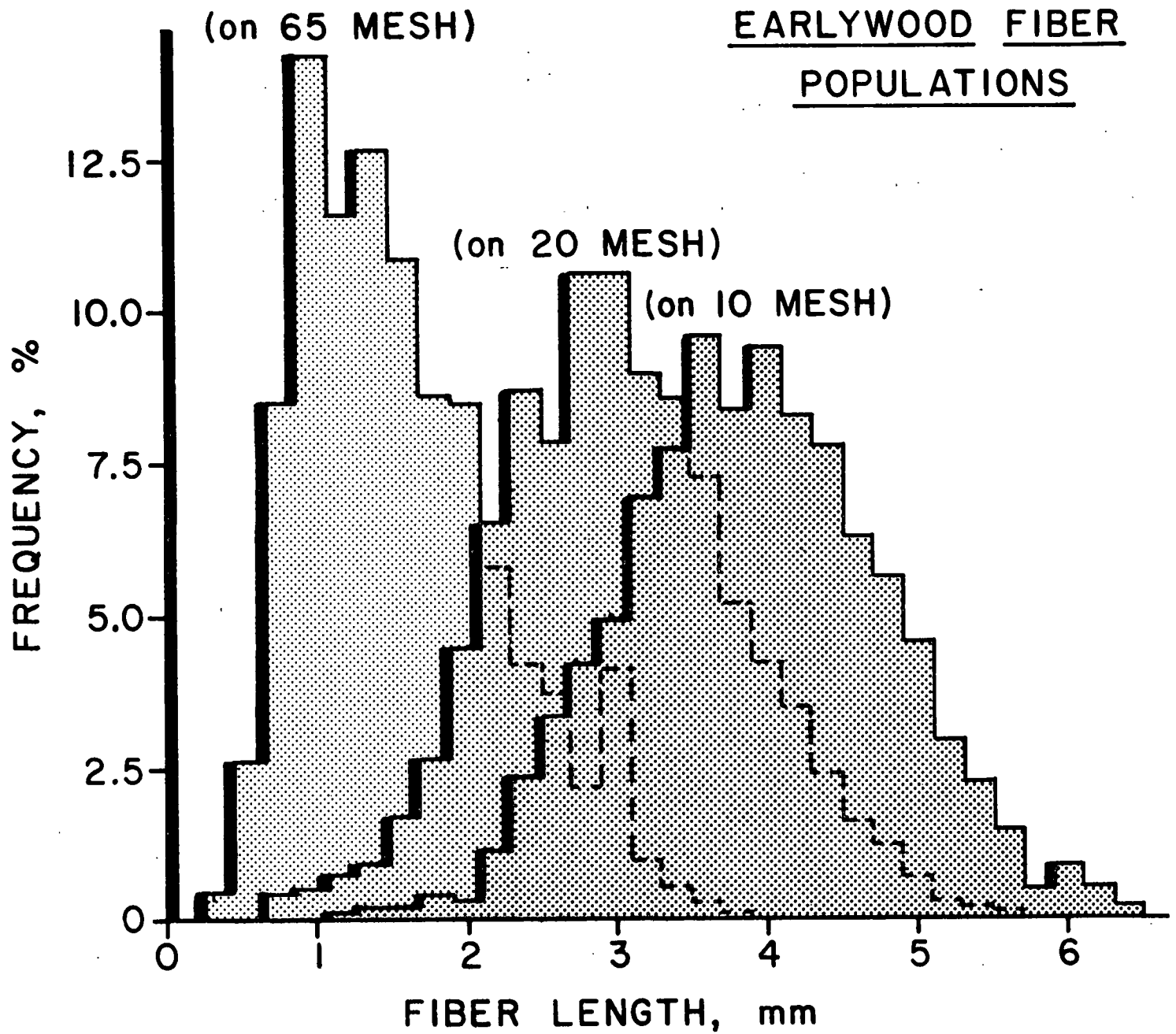


Figure 10. Fiber Length Distribution for Field Fraction Retained on 10, 20, and 65-Mesh Screens

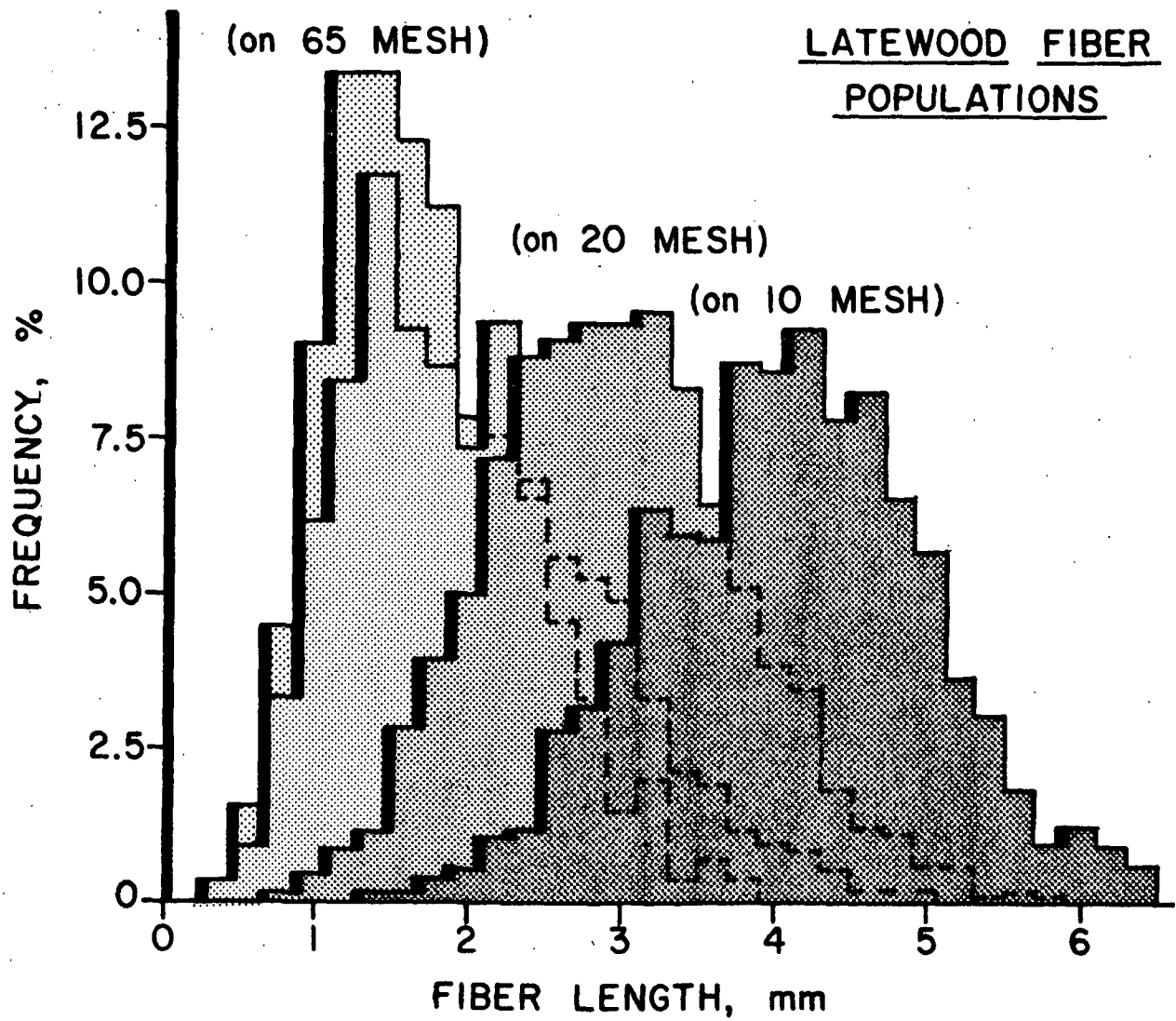


Figure 11. Fiber Length Distribution for Floc Fraction Retained on 10, 20, and 65-Mesh Screens. Double Peak for 65-Mesh Screen Described in Text

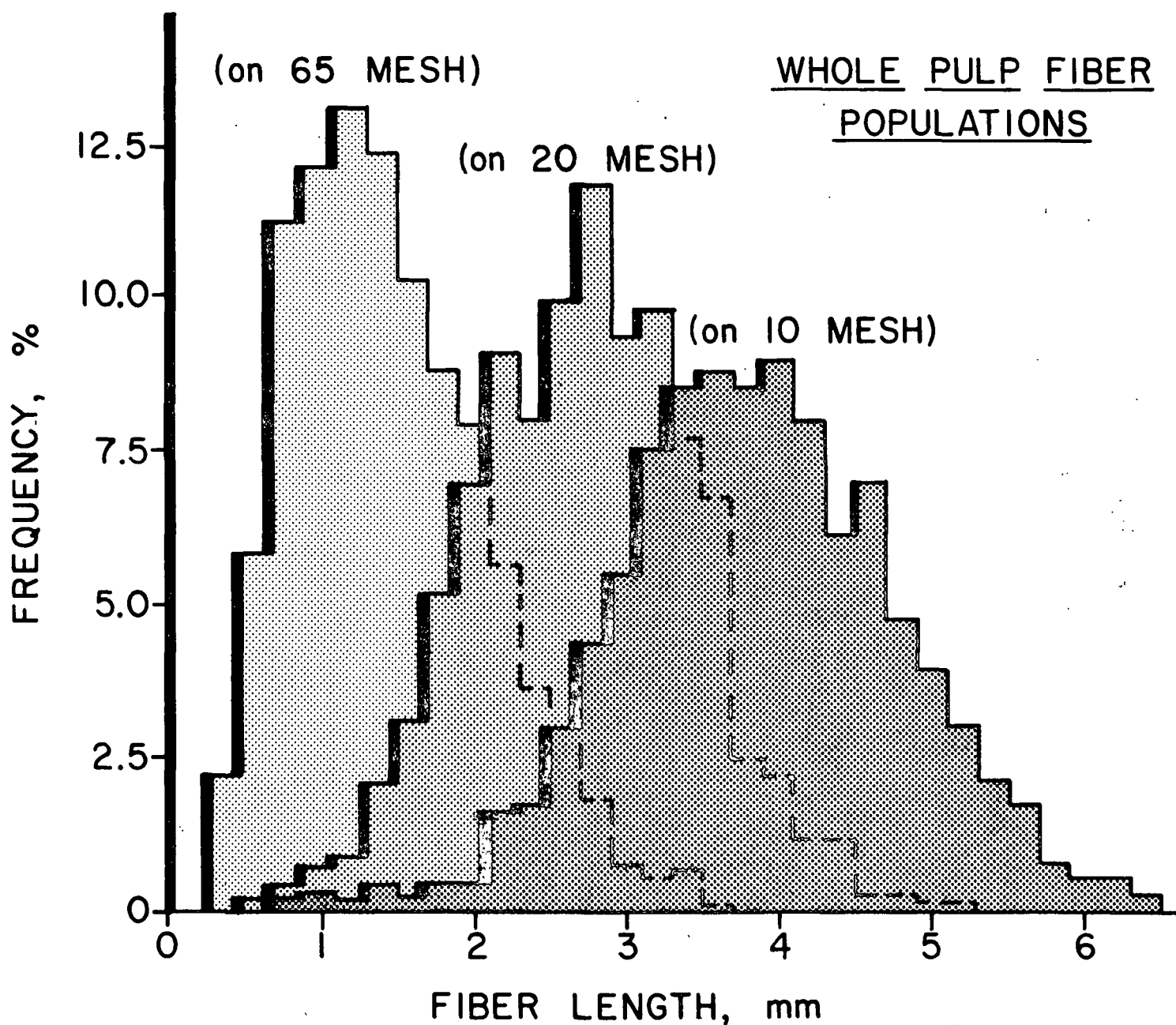


Figure 12. Fiber Length Distribution for Whole Pulp Retained on 10, 20, and 65-Mesh Screens

have a narrower length distribution; this is reflected in the 95% confidence limits.

Figure 13 is a comparison of scanning electron micrographs of handsheets composed of latewood fibers with respective mean fiber lengths of 1.74 and 4.13 mm. As previously reported by Dinwoodie (49), the micrographs show porosity increases with increasing fiber length. These qualitative results can be extrapolated to wet fiber mats; i.e., mats composed of short fibers should exhibit lower porosity than mats of long fibers of comparable wall fraction because short fibers, which are also thinner, pack tighter.

The measured morphological properties of the isolated fiber populations are summarized in Table V.

An additional indication of the separation into earlywood and latewood is given by the data on wall fraction, which was calculated from fiber diameters, $\underline{d_f}$, and wall thicknesses, \underline{WT} . The wall fraction of 30-32% for earlywood compared with 62-68% for latewood fiber fractions (resulting in fibers that are readily and less readily flattened as shown in Fig. 9) defines two distinct sets of fibers. Wall fraction data are in agreement with that calculated from previously reported fiber width and thickness measurements for loblolly pine (2). Earlywood and latewood are further subdivided in Table V according to $\underline{L_f}$. The range in $\underline{L_f}$ of 1.6-3.9 mm for earlywood is about comparable with that of 1.7-4.1 mm for latewood and also agrees with values previously reported for loblolly pine (2,3).

It is virtually impossible to chip, pulp, bleach, and isolate wood fibers without imparting some physical damage to the fibers. However, great care was taken during fiber isolation procedures to minimize the degree of damage. Table V shows that in both sets 50 to over 80% of the fibers were whole. Therefore, it was expected that the isolated fiber populations show similar variation in

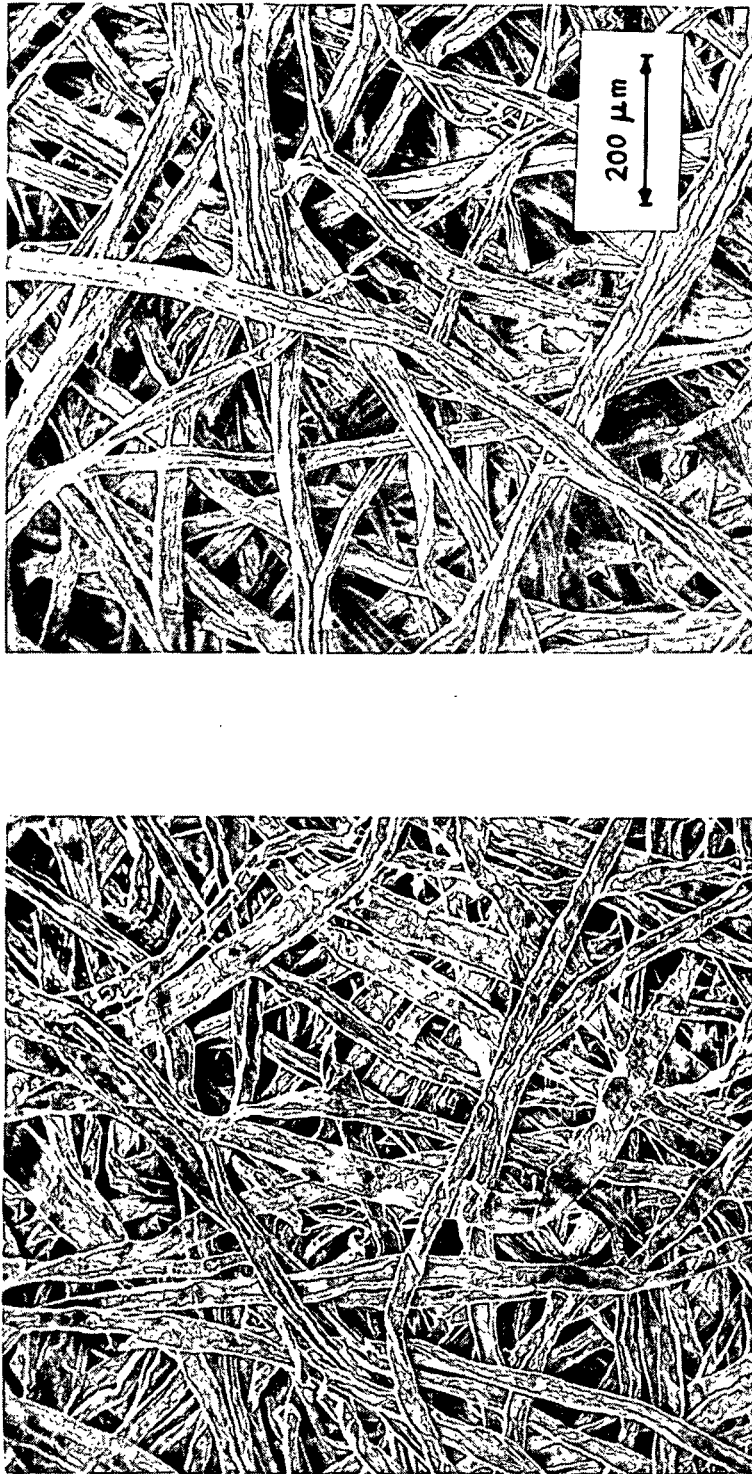


Figure 13. Comparison of Scanning Electron Micrographs of Handsheets Composed of Predominantly Latewood Fibers with Average Fiber Lengths of 1.74 μm (Left) and 4.13 mm

TABLE V
FIBER DIMENSIONS^a

Mean Fiber Length, \bar{L}_f , mm	Fiber Diameter, $\bar{d}_f \times 10^2$, mm	Cell Wall Thickness, $\frac{WT}{x 10^2 \text{ mm}}$	Wall Fraction, % ^b	Whole Fibers, %	No. Fibers ^f per Gram, $\times 10^{-5} \frac{g^{-1}}{\bar{n}_f}$
		<u>Earlywood</u>			$\frac{\bar{n}_f}{\bar{n}_{fg}}$
1.63 ± 0.02^c	3.99 ± 0.25	0.59 ± 0.05	30	51	21.46
3.05 ± 0.03^d	4.50 ± 0.22	0.73 ± 0.07	32	80	13.66
3.94 ± 0.04^e	4.96 ± 0.23	0.80 ± 0.07	32	89	9.40
		<u>Latewood</u>			
1.74 ± 0.03^c	3.24 ± 0.19	1.00 ± 0.05	62	50	22.73
2.07 ± 0.04^c	3.41 ± 0.17	1.13 ± 0.07	66	59	16.98
2.98 ± 0.03^d	3.57 ± 0.20	1.18 ± 0.06	66	73	11.12
4.13 ± 0.06^e	3.70 ± 0.17	1.26 ± 0.05	68	85	6.85
		<u>Whole Pulp</u>			
1.49 ± 0.31^c					
2.76 ± 0.75^d					
3.88 ± 0.77^e					

^aArithmetic mean \pm 95% confidence limits where applicable.

^bCalculated from fiber width and cell wall thickness.

^{c,d,e}On 65, 20, and 10-mesh screens, respectively.

^f \bar{n}_f = experimental, \bar{n}_{fg} = calculated.

fiber dimensions to that previously described for the tree. The increases in fiber width and cell wall thickness observed for earlywood and latewood fiber populations correspond to the increases in mean fiber length as expected.

In summary, the major variations in fiber characteristics and in the wall fraction for between-sets and in mean fiber length for within-sets of earlywood and latewood. However, within-sets, increases in fiber width and wall thickness accompany increases in mean fiber length. For convenience these joint trends will generally be referred to and indexed in terms of mean fiber length.

NUMBER OF FIBERS PER GRAM

The measured number of fibers per gram, $\underline{n_f}$, decreases as $\underline{L_f}$, $\underline{d_f}$, and \underline{WT} increase for earlywood and latewood fiber populations, and the values observed agree with calculated values of 10.3-13.3 and 6.9-10.0 x 10⁵, respectively, reported for earlywood and latewood fibers isolated from southern pine (50). Changes in $\underline{n_f}$ were also predicted by assuming a circular cylindrical model to calculate the volume of the fiber wall, $\underline{V_w}$:

$$\underline{V_w} = \pi \underline{L_f} \left[\left(\frac{\underline{d_f}}{2} \right)^2 - \left(\frac{\underline{d_f}}{2} - \underline{WT} \right)^2 \right] \quad (31)$$

The number of fibers per gram can then be calculated geometrically, $\underline{n_{fG}}$, using Equation (32) with an assumption of a fiber wall density, $\underline{\rho_w}$, for bleached loblolly pine earlywood and latewood:

$$\underline{n_{fG}} = 1/(\underline{V_w} \underline{\rho_w}) \quad (32)$$

Unfortunately, values for $\underline{\rho_w}$ are difficult to obtain experimentally and do not appear available in the general literature. However, calculated values for $\underline{\rho_w}$ of 0.27 and 0.36 for earlywood and latewood, respectively, were obtained to allow

\underline{n}_{FG} to agree closely with \underline{n}_F in Table V. They are in the range of 0.29 and 0.63, respectively, reported for extracted swollen earlywood and latewood (51).

CALCULATED MOMENTS OF INERTIA

Moment of inertia, \underline{I} , has been shown in a previous section to be an important fiber property influencing the behavior of wet mat compressibility [Equation (18)]. Since \underline{I} is a function of fiber dimensions, it may be calculated from the data in Table V with the assumption of an appropriate fiber model. Thus, \underline{I} might be expected to correlate with compressibility data to give some insight of the effects of morphology on compressibility.

Choice of an appropriate model for calculation of \underline{I} is critical because \underline{I} is also a strong function of cross-sectional shape. For this reason two fiber models are presented in Fig. 14: the upper model represents the fiber cross section as circular with the lumen uncollapsed; the lower model represents the fiber cross section as flattened into a rectangular shape with the lumen completely collapsed. Both models are based on experimentally measured fiber dimensions.

Although the models are a gross oversimplification of the real system, they enable calculation of trends in relative \underline{I} -values for fibers in the collapsed and uncollapsed state.

Assuming the fiber wall is homogeneous and of uniform mass distribution, moments of inertia for the circular, \underline{I}_C , and flattened, \underline{I}_F , cross sections may be obtained from Equations (33) and (34) which have been derived from the elementary principles of mechanics:

$$\underline{I}_C = \pi \frac{r_o^4 - r_i^4}{4} \quad (33)$$

where $\underline{r_o} = \underline{d_f}/2$ and $\underline{r_i} = (\underline{d_f}/2) - (\underline{WT})$,

$$I_F = 2/3 \underline{d_f} (\underline{WT})^3 \quad (34)$$

Calculated values for $\underline{I_C}$ and $\underline{I_F}$ are presented in Table VI and are related to fiber length in Fig. 15.

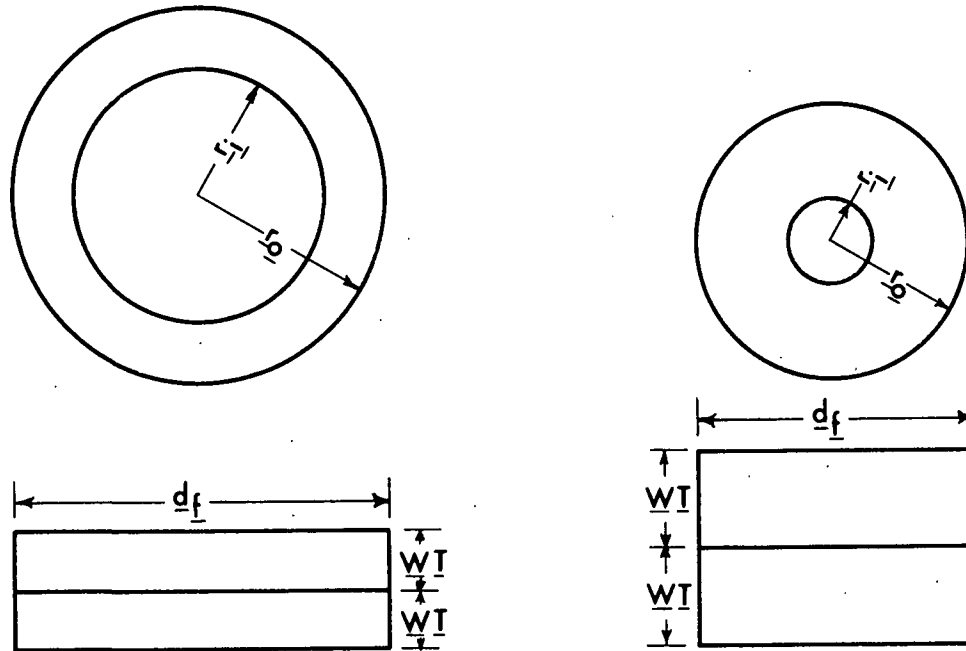


Figure 14. Scale Drawings (1000X) of Assumed Fiber Cross Sections for Calculation of \underline{I} Comparing 3.94 mm Earlywood (Left) and 4.13 mm Latewood

Both $\underline{I_C}$ and $\underline{I_F}$ increase with increasing $\underline{L_F}$ in expected agreement with corresponding increases in $\underline{d_f}$ and \underline{WT} . $\underline{I_C}$ is greater in all cases than $\underline{I_F}$ because the wall material is distributed further from the central axis of the fiber when the fiber is not collapsed.

It is interesting to note that $\underline{I_C}$ for earlywood is about 2 to 2.5 times larger than that of latewood and that this trend is reversed for $\underline{I_F}$. Logically, the trends of the flattened fiber model ($\underline{I_F}$) appear more reasonable; especially since in bending studies

of southern pine pulp fibers under water, latewood was shown to be five times stiffer than earlywood (52). This stiffness or flexural rigidity is a measure of the product, EI.

TABLE VI
CALCULATED MOMENTS OF INERTIA

$\frac{L_f}{\text{mm}}$	$\frac{d_f}{\text{mm}} \times 10^2,$	$\frac{WT}{\text{mm}} \times 10^2,$	$\frac{I_C^a}{\text{mm}^4} \times 10^8,$	$\frac{I_F^b}{\text{mm}^4} \times 10^8,$
<u>Earlywood</u>				
1.63	3.99	0.59	9.4	0.6
3.05	4.50	0.73	15.9	1.2
3.94	4.96	0.80	23.5	1.7
<u>Latewood</u>				
1.74	3.24	1.00	5.3	2.2
2.07	3.41	1.13	6.6	3.3
2.98	3.57	1.18	7.9	3.9
4.13	3.70	1.26	9.1	4.9

^aCalculated from circular cross-sectional model.

^bCalculated from flattened cross-sectional model.

Data for the elastic moduli of wet southern pine pulp are not available, but in general elastic moduli of latewood are greater than earlywood and E increases with increasing fiber length (10-14,23-25). However, there is no evidence to indicate that E is sufficiently low to compensate for the high moment values associated with the circular model. Therefore, on the basis of these studies (10-14, 23,25), it appears that the flattened fiber model may be more applicable to an understanding of fiber bending, whereas the circular model is more representative of the experimentally measured fiber dimensions.

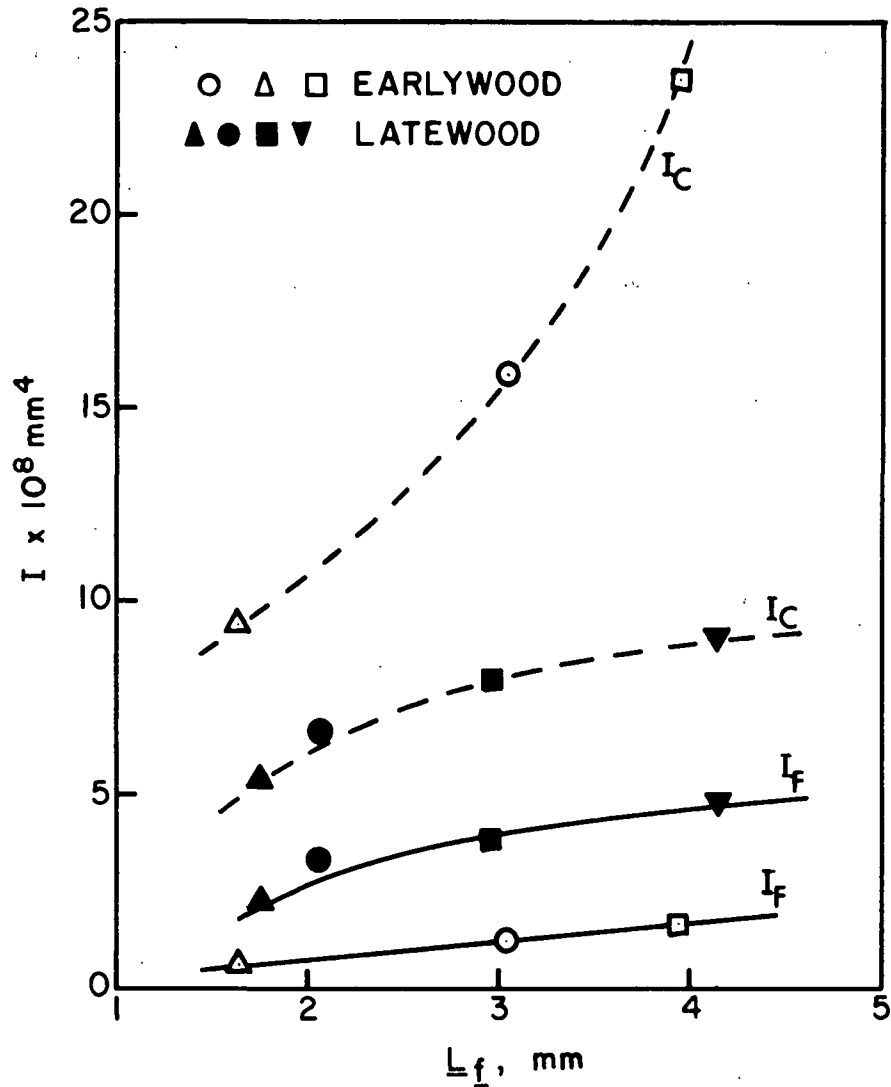


Figure 15: Relationship Between Fiber Length and Moments of Inertia for Circular, I_C , and Flattened, I_F , Models

CALCULATED SURFACE AND VOLUME TO MASS RATIOS

The information obtained in Table V can also be used to calculate an approximate surface to mass ratio, S_{WG} , and volume to mass ratio, v_G , for a fiber population assuming a circular cylindrical model to describe fiber shape as before. Since surface and volume to mass ratios are important hydrodynamic properties [see Equation (29)], calculations of this type will indicate the manner in which the morphological factors may be expected to influence hydrodynamic properties.

The model equations developed for \underline{S}_{WG} and \underline{v}_G are represented by Equations (35) and (36), respectively.

$$\underline{S}_{WG} = \pi d_f L_f n_f \quad (35)$$

$$\underline{v}_G = \pi d_f^2 L_f n_f / 4 \quad (36)$$

In Equation (36) \underline{v}_G represents the total volume of the fiber-wall volume plus lumen volume.

\underline{S}_{WG} and \underline{v}_G values for earlywood and latewood fiber populations are presented in Table VII.

TABLE VII
GEOMETRIC SURFACE- AND VOLUME-TO-MASS RATIOS

Mean Fiber Length, mm	$\frac{\underline{S}_{WG}}{\text{cm}^2/\text{g}}$	$\frac{\underline{v}_G}{\text{cm}^3/\text{g}}$
<u>Earlywood</u>		
1.63	4385 (7347) ^a	4.37 (7.33) ^a
3.05	5890	6.63
3.94	5771	7.16
<u>Latewood</u>		
1.74	4026	3.26
2.07	3766	3.21
2.98	3716	3.32
4.13	3290	3.04

^aCalculated using \underline{n}_{fG} .

As mean fiber length increases, \underline{S}_{WG} decreases for the latewood fiber populations. A similar trend is expected for earlywood, but is not observed because \underline{S}_{WG} for the 1.63 mm fiber population appears abnormally low. Experimental inaccuracy in the measurement of \underline{d}_f , \underline{L}_f , or \underline{n}_f could conceivably account for this

abnormality. Calculation of a value for \underline{S}_{WG} which is greater than 5890 cm²/g for this fiber population, through systematic variation of each of these fiber properties, reveals that experimental error could have reasonably occurred only in determination of \underline{n}_f . The value in parenthesis uses \underline{n}_{fG} in Equation (35) and demonstrates the expected trend. Also in Table VII, earlywood fibers have higher \underline{S}_{WG} values than latewood.

Values of \underline{v}_G for earlywood fiber populations are also higher than those for latewood but are not within the range of 1 to 4 cm³/g usually observed by measuring volume to mass ratios by filtration analysis (32).

The abnormally high value for earlywood may be a result of the change in swollen volume of the fiber with pressure. Fiber measurements were made on fibers with essentially circular cross sections, and the model reflects this cross-sectional shape in calculation of \underline{v}_G . Earlywood fibers, however, have thin cell walls and are more likely to collapse under pressure. Collapse of the fibers would cause expulsion of water from the lumen and subsequently lower the volume to mass ratio. On the other hand, thick-walled latewood fibers probably retain much of their cross-sectional shape under pressure.

Fiber collapse may cause a slight increase in surface to mass ratio as the fiber changes from circular to elliptical in cross section.

FIBER MORPHOLOGY AND WET MAT COMPRESSIBILITY.

COMPRESSIBILITY CONSTANTS \underline{M} AND \underline{N}

Initial compressibility constants for the various morphological fiber fractions described in Table V were obtained from linear regression of log-log plots of wet mat density, \underline{c} , vs. static load, \underline{P}_f , using the log form of Equation (2) in which the \underline{c}_0 term is neglected:

$$\log c = \log M + N \log P_f \quad (37)$$

The data and resulting best fit curves (solid line) for earlywood and latewood fiber fractions are presented in Fig. 16 and 17, respectively. The original data are presented in Appendix I, and applicability of Equation (37) to the data may be visually confirmed from these figures. Calculated values for the initial slopes, N_1 , and intercepts M_1 , are tabulated in Table VIII and are within the range of values previously reported by Han (9).

TABLE VIII
VALUES FOR COMPRESSIBILITY CONSTANTS N AND M

L_f , mm	L_f/d_f	N_1^a	$M_1 \times 10^3,^a$ c.g.s. units ^b	N^c	$M \times 10^3,^c$ c.g.s. units ^b
<u>Earlywood</u>					
1.63	40.9	0.361 ± 0.005^d	2.02 ± 0.01^d	0.373	1.79 ± 0.01^d
3.05	67.8	0.390 ± 0.010	1.43 ± 0.02	0.373	1.70 ± 0.02
3.94	79.4	0.376 ± 0.015	1.61 ± 0.03	0.373	1.66 ± 0.03
<u>Latewood</u>					
1.74	53.7	0.373 ± 0.017	1.65 ± 0.03	0.373	1.64 ± 0.03
2.07	60.7	0.376 ± 0.018	1.55 ± 0.03	0.373	1.60 ± 0.03
2.98	83.5	0.363 ± 0.013	1.73 ± 0.02	0.373	1.56 ± 0.02
4.13	111.6	0.366 ± 0.019	1.69 ± 0.03	0.373	1.57 ± 0.03

^aLinear regression of individual fiber populations.

^b $(g/cm^3)/(dynes/cm^2)^{1/N}$.

^cMultiple linear regression of total earlywood and latewood data, confidence limit negligible (0.0003) due to large sample size.

^d95% confidence limits.

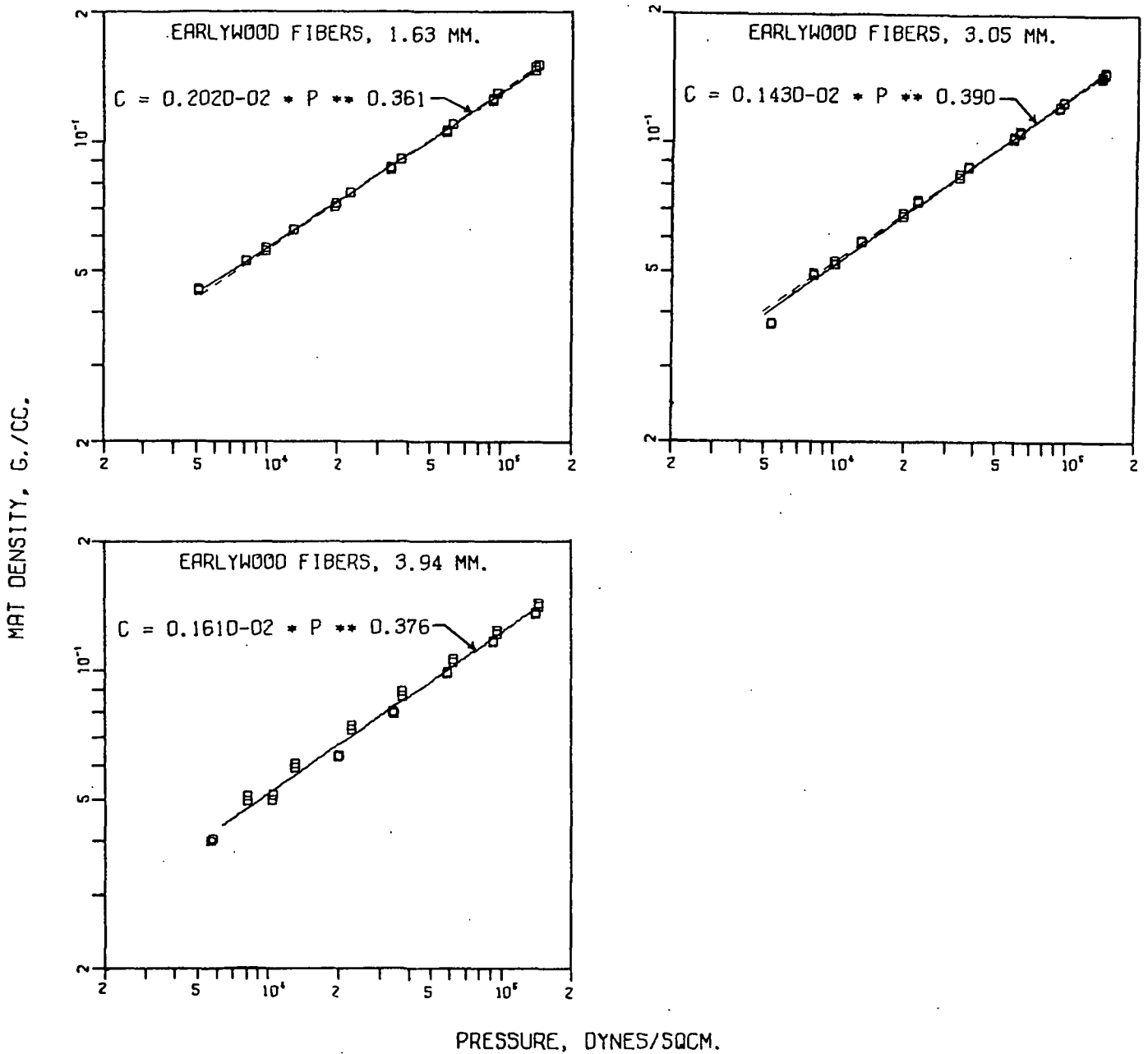


Figure 16. Compressibility Data and Resulting Best Fit Curves for Earlywood Fiber Fractions; Solid Line (Labelled)

Corresponds to $C = \frac{M_1 P^{N_1}}{F}$, Broken Line

Corresponds to $C = \frac{M P^N}{F}$

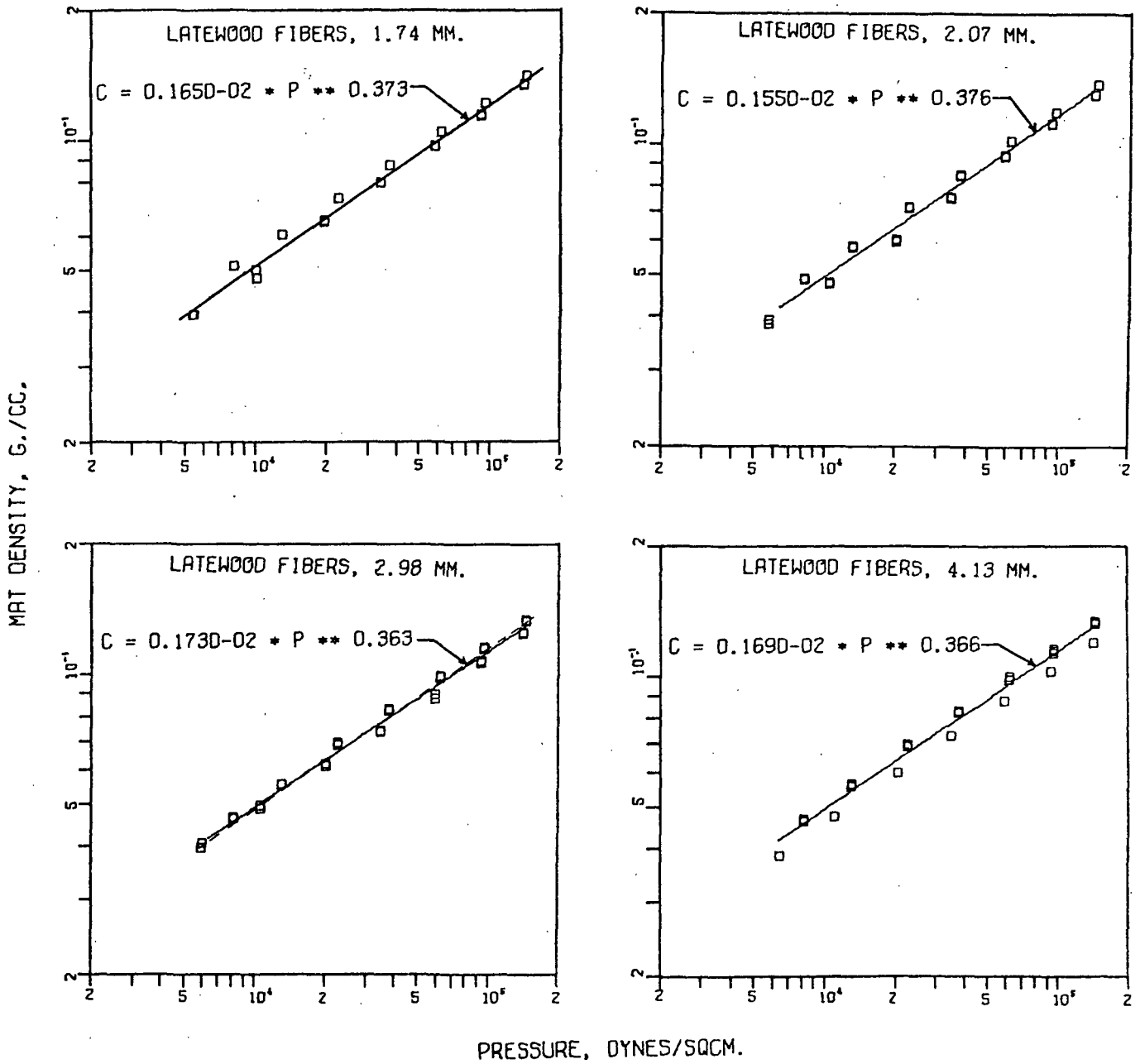


Figure 17. Compressibility Data and Resulting Best Fit Curves for Latewood Fiber Fractions (as in Fig. 16)

Although the \underline{M}_1 values were determined statistically, they are sensitive to the exact positioning of the slope (or \underline{N}_1 value), and normal variability in the experimental data results in uncertainty over what slope should be used. This uncertainty is manifested by the lack of correlation of \underline{M}_1 with fiber dimensions. Assuming the compressibility model, Equation (18), is applicable to wood pulp fiber systems, a more tenable result would be an observed correlation between \underline{M}_1 and \underline{L}_f in Table VIII [since \underline{M} in Equation (18) is a function of \underline{d}_f , \underline{I} , and \underline{E} , and increases in each of these fiber properties correspond to increases in \underline{L}_f , \underline{M} should also correlate to \underline{L}_f]. Also on the basis of Equation (18), \underline{N} would be expected to remain essentially constant with respect to changing fiber dimensions. This contention is supported by previous work in which beating and high consistency refining did not influence \underline{N} values appreciably (9).

Since \underline{N}_1 does not correlate with fiber dimensions (Table VIII) and in view of Equation (18), \underline{N} values for earlywood and latewood were assumed constant to facilitate further data analysis. Incorporation of the logs of the earlywood and latewood mat density vs. pressure data of Appendix I into a simultaneous linear multiple regression analysis in which the same value of \underline{N} is assumed for every group (53,54), gave an overall adjusted value of \underline{N} equal to 0.373 as well as an individual value of \underline{M} for each fiber population. These values corresponded to the weighted averages computed for separate independent regression runs. The results of this regression analysis are reported as \underline{N} and \underline{M} in Table VIII. Visual confirmation of the applicability of \underline{N} and \underline{M} to the experimental data is provided by the broken lines in Fig. 16 and 17. On the whole, respective values for \underline{N} and \underline{M} fit the data extremely well and in most cases the broken lines superimpose the solid lines calculated from \underline{N}_1 and \underline{M}_1 .

COMPRESSIBILITY

Further evidence that \underline{N} is essentially constant for the fiber populations results from defining compressibility as the change in mat density with pressure, i.e., $\underline{dc}/\underline{dP}_f$, which represents the slope at a given pressure for plots of \underline{c} vs. \underline{P}_f .

$$\frac{\underline{dc}}{\underline{dP}_f} = \frac{\underline{N}}{\underline{P}_f} \underline{M} \underline{P}_f^{\underline{N}} = \frac{\underline{N}}{\underline{P}_f} \underline{c} \quad (38)$$

From Equation (38) for a given pressure, $\underline{dc}/\underline{dP}_f$ is expected to be proportional to \underline{c} and \underline{M} if \underline{N} is essentially constant. Table IX shows $\underline{dc}/\underline{dP}_f$ remains practically constant at $\underline{P}_f = 10$ and 90 cm H₂O for earlywood and latewood fiber populations regardless of whether \underline{N}_1 and \underline{M}_1 or \underline{N} and \underline{M} are used in the calculation. However, only when \underline{N} is constant for the fiber populations is $\underline{dc}/\underline{dP}_f$ proportional to \underline{M} at a given pressure. Hence, this mean value of \underline{N} is believed more generally applicable to the experimental data than the individual initial values. Since for any two fiber fractions studied it would not necessarily be established that \underline{N} can be treated as constant, $\underline{dc}/\underline{dP}_f$ provides a more reliable indication of relative compressibility than the coefficient " \underline{M} ."

From Table IX it is observed at $\underline{P}_f = 10$ cm H₂O that the compressibility of earlywood fibers is greater than the compressibility of latewood. Also as fiber length increases, compressibility decreases for both earlywood and latewood fiber populations. At $\underline{P}_f = 90$ cm H₂O the compressibility of the mats has greatly diminished relative to $\underline{P}_f = 10$ cm H₂O; but differences between earlywood, latewood, and fiber lengths are still present albeit they are not as great.

TABLE IX

COMPRESSIBILITY VALUES, $d\bar{c}/dP_f$, FOR MATS OF EARLYWOOD AND LATEWOOD
FIBER FRACTIONS AT $P_f = 10$ AND 90 cm H₂O

Mean Fiber Length, mm	$P_f = 10$ cm H ₂ O		$P_f = 90$ cm H ₂ O	
	$\frac{(d\bar{c}/dP_f)_1^a}{x 10^7 \text{ g/cm-dyne}}$	$\frac{(d\bar{c}/dP_f)_1^b}{x 10^7 \text{ g/cm-dyne}}$	$\frac{(d\bar{c}/dP_f)_1^a}{x 10^7 \text{ g/cm-dyne}}$	$\frac{(d\bar{c}/dP_f)_1^b}{x 10^7 \text{ g/cm-dyne}}$
<u>Earlywood</u>				
1.63	21.0	21.0	5.0	5.3
3.05	20.5	19.9	5.4	5.0
3.94	19.6	19.5	4.9	4.9
<u>Latewood</u>				
1.74	19.3	19.2	4.9	4.8
2.07	18.9	18.8	4.8	4.7
2.98	18.1	18.3	4.4	4.6
4.13	18.3	18.4	4.5	4.6

^aCalculated using \bar{N}_1 and \bar{M}_1 .

^bCalculated using \bar{N} and \bar{M} .

WET MAT DENSITY

The systematic correlation of wet mat density and the major morphological variations represented by differences in wall fraction of earlywood compared with latewood and mean fiber length is shown in the three dimensional diagram of Fig. 18. For clarification of trends, tabulated values are presented in Table X and agree with results found earlier for first compression of loblolly pine latewood (5). Mat densities and pressures are interpolated values based on \bar{N} and \bar{M} as in Table VIII. The computer program used to develop the three-dimensional plot is given in Appendix II.

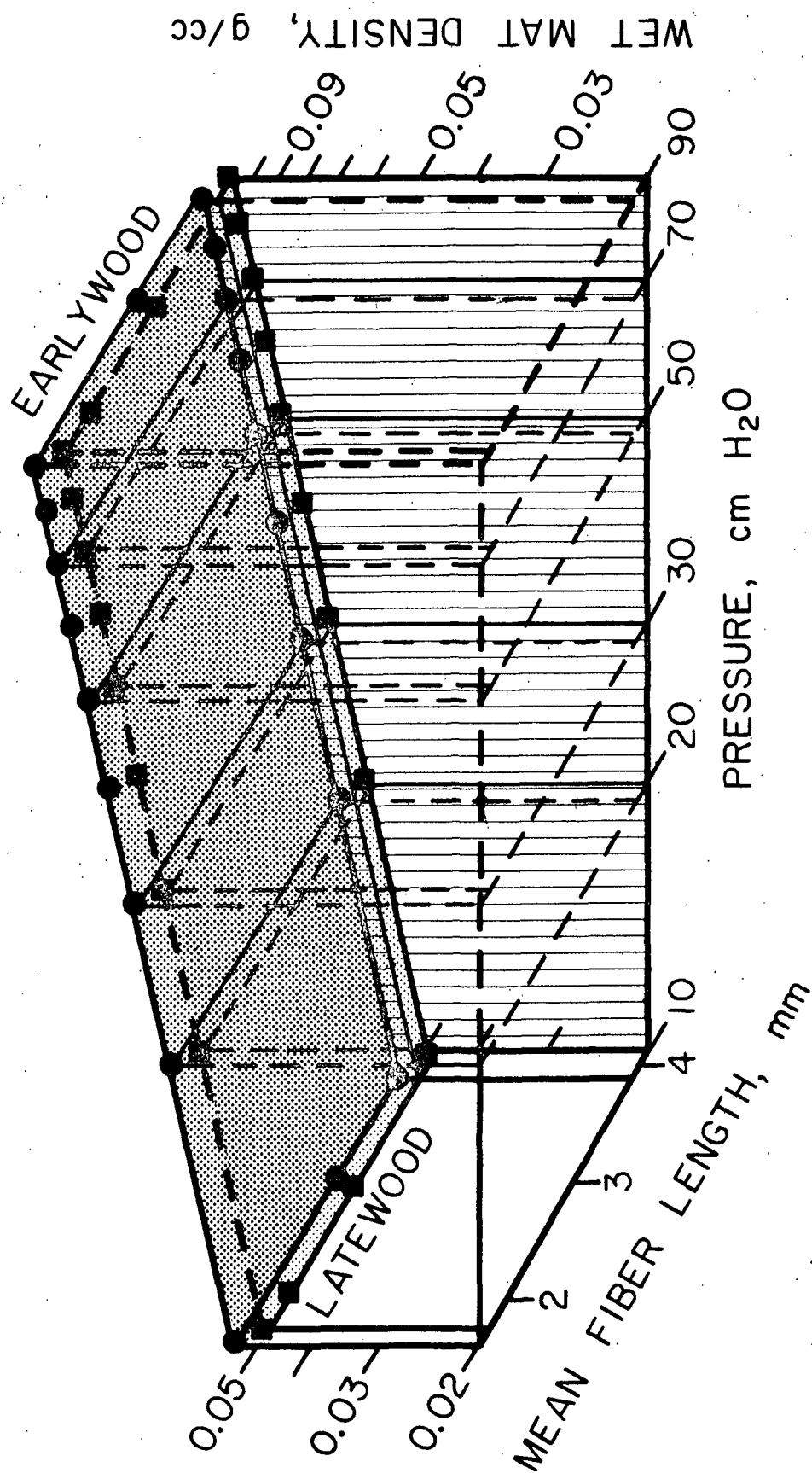


Figure 18. Log-log Plots of Interpolated Wet Mat Density vs. Pressure with Mean Fiber Length of Earlywood and Latewood Plotted Linearly on the z-Axis

TABLE X
INTERPOLATED WET MAT DENSITY,
G/CC

Pressure, cm H ₂ O	Earlywood Fiber Populations ^a			Latewood Fiber Populations ^a			
	1.63 mm	3.05 mm	3.94 mm	1.74 mm	2.07 mm	2.98 mm	4.13 mm
10	0.0552	0.0524	0.0512	0.0505	0.0493	0.0481	0.0484
20	0.0714	0.0679	0.0663	0.0655	0.0639	0.0623	0.0627
30	0.0831	0.0789	0.0771	0.0761	0.0743	0.0724	0.0729
40	0.0925	0.0879	0.0858	0.0848	0.0827	0.0864	0.0812
50	0.1006	0.0955	0.0933	0.0921	0.0899	0.0876	0.0882
60	0.1076	0.1022	0.0998	0.0986	0.0962	0.0938	0.0944
70	0.1140	0.1083	0.1057	0.1044	0.1019	0.0994	0.1000
80	0.1198	0.1138	0.1111	0.1098	0.1071	0.1044	0.1051
90	0.1252	0.1189	0.1161	0.1147	0.1119	0.1091	0.1098

^aMean fiber lengths.

The figure, although complex in appearance, is not difficult to analyze if one imagines it represents a box. Concentrating on the base of the box, the two horizontal lines (one in back and one in front) represent the pressure axis with pressure increasing from left to right as indicated. The two shorter lines forming the sides of the base are the fiber length axis with mean fiber length increasing from back to front. Wet mat density is represented by vertical distances from the base. Notice that wet mat density and pressure axes are logarithmic whereas the fiber length axis is linear.

Separation of the two planes is associated with wall fraction differences of earlywood compared to latewood (Table V), and reflects the ability of the more easily collapsible earlywood fibers to form mats of higher density. The planes are parallel because of the single value for N .

The trend of decreasing mat densities with increases in mean fiber length is shown by the tilting of the planes. Note that at all pressures in Fig. 18 or Table X, interpolated mat density is greater for smaller fibers, for which there are more fibers per gram (Table V). Probably greater density arises because smaller fibers cause a decrease in segment length, $\underline{L_s}$, and thus increase the number of contacts, $\underline{n_c}$, in the mat [Equation (6)].

The morphologically ranked \underline{M} values may be visualized as resulting from the extrapolation of the two planes in Fig. 18 to $\log \underline{P_f} = 0$ cm H₂O. But, if \underline{N} had not been smoothed, the calculated \underline{M} values would have been appreciably different as indicated in Table VIII.

CORRELATION OF \underline{M} AND FIBER DIMENSIONS

Latewood fibers with their characteristic high wall fraction and near circular cross section closely resemble the shape of the more intensively studied circular synthetic fiber systems. Therefore, a comparison of the mat density response to latewood fiber shape (length to diameter ratio, $\underline{L_f}/\underline{d_f}$) with that of a synthetic fiber system may indicate, at least partially, the extent to which the two systems are similar. Such a comparison is made in Fig. 19 between latewood fiber populations at $\underline{P_f} = 50$ and 90 cm H₂O and Nylon at $\underline{P_f} = 50$ and 100 cm H₂O.

The figure shows that the mat density response to $\underline{L_f}/\underline{d_f}$ for the two fiber systems is similar. Toward low axis ratios the curves for both latewood and Nylon fibers at comparable pressures begin to rise rapidly, while at high axis ratios the mat density appears to remain constant.

With \underline{N} constant for the fiber populations in this study, the effects of pressure may be eliminated from Fig. 19 by plotting fiber dimensions vs. compressibility constant \underline{M} . Figure 20 compares correlations of \underline{M} with $\underline{L_f}/\underline{d_f}$ as well

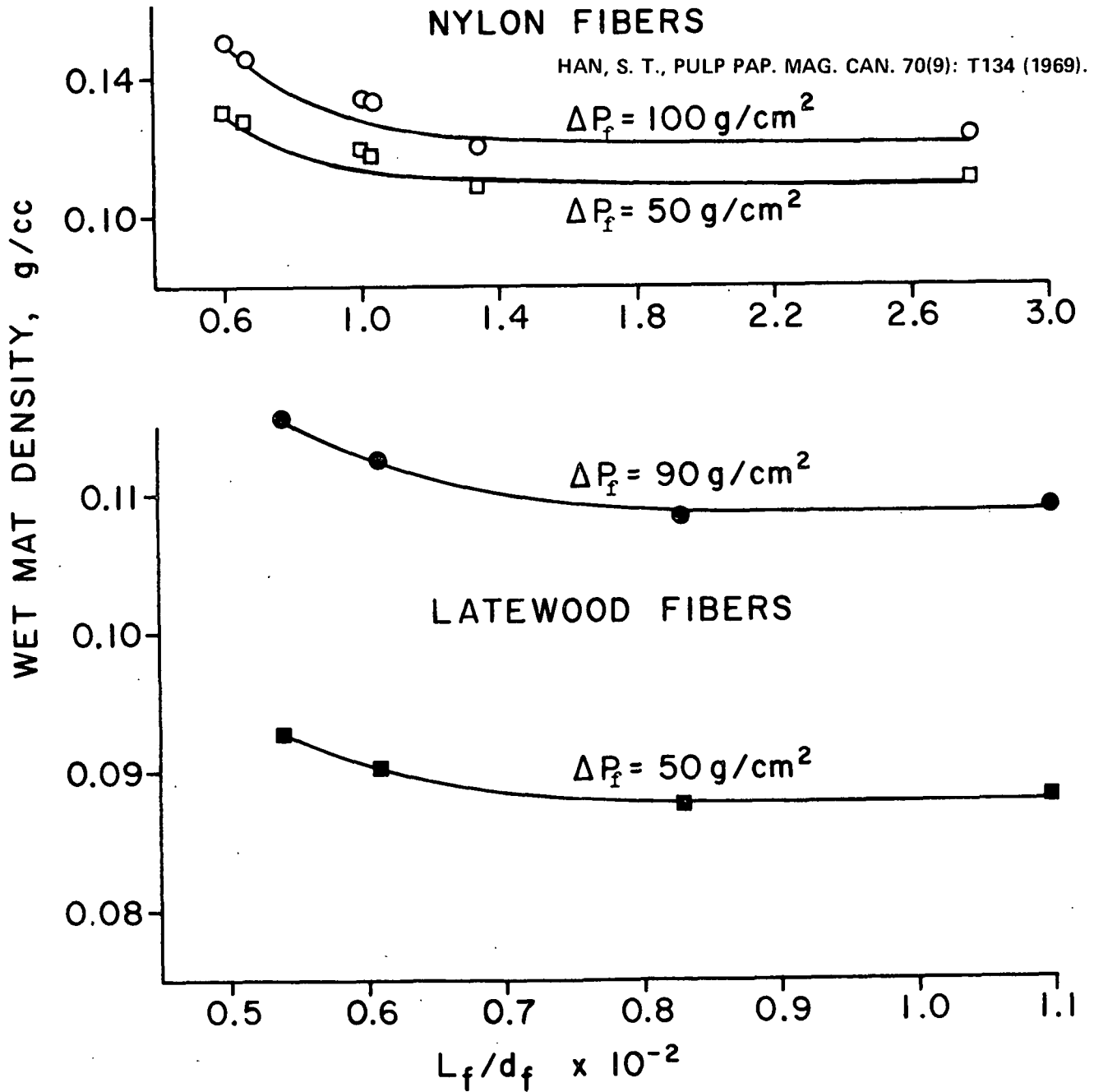


Figure 19. Comparison of Latewood to Nylon Fibers

as mean fiber length, \underline{L}_f , for earlywood and latewood fiber populations; and as anticipated the shape of the \underline{M} vs. $\underline{L}_f/\underline{d}_f$ curves are similar to that already discussed for Fig. 19. However, in Fig. 20, notice the comparable correlation of \underline{M} and \underline{L}_f . This is believed to result from the greater complexities of the natural fiber system in which variations in fiber diameter are biologically linked to changes in fiber length (Table V).

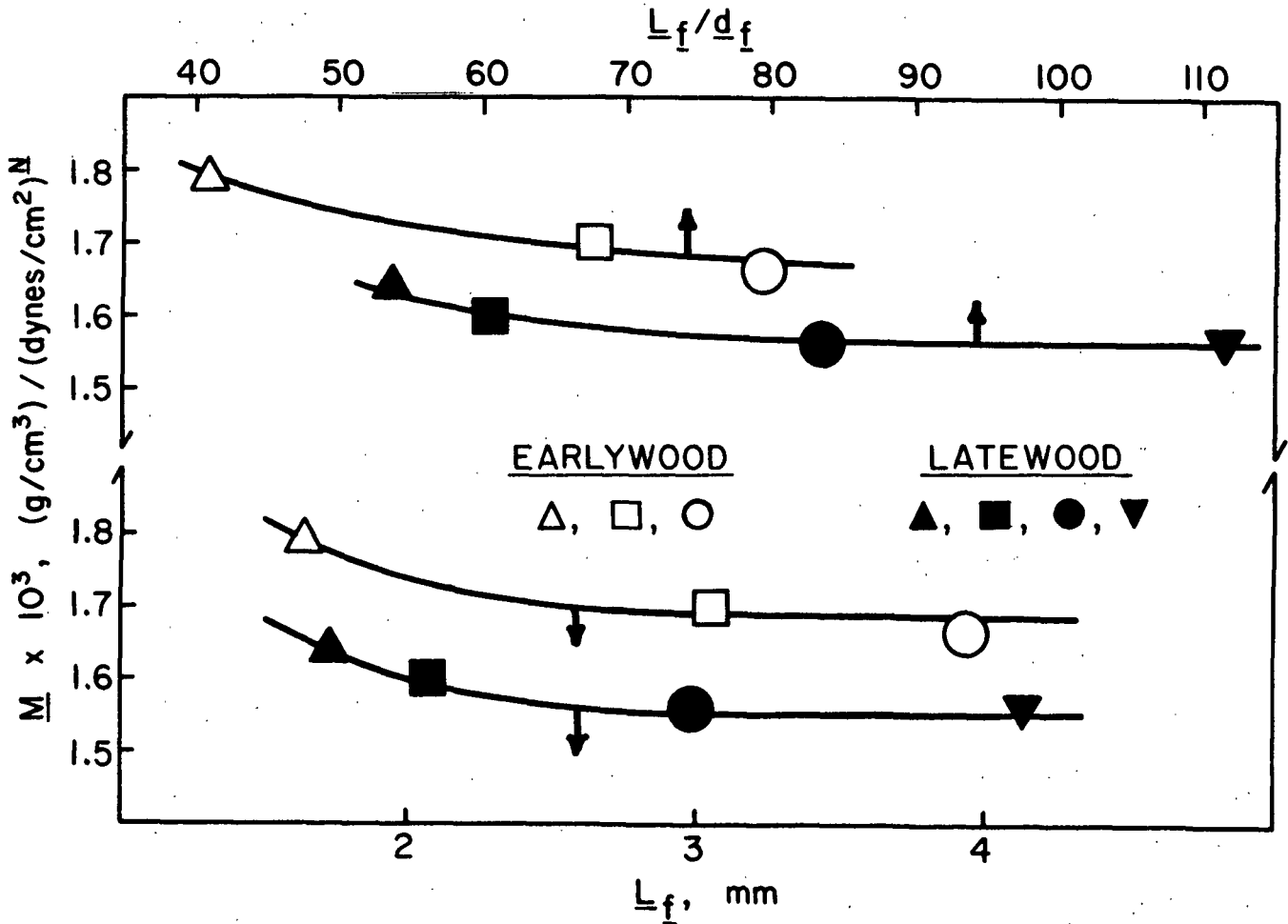


Figure 20. Compressibility Constant, \underline{M} , vs. Fiber Length to Fiber Diameter Ratio, $\underline{L}_f/\underline{d}_f$, (Upper Curves) and Fiber Length, \underline{L}_f , (Lower Curves)

As noted in development of Equation (18), the distance between points of contact in a fiber mat (segment length) is an important property of the mechanism of compressibility (9). The flat region of the curves in Fig. 20 corresponds to a condition in which the fiber length is sufficiently long so as to insure constant segment length. However, below a certain point, segment length will decrease with decreasing fiber length (6). Lower segment lengths cause higher mat density (9), and in this case the higher values of \underline{M} observed at low \underline{L}_f .

The separation of the curves for earlywood and latewood corresponds to differences in wall fraction, 32 vs. 66%, respectively. Using Equation (18) as a guide, this separation could be due to differences in \underline{d}_f , \underline{I} , and/or \underline{E} , since:

$$M \propto \left[\frac{\underline{d}_f^4}{\underline{E} \underline{I}} \right]^{1/3} \quad (39)$$

Attempts to correlate \underline{M} with \underline{d}_f and $(\underline{d}_f^4/\underline{I})^{1/3}$ failed to give meaningful results in agreement with studies by Jones (5) in which wet mat compression response was found to be independent of fiber diameter.

In view of the lack of correlation with \underline{d}_f and $(\underline{d}_f^4/\underline{I})^{1/3}$ in compressibility of wood pulp, it appears from Equation (39) that flexural rigidity (\underline{EI}) is the prominent fiber property contributing to the separation of the two curves in Fig. 20. In order to fully interpret flexural rigidity in terms of fiber dimensions, the moduli as well as the moment of the fibers must be known.

Wood pulp fibers are anisotropic, and the mechanism of bending, which is complex, involves more than a single modulus of the fiber wall. However, from the literature previously cited it is reasonable to expect that the elastic moduli for fiber bending would behave similarly to \underline{I}_F in Fig. 15. On this basis and Equation (39), \underline{M} would be expected to correlate with $(1/\underline{E} \underline{I}_F)^{1/3}$.

Since modulus values were not measured for the fiber populations studied, and cannot be quantified from the literature, a plot of \underline{M} vs. $(1/\underline{I}_F)^{1/3}$ is presented in Fig. 21.

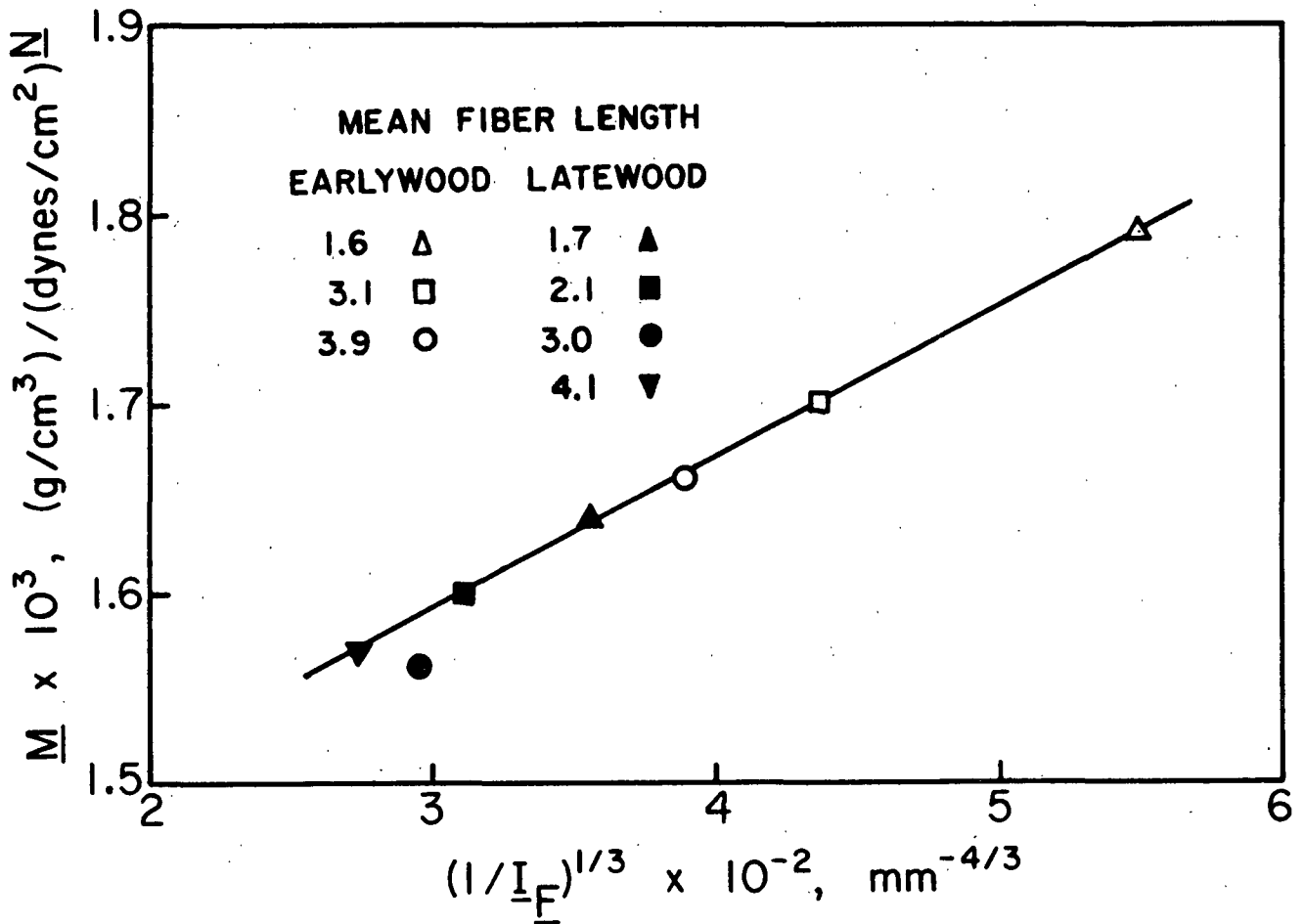


Figure 21. Plot of \underline{M} vs. $(1/\underline{I}_F)^{1/3}$ for Earlywood and Latewood Fiber Fractions

Amazingly, this figure reveals a straight line essentially connecting the seven fiber populations studied.*

* A constant area model based on the circular fiber model was also used to calculate \underline{I}_F . When plotted with \underline{M} a similar curve with a slight increase in the scatter of the data was obtained.

In view of the simplicity of the models involved, this result is quite significant; first, it supports bending as the dominant mechanism in compressibility of wood pulp; and second, it suggests that the wood pulp fiber is essentially flattened prior to bending. Since $\frac{I}{F}$ is predominantly a function of wall thickness [Equation (34)], it appears in a wood pulp fiber system that the relative compressibility of a wood pulp fiber mat is primarily influenced by fiber bending which in turn is governed by the thickness of the fiber walls, and to a lesser extent by the fiber diameter. These results do not imply, however, that modulus is not sharing at least an equally important role in the mechanism of wood pulp compressibility.

Not that decreases in \underline{M} in Fig. 21 also relate to an increase in mean fiber length (pyramids in circles) or earlywood and latewood (open and closed symbols, respectively). The relationship of \underline{M} with these morphological factors corresponds to observations on the increase in relative elastic modulus of earlywood and latewood in twenty successive growth rings of loblolly pine (13). Furthermore, this modulus for latewood was higher than that for earlywood by an amount about equal to the increase associated with growth. Growth, in turn, is accompanied by an increase in fiber length, with some trends toward increase in fiber width and wall thickness, particularly during the early decades of growth (21). Thus, the trend of changes in \underline{M} with changes in mean fiber length of earlywood and latewood tends to parallel previously reported changes in elastic modulus of earlywood and latewood in successive growth rings.

The observed correlation of \underline{M} with $(1/\frac{I}{F})^{1/3}$ also corresponds to high correlations of apparent axial modulus with fibril angle and fiber length (11,23,24). As longer fibers are formed during successive years of tree growth, fibril angle with respect to cell axis decreases [Equation (1)]; fiber axial modulus increases, and, on the basis of this study, \underline{M} decreases.

Differences in \bar{M} between the earlywood and latewood fiber fractions is also supported by elastic modulus data (10-12,14). Relatively large differences were observed between the axial modulus of latewood compared with earlywood and also in the collapse force of wet fibers. Differences in the transverse modulus between earlywood and latewood were not as great.

It may be interesting to notice that these differences between earlywood and latewood are visually supported by Fig. 22 which compares actual oven-dry samples of mats of comparable weight and mean fiber length previously subjected to compressibility experiments. The earlywood fiber mat is of significantly higher density than would be expected from Fig. 20. This is probably a result of the irreversible collapse and subsequent conformability of the earlywood fibers and subsequently less springback due to lower fiber stiffness.

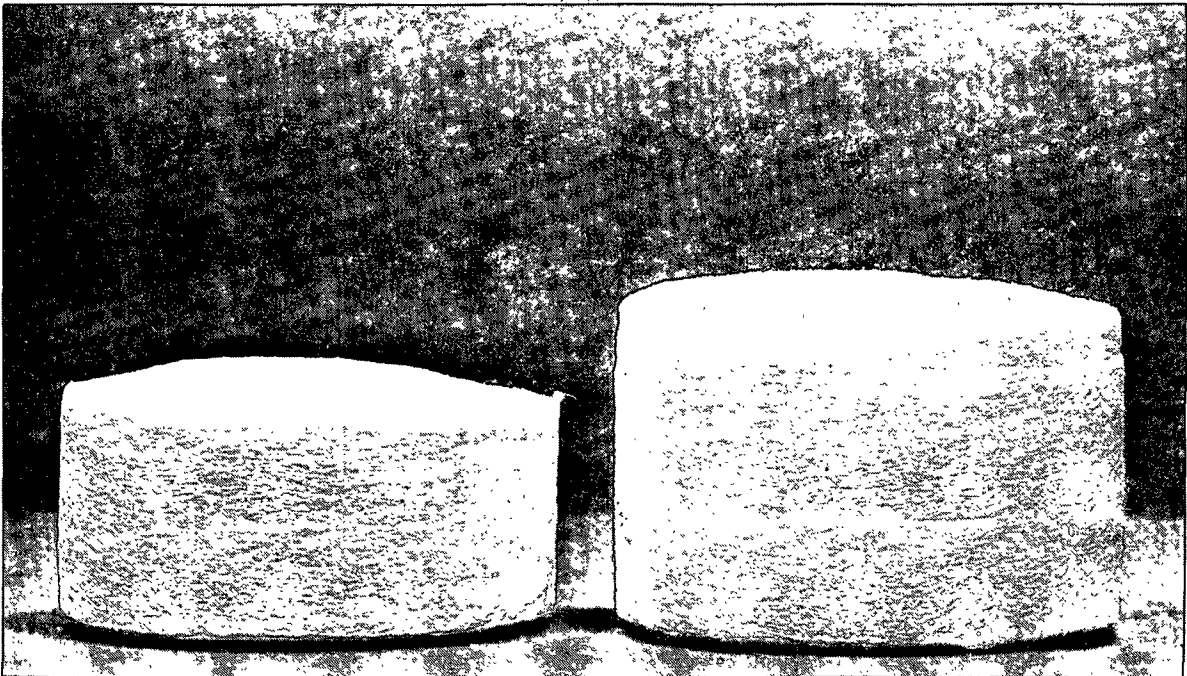


Figure 22. Comparison of 3.98 mm Earlywood (Left) and 4.13 mm Latewood Fiber Mats of Comparable Weight After Compressibility Experiments. Pad Diameters are Approximately 3 Inches

MATHEMATICAL PROCEDURE FOR DETERMINATION OF DERIVATIVES FROM CURVES OF EXPERIMENTAL DATA

During the course of data analysis, it is often desirable to fit a smooth curve as closely as possible to a set of experimental points. This is hand drawn (with a conventional French curve or similar aid). However, unless the curve is linear, the mathematical expression describing it is unknown.

One method of obtaining a mathematical expression to fit the data has been to use conventional statistical procedures. These procedures, based on least squares analysis, force the best linear, quadratic, cubic, or quartic expression to the experimental points. Unfortunately, plots of the experimental points and curves of the best fitting mathematical relationships are not always in close agreement over the entire range of data.

A review of the literature revealed that an equation of the form:

$$y = b_0 + b_1x^m + b_2x^n \quad (40)$$

has the capability of accurately fitting a wide variety of regularly curved plots of experimental data (55).

By combining the least squares approach used in conventional statistics with the versatile curve-fitting properties of Equation (40), a computerized method of accurately describing experimental data points mathematically was developed. This accurate mathematical description was easily differentiated, yielding a derivative of a curved plot of experimental data. Derivatives of this form were essential in solving many of the hydrodynamic equations.

LEAST SQUARES SOLUTION OF $y = b_0 + b_1x^m + b_2x^n$

The conventional least squares approach was used to fit experimental data to the form of Equation (40).

Let y_i = dependent variable and f_i = approximation to the dependent variable
 $= b_0 + b_1 x_i^m + b_2 x_i^n$. Then the square of the difference is:

$$\begin{aligned} S &= \sum \left[y_i - f_i \right]^2 \\ &= \sum \left[y_i^2 - 2b_0 y_i - 2b_1 x_i^m y_i - 2b_2 x_i^n y_i + b_0^2 + 2b_0 b_1 x_i^m + \right. \\ &\quad \left. 2b_0 b_2 x_i^n + b_1^2 x_i^{2m} + 2b_1 b_2 x_i^m x_i^n + b_2^2 x_i^{2n} \right] \end{aligned} \quad (41)$$

The conditions of a best fitting curve are achieved when S is minimized. This minimum occurs when the partial derivatives of S with respect to the five unknowns (b_0 , b_1 , b_2 , m , and n) in Equation (41) are zero. The result is the respective normalized Equations (42a) through (42e).

$$\sum y_i = Nb_0 + b_1 \sum x_i^m + b_2 \sum x_i^n \quad (42a)$$

$$\sum x_i^m y_i = b_0 \sum x_i^m + b_1 \sum x_i^{2m} + b_2 \sum x_i^m x_i^n \quad (42b)$$

$$\sum x_i^n y_i = b_0 \sum x_i^n + b_1 \sum x_i^m x_i^n + b_2 \sum x_i^{2n} \quad (42c)$$

$$\sum x_i^m y_i \ln(x_i) = b_0 \sum x_i^m \ln(x_i) + b_1 \sum x_i^{2m} \ln(x_i) + b_2 \sum x_i^m x_i^n \ln(x_i) \quad (42d)$$

$$\sum x_i^n y_i \ln(x_i) = b_0 \sum x_i^n \ln(x_i) + b_1 \sum x_i^m x_i^n \ln(x_i) + b_2 \sum x_i^{2n} \ln(x_i) \quad (42e)$$

To obtain values of b_0 , b_1 , b_2 , m , and n , this nonlinear system of normalized equations was solved simultaneously. The procedure used has been presented by Nelson (56), and the mathematical method employed is based on the truncation of a Taylor's expression. The procedure is detailed below.

Let the five normal equations be respectively represented by Equations (43a) through (43e):

$$F(b_0, b_1, b_2, m, n) = 0 \quad (43a)$$

$$G(b_0, b_1, b_2, m, n) = 0 \quad (43b)$$

$$H(b_0, b_1, b_2, m, n) = 0 \quad (43c)$$

$$I(b_0, b_1, b_2, m, n) = 0 \quad (43d)$$

$$J(b_0, b_1, b_2, m, n) = 0 \quad (43e)$$

Then let

$$f_1 = \frac{\partial F}{\partial b_0} = N$$

$$f_2 = \frac{\partial F}{\partial b_1} = \sum x_i^m$$

$$f_3 = \frac{\partial F}{\partial b_2} = \sum x_i^n$$

$$f_4 = \frac{\partial F}{\partial m} = b_1 \sum x_i^m \ln(x_i)$$

$$f_5 = \frac{\partial F}{\partial n} = b_2 \sum x_i^n \ln(x_i)$$

$$g_1 = \frac{\partial G}{\partial b_0} = \sum x_i^m$$

$$g_2 = \frac{\partial G}{\partial b_1} = \sum x_i^{2m}$$

$$g_3 = \frac{\partial G}{\partial b_2} = \sum x_i^m x_i^n$$

$$g_4 = \frac{\partial G}{\partial m} = b_0 \sum x_i^m \ln(x_i) + 2b_1 \sum x_i^{2m} \ln(x_i) +$$

$$b_2 \sum x_i^m x_i^n \ln(x_i) - \sum x_i^m y_i \ln(x_i)$$

$$g_5 = \frac{\partial G}{\partial n} = b_2 \sum x_i^m x_i^n \ln(x_i)$$

$$h_1 = \frac{\partial H}{\partial b_0} = \sum x_i^n$$

$$h_2 = \frac{\partial H}{\partial b_1} = \sum x_i^m x_i^n$$

$$h_3 = \frac{\partial H}{\partial b_2} = \sum x_i^{2n}$$

$$h_4 = \frac{\partial H}{\partial m} = \sum x_i^m x_i^n \ln(x_i)$$

$$h_5 = \frac{\partial H}{\partial n} = b_0 \sum x_i^n \ln(x_i) + b_1 \sum x_i^m x_i^n \ln(x_i) + \\ 2b_2 \sum x_i^{2n} \ln(x_i) - \sum x_i^n y_i \ln(x_i)$$

$$i_1 = \frac{\partial I}{\partial b_0} = \sum x_i^m \ln(x_i)$$

$$i_2 = \frac{\partial I}{\partial b_1} = \sum x_i^{2m} \ln(x_i)$$

$$i_3 = \frac{\partial I}{\partial b_2} = \sum x_i^m x_i^n \ln(x_i)$$

$$i_4 = \frac{\partial I}{\partial m} = b_0 \sum x_i^m [\ln(x_i)]^2 + 2b_1 \sum x_i^{2m} [\ln(x_i)]^2 + \\ b_2 \sum x_i^m x_i^n [\ln(x_i)]^2 - \sum x_i^m y_i [\ln(x_i)]^2$$

$$i_5 = \frac{\partial I}{\partial n} = b_2 \sum x_i^m x_i^n [\ln(x_i)]^2$$

$$j_1 = \frac{\partial J}{\partial b_0} = \sum x_i^n \ln(x_i)$$

$$j_2 = \frac{\partial J}{\partial b_1} = \sum x_i^m x_i^n \ln(x_i)$$

$$j_3 = \frac{\partial J}{\partial b_2} = \sum x_i^{2n} \ln(x_i)$$

$$j_4 = \frac{\partial J}{\partial m} = b_1 \sum x_i^m x_i^n [\ln(x_i)]^2$$

$$j_5 = \frac{\partial J}{\partial n} = b_0 \sum x_i^n [\ln(x_i)]^2 + b_1 \sum x_i^m x_i^n [\ln(x_i)]^2 + \\ 2b_2 \sum x_i^{2n} [\ln(x_i)]^2 - \sum x_i^n y_i [\ln(x_i)]^2$$

and let the displacements be defined as:

$$\delta b_0 = b_0 - \overline{b_0}$$

$$\delta b_1 = b_1 - \overline{b_1}$$

$$\delta b_2 = b_2 - \overline{b_2}$$

$$\delta m = m - \overline{m}$$

$$\delta n = n - \overline{n}$$

where $\overline{b_0}$, $\overline{b_1}$, $\overline{b_2}$, \overline{m} , and \overline{n} represent arbitrary first estimates of b_0 , b_1 , b_2 , m , and n , respectively.

A truncation of Taylor's theorem can then be applied to yield the following linearized equations:

$$f_1 \delta b_0 + f_2 \delta b_1 + f_3 \delta b_2 + f_4 \delta m + f_5 \delta n = - F(\overline{b_0}, \overline{b_1}, \overline{b_2}, \overline{m}, \overline{n}) \quad (44a)$$

$$g_1 \delta b_0 + g_2 \delta b_1 + g_3 \delta b_2 + g_4 \delta m + g_5 \delta n = - G(\overline{b_0}, \overline{b_1}, \overline{b_2}, \overline{m}, \overline{n}) \quad (44b)$$

$$h_1 \delta b_0 + h_2 \delta b_1 + h_3 \delta b_2 + h_4 \delta m + h_5 \delta n = - H(\overline{b_0}, \overline{b_1}, \overline{b_2}, \overline{m}, \overline{n}) \quad (44c)$$

$$i_1 \delta b_0 + i_2 \delta b_1 + i_3 \delta b_2 + i_4 \delta m + i_5 \delta n = - I(\overline{b_0}, \overline{b_1}, \overline{b_2}, \overline{m}, \overline{n}) \quad (44d)$$

$$j_1 \delta b_0 + j_2 \delta b_1 + j_3 \delta b_2 + j_4 \delta m + j_5 \delta n = - J(\overline{b_0}, \overline{b_1}, \overline{b_2}, \overline{m}, \overline{n}) \quad (44e)$$

Using Gaussian elimination, Equations (44a) through (44e) can be solved simultaneously for b_0 , b_1 , b_2 , m and n . The displacements are then calculated, respectively added to the initial estimates ($\overline{b_0}$, $\overline{b_1}$, $\overline{b_2}$, \overline{m} , and \overline{n}) to form a revised estimate, and the equations resolved. Values for b_0 , b_1 , b_2 , m , and n are obtained when the displacements become negligible.

COMPUTER PROGRAM

This numerical procedure has been incorporated into the computer program used to calculate local specific filtration resistance (next section) and is presented in its entirety in Appendix III. As written, the program requires the user to

estimate initial values of b_0 , b_1 , b_2 , m , and n . Initial estimates of b_0 , b_1 , and b_2 are relatively unimportant and may be assigned a value of 1.0. Initial estimates of m and n , however, are important. The number of iterations, and subsequently the time required for program execution, is greatly reduced if estimates of m and n are close to solution values.

More than one combination of values for b_0 , b_1 , b_2 , m , and n will satisfy the conditions for a solution. Therefore, the user must be cautious in using the accurate mathematical description of his data derived from this program in the development of theories.

If desired, output is computed which can be plotted. A plotting program used to plot the output is listed in Appendix IV.

The use of the program is exemplified in the sections on filtration resistance.

FIBER MORPHOLOGY AND SPECIFIC FILTRATION RESISTANCE

Specific filtration resistance obtained from constant rate filtration experiments may be calculated for either average, $\langle R \rangle$, or local, R , values by using Equations (23) or (22), respectively. The physical difference between these two values is that $\langle R \rangle$ represents an average filtration resistance for the whole mat during formation, whereas R represents the filtration resistance of a small but measurable section immediately above the septum. Since there is a pressure gradient throughout the mat (caused by the frictional force of the water as it flows around the fibers), $\langle R \rangle$ may be considered related to this gradient, whereas R is more closely related to the actual pressure drop measured.

Values for $\langle R \rangle$ and R were calculated for various pressures from averaged pressure vs. time data using the computer program listed in Appendix V; the

output for earlywood, latewood, and whole pulp fiber populations is presented in Appendix VI. Values are lower than those reported by other researchers for unbeaten softwood pulps (16,29) due to the lack of fines and fibrillations in the fiber systems.

AVERAGE SPECIFIC FILTRATION RESISTANCE

The systematic correlation of average specific filtration resistance and the major morphological variations represented by differences in wall fraction of earlywood compared with latewood and mean fiber length is shown in Fig. 23. Values are based on at least triplicate runs for each of the fiber fractions and the 95% confidence limits were ± 2 to 8.5% of the means ($\Delta P_f = 50$ cm H₂O) which ranked from 6.80×10^6 cm/g for the longest latewood fibers to 30.48×10^6 cm/g for the shortest earlywood (Appendix VI). It is evident from the figure that at a given pressure, populations of thin-walled earlywood fibers (top plane) attain higher $\langle R \rangle$ values at pressure drops between 10 and 90 cm H₂O than do the populations of thick-walled latewood fibers of comparable length, and, $\langle R \rangle$ increases as fiber length decreases for either earlywood or latewood fiber populations. Values for whole pulp data which are not displayed but may be obtained from Appendix VI fall between the earlywood and latewood planes, and analysis has shown that the higher percentage of latewood observed in the whole pulp (Table III) is reflected in the proximity of the whole pulp values to those of latewood.

These changes in average filtration resistance with fiber morphology may best be explained by qualitative analysis of the geometry of the fibers. Slight rearrangement of Equation (29) results in an expression for $\langle R \rangle$ in terms of its components, average specific surface, $\langle S_w \rangle$, and average specific volume, $\langle v \rangle$, as well as mat density, ρ :

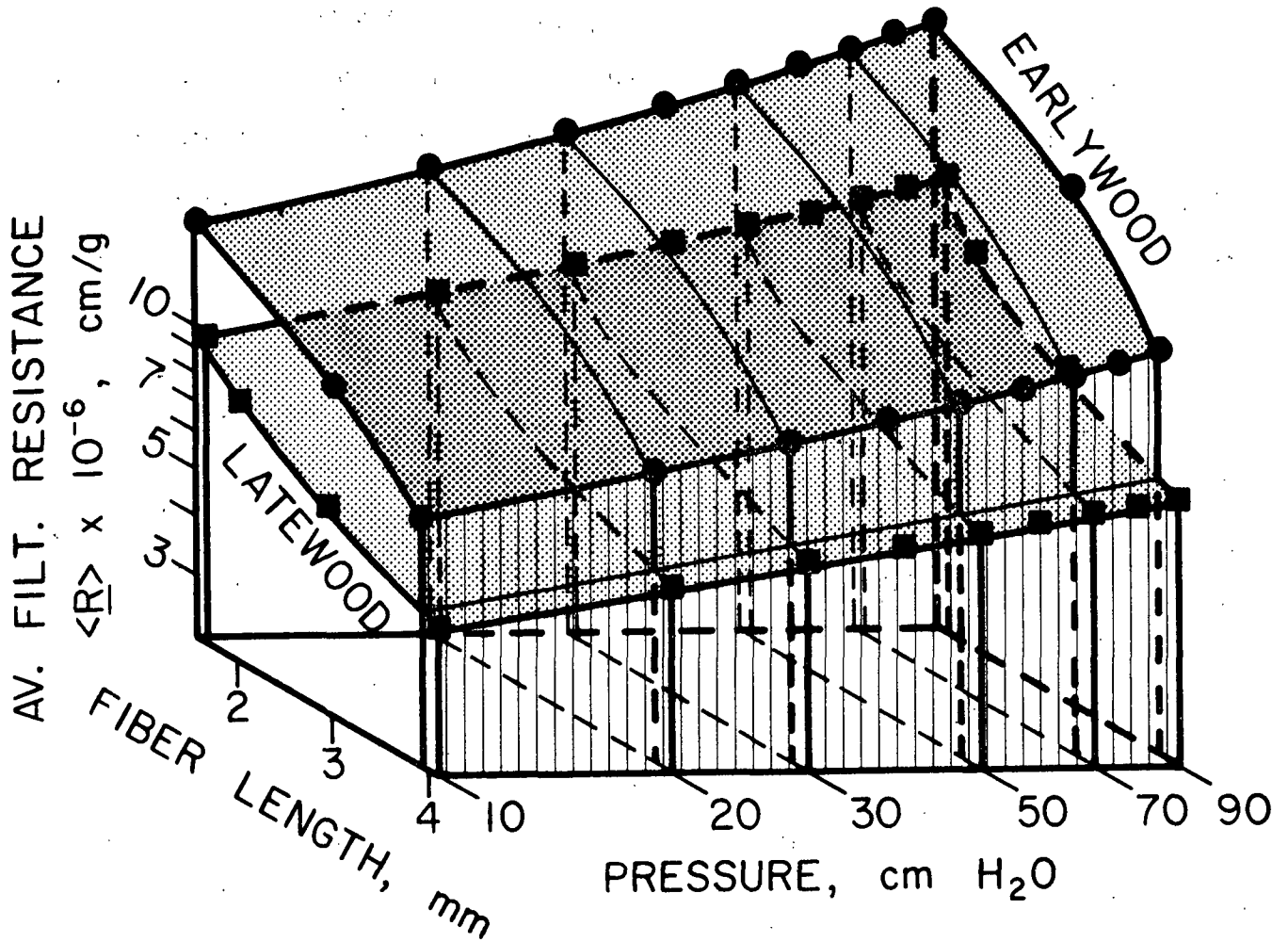


Figure 23. Log-log Plots of Average Specific Filtration Resistance vs. Pressure with Mean Fiber Length of Earlywood and Latewood Plotted Linearly on the z-Axis

$$\langle R \rangle = \langle S_W \rangle^2 \left\{ \frac{3.5 (1-N/2) c^{1/2}}{\langle v \rangle^{1/2}} [1 + 57 \langle v \rangle^3 (1-N/2)^6 c^3] \right\} \quad (45)$$

From Equation (45), $\langle R \rangle$ is observed to be proportional to $\langle S_W \rangle^2$ (a point discussed in detail in a later section). Table VII has already shown that the geometric surface to mass ratio, \underline{S}_{WG} , increases significantly as fiber length decreases. The corresponding increase in $\langle R \rangle$ is in accord with this finding.

The data presented in Table V show that the thinner-walled earlywood fiber populations are composed of fibers of greater width and generally lower mass than latewood fibers of comparable length. Thus, higher geometric surface to mass

ratios are expected for the earlywood fiber populations, and on this basis so are the higher values for $\langle R \rangle$. Qualitatively, this comparison may be visualized from Fig. 24 which compares identically formed handsheets of longest and shortest earlywood and latewood fiber fractions. By observation, fiber surface area per unit of mat exposed to fluid flow is highest for the 1.63 mm earlywood and lowest for the 4.13 mm latewood fibers.

The increase in $\langle R \rangle$ with increasing pressure drop also varies significantly, the greatest percent increase being for the smallest earlywood fibers. This variation in $\langle R \rangle$ with pressure is about comparable, on a percentage change basis, to those trends observed for wet mat density. However, the change in $\langle R \rangle$ with fiber length is much greater than the change found for c . This means that in a comparison of mats of constant density and varying fiber morphology, as in Table XI, about four times the filtration resistance for the shortest earlywood fibers occurs at a lower pressure compared to that of the longest latewood fibers.

LOCAL SPECIFIC FILTRATION RESISTANCE

Accurate calculation of local specific filtration resistance, R , results from the mathematical procedure for determining the derivative, dP_f/dt , using Equation (40). The precision with which Equation (40) fits the data is exemplified in the average pressure vs. time plots for earlywood, latewood, and whole pulp fiber populations shown in Fig. 25, 26, and 27, respectively. The empirical constants, b_0 , b_1 , b_2 , m , and n , which were statistically derived for each set of data are summarized in Table XII.

The effects of fiber morphological variation and pressure drop on R are shown in Fig. 28. Trends are similar to those previously described for average filtration resistance (Fig. 23); i.e., for a given pressure, thin-walled earlywood fibers (top plane) attain higher R values at pressure drops between 10 and

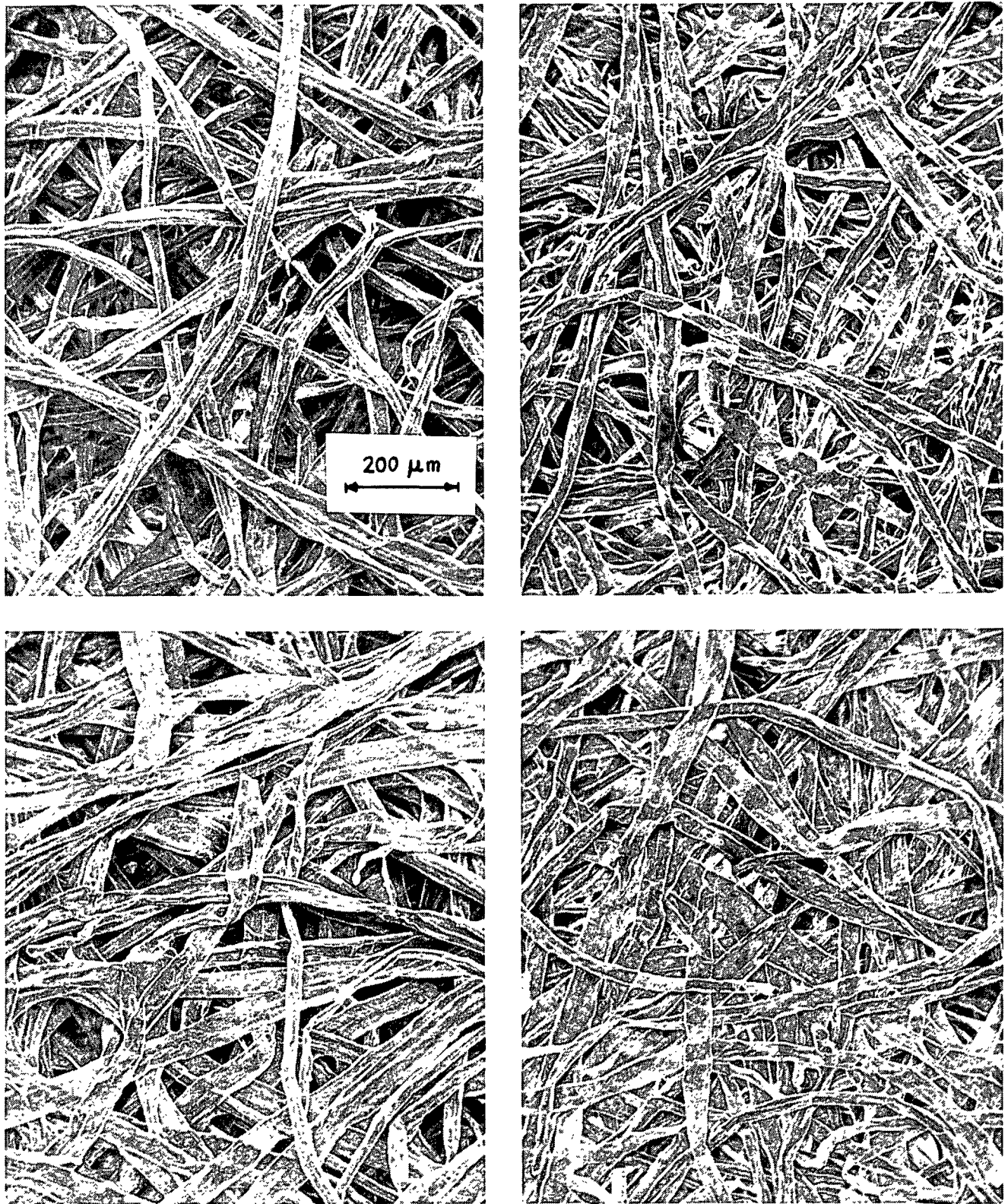


Figure 24. Scanning Electron Micrographs of 1.6 g Handsheets Wet Pressed to 50 psig of 4.13 mm Latewood (Upper Left), 1.74 mm Latewood (Upper Right), 3.94 mm Earlywood (Lower Left), and 1.63 mm Earlywood Fibers (Lower Right)

90 cm H₂O than do populations of thick-walled latewood fibers of comparable length, and \bar{R} increases as fiber length decreases for both fiber populations. Once again, whole pulp data (Appendix VI) falls between the earlywood and latewood planes.

TABLE XI

COMPARISON OF FIBER MORPHOLOGY AND FILTRATION RESISTANCE
AT CONSTANT MAT DENSITY ($\underline{c} = 0.10 \text{ g/cm}^3$)

Mean Fiber Length, mm	ΔP_f^a , cm H ₂ O	$\langle \bar{R} \rangle \times 10^{-6}$, cm/g	$\langle \bar{R} \rangle / \Delta P_f$, cm ³ /(g-dynes)
<u>Earlywood</u>			
1.63	49.1	30.2	627
3.05	56.2	21.4	388
3.94	60.2	13.1	222
<u>Latewood</u>			
1.74	61.5	17.1	284
2.07	66.3	13.5	208
2.98	70.7	10.3	149
4.13	70.1	7.4	108
<u>Whole Pulp</u>			
1.49	63.8	22.7	363
2.76	74.7	13.7	187
3.88	71.0	9.4	135
Not class.	74.3	18.0	247

^aCalculated from $\underline{c} = \frac{N}{M \Delta P_f}$.

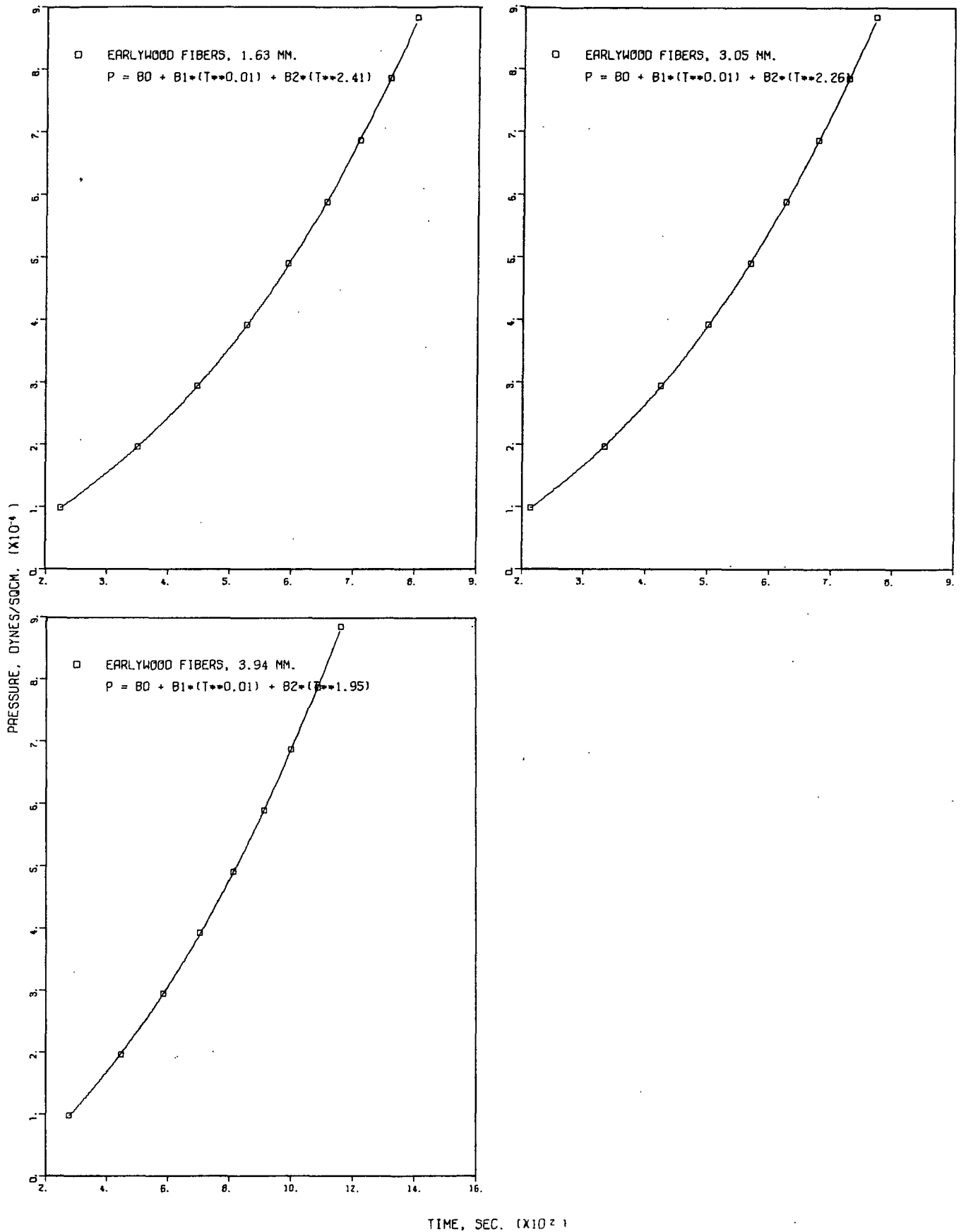


Figure 25. Averaged Pressure, ΔP_f , vs. Time, t , Data for Earlywood Fiber Populations Fitted with a Curve of the Form

$$\Delta P_f = b_0 + b_1 t^m + b_2 t^n$$

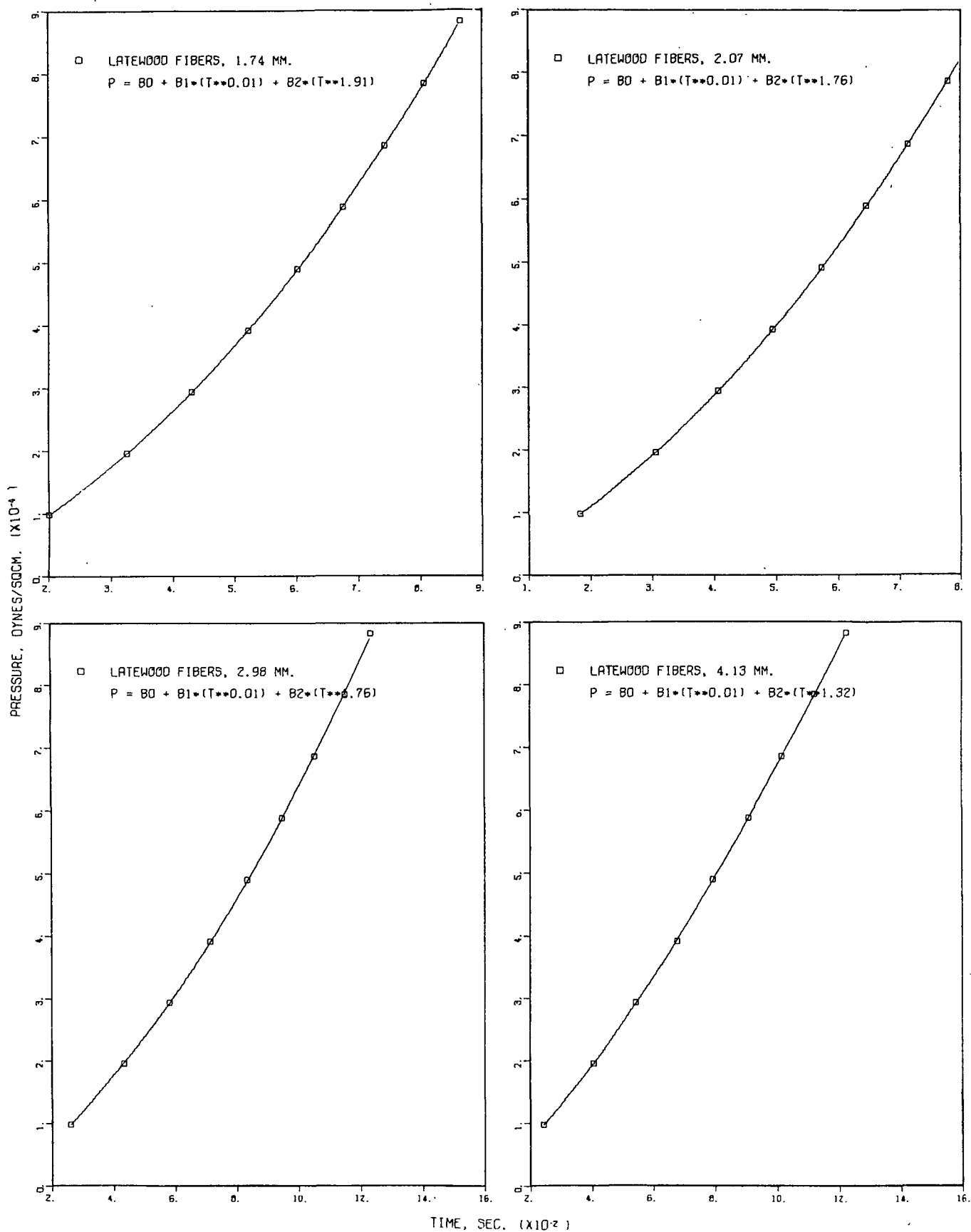


Figure 26. Averaged Pressure, ΔP_f , vs. Time, t , Data for Latewood Fiber Populations Fitted with a Curve of the Form

$$\Delta P_f = b_0 + b_1 t^m + b_2 t^n$$

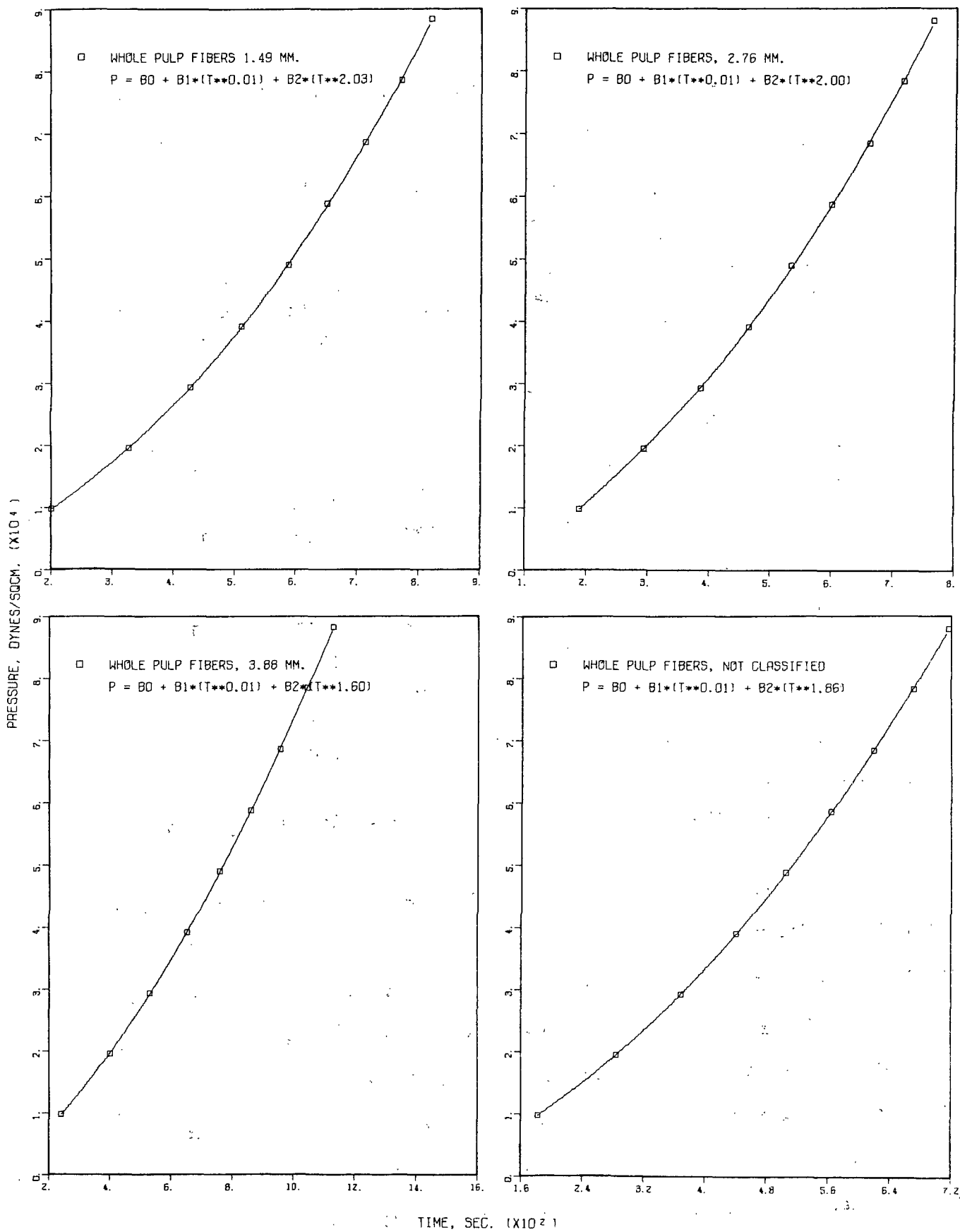


Figure 27. Averaged Pressure, ΔP_f , vs. Time, t , Data for Whole Pulp Fiber Populations Fitted with a Curve of the Form

$$\Delta P_f = b_0 + b_1 t^m + b_2 t^n$$

TABLE XII
EMPIRICAL CONSTANTS USED IN FILTRATION ANALYSIS^a

Fiber Length	b_0	b_1	b_2	m	n
<u>Earlywood</u>					
1.63	-777440	742610	0.0074	0.01	2.41
3.05	-641980	613810	0.0219	0.01	2.26
3.94	-637350	607420	0.0758	0.01	1.95
<u>Latewood</u>					
1.74	-561620	537580	0.1896	0.01	1.91
2.07	-394920	379010	0.5700	0.01	1.76
2.98	-584210	557390	0.2644	0.01	1.76
4.13	132160	-126080	7.6378	0.01	1.32
<u>Whole Pulp</u>					
1.49	-511760	490500	0.0927	0.01	2.03
2.76	-789060	753910	0.1245	0.01	2.00
3.88	-230480	220940	1.0664	0.01	1.60
Not class. cross	-408810	391560	0.3787	0.01	1.86

$$^a \Delta \underline{P}_f = \underline{b}_0 + \underline{b}_1 \underline{t}^{\underline{m}} + \underline{b}_2 \underline{t}^{\underline{n}}, \text{ where } \Delta \underline{P}_f = \text{pressure drop and } \underline{t} = \text{time.}$$

Although variations in \underline{R} with morphology are similar to those previously described for $\langle \underline{R} \rangle$, variations in \underline{R} with pressure are significantly different. Comparison of Fig. 23 and 28 reveal that at all pressures in the range studied, \underline{R} is greater than $\langle \underline{R} \rangle$, and the difference between these filtration resistance values increases with increasing pressure. Both figures show the increase in filtration resistance with pressure is greater for earlywood (in comparison to latewood fibers of comparable length) and short fibers (in comparison within sets), with the greatest increase being for the 1.63-mm earlywood fiber population;

however, these increases are much more pronounced in values for \underline{R} where pressure effects are localized and not averaged throughout the mat.

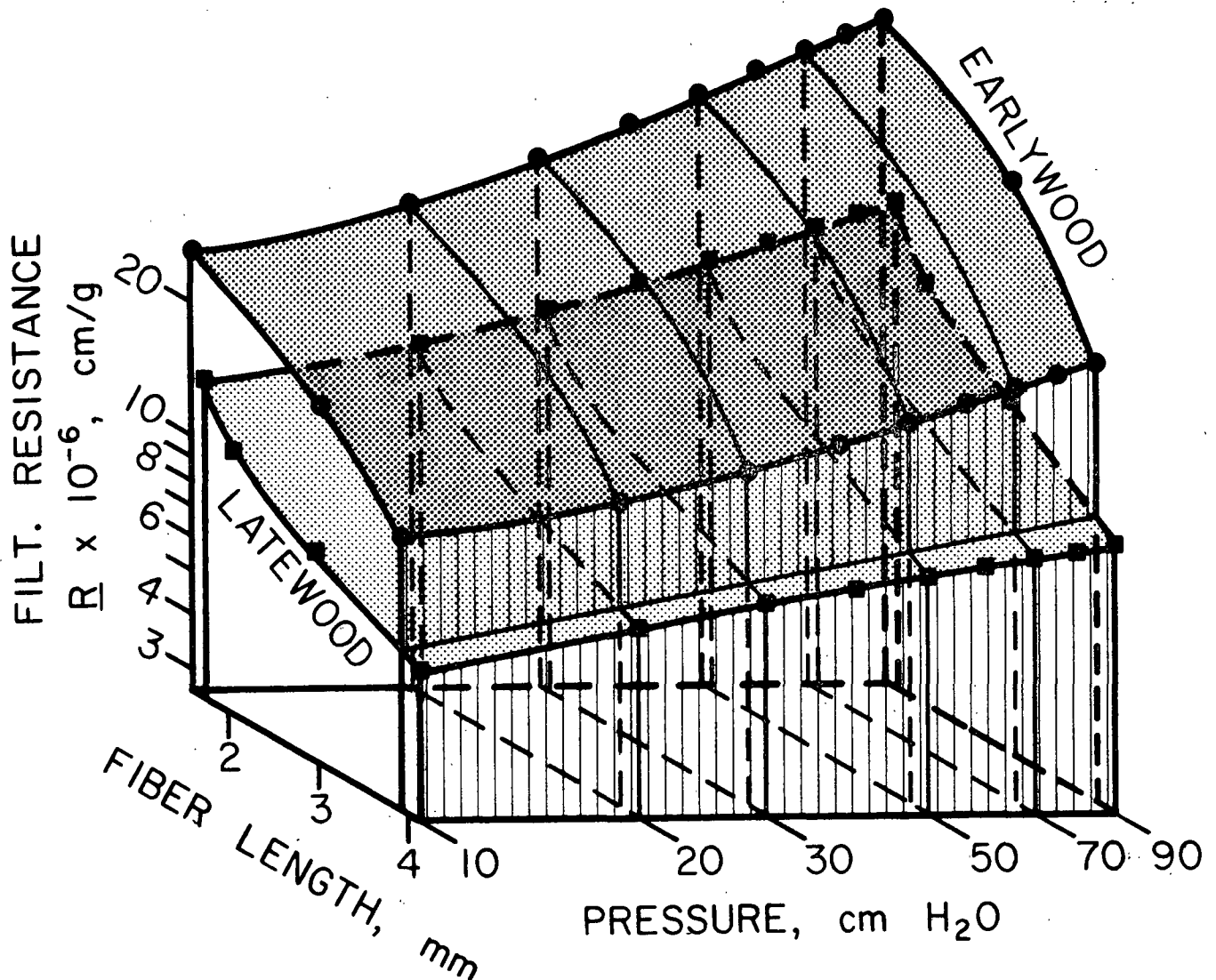


Figure 28. Log-log Plots of Local Specific Filtration Resistance vs. Pressure with Mean Fiber Length of Earlywood and Latewood Plotted Linearly on the z-Axis

FEASIBILITY OF DETERMINING \underline{S}_w AND \underline{v} AS FUNCTIONS OF PRESSURE

In the review section on hydrodynamic evaluation of pulp, Equation (29) was developed; it is generally used to calculate the average hydrodynamic specific surface and swollen volume. The solution procedure involves rectification (linear

interpretation) of a curved plot of $\Delta P_f / (c^{1/2} t)$ vs. c^3 . However, this procedure has been questioned (57), and as an alternative, Meyer (41) presented a procedure for determining $\langle v \rangle$ and $\langle S_w \rangle$ from Equation (29) which recognizes the physical phenomena of fiber deswelling with pressure. When the plot of $\Delta P_f / (c^{1/2} t)$ vs. c^3 was analyzed over narrow ranges of c^3 with the aid of Lagrange interpolation, values of $\langle v \rangle$ were observed to decrease with increasing pressure whereas $\langle S_w \rangle$ slightly increased (41,58).

As a second alternative, Meyer (42) solved Equation (19) in terms of pressure changes within a permeated mat, thereby establishing a means of eliminating the objectionable integration process in which S_w and v must be assumed constant. Equation (46) is the resulting equation in rectified form:

$$F = S_w^2 v^{-1/2} (1 + 57 v^3 X) \quad (46)$$

where F and X represent complex functions of experimentally measureable quantities involving pressure and mat density (45). A second equation was obtained by some authors (45,59) by taking the derivative of F with respect to X . In doing so it was assumed that S_w and v were insensitive to pressure over very narrow ranges. Accordingly, dS_w/dX and dv/dX were taken as zero and the resulting equations solved with the aid of quadratic smoothing. It was later recognized by the authors that the method was invalid (60), and the work was discontinued.

The advantage of these procedures was that they recognized the pressure dependence of S_w and v brought about through fiber conformability and deswelling. Their major drawback, however, was the inherent assumptions which cannot be justified but are necessary for solution. This section briefly describes refinements developed to improve these calculation procedures, analyzes the inherent assumptions involved in their calculation, and thus presents the basis for rejecting them in favor of adopting the method presented by Ingmanson and Andrews (40) for determining average values of specific surface and volume.

REFINEMENT OF CALCULATION PROCEDURES

As mentioned above, the curved plots of $\Delta P_f / (c^{1/2} t)$ vs. c^3 from Equation (29) and F vs. X from Equation (46) were analyzed using Lagrange interpolation and quadratic smoothing to determine values of specific surface and swollen volume as functions of pressure. Both of these procedures, however, are cumbersome. Prior to the realization that these procedures do not yield meaningful results, they were refined using the procedure for numerical differentiation presented earlier. Through computerization of these refined solution procedures for Equations (29) and (46), values of specific surface and swollen volume were obtained as functions of pressure which were in qualitative agreement with those presented previously (41,45,58,59). The computer programs describing the calculation procedure are presented with the results in Appendices VII and VIII, respectively.

ANALYSIS OF ASSUMPTION IN DETERMINING S_w AND v AS FUNCTIONS OF PRESSURE

The above methods of analyzing filtration and permeation data were once considered the best procedures for determining S_w and v for wood pulp fiber systems. But recently, Grace (61) and Nelson (53) have criticized the procedure involving constant rate filtration on the basis that it involved an unjustifiable assumption which had no physical significance. The assumption results from solving one basic equation containing two unknowns without additional information. The permeation procedure which also solves one equation with two unknowns is subject to a similar assumption. The mathematical argument leading to the exposure of the filtration assumption is presented in Appendix IX.

Clearly then, in order to establish the dependence of S_w and v on pressure, a second independent relationship is needed. Such a relationship is not now

available. Therefore, the procedure presented by Ingmanson and Andrews (40) which determines a single average value for surface and swollen volume from constant rate filtration and compressibility data was adopted for this study.

As already mentioned, this procedure involves drawing the best straight line through a curved plot of $\Delta P_f / (c^{1/2} t)$ vs. c^3 as shown in Fig. 29. Values for $\langle S_w \rangle$ were observed to be relatively insensitive to the exact positioning of this line. Variations observed were insignificant compared with changes in $\langle S_w \rangle$ between the fiber populations isolated. However, values for $\langle v \rangle$ were observed to be very sensitive to positioning of the best fit line.

To ensure unbiased results, linear regression was used to position the best straight line through the data for values of c^3 corresponding to $\Delta P_f = 50$ to 90 cm H₂O (Fig. 29). This pressure range corresponds to the approximately linear portion of the data.

Changes in $\langle S_w \rangle$ and $\langle v \rangle$ with wall fraction and fiber length using this calculation procedure are presented in the next section.

FIBER MORPHOLOGY AND AVERAGE SPECIFIC SURFACE AND VOLUME

Average specific surface, $\langle S_w \rangle$, and average specific volume, $\langle v \rangle$, were determined by graphical solution of Equation (29) involving linear regression of a plot of $\Delta P_f / (c^{1/2} t)$ vs. c^3 from $\Delta P_f = 50$ to 90 cm H₂O, utilizing filtration resistance and compressibility data. Details of the solution procedure are presented in the computer program of Appendix V. Results are included in Appendix VI and Table XIII.

Values for $\langle S_w \rangle$ are slightly lower than those reported previously for unbeaten bleached southern pine kraft (31). The difference is attributed to the lack of

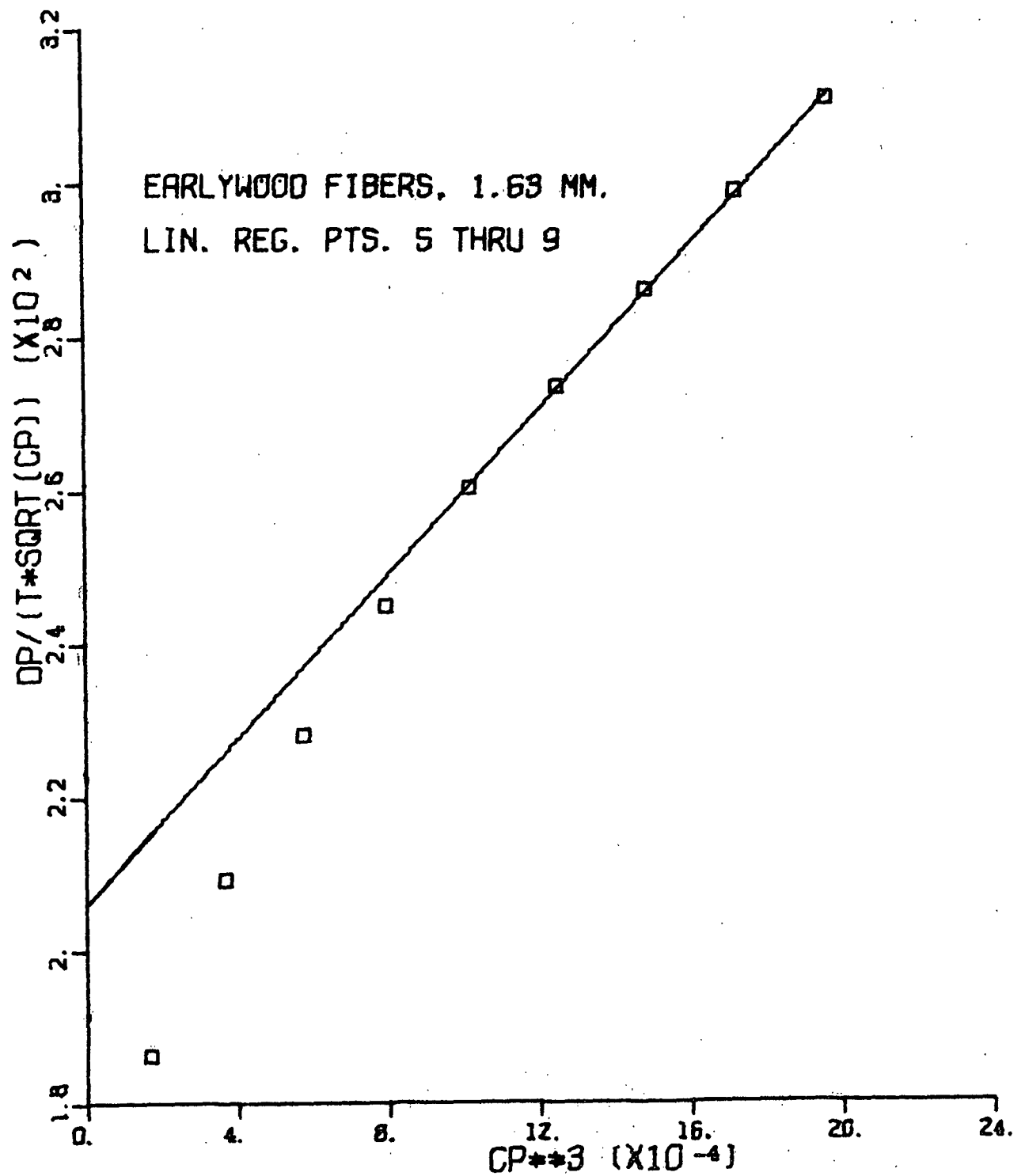


Figure 29. Experimental Plot of $\frac{\Delta P_c}{(c^{1/2} t)} \text{ vs. } c^3$

finer material in these highly classified pulp fiber populations. Values for $\langle v \rangle$ are within the usual range of 1 to 4 cm³/g observed for filtration data (32).

TABLE XIII

CORRELATION OF MORPHOLOGICAL VARIATION WITH AVERAGE SPECIFIC SURFACE, $\langle S_w \rangle$, AND AVERAGE SPECIFIC VOLUME, $\langle v \rangle$

Mean Fiber Length, mm	$\langle v \rangle$, cm ³ /g	τ_1^b	τ_2	$\langle R \rangle / \langle S_w \rangle^2^b$	$\langle S_w \rangle \times 10^{-3}$ cm ² /g	$S_{WG} \times 10^{-3}$ cm ² /g
<u>Earlywood</u>						
1.63	2.50 ± 0.03 ^a	0.57	0.15	0.72	6.50 ± 0.09 ^a	4.39 (7.35) ^c
3.05	2.59 ± 0.02	0.55	0.13	0.68	5.44 ± 0.13	5.89
3.94	2.30 ± 0.04	0.57	0.09	0.66	4.28 ± 0.13	5.71
<u>Latewood</u>						
1.74	2.27 ± 0.05	0.57	0.09	0.66	4.89 ± 0.21	4.03
2.07	2.19 ± 0.06	0.58	0.07	0.65	4.34 ± 0.11	3.77
2.98	2.11 ± 0.19	0.58	0.06	0.64	3.78 ± 0.04	3.72
4.13	1.66 ± 0.25	0.66	0.03	0.69	3.14 ± 0.09	3.29
<u>Whole Pulp</u>						
1.49	2.48 ± 0.03	0.55	0.10	0.65	5.62 ± 0.01	-- ^d
2.76	2.47 ± 0.05	0.53	0.09	0.62	4.34 ± 0.01	--
3.88	2.08 ± 0.05	0.58	0.06	0.64	3.61 ± 0.06	--
Not class.	2.52 ± 0.03	0.53	0.09	0.62	5.00 ± 0.05	--

^a95% Confidence limits.

$$\frac{\langle R \rangle}{\langle S_w \rangle^2} = \frac{3.5(1-N/2)\underline{c}^{1/2}}{\langle v \rangle^{1/2}} \left[1 + 57 \langle v \rangle^3 (1-N/2)^6 \underline{c}^3 \right] = \tau_1 + \tau_2.$$

^cFrom Table VII.

^dValues for \underline{d}_f and \underline{n}_f not available.

AVERAGE SPECIFIC SURFACE

A log-log plot of average specific filtration resistance, $\langle R \rangle$, vs. average specific surface, $\langle S_w \rangle$, is presented for earlywood, latewood, and whole pulp fiber populations in Fig. 30. The figure shows that there is an essentially linear relationship between $\log \langle R \rangle$ and $\log \langle S_w \rangle$ which agrees with results presented previously (26). The slope of the line connecting the data equals 2.0 and implies that in Equation (45) the sum of the terms containing c and $\langle v \rangle$ does not vary significantly for the various fiber fractions.

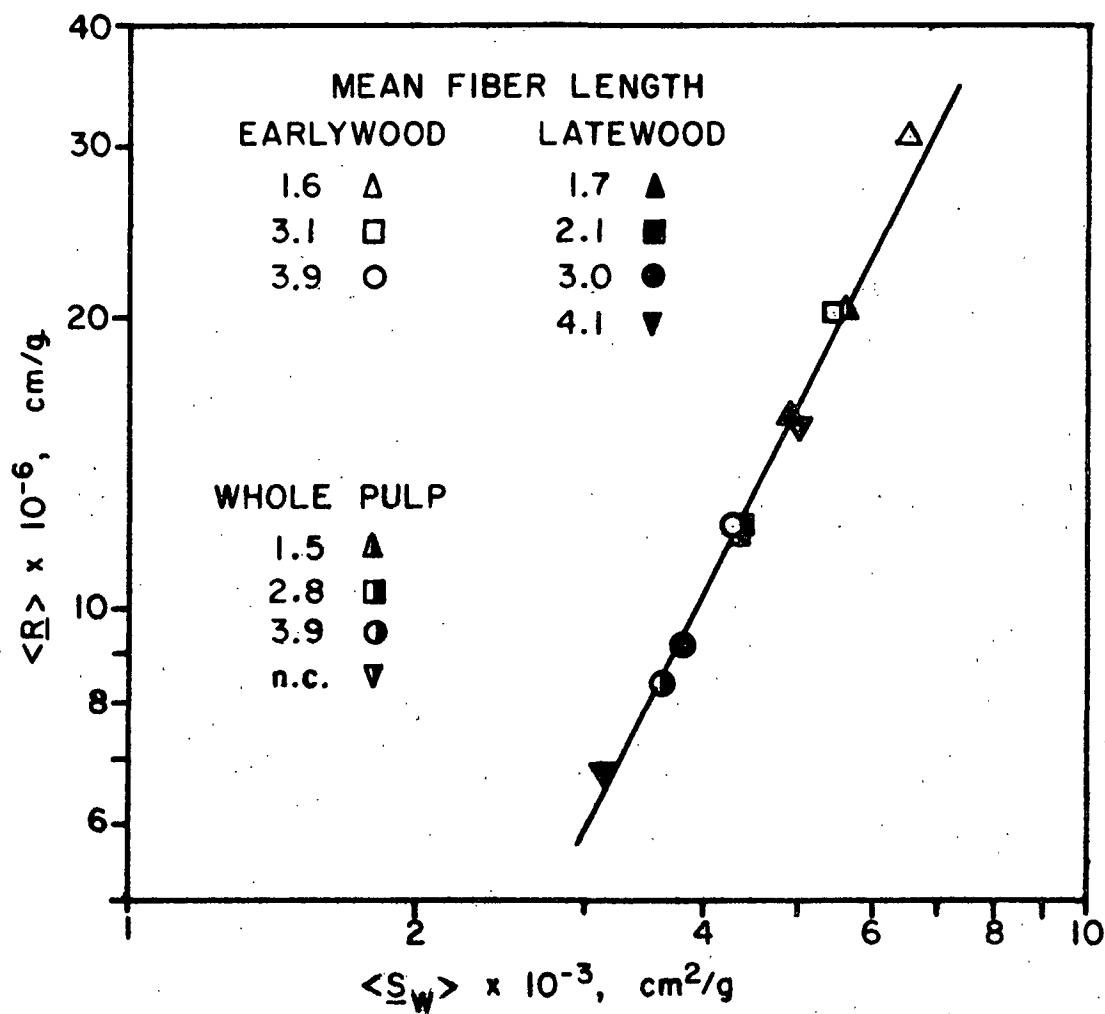


Figure 30. Plot of Average Specific Filtration Resistance, $\langle R \rangle$, vs. Average Specific Surface, $\langle S_w \rangle$, with Slope of Line = 2.0 at $\Delta P_f = 50$ cm H₂O

The values for each term, τ_1 and τ_2 are shown in Table XIII. Although the second term has a clear trend, its value is significantly less than that of the other term, which varies relatively little. Consequently, whatever trend there may be in the sum of the terms, $\langle \underline{R} \rangle / \langle \underline{S}_W \rangle^2$, it is insufficient to cause the slope in Fig. 30 to vary significantly from a value of 2.

Hence, for the various fiber fractions under study, $\langle \underline{R} \rangle$ is essentially a reflection of $\langle \underline{S}_W \rangle^2$ and is relatively insensitive to changes in mat density and specific volume. Therefore, variation in $\langle \underline{S}_W \rangle$ with fiber morphology will be relatively the same as those previously described for $\langle \underline{R} \rangle$.

The tendency of the longest latewood fibers (4.13 mm fraction) to resist collapse, as shown in Fig. 24, indicates that aqueous suspensions of these fibers compared with those in other fractions probably would be closest in behavior to fibers with circular cross section. This is supported by the similarity in the corresponding hydrodynamic, $\langle \underline{S}_W \rangle$, and geometric, \underline{S}_{WG} , specific surface data in Table XIII. Changes in morphology, such as in more flattened cross section (Fig. 24) and significantly more broken fibers with open ends (Table V) for the shortest compared with the longest fibers, are believed to result in the greater differences between the corresponding values for $\langle \underline{S}_W \rangle$ and \underline{S}_{WG} presented in Table XIII.

Thus, the latewood fraction with the greatest mean fiber length, which is probably nearest in behavior to the circular fibers, has a hydrodynamic specific surface closest to the calculated geometric specific surface.

AVERAGE SPECIFIC VOLUME

Table XIV compares the average specific volume, $\langle \underline{v} \rangle$, obtained from filtration resistance data with the geometric volume, \underline{v}_G , calculated from the fiber dimensions using a circular cylindrical model (Table VII).

TABLE XIV
COMPARISON OF SWOLLEN VOLUMES

$\frac{L_f}{\text{mm}}$	$\langle v \rangle, \text{cm}^3/\text{g}$	$\frac{v_G}{\text{cm}^3/\text{g}}$	$\frac{v_G}{\langle v \rangle}$	Rectangular Volume ^b , cm^3/g
<u>Earlywood</u>				
1.63	2.50	(7.33) ^a	2.9	(1.38) ^a
3.05	2.59	6.63	2.6	1.37
3.94	2.30	7.16	3.1	1.47
<u>Latewood</u>				
1.74	2.27	3.26	1.4	1.28
2.07	2.19	3.21	1.5	1.35
2.98	2.11	3.32	1.6	1.40
4.13	1.66	3.04	1.8	1.32

^aBased on $\frac{n_{fG}}{L_f}$.

^bRectangular volume = $2(\text{WT}) \frac{d_f}{L_f} \frac{L_f}{n_f}$.

The values for $\langle v \rangle$ are considerably lower than those for $\frac{v_G}{L_f}$, with the ratios of the two volumes equal to about 3 for earlywood and 1.6 for latewood. The large differences observed between $\langle v \rangle$ and $\frac{v_G}{L_f}$ are in part a reflection of the inability of the circular model to account for a decrease in swollen volume due to collapse of the fiber lumen. However, the collapse of the lumen is probably not complete since calculated rectangular volumes in which the fiber is assumed completely collapsed, as in the lower portion of Fig. 14, are lower than corresponding values of $\langle v \rangle$.

The average specific volume, $\langle v \rangle$, of fibers presented in Table XIII is in essence the volume of dry fibers plus their associated immobilized water per gram of dry fiber (31). By subtracting an assumed constant inverse pycnometric density of 0.62 cc/g for dry fibers from the specific volume (29), the increase

in $\langle v \rangle$ in Table XIII can be observed to correspond to an increase in immobilized water of 1.04 to 1.97 cm³ water per g fiber. Further assuming there is no increase in fiber swelling as found when fibers are beaten (29), it is concluded that most of this increase arises from more water being immobilized in the interstitial regions of the fiber mat as a reflection of changes in fiber morphology, particularly decreases in fiber length (accompanied by decreases in fiber width and wall thickness) and wall fraction.

Specific volume data may also be converted to pulp consistency [consistency = mass dry fibers/(mass of dry fibers + water)]. For specific volume of 1.66 to 2.59 cc/g, the apparent fiber consistency is approximately 49 to 33%, respectively. A consistency of about 33% would be a more credible maximum since fibers at this consistency are to a great extent considered dewatered. This discrepancy is probably a reflection of the limitations of the assumptions made in deriving Equation (29). Nevertheless, a relatively high consistency suggests that the immobile water is not in a free flowing form, but physically entrapped in the micropores and lumens.

CONCLUSIONS

Mechanical separation of unbeaten, bleached loblolly pine kraft pulp resulted in fiber populations of predominantly unbroken fibers which could be characterized by wall fraction and mean fiber length. Furthermore, variation in fiber length within the set of earlywood (low wall fraction) and latewood (high wall fraction) fiber populations correlated with wall thickness, fiber diameter, and number of fibers per gram in a manner similar to that within a tree.

Static compressibility data show the relationship between mat density, \underline{c} , and pressure, \underline{P}_f , followed the usual power function $\underline{c} = \underline{M} \underline{P}_f^{\underline{N}}$ for \underline{P}_f of about 10 to 150 cm H₂O. In this expression the compressibility constant \underline{N} was found to equal 0.373 for earlywood and latewood fiber populations and the compressibility constant \underline{M} correlated with fiber length for all fiber fractions. Compressibility, $d\underline{c}/d\underline{P}_f$, was greatest for shortest earlywood fibers and least for longest latewood fibers. \underline{M} was found to be linearly related to $(1/\underline{I}_f)^{1/3}$, where \underline{I}_f represents the moment of inertia for a flattened fiber model, in agreement with the simple compressibility model originally developed by Wilder. The linearity of the relationship supports bending as the dominant mechanism in compressibility of wood pulp, and suggests that the wood pulp fiber is essentially flattened prior to bending. Since \underline{I}_f was defined as $2/3 (\underline{WT})^3 \underline{d}_f$, where \underline{WT} is wall thickness and \underline{d}_f fiber diameter, it appears that the wood pulp fiber dimensions influencing compressibility are primarily wall thickness and to a lesser degree fiber diameter. Trends in \underline{M} with changes in mean fiber length of earlywood and latewood fibers tend to follow previously reported changes in elastic modulus of earlywood and latewood in successive growth rings, and also in elastic moduli and fibril angle.

Average specific filtration resistance, $\langle \underline{R} \rangle$, obtained from constant rate filtration data at a given pressure drop, $\Delta \underline{P}_f$, in the range 10 to 90 cm H₂O

also correlated with wall fraction and fiber length. Percentage change in $\langle R \rangle$ with pressure was comparable to that trend observed for c ; however, change in $\langle R \rangle$ with L_f was much greater. Smallest earlywood fibers had highest $\langle R \rangle$ values and these increased most with increases in ΔP_f compared with other fiber fractions.

Local specific filtration resistance, R , was calculated from pressure vs. time data obtained from constant rate filtration using a newly developed statistical procedure for determining derivatives. Changes in R with fiber wall fraction and length were similar to those found for $\langle R \rangle$, but R values were much higher and increased significantly more with pressure.

The square of average hydrodynamic specific surface, $\langle S_w \rangle^2$, is proportional to $\langle R \rangle$, and this relationship was comparatively insensitive to changes in c and average specific volume, $\langle v \rangle$. Calculated geometric specific surface is closest to $\langle S_w \rangle$ for latewood with greatest fiber length, probably because these fibers most closely approximate circular fibers. Values for $\langle v \rangle$ were considerably lower than calculated values, v_G , using a circular cylindrical model, indicating that the fibers collapse under fluid drag forces. The ratios of the two corresponding volumes was almost 3 for earlywood and about 1.6 for latewood. Data for $\langle v \rangle$ indicate immobilized water varies from 1.04 to 1.97 cc/g with morphological changes. Apparently most of this water is within the fiber walls or uncollapsed lumina and not elsewhere.

IMPLICATIONS OF RESULTS

The results of this study imply that alteration of fiber properties in the chip supply by inclusion of more juvenile wood, whole-tree chips, and/or low or high density logs may alter the compressibility and filtration resistance properties of the unbeaten pulp.

Compressibility and filtration resistance are important parameters in processes involving water flow through pulp fiber mats; and, the experimental conditions used closely approximate conditions of displacement bleaching and washing. Since the displacement process also involves diffusion which was not studied, little can be concluded about the effects of fiber properties on washing efficiency, however, the results of this study do apply to the gross transport of fluid through the mat.

From the text it is apparent that morphological variation which relates to growth within a tree can result in relatively large changes in filtration resistance at 5-10% consistency, which is the practical range encountered in displacement bleaching and washing. As a result, if more juvenile wood were included in a chip supply, filtration resistance would tend to increase, whereas if more mature wood were included, filtration resistance would tend to decrease. A similar argument is valid for low density (more earlywood) vs. high density (more latewood) wood sources.

However, a displacement bleaching process is more precisely a permeation, so that Equations (22) and (23) cannot be used in their present form to relate filtration resistance to the displacement processes. But these equations may be rearranged into the form applicable to permeation:

$$\frac{\langle R \rangle}{\Delta P_f} = \frac{\mu W}{A^2} \frac{1}{dV/dt} \quad (47)$$

which defines the volumetric flow rate (dV/dt) in terms of the cross-sectional area, A , of the bed; fluid viscosity, μ ; total mass, W' , of the fibers in bed; total pressure drop, ΔP_f , across the bed; and average filtration resistance, $\langle R \rangle$, (31). For displacement bleaching or washing equipment operating at constant consistency, μ , W' , and A^2 are constant so that in Table XI the sixfold change for $\langle R \rangle / \Delta P_f$ arising from fiber length and wall fraction variation, results in an inversely proportional change in (dV/dt). Similarly, if a constant flow rate is maintained by changing the drainage area, A , and since the square of this is proportional to $\langle R \rangle / \Delta P_f$, there would be a two- to threefold change in A arising from morphological variation.

Thus, if more juvenile wood is utilized, it probably would be necessary in displacement bleaching and washing at constant average consistency to use a lower maximum pressure between the washer head and screen to avoid significant thickening of the mat. In existing equipment the increased filtration resistance, even at lower pressure, would be expected to result in a slower flow of liquor through the pulp mat. For new equipment assuming constant flow rate is maintained, the increased filtration resistance could imply a need for more drainage area at increase in capital cost. When utilizing more mature wood the converse would tend to apply.

A similar argument is applicable to a discussion of high density vs. low density wood.

SUGGESTIONS FOR FUTURE WORK

Understanding the effects of fiber morphology on process parameters, such as the hydrodynamic properties of pulp, necessitates use of two major approaches to solving problems: the theoretical approach of "predicting and proving" and the experimental approach of "learning and discovery."

In the theoretical area there remains the definite desire to be able to mathematically predict the changes in hydrodynamic surface and volume of wood pulp resulting from changes in fluid stress using filtration and permeation experiments. Attempts in this area have failed the rigors of being mathematically justifiable.

In the experimental area it would be desirable to extend the correlative aspects of wet mat compressibility and fiber morphology by quantifying the modulus values descriptive of wet fiber collapse and bending. Also, the implications of the research described in this dissertation concerning displacement bleaching and washing would be greatly enhanced with quantitative information correlating rates of diffusion with fiber properties.

LIST OF SYMBOLS

\underline{A}	= area, empirical constant
\underline{B}	= filtration constant; empirical constant
$\underline{b_0}, \underline{b_1}, \underline{b_2}$	= empirical constants
\underline{C}	= stock consistency, empirical constant
\underline{c}	= mat density
$\underline{c_{avg}}$	= average mat density
$\underline{c_L}$	= initial mat density
$\underline{c_O}$	= initial mat density
$\underline{d_f}$	= fiber diameter
\underline{E}	= apparent modulus
\underline{I}	= moment of inertia
$\underline{I_C}$	= moment of inertia for circular fiber cross section
$\underline{I_F}$	= moment of inertia for flattened fiber cross section
\underline{K}	= Darcy permeability coefficient
$\underline{K_n}$	= constant depending on load distribution
\underline{k}	= Kozeny factor
$\underline{k_1}, \underline{k_2}$	= constants
\underline{L}	= pad thickness
$\underline{L_f}$	= fiber length
$\underline{L_n}$	= free span between two supports
$\underline{L_s}$	= segment length
$\underline{L_{s,0}}$	= initial segment length
$\underline{M}, \underline{N}$	= compressibility constants
$\underline{M_1}, \underline{N_1}$	= initial compressibility constants
$\underline{m}, \underline{n}$	= empirical constants
\underline{n}	= number of layers in mat

$\underline{n_c}$	= number of contacts per layer
$\underline{n_{c,o}}$	= initial number of contacts per layer
$\underline{n_f}$	= number fibers per gram
$\underline{n_{fG}}$	= calculated number fibers per gram
$\underline{P_f}$	= static pressure
$\underline{P_n}$	= magnitude of total load in bending
$\underline{\Delta P_f}$	= fluid pressure drop
$\underline{\Delta P_L}$	= total pressure drop across the mat
$\underline{\Delta P_z}$	= pressure drop at distance \underline{z} from top of mat
\underline{q}	= volumetric flow rate
\underline{R}	= local specific filtration resistance
$\langle \underline{R} \rangle$	= average specific filtration resistance
$\underline{r_o}$	= outside fiber diameter
$\underline{r_i}$	= inside fiber diameter
$\underline{S_v}$	= specific surface per unit volume
$\langle \underline{S_v} \rangle$	= average specific surface per unit volume
$\underline{S_w}$	= specific surface per unit mass
$\langle \underline{S_w} \rangle$	= geometric surface to mass ratio
\underline{t}	= time
\underline{U}	= superficial fluid velocity
\underline{V}	= filtrate volume
$\underline{V_w}$	= volume of fiber wall
\underline{v}	= specific volume
$\underline{v_G}$	= geometric volume to mass ratio
$\langle \underline{v} \rangle$	= average specific volume
\underline{W}	= mass of fibers per unit area
$\underline{W'}$	= mass of fibers in bed
\underline{WT}	= wall thickness

$\underline{x}, \underline{y}$	= defined variables
\underline{z}	= mat thickness; distance from top of mat
α, β	= constants associated with load distribution
δ	= deflection
ϵ	= porosity
θ	= \underline{S}_2 fibril angle
μ	= fluid viscosity
$\rho_{\underline{f}}$	= fiber density
$\rho_{\underline{w}}$	= fiber wall density
τ_1	= $3.5 (1 - N/2) \underline{c}^{1/2} / \langle \underline{v} \rangle^{1/2}$
τ_2	= $\tau_1 57 \langle \underline{v} \rangle^3 (1 - N/2)^6 \underline{c}^3$

ACKNOWLEDGMENTS

Sincere appreciation is expressed to the many people who assisted in the completion of this thesis.

The author is especially grateful for the encouragement and advice of Dr. Gordon A. Nicholls, Thesis Chairman and to Mr. N. L. Chang, Mr. S. T. Han, and Mr. H. Meyer, members of his Advisory Committee.

Special acknowledgments for their advice and assistance are also extended to Mr. B. D. Andrews, Dr. G. A. Baum, Dr. T. M. Grace, Dr. R. W. Nelson, and Mr. V. J. Van Drunen.

The assistance of the following people is also appreciated: Mr. H. Bailey of the Union Camp Corporation for the selection, harvesting, and delivery of a complete loblolly pine; Mr. M. C. Filz, Jr. and Mr. P. F. Van Rossum, whose skillful construction of much of the equipment used in this study greatly contributed to the success of this investigation; Mr. J. D. Hankey, Mrs. H. M. Kaustinen, and Dr. R. A. Parham for their assistance in microscopy; Mr. J. J. Bachhuber and Mr. J. O. Church for their assistance in computer programming; Mr. D. E. Beyer, Mr. C. H. Schabo, and Mr. F. R. Sweeney for their assistance in photographing and reducing the many figures; and Mr. H. J. Grady, Mr. O. C. Kuehl, and Mr. J. Tierney for their assistance on special problems.

LITERATURE CITED

1. Einspahr, D. W., Tappi 47(4):180(1964).
2. Einspahr, D. W., van Buijtenen, J. P., and Peckham, J. R., *Silvae Genet.* 18(3):57(1969).
3. Barefoot, A. C., Hitchings, R. G., Ellwood, E. L., Wilson, E. H. The relationship between loblolly pine fiber morphology and kraft paper properties. North Carolina Agr. Expt. Sta. Tech. Bull. No. 202, Dec., 1970. 89 p.
4. van Buijtenen, J. P., Alexander, S. D., Einspahr, D. W., Ferrie, A. E., Hart, T., Kellog, R. M., Porterfield, R. L., and Zobel, B. J., Tappi 58(9):129(1975).
5. Jones, R. L. An investigation of the effect of fiber structural properties on the compression response of fibrous beds. Doctoral Dissertation, Appleton, Wisconsin, The Institute of Paper Chemistry, 1962. Tappi 46(1):20(1963).
6. Elias, T. C. An investigation of the compression response of ideal unbonded fibrous structures by direct observation. Doctoral Dissertation, Appleton, Wisconsin, The Institute of Paper Chemistry, 1965. Tappi 50(3):125(1967).
7. Bliesner, W. C. A study of the porous structure of fibrous sheets using permeability techniques. Doctoral Dissertation, Appleton, Wisconsin, The Institute of Paper Chemistry, 1963. Tappi 47(7):392(1964).
8. Labrecque, R. P. An investigation of the effects of fiber cross-sectional shape on the resistance to the flow of fluids through fiber mats. Doctoral Dissertation, Appleton, Wisconsin, The Institute of Paper Chemistry, 1967. Tappi 51(1):8(1968).
9. Han, S. T., *Pulp Paper Mag. Can.* 70(9):T134(1969).
10. Hardacker, K. W. The physics and chemistry of wood pulp fibers. TAPPI/STAP No. 8:201(1970).
11. Alexander, S. D., Marton, R., and McGovern, S. D., Tappi 51(6):277(1968).
12. Leopold, B. and Thorpe, J. L., Tappi 51(7):304(1968).
13. Yiannos, P. N. and Taylor, D. L., Tappi 50(1):40(1967).
14. Hartler, N. and Nyren, J. TAPPI Paper Physics Seminar, "The physics and chemistry of wood pulp fiber." p. 76. Appleton, Wisconsin, May, 1969. Tappi 53(5):820(1970).
15. Gren, U. B., *Svensk Papperstid.* 75(19):785(1972).
16. Andrews, B. D. and Nicholls, G. A., *Appita* 27(6):411(1974).
17. Gullichsen, J., Personal communication.

18. Jacquelin, G., Tech. Rech. Pepet. 7:22(1966).
19. Chang, N. L. and Meyer, H., Unpublished work, Appleton, Wisconsin; The Institute of Paper Chemistry, 1967.
20. Nicholls, G. A. and Jamieson, R. G., Appita 29(5):339(1976).
21. Wardrop, A. B. and Dadswell, H. E., Holzforschung 7(2/3):33(1953).
22. McMillin, C. W., Wood Sci. Technol. 2(3):166(1968).
23. Panshin, A. J. and deZeeuw, C. Textbook of wood technology. Vol. I. Chap. 7. New York, McGraw Hill Book Company, 1970.
24. Mark, R. E. Cell wall mechanics of tracheids. Chap. 7. p. 168-170. New Haven and London, Yale Univ. Press, 1967.
25. Cowdry, D. R. and Preston, R. D. In Cote's The cellular ultrastructure of woody plants. Syracuse Univ. Press, 1965.
26. Han, S. T. Hydrodynamic evaluation of fiber surface area and swollen volume. A critical review. Appleton, Wisconsin, The Institute of Paper Chemistry, 1967.
27. Han, S. T. The status of the sheet-forming process. A critical review. Appleton, Wisconsin, The Institute of Paper Chemistry, 1965.
28. Kesler, R. B., Unpublished work, Appleton, Wisconsin, The Institute of Paper Chemistry, 1969.
29. Ingmanson, W. L. and Andrews, B. D., Tappi 42(1):29(1959).
30. Campbell, W. B., Pulp Paper Mag. Can. 48(3):103(1947).
31. Ingmanson, W. L. and Whitney, R. P., Tappi 37(11):523(1954).
32. Ingmanson, W. L., Tappi 35(10):439(1952).
33. Wilder, H. D. The compression creep properties of wet pulp mats. Doctoral Dissertation, Appleton, Wisconsin, The Institute of Paper Chemistry, 1960. Tappi 43(8):715(1960).
34. Ingmanson, W. L., Chem. Eng. Progr. 49(11):577(1953).
35. Whitney, R. P., Ingmanson, W. L., and Han, S. T., Tappi 38(3):157(1955).
36. Kozeny, J., Sitzber. Akad. Wiss. Wein, Math. Naturw. Kl., 136(Abt. IIa):271 (1927).
37. Carman, P. C., Trans. Inst. Chem. Eng. (London) 15:150(1937).
38. Davies, C. N., Proc. Inst. Mech. Engr. (London) 1B:185(1952).
39. Ingmanson, W. L., Andrews, B. D., and Johnson, R. C., Tappi 42(10):840(1959).

40. Ingmanson, W. L. and Andrews, B. D., Tappi 46(3):150(1963).
41. Meyer, H., Tappi 52(9):1716(1969).
42. Meyer, H., see Ref. 9.
43. Chang, N. L., Unpublished work, Appleton, Wisconsin, The Institute of Paper Chemistry, 1967.
44. Illvessalo-Pfaffli, M. S. and Alfthan, G. V., Paperi Puu 39(11):509(1957).
45. Chang, N. L. and Han, S. T., Unpublished work, Appleton, Wisconsin, The Institute of Paper Chemistry, 1969.
46. Jacquelin, G. Cohesion of papermaking fibrous networks in aqueous medium. ATIP Rev. 20:4-153(1966).
47. Jacquelin, G. Cohesion of fibrous networks in suspension. Influence of physico-chemical factors. C.T.P. Document No. 322, 1968.
48. Jacquelin, G. Cohesion of fibrous networks in suspension - the influence of physico-chemical factors. ATIP Rev. 23:5-293(1969).
49. Dinwoodie, J. M., Tappi 48(8):440(1968).
50. Horn, R. A. and Coens, C. L., Tappi 53(11):2120(1970).
51. Koch, P. Utilization of the southern pines. Chap. 7. p. 235-264. U.S. Dept. Agri. Forest Serv., 1972.
52. Seborg, C. O. and Simmonds, F. A., Paper Trade J. 113(17):49(Oct. 23, 1941).
53. Nelson, R. W., Personal communication, 1976.
54. Draper, N. R. and Smith, H. Applied regression analysis. p. 134. New York, Wiley, 1966.
55. Jensen, C. E. Matchcurve-3: Multiple-component and multidimensional mathematical models for natural resource studies. USDA Forest Serv. Res. Paper INT-146, Dec., 1973.
56. Nelson, R. W., Personal communication, 1975.
57. Meyer, H., Tappi 45(4):292(1962).
58. Chang, N. L., Tappi 52(5):923(1969).
59. Chang, N. L. and Han, S. T., Unpublished work, Appleton, Wisconsin, The Institute of Paper Chemistry, 1969.
60. Chang, N. L., Personal communication, 1976.
61. Grace, T. M., Personal communication, 1976.
62. Onagi, S. and Sasaguri, K., Tappi 44(12):874(1961).

APPENDIX I

ORIGINAL MAT DENSITY DATA

MAT DENSITY VS. PRESSURE FOR EARLYWOOD FIBERS

Earlywood - 1.63 mm			Earlywood - 3.05 mm		
P_f , dynes/cm ²		ρ , g/cm ³	P_f , dynes, cm ²		ρ , g/cm ³
0.81500000	04	0.52799180-01	0.81500000	04	0.49270900-01
0.13100000	05	0.62382180-01	0.13100000	05	0.58781550-01
0.22900000	05	0.76386100-01	0.22900000	05	0.73146380-01
0.37700000	05	0.91424080-01	0.37700000	05	0.88058620-01
0.62300000	05	0.11024160 00	0.62300000	05	0.10617140 00
0.96400000	05	0.12961170 00	0.96400000	05	0.12493500 00
0.14580000	06	0.15107790 00	0.14580000	06	0.14531220 00
0.51697050	04	0.44783180-01	0.81500000	04	0.49598010-01
0.99608450	04	0.55714800-01	0.13100000	05	0.59236860-01
0.19686040	05	0.70803140-01	0.22900000	05	0.73710800-01
0.34331450	05	0.86163400-01	0.37700000	05	0.88831350-01
0.58810470	05	0.10583760 00	0.62300000	05	0.10725660 00
0.92780040	05	0.12484140 00	0.96400000	05	0.12576180 00
0.14185000	06	0.14707130 00	0.14580000	06	0.14675710 00
0.51564550	04	0.45297200-01	0.54313710	04	0.37645770-01
0.99484720	04	0.56555410-01	0.10125750	05	0.52079570-01
0.19814600	05	0.71849010-01	0.19811240	05	0.67797960-01
0.34323470	05	0.87296770-01	0.34431780	05	0.83789220-01
0.58805280	05	0.10649860 00	0.58894880	05	0.10262390 00
0.92774780	05	0.12618440 00	0.92850280	05	0.12223490 00
0.14184470	06	0.14939950 00	0.14191070	06	0.14380700 00
			0.54196690	04	0.37859010-01
			0.10109730	05	0.53090190-01
			0.19800440	05	0.68743490-01
			0.34423410	05	0.84789410-01
			0.58888430	05	0.10364000 00
			0.92848090	05	0.12177770 00
			0.14190990	06	0.14250720 00

Earlywood - 3.94 mm		
P_f , dynes/cm ²		ρ , g/cm ³
0.81500000	04	0.50717000-01
0.13100000	05	0.60491660-01
0.22900000	05	0.74377240-01
0.37700000	05	0.89026080-01
0.62300000	05	0.10636830 00
0.96400000	05	0.12374330 00
0.14580000	06	0.14320010 00
0.81500000	04	0.49466010-01
0.13100000	05	0.59047570-01
0.22900000	05	0.72747010-01
0.37700000	05	0.87060510-01
0.62300000	05	0.10428590 00
0.96400000	05	0.12149080 00
0.14580000	06	0.14038270 00
0.58662040	04	0.40265330-01
0.10548500	05	0.51007820-01
0.20195560	05	0.63240060-01
0.34751990	05	0.79062260-01
0.59155590	05	0.98981620-01
0.93079100	05	0.11688530 00
0.14211380	06	0.13598930 00
0.57581520	04	0.39894850-01
0.10465610	05	0.49693670-01
0.20111980	05	0.62677050-01
0.34669430	05	0.79974590-01
0.59093940	05	0.98388450-01
0.93025440	05	0.11609900 00
0.14206490	06	0.13567710 00

MAT DENSITY VS. PRESSURE FOR LATEWOOD FIBERS

Latewood - 1.74 mm	
P_f , dynes/cm ²	ρ , g/cm ³
0.81500000 04	0.51254000-01
0.13100000 05	0.60885090-01
0.22900000 05	0.73822380-01
0.37700000 05	0.87871520-01
0.62300000 05	0.10495880 00
0.96400000 05	0.12225710 00
0.14580000 06	0.14163540 00
0.54969030 04	0.39637380-01
0.10254030 05	0.48038510-01
0.19893310 05	0.65504950-01
0.34504510 05	0.80197960-01
0.58958460 05	0.97531380-01
0.92907220 05	0.11522140 00
0.14196120 06	0.13485820 00
0.54798840 04	0.39696560-01
0.10214580 05	0.50169900-01
0.19884840 05	0.65137790-01
0.34496400 05	0.79933170-01
0.58951470 05	0.97239330-01
0.92901530 05	0.11473780 00
0.14195470 06	0.13513010 00

Latewood - 1.07 mm	
P_f , dynes/cm ²	ρ , g/cm ³
0.81500000 04	0.48893480-01
0.13100000 05	0.58181560-01
0.22900000 05	0.71410210-01
0.37700000 05	0.85225750-01
0.62300000 05	0.10211060 00
0.96400000 05	0.11896480 00
0.14580000 06	0.13739690 00
0.81500000 04	0.48768130-01
0.13100000 05	0.57805390-01
0.22900000 05	0.71820540-01
0.37700000 05	0.85548110-01
0.62300000 05	0.10211130 00
0.96400000 05	0.11880580 00
0.14580000 06	0.13763190 00
0.58021300 04	0.39144250-01
0.10517260 05	0.47966420-01
0.20158380 05	0.60337260-01
0.34718490 05	0.75646380-01
0.59129850 05	0.94204430-01
0.93053760 05	0.11197440 00
0.14209050 06	0.13059480 00
0.57868170 04	0.38387790-01
0.10493470 05	0.47663130-01
0.20140540 05	0.59703690-01
0.34695630 05	0.75879850-01
0.59110320 05	0.94532600-01
0.93036950 05	0.11231540 00
0.14207670 06	0.13063680 00

Latewood - 2.98 mm	
P_f , dynes/cm ²	ρ , g/cm ³
0.81500000 04	0.46375850-01
0.13100000 05	0.55741810-01
0.22900000 05	0.69563780-01
0.37700000 05	0.83340800-01
0.62300000 05	0.99330610-01
0.96400000 05	0.11556840 00
0.14580000 06	0.13382400 00
0.81500000 04	0.46625250-01
0.13100000 05	0.55734230-01
0.22900000 05	0.68968660-01
0.37700000 05	0.82829320-01
0.62300000 05	0.99174760-01
0.96400000 05	0.11536880 00
0.14580000 06	0.13353430 00
0.59945650 04	0.39492220-01
0.10682060 05	0.48960030-01
0.20305120 05	0.61396050-01
0.34870530 05	0.74075930-01
0.59272710 05	0.90209330-01
0.93175160 05	0.10798420 00
0.14219810 06	0.12585770 00
0.60096600 04	0.40751550-01
0.10709050 05	0.49761800-01
0.20334610 05	0.61959280-01
0.34903860 05	0.74005660-01
0.59315320 05	0.88183200-01
0.93207910 05	0.10645290 00
0.14222290 06	0.12517930 00

Latewood - 4.13 mm	
P_f , dynes/cm ²	ρ , g/cm ³
0.81500000 04	0.46615660-01
0.13100000 05	0.56377590-01
0.22900000 05	0.69656990-01
0.37700000 05	0.83370500-01
0.62300000 05	0.99752070-01
0.96400000 05	0.11591200 00
0.14580000 06	0.13405850 00
0.81500000 04	0.46680120-01
0.13100000 05	0.55767470-01
0.22900000 05	0.68890820-01
0.37700000 05	0.82647650-01
0.62300000 05	0.98370120-01
0.96400000 05	0.11463310 00
0.14580000 06	0.13252340 00
0.81500000 04	0.46035970-01
0.13100000 05	0.56016560-01
0.22900000 05	0.68998320-01
0.37700000 05	0.82683380-01
0.62300000 05	0.98489660-01
0.96400000 05	0.11347320 00
0.14580000 06	0.13296100 00
0.64638320 04	0.38407690-01
0.11133510 05	0.47286750-01
0.20709110 05	0.59843350-01
0.35229750 05	0.72845980-01
0.59600920 05	0.87724080-01
0.93481730 05	0.10281310 00
0.14247400 06	0.11963640 00

MAT DENSITY VS. PRESSURE FOR WHOLE PULP FIBERS

Whole Pulp - 1.49 mm		
P_f , dynes/cm ²	c , g/cm ³	
0.8150000D 04	0.4869344D-01	
0.1310000D 05	0.5783450D-01	
0.2290000D 05	0.7101295D-01	
0.3770000D 05	0.8548899D-01	
0.6230000D 05	0.1029136D 00	
0.9640000D 05	0.1205749D 00	
0.1458000D 06	0.1403368D 00	
0.5492390D 04	0.3761313D-01	
0.1021763D 05	0.4816187D-01	
0.1986255D 05	0.6595798D-01	
0.3447869D 05	0.8069782D-01	
0.5893322D 05	0.9915962D-01	
0.9288573D 05	0.1170050D 00	
0.1419423D 06	0.1370937D 00	
0.5485009D 04	0.3752867D-01	
0.1021212D 05	0.4799393D-01	
0.1986058D 05	0.6538658D-01	
0.3447734D 05	0.7993203D-01	
0.5893465D 05	0.9744221D-01	
0.9288647D 05	0.1151867D 00	
0.1419423D 06	0.1353157D 00	

Whole Pulp - 2.76 mm		
P_f , dynes/cm ²	c , g/cm ³	
0.8150000D 04	0.4676894D-01	
0.1310000D 05	0.5591713D-01	
0.2290000D 05	0.6967646D-01	
0.3770000D 05	0.8348040D-01	
0.6230000D 05	0.1004957D 00	
0.9640000D 05	0.1175662D 00	
0.1458000D 06	0.1364895D 00	
0.5971225D 04	0.3783484D-01	
0.1065706D 05	0.4710987D-01	
0.2027248D 05	0.5991390D-01	
0.3483545D 05	0.7295845D-01	
0.5922985D 05	0.9079601D-01	
0.9313734D 05	0.1087654D 00	
0.1421610D 06	0.1278166D 00	
0.5922493D 04	0.3732386D-01	
0.1061038D 05	0.4661501D-01	
0.2023923D 05	0.5866763D-01	
0.3481037D 05	0.7097254D-01	
0.5919366D 05	0.9076442D-01	
0.9310808D 05	0.1082059D 00	
0.1421368D 06	0.1266825D 00	

Whole Pulp - 3.88 mm		
P_f , dynes/cm ²	c , g/cm ³	
0.8150000D 04	0.4704740D-01	
0.1310000D 05	0.5626533D-01	
0.2290000D 05	0.6950423D-01	
0.3770000D 05	0.8327794D-01	
0.6230000D 05	0.9996938D-01	
0.9640000D 05	0.1164388D 00	
0.1458000D 06	0.1351842D 00	
0.6080014D 04	0.4387227D-01	
0.1078113D 05	0.5316521D-01	
0.2040875D 05	0.6543423D-01	
0.3497533D 05	0.7766837D-01	
0.5938074D 05	0.9231913D-01	
0.9328111D 05	0.1084817D 00	
0.1422869D 06	0.1277465D 00	
0.6159665D 04	0.3982958D-01	
0.1084314D 05	0.4893220D-01	
0.2045712D 05	0.6079975D-01	
0.3501379D 05	0.7269041D-01	
0.5941154D 05	0.8687168D-01	
0.9330871D 05	0.1020787D 00	
0.1423108D 06	0.1203493D 00	

Whole Pulp - Not Class.		
P_f , dynes/cm ²	c , g/cm ³	
0.8150000D 04	0.4562335D-01	
0.1310000D 05	0.5494349D-01	
0.2290000D 05	0.6836177D-01	
0.3770000D 05	0.8247910D-01	
0.6230000D 05	0.9896725D-01	
0.9640000D 05	0.1157578D 00	
0.1458000D 06	0.1343930D 00	
0.5697347D 04	0.3671692D-01	
0.1042189D 05	0.4510315D-01	
0.2007172D 05	0.5713932D-01	
0.3462116D 05	0.7503564D-01	
0.5905279D 05	0.9234183D-01	
0.9298851D 05	0.1092652D 00	
0.1420306D 06	0.1284662D 00	
0.5660418D 04	0.3738418D-01	
0.1039292D 05	0.4567838D-01	
0.2004159D 05	0.5839888D-01	
0.3460246D 05	0.7576348D-01	
0.5903935D 05	0.9269678D-01	
0.9297538D 05	0.1101282D 00	
0.1420200D 06	0.1291505D 00	
0.5631177D 04	0.3784716D-01	
0.1036408D 05	0.4644513D-01	
0.1999431D 05	0.6183906D-01	
0.3457902D 05	0.7760351D-01	
0.5901768D 05	0.9536743D-01	
0.9295732D 05	0.1130746D 00	
0.1420037D 06	0.1328685D 00	

Variability in the mat density vs. pressure data for the whole pulp fiber populations was found to be abnormally high. This variation has been attributed to difficulties in eliminating vibrations from the environment during some of the experiments. For this reason, compressibility data for whole pulp has been eliminated from the body of this report. However, Table XV and Figure 31 show that $\underline{N} = 0.373$ is generally applicable to the data.

TABLE XV

VALUES FOR COMPRESSIBILITY CONSTANTS \underline{N} AND \underline{M}^a FOR WHOLE PULP

\underline{L}_f , mm	\underline{N}_1^a	$\underline{M}_1 \times 10^3,^a$ c.g.s. units ^b	\underline{N}	$\underline{M} \times 10^3,$ c.g.s. units ^b
1.49	0.389	1.37	0.373	1.62
2.76	0.384	1.37	0.373	1.53
3.88	0.350	1.99	0.373	1.56
Not class. c13	0.392	1.27	0.373	1.53

^aAs described in text.

^b $(g/cm^3)/(\text{dynes}/cm^2)^{\underline{N}}$.

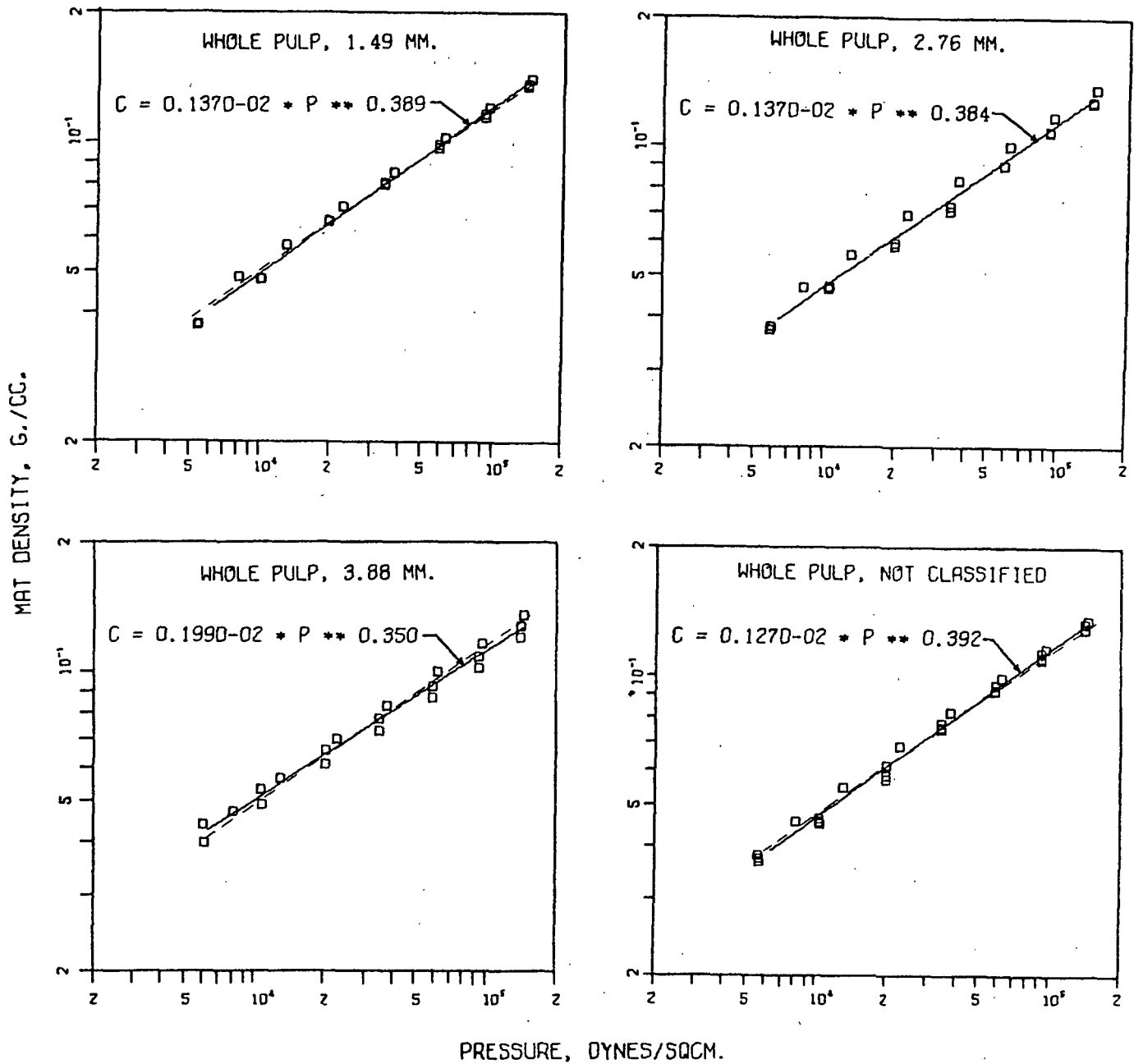


Figure 31. Compressibility Data and Resulting Best Fit Curves for Whole Pulp Fiber Fractions (as in Fig. 16)

APPENDIX II

THREE-DIMENSIONAL PLOTTING PROGRAM

```

/JOB G0,TIME=20
LE DISK=(1,PLUTS,NREC=5000),RSIZ=80,VCL=SYSFL1,DISP=(OLD,DELETE)

      XYZPLT == 3-DIMENSIONAL PLOTTING

      ANTHONY P. BINOTTO
      JUNE 1, 1975

THIS PROGRAM WILL PLOT ANY SET OF NUMBERS ON X-Y COORDINATES
UTILIZING RETZKE'S PLOTTING PROGRAM.
THE USER MUST ENTER THE FOLLOWING CARDS IN ORDER.

      /ID
      /INCLUDE ABPLOT
DATA CARD 1. LABEL FOR X AXIS
DATA CARD 2. LABEL FOR Y AXIS
DATA CARD 3. TITLE OF PLOT
DATA CARD 4. N,NX,NY,LT,IEQ (IN FORMAT 513)
      WHERE...
      N = TOTAL NUMBER OF X,Y-PAIRS
      NX = 1 IF X IS PLOTTED AS LINEAR
           2 IF X IS PLOTTED AS LOG10(X)
           -1 OR -2 IF NEW SET OF AXIS IS NOT MADE
      NY = SAME AS FOR NX EXCEPT MINUS HAS NO EFFECT
      LT = -1 IF SYMBOLS ONLY ARE PLOTTED FOR EACH DATA POINT
           0 IF A LINE ONLY CONNECTS EACH DATA POINT
           +1 IF BOTH LINE AND SYMBOLS ARE PLOTTED
      IEQ = INTERGER EQUIVALENT OF PLOTTING SYMBOL (1-16)
DATA CARD 5-N. X AND Y COORDINATES IN ZE15.7 FORMAT
      /END

1  DIMENSION X(900),Y(900)
2  COMMON LX(7),LY(7),ID(13),SVAL(4),FIRSTX,XSCALE,FIRSTY,YSCALE
3  COMMON FIRSTZ,ZSCALE,LZ(7),XPRIME,YPRIME,ZANGLE
4  9006 FORMAT (E11.4,44X,E11.4)
5  ID(13) = 0
6  FIRSTX = 1.
7  XSCALE = 7./1.
8  FIRSTY = 2.
9  YSCALE = 8.5/2.
10 FIRSTZ = 0.
11 ZSCALE = 1.
12 ZANGLE = 330.
13 IN = 5
14 C
15 REWIND IN
16 CALL GET(LX,24,IN)
17 CALL GET(LY,24,IN)
18 CALL GET(LZ,24,IN)
19 LX(7) = IVERR(LX,1,24)
20 LY(7) = IVERR(LY,1,24)
21 LZ(7) = IVERR(LZ,1,24)
22 1 READ (IN,9004) (ID(1),I=1,12),Z
23 IF (ICOMP(ID,1,249,4,1)) 2,3,2
24 2 READ (IN,9005) N,NX,NY,LT,IEQ
25 READ (IN,9006) (X(I),Y(I),I=1,N)
26 XPRIME = Z * COS(ZANGLE/57.2958)
27 YPRIME = Z * SIN(ZANGLE/57.2958)
28 CALL GRAPH (X,Y,NX,NY,N,LT,IEQ)
29 GO TO 1
30 3 CALL FINAL
31 CALL EXIT
32 9004 FORMAT (12A4,F6.2)
33 9005 FORMAT (5I3)
34 END

C
1 SUBROUTINE GRAPH (X,Y,NX,NY,N,LT,IEQ)
2 DIMENSION X(1),Y(1),ISMBL(16)
3 COMMON LX(7),LY(7),ID(13),SVAL(4),FIRSTX,XSCALE,FIRSTY,YSCALE
4 COMMON FIRSTZ,ZSCALE,LZ(7),XPRIME,YPRIME,ZANGLE
5 ISMBL(1)=170
6 ISMBL(2)=183
7 ISMBL(3)=175
8 ISMBL(4)=176
9 ISMBL(5)=181
10 ISMBL(6)=182
11 ISMBL(7)=185
12 ISMBL(8)=171
13 ISMBL(9)=172
14 ISMBL(10)=173
15 ISMBL(11)=174
16 ISMBL(12)=177
17 ISMBL(13)=178
18 ISMBL(14)=179
19 ISMBL(15)=180
20 ISMBL(16)=184
21 IF (ID(13)) 13,1,2
22 1 CALL ITLZ
23 CALL DPY(1,4)
24 CALL PLOT(0.0,-11.0,-3)
25 CALL PLOT(6.0,1.5,-3)
26 2 IF (NX) 10,13,3
27 ID(13)=1
28 CALL PLOT(10.75,-1.5,3)
29 CALL PLOT(10.75,9.0,2)
30 CALL PLOT(12.0,0.75,-3)
31 CALL AXIS(10.0,0.0,LZ(7),0.0,ZANGLE,FIRSTZ,ZSCALE)
32 CALL AXLOG(0.0,0.0,LX(7),7.0,0.0,FIRSTX,XSCALE)
33 CALL AXLOG(0.0,0.0,LY(7),8.5,90.0,FIRSTY,YSCALE)
34 10 YPAGE=8.5-(ID(13)*0.30)
35 IF (LT) 11,12,11
36 11 CALL DRAWHC(YPAGE+0.08,0.0,ISMBL(IEQ),1.0,0.0,0.35)
37 12 CALL SYMBOL(1.0,YPAGE,0.14,ID(0.0,48))
38 ID(13)=ID(13)+1
39 MX=IABS(NX)
40 MY=IABS(NY)
41 X(N+1)=FIRSTX
42 X(N+2)=XSCALE
43 Y(N+1)=FIRSTY
44 Y(N+2)=YSCALE
45 CALL PLOT (XPRIME,YPRIME,-3)
46 CALL LILOG(X,MX,Y,MY,N,1,LT,IEQ)
47 XPRIME = -1.* XPRIME
48 YPRIME = -1.* YPRIME
49 CALL PLOT (XPRIME,YPRIME,-3)
50 13 RETURN
51 END

```

APPENDIX III

COMPUTER PROGRAM USED TO CALCULATE
AN EQUATION OF THE FORM

$$y = b_0 + b_1 x^m + b_2 x^n$$

```

/JOE GO,TIME=20
/FILE DISK=(2,CRVFIT,NREC=9000),RSIZ=80,VOL=SYSFL1,DISP=(NEW,KEEP)
CRVFIT === CURVE FITTING
ANTHONY P. BINOTTO
AUGUST 25, 1975
THIS PROGRAM IS DESIGNED TO CALCULATE THE BEST EQUATION
OF THE FORM...
Y = B0 + B1*(X**M) + B2*(X**N)
TO ANY SET OF DATA. THE PROCEDURE INVOLVES MINIMIZING THE
SUM OF SQUARES.
*** WARNING*** THE RESULTING EQUATION WILL ONLY BE ONE OF
MANY COMBINATIONS OF B0,B1,B2,M,N WHICH GIVE A "BEST"
FIT TO THE DATA. THE FINAL EQUATION IS THEREFORE DEPENDENT
ON THE INITIAL ESTIMATE OF M AND N.
THE USER MUST ENTER THE FOLLOWING CARDS IN ORDER.
/IO *****
/INCLUDE CRVFIT
DATA CARD 1. TITLE FOR DATA SET 1
DATA CARD 2. NUMBER OF X,Y-PAIRS IN I3 FORMAT
DATA CARD 3+ X,Y-PAIRS OF DATA IN 2E15.7 FORMAT
REPEAT DATA CARDS 1 THROUGH 3+ FOR SUBSEQUENT DATA SETS
99999999999999999999
/END
DIMENSION ITITLE(20),X(200),Y(200),A(5,6)
DOUBLE PRECISION X,Y,B0,B1,B2,M,N,A
DOUBLE PRECISION DELB0,DELB1,DELB2,DELM,DELN
C**** IOUT == OUTPUT STORED ON DISK OR TAPE FOR PLOTTING.
IOUT = 2
NCOUNT = 0.0
WRITE (IOUT,300)
WRITE (IOUT,200)
FORMAT ('CP**3')
300 FORMAT ('DP/T(SORT(CP))')
200 FORMAT ('DP/T(SORT(CP))')
100 READ (5,2) ITITLE
1 IF (ICOMP(ITITLE,1,249,4,1)) 1,14,1
1 READ (5,3) NPTS
1 READ (5,4) (X(I),Y(I),I=1,NPTS)
1 WRITE (IOUT,2) ITITLE
1 WRITE (IOUT,5) NPTS
1 WRITE (IOUT,4) (X(I),Y(I),I=1,NPTS)
1 WRITE (6,6) ITITLE
2 FORMAT (20A4)
3 FORMAT (13)
4 FORMAT (2E15.7)
5 FORMAT (13,' 1 -1 3')
6 FORMAT ('0',20A4, '/')
C**** ESTIMATE VALUES OF B0,B1,B2,M,N
B0 = 200.0
B1 = 1000.0
B2 = 1000.0
M = 0.120
N = 0.500
TEST1 = 0.0
7 CALL SUM (X,Y,NPTS,B0,B1,B2,M,N,A)
7 CALL SIMEQN (A,5,6)
7 DELB0 = A(1,6) / A(1,1)
7 DELB1 = A(2,6) / A(2,2)
7 DELB2 = A(3,6) / A(3,3)
7 DELM = A(4,6) / A(4,4)
7 DELN = A(5,6) / A(5,5)
C**** DATA FIT MAY BE IMPROVED AT THE EXPENSE OF CALCULATION TIME
C**** BY REDUCING THE VALUE OF "TEST".
TEST = 10.
TEST2 = DELB0 + DELB1 + DELB2 + DELM + DELN
DIFF = TEST2 - TEST1
8 IF (ABS(DIFF)-TEST) 12,12,8
8 TEST1 = TEST2
8 NCOUNT = NCOUNT + 1
8 B0 = B0 + DELB0
8 B1 = B1 + DELB1
8 B2 = B2 + DELB2
8 IF (NCOUNT-100) 7,7,9
9 NCOUNT = 0
9 WRITE (6,10) DIFF,B0,B1,B2,M,N,NCOUNT
9 WRITE (6,11) DELB0,DELB1,DELB2,DELM,DELN
10 FORMAT ('0',6E15.4,15)
11 FORMAT (' ',15X,5E15.4)
11 M = M + DELM
11 N = N + DELN
11 GO TO 7
12 WRITE (6,13)B0,B1,B2,M,N,NCOUNT
13 FORMAT ('0 B0 = ',E12.4,5X,'B1 = ',E12.4,5X,'B2 = ',E12.4,5X,
* 'M = ',E12.4,5X,'N = ',E12.4,15, '/')
13 CALL EQN (B0,B1,B2,M,N,IOUT,X,Y)
13 GO TO 100
14 WRITE (IOUT,9999)
9999 FORMAT ('99999999999999999999')
CALL EXIT
END
C
C SUBROUTINE EQN === GENERATION OF PLOTTING POINTS
C
C THIS SUBROUTINE GENERATES DATA POINTS FROM THE CALCULATED
C EQUATION TO BE USED IN PLOTTING PROGRAM "ABPLOT".
SUBROUTINE EQN (B0,B1,B2,M,N,IOUT,X,Y)
DIMENSION X(200),Y(200)
DOUBLE PRECISION X,Y,DPTS,XFIRST,XLAST,XINCR,B0,B1,B2,M,N
NPTS = 100
XFIRST = X(1)
XLAST = X(9)
DPTS = NPTS
XINCR = (XLAST - XFIRST) / DPTS
WRITE (IOUT,1) M,N
WRITE (IOUT,2) NPTS
1 FORMAT ('Y = B0 + B1*(X**',F4.2,') + B2*(X**',F4.2,')')
2 FORMAT (13,' -1 -1 0')
X(1) = XFIRST
DO 3 I=1,NPTS
Y(I) = B0 + B1*(X(I)**M) + B2*(X(I)**N)
X(I+1) = X(I) + XINCR
3 WRITE (IOUT,4) X(I),Y(I)
4 FORMAT (2E15.7)
RETURN
END

```

```

SUBROUTINE SUM == CALCULATION OF SUM OF SQUARES
SUBROUTINE SUM (X,Y,NPTS,B0,B1,B2,M,N,A,PTS,SXMYR2
DIMENSION X(20),Y(20),A(5,6)
DOUBLE PRECISION X,Y,B0,B1,B2,M,N,A,PTS,SXMYR2
DOUBLE PRECISION SX,SXM,SXN,SXMY,SX2M,SXMXN,SXNY,SX2N,SXMYR,SXMR
DOUBLE PRECISION SX2MR,SXMXNR,SXNYR,SXNR,SXMR2,SX2MR2,SXMYR2
DOUBLE PRECISION SXNR2,SX2NR2,SXNYR2,SX2NR,XN,XM,X2M,X2N,R,R2
PTS = NPTS
SY = 0.0
SXM = 0.0
SXN = 0.0
SXMY = 0.0
SX2M = 0.0
SXMXN = 0.0
SXNY = 0.0
SX2N = 0.0
SXMYR = 0.0
SXMR = 0.0
SX2MR = 0.0
SXMXNR = 0.0
SXNYR = 0.0
SXNR = 0.0
SX2NR = 0.0
SXMR2 = 0.0
SX2MR2 = 0.0
SXMXNR2 = 0.0
SXMYR2 = 0.0
SXNR2 = 0.0
SX2NR2 = 0.0
SXNYR2 = 0.0
ON 1 I=1,NPTS
XM = X(I) ** M
XN = X(I) ** N
X2M = XM ** 2
X2N = XN ** 2
R = DLOG(X(I))
R2 = R ** 2
SY = SY + Y(I)
SXM = SXM + XM
SXN = SXN + XN
SXMY = SXMY + (XM * Y(I))
SX2M = SX2M + X2M
SXMXN = SXMXN + (XM * XN)
SXNY = SXNY + (XN * Y(I))
SX2N = SX2N + X2N
SXMYR = SXMYR + (XM * Y(I) * R)
SXMR = SXMR + (XM * R)
SX2MR = SX2MR + (X2M * R)
SXMXNR = SXMXNR + (XM * XN * R)
SXNYR = SXNYR + (XN * Y(I) * R)
SX2NR = SX2NR + (XN * R)
SXMR2 = SXMR2 + (XM * R2)
SX2MR2 = SX2MR2 + (X2M * R2)
SXMXNR2 = SXMXNR2 + (XM * XN * R2)
SXMYR2 = SXMYR2 + (XM * Y(I) * R2)
SXNR2 = SXNR2 + (XN * R2)
SX2NR2 = SX2NR2 + (X2N * R2)
SXNYR2 = SXNYR2 + (XN * Y(I) * R2)
A(1,1) = PTS
A(1,2) = SXM
A(1,3) = SXN
A(1,4) = B1 * SXMR
A(1,5) = B2 * SXNR
A(1,6) = -B0*PTS*B0 + B1*SXM + B2*SXN - SY)
A(2,1) = SXM
A(2,2) = SX2M
A(2,3) = SXMXN
A(2,4) = B0*SXMR + 2.0*B1*SX2MR + B2*SXMXNR - SXMYR
A(2,5) = B2*SXMXNR
A(2,6) = -(B0*SXM + B1*SX2M + B2*SXMXN - SXMY)
A(3,1) = SXN
A(3,2) = SXMXN
A(3,3) = SX2N
A(3,4) = SXMXNR
A(3,5) = B0*SXNR + B1*SXMXNR + 2.0*B2*SX2NR - SXNYR
A(3,6) = -(B0*SXN + B1*SXMXN + B2*SX2N - SXNY)
A(4,1) = SXMR
A(4,2) = SX2MR
A(4,3) = SXMXNR
A(4,4) = B0*SXMR2 + 2.0*B1*SX2MR2 + B2*SXMXNR2 - SXMYR2
A(4,5) = B2*SXMXNR2
A(4,6) = -(B0*SXMR + B1*SX2MR + B2*SXMXNR - SXMYR)
A(5,1) = SXNR
A(5,2) = SXMXNR
A(5,3) = SX2NR
A(5,4) = B0*SXNR2
A(5,5) = B0*SXNR2 + B1*SXMXNR2 + 2.0*B2*SX2NR2 - SXNYR2
A(5,6) = -(B0*SXNR + B1*SXMXNR + B2*SX2NR - SXNYR)
RETURN
END

SUBROUTINE SIMEQN == SOLUTION OF SIMULTANEOUS LINEAR EQUATIONS
SUBROUTINE SIMEQN (A,NR,NC)
DIMENSION A(6,100)
DOUBLE PRECISION A,R,D,T
IF(NR - NC) 4,4,3
3 NCT = NC
GO TO 5
4 NCT = NR
5 K = 1
D = 1.
7 IF(A(K,K)) 12,8,12
8 DO 9 I = 1,K,NR
IF(A(I,K)) 10,9,10
9 CONTINUE
GO TO 17
10 DO 11 J = 1,NC
T = A(I,J)
A(I,J) = A(K,J)
11 A(K,J) = T
12 DO 16 I = 1,NR
IF(I - K) 13,16,13
13 DO 14 J = 1,NC
R(I) = (A(I,J)*A(K,K) - A(I,K)*A(K,J))/D
DO 15 J = 1,NC
A(I,J) = R(I)
14 CONTINUE
D = A(K,K)
K = K + 1
IF(K - NCT) 7,7,17
17 RETURN
END

```

APPENDIX IV

TWO-DIMENSIONAL PLOTTING PROGRAM

```

/JOB GO,TIME=20
/FILE DISK=(1,CRVFIT,NREC=9000),RSIZ=80,VOL=SYSFL1,DISP=(OLD,DELETE)

ABPLOT === PLOTTING PROGRAM

      ANTHONY P. BINOTTO
      JUNE 1, 1975

THIS PROGRAM WILL PLOT ANY SET OF NUMBERS ON X-Y COORDINATES
UTILIZING RETZKE'S PLOTTING PROGRAM.
THE USER MUST ENTER THE FOLLOWING CARDS IN ORDER.
/ID
/INCLUDE ABPLOT
DATA CARD 1. LABEL FOR X AXIS
DATA CARD 2. LABEL FOR Y AXIS
DATA CARD 3. TITLE OF PLOT
DATA CARD 4. N,NX,NY,LT,IEQ (IN FORMAT 513)
      WHERE...
      N = TOTAL NUMBER OF X,Y-PAIRS
      NX = 1 IF X IS PLOTTED AS LINEAR
           2 IF X IS PLOTTED AS LOG10(X)
           -1 OR -2 IF NEW SET OF AXIS IS NOT MADE
      NY = SAME AS FOR NX EXCEPT MINUS HAS NO EFFECT
      LT = -1 IF SYMBOLS ONLY ARE PLOTTED FOR EACH DATA POINT
           0 IF A LINE ONLY CONNECTS EACH DATA POINT
           +1 IF BOTH LINE AND SYMBOLS ARE PLOTTED
      IEQ = INTERGER EQUIVALENT OF PLOTTING SYMBOL (1-16)
DATA CARD 5-N. X AND Y COORDINATES IN 2E15.7 FORMAT
/END

      DIMENSION X(900),Y(900)
      COMMON LX(7),LY(7),ID(13),SVAL(4)
      ID(13) = 0
      IN = 1
      REMTND IN
      CALL GET(LX,24,IN)
      CALL GET(LY,24,IN)
      LX(7) = IVERR(LX,1,24)
      LY(7) = IVERR(LY,1,24)
1  READ (IN,2)(ID(I),I=1,12)
2  FORMAT (12A4)
3  IF (ICOMP(ID,1,249,4,1)) 3,6,3
4  READ (IN,4) N,NX,NY,LT,IEQ
5  FORMAT (5I3)
6  READ (IN,5)(X(I),Y(I),I=1,N)
7  FORMAT (2E15.7)
8  CALL GRAPH (X,Y,NX,NY,N,LT,IEQ)
9  GO TO 1
10 CALL FINAL
11 CALL EXIT
12 END

SUBROUTINE GRAPH - WRITTEN BY JAMES R RETZKE. 30 OCTOBER 1972

SUBROUTINE GRAPH (X,Y,NX,NY,N,LT,IEQ)
  DIMENSION X(1),Y(1),ISMBL(16)
  COMMON LX(7),LY(7),ID(13),SVAL(4)
  ISMBL(1)=170
  ISMBL(2)=183
  ISMBL(3)=175
  ISMBL(4)=176
  ISMBL(5)=181
  ISMBL(6)=182
  ISMBL(7)=185
  ISMBL(8)=171
  ISMBL(9)=172
  ISMBL(10)=173
  ISMBL(11)=174
  ISMBL(12)=177
  ISMBL(13)=178
  ISMBL(14)=179
  ISMBL(15)=180
  ISMBL(16)=184
  IF (ID(13)) 100,10,11
10 CALL ITLZ
  CALL OPT(1,4)
  CALL PLOT(0.0,-11.0,-3)
  CALL PLOT(0.0,1.5,-3)
11 IF (NX) 18,100,7
7  ID(13)=1
  CALL PLOT(7.75,-1.5,3)
  CALL PLOT(7.75,9.0,2)
  CALL PLOT(8.5,0.0,-3)
  IF (NX-1) 100,1,2
1  CALL SCALE(X,7.0,N,1)
  CALL AXIS(0.0,0.0,LX,-LX(7),7.0,0.0,X(N+1),X(N+2))
  GO TO 3
2  CALL SCALOG(X,7.0,N,1)
  CALL AXLOG(0.0,0.0,LX,-LX(7),7.0,0.0,X(N+1),X(N+2))
3  IF (NY-1) 100,4,5
4  CALL SCALE(Y,7.0,N,1)
  CALL AXIS(0.0,0.0,LY,LY(7),7.0,90.0,Y(N+1),Y(N+2))
  GO TO 6
5  CALL SCALOG(Y,7.0,N,1)
  CALL AXLOG(0.0,0.0,LY,LY(7),7.0,90.0,Y(N+1),Y(N+2))
6  SVAL(1)=X(N+1)
  SVAL(2)=X(N+2)
  SVAL(3)=Y(N+1)
  SVAL(4)=Y(N+2)
8  YPAGE=7.2-(ID(13)*0.35)
  IF (LT) 45,44,45
45 CALL DRAW(0.5,YPAGE+0.08,0.0,ISMBL(IEQ),1.0,0.0,0.35)
44 CALL SYMBOL(1.0,YPAGE,0.14,ID(0.0,48))
  ID(13)=ID(13)+1
  MX=IABS(NX)
  MY=IABS(NY)
  X(N+1)=SVAL(1)
  X(N+2)=SVAL(2)
  Y(N+1)=SVAL(3)
  Y(N+2)=SVAL(4)
  CALL LLOG(X,MX,Y,MY,N,1,LT,IEQ)
100 RETURN
  END
/DATE

```

00010
00020
00030
00040
00050
00060
00070
00080
00090
00100
00110
00120
00130
00140
00150
00160
00170
00180
00190
00200
00210
00220
00230
00240
00250
00260
00270
00280
00290
00300
00310
00320
00330
00340
00350
00360
00370
00380
00390
00400
00410
00420
00430
00440
00450
00460
00470
00480
00490
00500
00510
00520
00530
00540
00550
00560
00570
00580
00590
00600
00610
00620
00630
00640
00650
00660
00670
00680
00690
00700
00710
00720
00730
00740
00750
00760
00770
00780
00790
00800
00810
00820
00830
00840
00850
00860
00870
00880
00890
00900
00910
00920
00930
00940
00950
00960
00970
00980
00990
01000
01010
01020
01030
01040
01050
01060
01070
01080
01090
01100
01110
01120
01130
01140
01150

APPENDIX V

COMPUTER PROGRAM FOR THE ANALYSIS OF CONSTANT RATE FILTRATION DATA

```
/JOB GO,TIME=99
/FILE DISK=(1,NREC=10000),RSIZ=128
/FILE DISK=(2,PLOT1,NREC=3000),RSIZ=80,VOL=SYSFL1,DISP=(NEW,DELETE)
/FILE DISK=(3,PLOTJ,NREC=3000),RSIZ=80,VOL=SYSFL1,DISP=(NEW,KEEP)
/FILE DISK=(4,PRTOUT,NREC=1000),RSIZ=128,VOL=SYSFL1,DISP=(NEW,DELETE)
```

CRFILT == CONSTANT RATE FILTRATION

ANTHONY P. BINOTTO
NOVEMBER 13,1974

THIS PROGRAM IS DESIGNED TO CALCULATE...

1. AVERAGE SPECIFIC FILTRATION RESISTANCE
2. LOCAL SPECIFIC FILTRATION RESISTANCE
3. WET MAT DENSITY
4. COMPRESSIBILITY CONSTANTS M AND N
5. AVERAGE SPECIFIC SURFACE
6. AVERAGE SPECIFIC VOLUME

FROM DATA OBTAINED THROUGH CONSTANT RATE FILTRATION AND WET MAT COMPRESSIBILITY EXPERIMENTS. FOR ADDITIONAL INFORMATION REFER TO THE AUTHOR'S THESIS.

THE USER'S CARD DECK SHOULD CONTAIN THE FOLLOWING CARDS IN ORDER...

1. /ID XXXXXXXX
2. /INCLUDE CRFILT
3. /INCLUDE CMRPS
4. /INCLUDE FILTCV
5. /INCLUDE AVEVS
6. /DATA
 - A. TITLE IN A4 FORMAT (ALL OTHER DATA IN 9F8.0)
 - B. CHART READINGS FROM FILT. EXP., NOTE THAT
CHTSPD = 2 IN/MIN. CHANGE IF NECESSARY.
 - C. FILT. PAD WT. IN GRAMS, FLOW RATE IN CC./SEC.,
TEMP. IN DEG. C, AND EQUIV. VOLUME
 - D. COMP. PAD WT. AND PAD THICK. IN INCHES FOR WTS.
1 THRU 7 IN 9F8.0.
7. 999999999999
8. /END

```
DIMENSION DP(20),CP(20),CP3(20),T(20),Y(20),CHTRD(20),LOCR(20)
DIMENSION DP2(20),SCONC(20),PDTHCK(20),DPDT(20),DPTCP(20)
DIMENSION WPRESS(20),ITITLE(20),AVER(20)
DOUBLE PRECISION DP,CP,M,N,CP3,T,Y,DP2,SCONC,PDTHCK,MU,WR,UO,TEMP
DOUBLE PRECISION EQVOL,A,B0,B1,B2,EXPM,EXPN,DPDT,C1,B,AVESV,AVESW
DOUBLE PRECISION AVER,LOCR,WCP,DPTCP,AVEV
COMMON ITITLE,K,IOUT,JOUT,KOUT
COMMON M,N,MU,UO,A,WR,EQVOL
```

*** SAVE IOUT FOR PLOTS OF P VS T

*** SAVE JOUT FOR PLOTS OF DP/(T*SQRT(CP)) VS. CP**3

*** SAVE LOUT FOR PUNCHED OUTPUT

*** SAVE MOUT FOR PRINTED OUTPUT

MOUT = 1

J = 1

K = 9

CHTSPD = 2.

A = 45.51

WRITE (IOUT,9037)

WRITE (IOUT,9038)

WRITE (JOUT,9052)

WRITE (JOUT,9053)

WRITE (LOUT,9046)

WRITE (LOUT,9052)

WRITE (LOUT,9048)

1 READ (5,9009) ITITLE

IF (ICOMP (ITITLE,1,249,4,1)) 2,8,2

2 READ (5,9010) (CHTRD(I),I=J,K)

READ (5,9010) WR,UO,TEMP,EQVOL

READ (5,9010) WCP,(PDTHCK(I),I=1,7)

*** CALCULATION OF VISCOSITY (MU) FROM WATER TEMPERATURE

IF (TEMP - 20.) 3,3,4

3 ETA=(1301.7/(998.333+8.1855*(TEMP-20.))+.00585*((TEMP-20.)**2)))

MU = 10. ** (ETA - 3.30233)

GO TO 5

4 ETA=(1.3272*(20.-TEMP)-.001053*((TEMP-20.)**2))/(TEMP+105.)

MU = (10. ** ETA) * .01002

5 WRITE (MOUT,9011)

WRITE (MOUT,9012)

WRITE (MOUT,9012)

Appendix V (Continued)

```

WRITE (MOUT,9013) ITITLE
WRITE (MOUT,9012)
WRITE (MOUT,9012)
WRITE (MOUT,9014)
WRITE (MOUT,9015)
WRITE (MOUT,9016)
WRITE (MOUT,9017)
WRITE (MOUT,9018)
WRITE (MOUT,9019)
C1 = WR / EQVOL
CIP = C1 * 100.
DO 6 I=J,K
  T(I) = (CHTRD(I) * 60.D0) / CHTSPD
  WPRESS(I) = (I) * 10
  DP(I) = WPRESS(I) * 980.665D0
C*** 6 CALCULATION OF COMPRESSIBILITY CONSTANTS IN SUBROUTINE CMPRSS
  CALL CMPRSS (WCP,PDTHCK,N,M,CP,DP2,DP,T,SCONC,CP3,DPTCP)
  WRITE (MOUT,9020) (WPRESS(I),CHTRD(I),T(I),DP2(I),PDTHCK(I),
    * SCJNC(I),I=J,7)
  WRITE (MOUT,9120) (WPRESS(I),CHTRD(I),T(I),I=8,K)
  WRITE (MOUT,9021) WR,EQVOL,CIP
  WRITE (MOUT,9022) UO,MU,WCP
C*** CALCULATION OF AVERAGE AND LOCAL FILTRATION RESISTANCES
  B = (A**2) / (MU * (UO**2) * C1)
  CALL CRVFIT (T,DP,B0,B1,B2,EXPM,EXPN,J,K)
  DO 7 I=J,K
    DPDT(I) = EXPM*B1*(T(I)**(EXPM-1.)) + EXPN*B2*(T(I)**(EXPN-1.))
    AVER(I) = B * DP(I) / T(I)
    LOCR(I) = B * DPDT(I)
C*** 7 CALCULATION OF AVERAGE VALUES FOR V, SW, AND SV FROM SUB. AVEVS
  CALL AVEVS (DPTCP,CP3,B,N,AVEV,AVESW,AVESV,JOUT,ITITLE)
  WRITE (MOUT,9044)
  WRITE (MOUT,9023)
  WRITE (MOUT,9024)
  WRITE (MOUT,9025)
  WRITE (MOUT,9026)
  WRITE (MOUT,9027)
  WRITE (MOUT,9028)
  WRITE (MOUT,9029) (WPRESS(I),DP(I),AVER(I),LOCRI(I),CP(I),DPDT(I),
    *I=J,K)
  WRITE (MOUT,9044)
  WRITE (MOUT,9030)
  WRITE (MOUT,9031)
  WRITE (MOUT,9032)
  WRITE (MOUT,9033)
  WRITE (MOUT,9034) M,B0,EXPM
  WRITE (MOUT,9035) N,B1,EXPN
  WRITE (MOUT,9036) B2
  WRITE (MOUT,9044)
  WRITE (MOUT,9139)
  WRITE (MOUT,9140)
  WRITE (MOUT,9141) AVEV
  WRITE (MOUT,9142) AVESW
  WRITE (MOUT,9143) AVESV
  WRITE (MOUT,9044)
  WRITE (LOUT,9009) ITITLE
  WRITE (LOUT,9050)
  WRITE (LOUT,9045) (WPRESS(I),AVER(I),LOCRI(I),CP(I),I=J,K)
  GO TO 1
8 WRITE (IOUT,9051)
  WRITE (JOUT,9051)
  WRITE (LOUT,9051)
  WRITE (MOUT,9051)
  END FILE 1
  END FILE 2
  END FILE 3
  END FILE 4
  CALL EXIT
9009 FORMAT (20A4)
9010 FORMAT (9F8.0)
9011 FORMAT (1H1,16X,'*****')
9012 FORMAT (' ',16X,'*',85X,'*')
9013 FORMAT (' ',16X,'*',3X,20A4,2X,'*')
9014 FORMAT (' ',16X,'*****')
9015 FORMAT ('0','ORIGINAL DATA')
9016 FORMAT (' ','-----',//)
9017 FORMAT ('0',10X,'FILTRATION EXPERIMENT',31X,'COMPRESSIBILITY EXPE
  IRIMENT',/)
9018 FORMAT(' ',10X,'PRESSURE',7X,'CHART',9X,'TIME',20X,'PRESSURE',10X,
  1'PAD THICK.',8X,'SOLIDS CONC. ')
9019 FORMAT(' ',10X,'CM. H2O',8X,'READING',7X,'SEC.',20X,'DYNES/SQCM.'
  1,7X,'INCHES',12X,'G./CC.',//)
9020 FORMAT ('0',12X,F4.0,8X,F6.2,7X,F8.2,16X,F10.0,10X,F8.4,11X,F6.4)
9120 FORMAT ('0',12X,F4.0,8X,F6.2,7X,F8.2)
9021 FORMAT ('0',FILT. PAD WT. =',F7.4,' G.',5X,'EQ. VOL. =',F9.2,
  1' CC.',7X,'CONSISTENCY =',F5.3,' PERCENT')

```

```

C C C
C          FILTCV ==== CURVE FITTING
C
SUBROUTINE CRVFIT(X,Y,B0,B1,B2,M,N,J,K)
DIMENSION ITITLE(20),A(5,6),X(20),Y(20)
DOUBLE PRECISION X,Y,B0,B1,B2,M,N,A,ORIGM,ORIGN,DPTS
DOUBLE PRECISION DELB0,DELB1,DELB2,DELM,DELN
COMMON ITITLE,NPTS,IDOUT,JOUT,KOUT
C****  IOUT == OUTPUT STORED ON DISK OR TAPE FOR PLOTTING
WRITE (IDOUT,9001) ITITLE
WRITE (IDOUT,9002) NPTS
WRITE (IDOUT,9003) (X(I),Y(I),I=1,NPTS)
9001  FORMAT (20A4)
9002  FORMAT (I3,' 1 1 -1 3')
9003  FORMAT (2E15.7)
DPTS = 9.00
C****  INITIAL VALUES OF B0, B1, AND M ESTIMATED BY 'SUBROUTINE XM'
M = .01
N = 1.00
B0 = 27000.
B1 = 10000.
B2 = 75000.
TEST = 1000.
C***  DATA FIT MAY BE IMPROVED AT THE EXPENSE OF CALCULATION TIME
C***  BY DECREASING THE VALUE OF 'TEST'.
1  MCOUNT = 0
   NCOUNT = 0
   ORIGM = M
   ORIGN = N
   TEST1 = 0.0
2  CALL SUM (X,Y,NPTS,B0,B1,B2,M,N,A,J,K)
   CALL SIMEQ (A,5,6)
   DELB0 = A(1,6) / A(1,1)
   DELB1 = A(2,6) / A(2,2)
   DELB2 = A(3,6) / A(3,3)
   DELM = A(4,6) / A(4,4)
   DELN = A(5,6) / A(5,5)
   TEST2 = DABS(DELB0) + DABS(DELB1) + DABS(DELB2) + DABS(DELM)
*  DABS(DELN)
   DIFF = TEST2 - TEST1
   IF (ABS(DIFF)-TEST) 6,6,3
3  TEST1 = TEST2
   NCOUNT = NCOUNT + 1
   B0 = B0 + DELB0
   B1 = B1 + DELB1
   B2 = B2 + DELB2
   IF (NCOUNT-100) 2,2,4.
C  4  NCOUNT = 0
C     M = M + DELM
C     N = N + DELN
C     MCOUNT = MCOUNT + 1

```


Appendix V (Continued)

```

5  IF (MCDUNT - 99) 2,2,5
    M = ORIGM
    N = ORIGN + 0.01
    GO TO 1
6  CALL EQN (B0,B1,B2,M,N,IOUT,X,J,K)
    RETURN
END

C
C
C
C
SUBROUTINE EQN === GENERATION OF PLOTTING POINTS

THIS SUBROUTINE GENERATES DATA POINTS FROM THE CALCULATED
EQUATION TO BE USED IN PLOTTING PROGRAM 'ABPLOT'.
SUBROUTINE EQN (B0,B1,B2,M,N,IOUT,X,J,K)
DIMENSION X(20)
DOUBLE PRECISION X,DPTS,XINCR,B0,B1,B2,M,N,P,R
NPTS = 200
DPTS = NPTS
XINCR = (X(K) - X(J)) / DPTS
WRITE (IOUT,9002) M,N
WRITE (IOUT,9003) NPTS
P = X(J)
DO 1 I=1,NPTS
  R = B0 + B1 * (P ** M) + B2 * (P ** N)
  WRITE (IOUT,9004) P,R
  P = P + XINCR
1 RETURN
9002 FORMAT ('P = B0 + B1*(T**',F4.2,',) + B2*(T**',F4.2,',)')
9003 FORMAT (I3,' -1 -1 0')
9004 FORMAT (2D15.7)
END

C
C
C
SUBROUTINE SUM === CALCULATION OF SUM OF SQUARES

SUBROUTINE SUM (X,Y,NPTS,B0,B1,B2,M,N,A,J,K)
DIMENSION X(12),Y(12),A(5,6)
DOUBLE PRECISION X,Y,B0,B1,B2,M,N,A,PTS,SXMYR2
DOUBLE PRECISION SY,SXM,SXN,SXMY,SX2M,SXMXN,SXNY,SX2N,SXMYR,SXMR
DOUBLE PRECISION SX2MR,SXMXNR,SXNYR,SXNR,SXMR2,SX2MR2,SXMNR2
DOUBLE PRECISION SXNR2,SX2NR2,SXNYR2,SX2NR,XN,XM,X2M,X2N,R,R2
PTS = NPTS
SY = 0.0
SXM = 0.0
SXN = 0.0
SXMY = 0.0
SX2M = 0.0
SXMXN = 0.0
SXNY = 0.0
SX2N = 0.0
SXMYR = 0.0
SXMR = 0.0
SX2MR = 0.0
SXMXNR = 0.0
SXNYR = 0.0
SXNR = 0.0
SX2NR = 0.0
SXMR2 = 0.0
SX2MR2 = 0.0
SXMYR2 = 0.0
SXNR2 = 0.0
SX2NR2 = 0.0
SXVYR2 = 0.0
DO 1 I=J,K
  XM = X(I) ** M
  XN = X(I) ** N
  X2M = XM ** 2
  X2N = XN ** 2
  R = DLOG(X(I))
  R2 = R ** 2
  SY = SY + Y(I)
  SXM = SXM + XM
  SXN = SXN + XN
  SXMY = SXMY + (XM * Y(I))
  SX2M = SX2M + X2M
  SXMXN = SXMXN + (XM * XN)
  SXNY = SXNY + (XN * Y(I))
  SX2N = SX2N + X2N
  SXMYR = SXMYR + (XM * Y(I) * R)
  SXMR = SXMR + (XM * R)
  SX2MR = SX2MR + (X2M * R)
  SXMXNR = SXMXNR + (XM * XN * R)
  SXNYR = SXNYR + (XN * Y(I) * R)
  SXNR = SXNR + (XN * R)
  SX2NR = SX2NR + (X2N * R)
  SXMR2 = SXMR2 + (XM * R2)
  SX2MR2 = SX2MR2 + (X2M * R2)
  SXMNR2 = SXMNR2 + (XM * XN * R2)
  SXMYR2 = SXMYR2 + (XM * Y(I) * R2)

```

Appendix V (Continued)

```

1  SXNR2 = SXNR2 + (XN * R2)
   SX2NR2 = SX2NR2 + (X2N * R2)
   SXNYR2 = SXNYR2 + (XN * Y(I) * R2)
   A(1,1) = PTS
   A(1,2) = SXM
   A(1,3) = SXN
   A(1,4) = B1 * SXMR
   A(1,5) = B2 * SXNR
   A(1,6) = -(PTS*B0 + B1*SXM + B2*SXN - SY)
   A(2,1) = SXM
   A(2,2) = SX2M
   A(2,3) = SXXN
   A(2,4) = B0*SXMR + 2.0*B1*SX2MR + B2*SXXNR - SXMYR
   A(2,5) = B2*SXXNR
   A(2,6) = -(B0*SXM + B1*SX2M + B2*SXXN - SXMY)
   A(3,1) = SXN
   A(3,2) = SXXN
   A(3,3) = SX2N
   A(3,4) = SXXNR
   A(3,5) = B0*SXNR + B1*SXXNR + 2.0*B2*SX2NR - SXNYR
   A(3,6) = -(B0*SXN + B1*SXXN + B2*SX2N - SXNY)
   A(4,1) = SXMR
   A(4,2) = SX2MR
   A(4,3) = SXXNR
   A(4,4) = B0*SXMR2 + 2.0*B1*SX2MR2 + B2*SXXNR2 - SXMYR2
   A(4,5) = B2*SXXNR2
   A(4,6) = -(B0*SXMR + B1*SX2MR + B2*SXXNR - SXMYR)
   A(5,1) = SXNR
   A(5,2) = SXXNR
   A(5,3) = SX2NR
   A(5,4) = B1*SXXNR2
   A(5,5) = B0*SXNR2 + B1*SXXNR2 + 2.0*B2*SX2NR2 - SXNYR2
   A(5,6) = -(B0*SXNR + B1*SXXNR + B2*SX2NR - SXNYR)
   RETURN
END

```

SUBROUTINE SIMEQN == SOLUTION OF SIMULTANEOUS LINEAR EQUATIONS

```

SUBROUTINE SIMEQ (A,NR,NC)
  DIMENSION A(5,6),R(100)
  DOUBLE PRECISION A,R,D,T
  IF(NR - NC) 2,2,1
1  NCT = NC
  GO TO 3
2  NCT = NR
3  K = 1
  D = 1.
4  IF(A(K,K)) 9,5,9
5  DO 6 I = K,NR
  IF(A(I,K)) 7,6,7
6  CONTINUE
  GO TO 14
7  DO 8 J = 1,NC
  T = A(I,J)
  A(I,J) = A(K,J)
8  A(K,J) = T
9  DO 13 I = 1,NR
  IF(I - K) 10,13,10
10 DO 11 J = 1,NC
  R(J) = (A(I,J)*A(K,K) - A(I,K)*A(K,J))/D
  DO 12 J = 1,NC
12 A(I,J) = R(J)
13 CONTINUE
  D = A(K,K)
  K = K + 1
  IF(K - NCT) 4,4,14
14 RETURN
END

```

SUBROUTINE EXPDNM = ESTIMATION OF INITIAL VALUE OF EXPONENT ***

```

SUBROUTINE EXPDNM (X,Y,NPTS,BOMIN,B1MIN,MMIN,G,H,MAXM)
  DIMENSION X(12),Y(12)
  DOUBLE PRECISION X,XM,Y,M,PTS,SUMXM,SUMX2M,SUMY,SUMXMY,SMIN
  DOUBLE PRECISION S,B0,B1,MMIN,BOMIN,B1MIN,MAXM
  INTEGER G,H
  PTS = NPTS
  M = MMIN
  UNIT = .0001
  SMIN = 16.0070
  J = 1
  SUMXM = 0.
  SUMX2M = 0.
  SUMY = 0.
  SUMXMY = 0.
  DO 7 I=G,H
  XM = X(I) ** M
  SUMXM = SUMXM + XM

```

Appendix V (Continued)

```

SUMX2M = SUMX2M + (XM**2)
SUMY = SUMY + Y(I)
7 SUMXMY = SUMXMY + (XM * Y(I))
Q1 = SUMXMY - (SUMXM * SUMY)/PTS
Q2 = SUMX2M - (SUMXM ** 2)/PTS
B1 = Q1 / Q2
B0 = (SUMY - B1 * SUMXM) / PTS
S = DSQRT(B0**2 + B1**2)
IF (S - SMIN) 8,9,9
8 SMIN = S
B0MIN = B0
B1MIN = B1
MMIN = M
9 J = J + 1
M = M + UNIT
IF (M - MAXM) 6,6,11
11 RETURN
END

```

SUBROUTINE CMPRSS === COMPRESSIBILITY

ANTHONY P. BINOTTO
JUNE 16, 1975

THIS SUBROUTINE IS USED TO CALCULATE THE MAT SOLIDS
CONCENTRATION FROM MEASUREMENTS OF PAD THICKNESS AND THE
O.D. WT. OF THE MAT. THE PROCEDURE INVOLVES A LEAST SQUARES
APPROACH TO COMPUTING COMPRESSIBILITY CONSTANTS M AND N.

```

C
C
C
C
C
C
C
SUBROUTINE CMPRSS (W,PDTHCK,N,M,CP,DP2,DP,T,MATCON,CP3,DPTCP)
DIMENSION PDTHCK(20),MATCON(20),LMC(20),LDP2(20),DP2(20)
DIMENSION DP(20),CP(20),T(20),CP3(20),DPTCP(20)
DOUBLE PRECISION MATCON,LMC,LDP2,SUMY,SUMY2,SUMX,SUMX2,SUMXY,Q1
DOUBLE PRECISION Q2,N,M,SUMM,DP2,CP,CP3,DPTCP,DP,PDTHCK,T,W
AREA = 45.5400
NPTS = 7
DP2(1) = 8150.00
DP2(2) = 13100.00
DP2(3) = 22900.00
DP2(4) = 37700.00
DP2(5) = 62300.00
DP2(6) = 96400.00
DP2(7) = 145800.00
DO 1 I=1,7
MATCON(I) = W / (AREA * PDTHCK(I) * 2.54)
LMC(I) = DLOG(MATCON(I))
1 LDP2(I) = DLOG(DP2(I))
CALL LINREG (LDP2,LMC,NPTS,M,N,1,7)
M = DEXP(M)
DO 2 I=1,9
CP(I) = M * DP(I) ** N
CP3(I) = CP(I) ** 3
2 DPTCP(I) = DP(I) / (T(I) * DSQRT(CP(I)))
RETURN
END

```

LINREG === LINEAR REGRESSION
ANTHONY P. BINOTTO
JUNE 16, 1975

THIS SUBROUTINE IS USED TO CALCULATE THE STRAIGHT LINE
RELATIONSHIP BETWEEN PAIRS OF X,Y-DATA

```

C
C
C
C
C
C
C
SUBROUTINE LINREG (X,Y,NPTS,INTCPT,SLOPE,J,K)
DIMENSION X(20),Y(20)
DOUBLE PRECISION X,Y,SUMX,SUMX2,SUMY,SUMXY,SLOPE,INTCPT,Q1,Q2,PTS
DOUBLE PRECISION STDERR,XBAR,YBAR,SYP2,S2X
PTS = NPTS
SUMY = 0.00
SUMX = 0.00
SUMX2 = 0.00
SUMXY = 0.00
SYP2 = 0.00
DO 1 I=J,K
SUMY = SUMY + Y(I)
SUMX = SUMX + X(I)
SUMX2 = SUMX2 + (X(I) ** 2)
SUMXY = SUMXY + (X(I) * Y(I))
1 Q1 = SUMXY - (SUMX * SUMY)/PTS
Q2 = SUMX2 - (SUMX ** 2)/PTS
SLOPE = Q1/Q2
INTCPT = (SUMY - SLOPE * SUMX) / PTS
YBAR = SUMY / PTS
XBAR = SUMX / PTS
C*** CALCULATION OF STATISTICAL QUANTITIES USED TO COMPUTE C.L.
DO 2 I=J,K
2 SYP2 = SYP2 + (Y(I) - (YBAR + SLOPE*(X(I) - XBAR))) ** 2
STDERR = SYP2 / (PTS - 2.00)
S2X = (SUMX2 - (SUMX**2)/PTS)/(PTS - 1.00)
RETURN
END

```

```
C
      AVEVS === CALCULATION OF (V), (SW), AND (SV)
      SUBROUTINE AVEVS (DPTCP, CP3, B, N, AVEV, AVESW, AVESV, JOUT, ITITLE)
      DIMENSION DPTCP(20), CP3(20), ITITLE(20)
      DOUBLE PRECISION DPTCP, CP3, B, N, NOVER2, AVEV, AVESW, AVESV, SLOPE
      DOUBLE PRECISION INTCP
      WRITE (JOUT, 9001) ITITLE
      WRITE (JOUT, 9002)
      WRITE (JOUT, 9003) (CP3(I), DPTCP(I), I=1, 9)
C*** J IS THE INITIAL POINT OF LINEAR INTERPRETATION OF THE DPTCP
C*** VS. CP3 PLOT. K IS THE FINAL POINT.
      J = 5
      K = 9
      NPTS = K - J + 1
      WRITE (JOUT, 9004) J, K
      WRITE (JOUT, 9005)
      NOVER2 = 1.00 - N / 2.00
      CALL LINREG (CP3, DPTCP, NPTS, INTCP, SLOPE, J, K)
      AVEV = ((SLOPE/INTCP) / (.57.D0*(NOVER2**6))) ** (1.00/3.00)
      DPTCP(1) = INTCP + SLOPE * CP3(1)
      DPTCP(K) = INTCP + SLOPE * CP3(K)
      AVESW = DSQRT((B*DSQRT(AVEV)*INTCP) / (3.500*NOVER2))
      AVESV = AVESW / AVEV
      WRITE (JOUT, 9003) CP3(1), DPTCP(1), CP3(K), DPTCP(K)
9001 FORMAT (20A4)
9002 FORMAT (' 9 1 1 -1 3')
9003 FORMAT (2E15.7)
9004 FORMAT ('LIN. REG. PTS. ', 11, ' THRU ', 11)
9005 FORMAT (' 2 -1 -1 0')
      RETURN
      END

/DATA
      FIELD FRACTION RETAINED ON 65 MESH          FIBER LENGTH = 1.63 MM.
      7.4633 11.6833 14.9100 17.5500 19.8000 21.8667 23.6967 25.2900 26.7633
      6.7979 78.5667 26.0000 65132.2
      6.1767 1.0338 0.8665 0.7039 0.5848 0.4851 0.4124 0.3536 F-65AVE
      FIELD FRACTION RETAINED ON 20 MESH          FIBER LENGTH = 3.05 MM.
      7.1475 11.1175 14.1275 16.6725 18.9375 20.8100 22.5775 24.2050 25.6825
      9.7035 78.2499 23.1250 62375.0
      7.2896 1.2830 1.0754 0.8736 0.7258 0.6021 0.5118 0.4388 F-20AVE
      FIELD FRACTION RETAINED ON 10 MESH          FIBER LENGTH = 3.94 MM.
      9.2700 14.9000 19.5067 23.4800 27.1100 30.4233 33.3600 36.1167 38.6800
      16.8514 81.1000 24.4000 97743.3
      11.2539 2.0327 1.7037 1.3841 1.1498 0.9538 0.8109 0.6952 F-10AVE
      FLOC FRACTION RETAINED ON 65 MESH          FIBER LENGTH = 1.74 MM.
      6.6767 10.8633 14.3600 17.4400 20.0733 22.5233 24.7666 26.8633 28.8267
      11.2212 84.9000 20.1667 75825.4
      8.8940 1.6190 1.3570 1.1024 0.9158 0.7597 0.6458 0.5537 B-65IIAV
      FLOC FRACTION RETAINED ON 65 MESH          FIBER LENGTH = 2.07 MM.
      6.1280 10.1960 13.5600 16.5120 19.1300 21.5700 23.8380 26.0020 27.9060
      15.3695 87.3800 23.5000 74956.9
      10.9453 2.0490 1.7174 1.3952 1.1590 0.9615 0.8174 0.7008 B-65IAVE
      FLOC FRACTION RETAINED ON 20 MESH          FIBER LENGTH = 2.98 MM.
      8.6375 14.4900 19.3725 23.7925 27.8100 31.5525 35.0875 38.3225 41.1600
      20.8284 87.6000 23.7000 110658.8
      13.3006 2.5497 2.1370 1.7361 1.4422 1.1964 1.0171 0.8720 B-20AVE
      FLOC FRACTION RETAINED ON 10 MESH          FIBER LENGTH = 4.13 MM.
      8.1100 13.5100 18.1433 22.5133 26.3867 30.1700 33.8033 37.2933 40.7133
      30.3815 89.9666 26.8000 111436.7
      11.5314 2.2036 1.8469 1.5004 1.2465 1.0340 0.8790 0.7536 B-10AVE
      WHOLE PULP RETAINED ON 65 MESH          FIBER LENGTH = 1.49 MM.
      6.71 10.93 14.28 17.08 19.62 21.73 23.84 25.77 27.42 W-65-1F
      9.8641 77.3 21.9 66882.94 19.62 21.73 23.84 25.77 27.42 W-65-1F
      8.5246 1.5735 1.3188 1.0714 0.8900 0.7383 0.6277 0.5381 W-65AVE
      WHOLE PULP RETAINED ON 20 MESH          FIBER LENGTH = 2.76 MM.
      6.29 9.82 12.90 15.50 17.76 19.97 22.00 23.80 25.39 W-20-1F
      17.1414 77.3 21.4 61389.57 19.97 22.00 23.80 25.39 W-20-1F
      13.9570 2.7308 2.2888 1.8594 1.5447 1.2814 1.0893 0.9339 W-20AVE
      WHOLE PULP RETAINED ON 10 MESH          FIBER LENGTH = 3.88 MM.
      8.00 13.40 17.75 21.77 25.33 28.72 31.95 34.86 37.65 W-10-1F
      24.8004 77.3 21.3 90146.69 28.72 31.95 34.86 37.65 W-10-1F
      17.9365 3.4449 2.8874 2.3457 1.9486 1.6165 1.3742 1.1782 W-10AVE
      WHOLE PULP -- NOT CLASSIFIED
      6.07 9.50 12.30 14.69 16.83 18.80 20.65 22.37 23.88 W-NC-AF
      13.5742 77.3 22.5 58602.66 16.83 18.80 20.65 22.37 23.88 W-NC-AF
      10.9475 2.1378 1.7918 1.4557 1.2093 1.0032 0.8528 0.7311 W-NC-AVE
      999999999999999999
```

APPENDIX VI

OUTPUT FROM PROGRAM CRFILT USING AVERAGED PRESSURE VS. TIME
DATA FROM CONSTANT RATE FILTRATION, AND AVERAGED
COMPRESSIBILITY DATA

Calculated values are presented for:

Average specific filtration resistance;

Local specific filtration resistance;

Apparent wet mat density;

Average specific surface; and

Average specific volume.

Appendix VI (Continued)

 * FIELD FRACTION RETAINED ON 65 MESH FIBER LENGTH = 1.63 MM. *
 * *****

ORIGINAL DATA

FILTRATION EXPERIMENT			COMPRESSIBILITY EXPERIMENT		SOLIDS CONC. G./CC.
PRESSURE CM. H ₂ O	CHART READING	TIME SEC.	PRESSURE DYNES/SQCM.	PAD THICK. INCHES	
10.	7.46	223.90	8150.	1.0338	0.0517
20.	11.68	350.50	13100.	0.8665	0.0616
30.	14.91	447.30	22900.	0.7039	0.0759
40.	17.55	526.50	37700.	0.5848	0.0913
50.	19.80	594.00	62300.	0.4851	0.1101
60.	21.87	656.00	96400.	0.4124	0.1295
70.	23.70	710.90	145800.	0.3536	0.1510
80.	25.29	758.70			
90.	26.76	802.90			

FILT. PAD WT. = 6.7979 G. EQ. VOL. = 65132.20 CC. CONSISTENCY = 0.010 PERCENT
 FLOW RATE = 78.6 CC./SEC. H₂O VISC. = 0.008705 POISE COMP. PAD WT. = 6.1767 G.

FILTRATION RESISTANCE AND MAT SOLIDS CONCENTRATION AS FUNCTIONS OF PRESSURE

PRESSURE		FILTRATION RESISTANCE		MAT DENSITY C G./CC.	DP/DT
P CM. H ₂ O	DYNES/SQCM.	AVERAGE (R) CM./G.	LOCAL R CM./G.		
10.	9807.	0.1617D 08	0.2608D 08	0.0553	70.63
20.	19613.	0.2066D 08	0.3298D 08	0.0716	89.32
30.	29420.	0.2429D 08	0.4130D 08	0.0833	111.82
40.	39227.	0.2751D 08	0.4928D 08	0.0927	133.44
50.	49033.	0.3048D 08	0.5673D 08	0.1007	153.63
60.	58840.	0.3312D 08	0.6403D 08	0.1078	173.39
70.	68647.	0.3566D 08	0.7081D 08	0.1141	191.75
80.	78453.	0.3819D 08	0.7694D 08	0.1199	208.35
90.	88260.	0.4059D 08	0.8278D 08	0.1253	224.17

EXPERIMENTAL EMPIRICAL CONSTANTS

$$C = M * (P ** N)$$

WHERE...

$$M = 0.1812D-02$$

$$N = 0.3720$$

$$P = B0 + B1*(T**EXPM) + B2*(T**EXPN)$$

WHERE...

$$B0 = -3.77744D 06 \quad \text{EXPM} = 0.10002D-01$$

$$B1 = 3.74261D 06 \quad \text{EXPN} = 0.24054D 01$$

$$B2 = 0.73725D-02$$

AVERAGE VALUES FOR SPECIFIC VOLUME AND SURFACE

$$\text{AVERAGE SPECIFIC VOLUME, (V)} = 2.50$$

$$\text{AVERAGE SPECIFIC SURFACE, (SW)} = 6500.$$

$$\text{AVERAGE SPECIFIC SURFACE, (SV)} = 2602.$$

Appendix VI (Continued)

*
* FIELD FRACTION RETAINED ON 20 MESH FIBER LENGTH = 3.05 MM. *
*

ORIGINAL DATA

FILTRATION EXPERIMENT			COMPRESSIBILITY EXPERIMENT		
PRESSURE CM. H ₂ O	CHART READING	TIME SEC.	PRESSURE DYNES/SQCM.	PAD THICK. INCHES	SOLIDS CONC. G./CC.
10.	7.15	214.42	8150.	1.2830	0.0491
20.	11.12	333.52	13100.	1.0754	0.0586
30.	14.13	423.82	22900.	0.8736	0.0721
40.	16.67	500.17	37700.	0.7258	0.0868
50.	18.94	568.13	62300.	0.6021	0.1047
60.	20.81	624.30	96400.	0.5118	0.1231
70.	22.58	677.32	145800.	0.4388	0.1436
80.	24.20	726.15			
90.	25.68	770.47			

FILT. PAD WT. = 9.7035 G. EQ. VOL. = 62375.00 CC. CONSISTENCY = 0.016 PERCENT
FLOW RATE = 78.2 CC./SEC. H₂O VISC. = 0.009299 POISE COMP. PAD WT. = 7.2896 G.

FILTRATION RESISTANCE AND MAT SOLIDS CONCENTRATION AS FUNCTIONS OF PRESSURE

PRESSURE		FILTRATION RESISTANCE		MAT	DP/DT
P		AVERAGE	LOCAL	DENSITY	
CM. H ₂ O	DYNES/SQCM.	(R)	R	C	
		CM./G.	CM./G.	G./CC.	
10.	9807.	0.1069D 08	0.1721D 08	0.0526	73.58
20.	19613.	0.1375D 08	0.2227D 08	0.0681	95.24
30.	29420.	0.1623D 08	0.2756D 08	0.0792	117.85
40.	39227.	0.1834D 08	0.3258D 08	0.0881	139.35
50.	49033.	0.2018D 08	0.3737D 08	0.0958	159.82
60.	58840.	0.2204D 08	0.4151D 08	0.1025	177.53
70.	68647.	0.2370D 08	0.4555D 08	0.1085	194.82
80.	78453.	0.2526D 08	0.4938D 08	0.1140	211.17
90.	88260.	0.2679D 08	0.5293D 08	0.1192	226.34

EXPERIMENTAL EMPIRICAL CONSTANTS

$$C = M * (P ** N)$$

WHERE...

$$M = 0.1723D-02$$

$$N = 0.3720$$

$$P = B0 + B1*(T**EXPM) + B2*(T**EXPN)$$

WHERE...

$$B0 = -0.64198D 06$$

$$B1 = 0.61381D 06$$

$$B2 = 0.21936D-01$$

$$EXPM = 0.10000D-01$$

$$EXPN = 0.22618D 01$$

AVERAGE VALUES FOR SPECIFIC VOLUME AND SURFACE

$$\text{AVERAGE SPECIFIC VOLUME, (V)} = 2.59$$

$$\text{AVERAGE SPECIFIC SURFACE, (SW)} = 5438.$$

$$\text{AVERAGE SPECIFIC SURFACE, (SV)} = 2099.$$

Appendix VI (Continued)

 *
 * FIELD FRACTION RETAINED ON 10 MESH FIBER LENGTH = 3.94 MM. *
 *

ORIGINAL DATA

FILTRATION EXPERIMENT			COMPRESSIBILITY EXPERIMENT		
PRESSURE CM. H2O	CHART READING	TIME SEC.	PRESSURE DYNES/SQCM.	PAD THICK. INCHES	SOLIDS CONC. G./CC.
10.	9.27	278.10	8150.	2.0327	0.0479
20.	14.90	447.00	13100.	1.7037	0.0571
30.	19.51	585.20	22900.	1.3841	0.0703
40.	23.48	704.40	37700.	1.1498	0.0846
50.	27.11	813.30	62300.	0.9538	0.1020
60.	30.42	912.70	96400.	0.8109	0.1200
70.	33.36	1000.80	145800.	0.6952	0.1399
80.	36.12	1083.50			
90.	38.68	1160.40			

FILT. PAD WT. = 16.8514 G. EQ. VOL. = 97743.30 CC. CONSISTENCY = 0.017 PERCENT
 FLOW RATE = 81.1 CC./SEC. H2O VISC. = 0.009028 POISE COMP. PAD WT. = 11.2539 G.

FILTRATION RESISTANCE AND MAT SOLIDS CONCENTRATION AS FUNCTIONS OF PRESSURE

PRESSURE		FILTRATION RESISTANCE		MAT	DP/DT
P		AVERAGE	LOCAL	DENSITY	
CM. H2O	DYNES/SQCM.	(R)	R	C	
		CM./G.	CM./G.	G./CC.	
10.	9807.	0.71340 07	0.11100 08	0.0513	54.87
20.	19613.	0.88770 07	0.13030 08	0.0664	64.38
30.	29420.	0.10170 08	0.15300 08	0.0772	75.62
40.	39227.	0.11270 08	0.17450 08	0.0859	86.25
50.	49033.	0.12200 08	0.19490 08	0.0933	96.35
60.	58840.	0.13040 08	0.21400 08	0.0999	105.76
70.	68647.	0.13880 08	0.23100 08	0.1057	114.20
80.	78453.	0.14650 08	0.24720 08	0.1111	122.18
90.	88260.	0.15390 08	0.26230 08	0.1161	129.63

EXPERIMENTAL EMPIRICAL CONSTANTS

$$C = M * (P ** N)$$

WHERE...

$$M = 0.16790-02$$

$$N = 0.3720$$

$$P = B0 + B1*(T**EXPM) + B2*(T**EXPN)$$

WHERE...

$$B0 = -0.637350 06$$

$$B1 = 0.607420 06$$

$$B2 = 0.758080-01$$

$$EXPM = 0.100060-01$$

$$EXPN = 0.195380 01$$

AVERAGE VALUES FOR SPECIFIC VOLUME AND SURFACE

$$\text{AVERAGE SPECIFIC VOLUME, (V)} = 2.30$$

$$\text{AVERAGE SPECIFIC SURFACE, (SW)} = 4277.$$

$$\text{AVERAGE SPECIFIC SURFACE, (SV)} = 1856.$$

Appendix VI (Continued)

 * FLOC FRACTION RETAINED ON 65 MESH FIBER LENGTH = 1.74 MM. *
 * *****

ORIGINAL DATA

FILTRATION EXPERIMENT			COMPRESSIBILITY EXPERIMENT		SOLIDS CONC. G./CC.
PRESSURE CM. H2O	CHART READING	TIME SEC.	PRESSURE DYNES/SQCM.	PAD THICK. INCHES	
10.	6.68	200.30	8150.	1.6190	0.0475
20.	10.86	325.90	13100.	1.3570	0.0567
30.	14.36	430.80	22900.	1.1024	0.0697
40.	17.44	523.20	37700.	0.9158	0.0840
50.	20.07	602.20	62300.	0.7597	0.1012
60.	22.52	675.70	96400.	0.6458	0.1191
70.	24.77	743.00	145800.	0.5537	0.1389
80.	26.86	805.90			
90.	28.83	864.80			

FILT. PAD WT. = 11.2212 G. EQ. VOL. = 75825.40 CC. CONSISTENCY = 0.015 PERCENT
 FLOW RATE = 84.9 CC./SEC. H2O VISC. = 0.009979 POISE COMP. PAD WT. = 8.8940 G.

FILTRATION RESISTANCE AND MAT SOLIDS CONCENTRATION AS FUNCTIONS OF PRESSURE

PRESSURE		FILTRATION RESISTANCE AVERAGE	LOCAL	MAT DENSITY	DP/DT
P		(R)	R	C	
CM. H2O	DYNES/SQCM.	CM./G.	CM./G.	G./CC.	
10.	9807.	0.9526D 07	0.1403D 08	0.0509	72.08
20.	19613.	0.1171D 08	0.1664D 08	0.0658	85.51
30.	29420.	0.1329D 08	0.1962D 08	0.0766	100.85
40.	39227.	0.1459D 08	0.2245D 08	0.0852	115.37
50.	49033.	0.1584D 08	0.2493D 08	0.0926	128.13
60.	58840.	0.1694D 08	0.2727D 08	0.0991	140.14
70.	68647.	0.1798D 08	0.2942D 08	0.1049	151.19
80.	78453.	0.1894D 08	0.3143D 08	0.1103	161.54
90.	88260.	0.1986D 08	0.3332D 08	0.1152	171.24

EXPERIMENTAL EMPIRICAL CONSTANTS

$$C = M * (P ** N)$$

WHERE...

$$N = 0.1666D-02$$

$$M = 0.3720$$

$$P = 80 + B1*(T**EXPM) + B2*(T**EXPN)$$

WHERE...

$$B0 = -0.56162D 06$$

$$B1 = 0.53758D 06$$

$$B2 = 0.18961D 00$$

$$EXPM = 0.99979D-02$$

$$EXPN = 0.19052D 01$$

AVERAGE VALUES FOR SPECIFIC VOLUME AND SURFACE

$$\text{AVERAGE SPECIFIC VOLUME, (V)} = 2.27$$

$$\text{AVERAGE SPECIFIC SURFACE, (SW)} = 4891.$$

$$\text{AVERAGE SPECIFIC SURFACE, (SV)} = 2158.$$

Appendix VI (Continued)

 * FLOC FRACTION RETAINED ON 65 MESH FIBER LENGTH = 2.07 MM. *
 * *****

ORIGINAL DATA

FILTRATION EXPERIMENT			COMPRESSIBILITY EXPERIMENT		
PRESSURE CM. H2O	CHART READING	TIME SEC.	PRESSURE DYNES/SQCM.	PAD THICK. INCHES	SOLIDS CONC. G./CC.
10.	6.13	183.84	8150.	2.0490	0.0462
20.	10.20	305.88	13100.	1.7174	0.0551
30.	13.56	406.80	22900.	1.3952	0.0678
40.	16.51	495.36	37700.	1.1590	0.0816
50.	19.13	573.90	62300.	0.9615	0.0984
60.	21.57	647.10	96400.	0.8174	0.1158
70.	23.84	715.14	145800.	0.7008	0.1350
80.	26.00	780.06			
90.	27.91	837.18			

FILT. PAD WT. = 15.3695 G. EQ. VOL. = 74956.90 CC. CONSISTENCY = 0.021 PERCENT
 FLOW RATE = 87.4 CC./SEC. H2O VISC. = 0.009218 POISE COMP. PAD WT. = 10.9453 G.

FILTRATION RESISTANCE AND MAT SOLIDS CONCENTRATION AS FUNCTIONS OF PRESSURE

PRESSURE		FILTRATION RESISTANCE		MAT DENSITY C G./CC.	DP/DT
P CM. H2O	DYNES/SQCM.	AVERAGE (R) CM./G.	LOCAL R CM./G.		
10.	9807.	0.7656D 07	0.1054D 08	0.0495	73.46
20.	19613.	0.9203D 07	0.1280D 08	0.0640	89.15
30.	29420.	0.1038D 08	0.1496D 08	0.0744	104.21
40.	39227.	0.1137D 08	0.1688D 08	0.0829	117.59
50.	49033.	0.1226D 08	0.1857D 08	0.0900	129.37
60.	58840.	0.1305D 08	0.2012D 08	0.0963	140.19
70.	68647.	0.1378D 08	0.2155D 08	0.1020	150.12
80.	78453.	0.1443D 08	0.2289D 08	0.1072	159.46
90.	88260.	0.1513D 08	0.2405D 08	0.1120	167.57

EXPERIMENTAL EMPIRICAL CONSTANTS

$$C = M * (P ** N)$$

WHERE...

$$M = 0.1620D-02$$

$$N = 0.3720$$

$$P = B0 + B1*(T**EXPM) + B2*(T**EXPN)$$

WHERE...

$$B0 = -0.39492D 06$$

$$B1 = 0.37901D 06$$

$$B2 = 0.57300D 00$$

$$EXPM = 0.99969D-02$$

$$EXPN = 0.17557D 01$$

AVERAGE VALUES FOR SPECIFIC VOLUME AND SURFACE

$$\text{AVERAGE SPECIFIC VOLUME, (V)} = 2.19$$

$$\text{AVERAGE SPECIFIC SURFACE, (SW)} = 4344.$$

$$\text{AVERAGE SPECIFIC SURFACE, (SV)} = 1983.$$

Appendix VI (Continued)

 * FLOC FRACTION RETAINED ON 20 MESH FIBER LENGTH = 2.98 MM. *
 * *****

ORIGINAL DATA

FILTRATION EXPERIMENT			COMPRESSIBILITY EXPERIMENT		SOLIDS CONC. G./CC.
PRESSURE CM. H2O	CHART READING	TIME SEC.	PRESSURE DYNES/SQCM.	PAD THICK. INCHES	
10.	8.64	259.12	8150.	2.5497	0.0451
20.	14.49	434.70	13100.	2.1370	0.0538
30.	19.37	581.17	22900.	1.7361	0.0662
40.	23.79	713.77	37700.	1.4422	0.0797
50.	27.81	834.30	62300.	1.1964	0.0961
60.	31.55	946.57	96400.	1.0171	0.1131
70.	35.09	1052.62	145800.	0.8720	0.1319
80.	38.32	1149.67			
90.	41.16	1234.80			

FILT. PAD WT. = 20.8284 G. EQ. VOL. = 110658.80 CC. CONSISTENCY = 0.019 PERCENT
 FLOW RATE = 87.6 CC./SEC. H2O VISC. = 0.009175 POISE COMP. PAD WT. = 13.3006 G.

FILTRATION RESISTANCE AND MAT SOLIDS CONCENTRATION AS FUNCTIONS OF PRESSURE

PRESSURE		FILTRATION RESISTANCE		MAT DENSITY C G./CC.	DP/DT
P CM. H2O	DYNES/SQCM.	AVERAGE (R) CM./G.	LOCAL R CM./G.		
10.	9807.	0.5915D 07	0.8555D 07	0.0483	54.74
20.	19613.	0.7052D 07	0.9540D 07	0.0625	61.04
30.	29420.	0.7912D 07	0.1084D 08	0.0727	69.36
40.	39227.	0.8589D 07	0.1211D 08	0.0809	77.49
50.	49033.	0.9186D 07	0.1329D 08	0.0879	85.01
60.	58840.	0.9715D 07	0.1438D 08	0.0941	92.02
70.	68647.	0.1019D 08	0.1541D 08	0.0996	98.60
80.	78453.	0.1067D 08	0.1634D 08	0.1047	104.58
90.	88260.	0.1117D 08	0.1716D 08	0.1094	109.78

EXPERIMENTAL EMPIRICAL CONSTANTS

$$C = M * (P ** N)$$

WHERE...

$$M = 0.1582D-02$$

$$N = 0.3720$$

$$P = B0 + B1*(T**EXPM) + B2*(T**EXPX)$$

WHERE...

$$B0 = -0.58421D 06$$

$$B1 = 0.55739D 06$$

$$B2 = 0.26444D 00$$

$$EXPM = 0.10009D-01$$

$$EXPX = 0.17610D 01$$

AVERAGE VALUES FOR SPECIFIC VOLUME AND SURFACE

$$\text{AVERAGE SPECIFIC VOLUME, (V)} = 2.11$$

$$\text{AVERAGE SPECIFIC SURFACE, (SW)} = 3779.$$

$$\text{AVERAGE SPECIFIC SURFACE, (SV)} = 1790.$$

Appendix VI (Continued)

 * FLOC FRACTION RETAINED ON 10 MESH FIBER LENGTH = 4.13 MM. *
 *

ORIGINAL DATA

FILTRATION EXPERIMENT			COMPRESSIBILITY EXPERIMENT		SOLIDS CONC. G./CC.
PRESSURE CM. H2O	CHART READING	TIME SEC.	PRESSURE DYNES/SQCM.	PAD THICK. INCHES	
10.	8.11	243.30	8150.	2.2036	0.0452
20.	13.51	405.30	13100.	1.8469	0.0540
30.	18.14	544.30	22900.	1.5004	0.0664
40.	22.51	675.40	37700.	1.2465	0.0800
50.	26.39	791.60	62300.	1.0340	0.0964
60.	30.17	905.10	96400.	0.8790	0.1134
70.	33.80	1014.10	145800.	0.7536	0.1323
80.	37.29	1118.80			
90.	40.71	1221.40			

FILT. PAD WT. = 30.3815 G. EQ. VOL. = 111436.70 CC. CONSISTENCY = 0.027 PERCENT
 FLOW RATE = 90.0 CC./SEC. H2O VISC. = 0.008551 POISE COMP. PAD WT. = 11.5314 G.

FILTRATION RESISTANCE AND MAT SOLIDS CONCENTRATION AS FUNCTIONS OF PRESSURE

PRESSURE		FILTRATION RESISTANCE		MAT DENSITY	DP/DT
P		AVERAGE	LOCAL		
CM. H2O	DYNES/SQCM.	(R)	R	C	
		CM./G.	CM./G.	G./CC.	
10.	9807.	0.44240 07	0.58700 07	0.0485	53.48
20.	19613.	0.53120 07	0.72610 07	0.0627	66.16
30.	29420.	0.59330 07	0.81110 07	0.0729	73.89
40.	39227.	0.63750 07	0.87640 07	0.0812	79.85
50.	49033.	0.67990 07	0.92660 07	0.0882	84.42
60.	58840.	0.71350 07	0.97050 07	0.0944	88.42
70.	68647.	0.74300 07	0.10090 08	0.1000	91.93
80.	78453.	0.76970 07	0.10430 08	0.1050	95.04
90.	88260.	0.79310 07	0.10740 08	0.1098	97.89

EXPERIMENTAL EMPIRICAL CONSTANTS

$$C = M * (P ** N)$$

WHERE...

$$M = 0.15870-02$$

$$N = 0.3720$$

$$P = B0 + B1*(T**EXPM) + B2*(T**EXPN)$$

WHERE...

$$B0 = 0.132160 06$$

$$B1 = -0.126080 06$$

$$B2 = 0.763780 01$$

$$EXPM = 0.999970-02$$

$$EXPN = 0.132130 01$$

AVERAGE VALUES FOR SPECIFIC VOLUME AND SURFACE

$$\text{AVERAGE SPECIFIC VOLUME, (V)} = 1.66$$

$$\text{AVERAGE SPECIFIC SURFACE, (SM)} = 3139.$$

$$\text{AVERAGE SPECIFIC SURFACE, (SV)} = 1895.$$

Appendix VI (Continued)

 *
 * WHOLE PULP RETAINED ON 65 MESH FIBER LENGTH = 1.49 MM. *
 *
 *

ORIGINAL DATA

FILTRATION EXPERIMENT			COMPRESSIBILITY EXPERIMENT		
PRESSURE CM. H ₂ O	CHART READING	TIME SEC.	PRESSURE DYNES/SQCM.	PAD THICK. INCHES	SOLIDS CONC. G./CC.
10.	6.71	201.30	8150.	1.5735	0.0468
20.	10.93	327.90	13100.	1.3188	0.0559
30.	14.28	428.40	22900.	1.0714	0.0688
40.	17.08	512.40	37700.	0.8900	0.0828
50.	19.62	588.60	62300.	0.7383	0.0998
60.	21.73	651.90	96400.	0.6277	0.1174
70.	23.84	715.20	145800.	0.5381	0.1370
80.	25.77	773.10			
90.	27.42	822.60			

FILT. PAD WT. = 9.8641 G. EQ. VOL. = 66882.94 CC. CONSISTENCY = 0.015 PERCENT
 FLOW RATE = 77.3 CC./SEC. H₂O VISC. = 0.009571 POISE COMP. PAD WT. = 8.5246 G.

FILTRATION RESISTANCE AND MAT SOLIDS CONCENTRATION AS FUNCTIONS OF PRESSURE

PRESSURE		FILTRATION RESISTANCE		MAT	DP/DT
P		AVERAGE	LOCAL	DENSITY	
CM. H ₂ O	DYNES/SQCM.	(R)	R	C	
		CM./G.	CM./G.	G./CC.	
10.	9807.	0.1196D 08	0.1703D 08	0.0502	69.36
20.	19613.	0.1469D 08	0.2159D 08	0.0649	87.93
30.	29420.	0.1686D 08	0.2628D 08	0.0755	107.03
40.	39227.	0.1880D 08	0.3050D 08	0.0840	124.20
50.	49033.	0.2046D 08	0.3446D 08	0.0913	140.35
60.	58840.	0.2216D 08	0.3782D 08	0.0977	154.03
70.	68647.	0.2357D 08	0.4123D 08	0.1035	167.91
80.	78453.	0.2492D 08	0.4438D 08	0.1088	180.73
90.	88260.	0.2635D 08	0.4709D 08	0.1136	191.78

EXPERIMENTAL EMPIRICAL CONSTANTS

$$C = M * (P ** N)$$

WHERE...

$$M = 0.1643D-02$$

$$N = 0.3720$$

$$P = B0 + B1*(T**EXPM) + B2*(T**EXPN)$$

WHERE...

$$B0 = -0.51176D 06$$

$$B1 = 0.49050D 06$$

$$B2 = 0.92674D-01$$

$$EXPM = 0.99991D-02$$

$$EXPN = 0.20271D 01$$

AVERAGE VALUES FOR SPECIFIC VOLUME AND SURFACE

$$\text{AVERAGE SPECIFIC VOLUME, (V)} = 2.48$$

$$\text{AVERAGE SPECIFIC SURFACE, (SW)} = 5616.$$

$$\text{AVERAGE SPECIFIC SURFACE, (SV)} = 2261.$$

Appendix VI (Continued)

*
* WHOLE PULP RETAINED ON 20 MESH FIBER LENGTH = 2.76 MM. *
*

ORIGINAL DATA

FILTRATION EXPERIMENT			COMPRESSIBILITY EXPERIMENT		
PRESSURE CM. H ₂ O	CHART READING	TIME SEC.	PRESSURE DYNES/SQCM.	PAD THICK. INCHES	SOLIDS CONC. G./CC.
10.	6.29	188.70	8150.	2.7308	0.0442
20.	9.82	294.60	13100.	2.2888	0.0527
30.	12.90	387.00	22900.	1.8594	0.0649
40.	15.50	465.00	37700.	1.5447	0.0781
50.	17.76	532.80	62300.	1.2814	0.0942
60.	19.97	599.10	96400.	1.0893	0.1108
70.	22.00	660.00	145800.	0.9339	0.1292
80.	23.80	714.00			
90.	25.39	761.70			

FILT. PAD WT. = 17.1414 G. EQ. VOL. = 61389.57 CC. CONSISTENCY = 0.028 PERCENT
FLOW RATE = 77.3 CC./SEC. H₂O VISC. = 0.009686 POISE COMP. PAD WT. = 13.9570 G.

FILTRATION RESISTANCE AND MAT SOLIDS CONCENTRATION AS FUNCTIONS OF PRESSURE

PRESSURE		FILTRATION RESISTANCE		MAT DENSITY C	DP/DT
P		AVERAGE	LOCAL		
CM. H ₂ O	DYNES/SQCM.	(R)	R	G./CC.	
		CM./G.	CM./G.		
10.	9807.	0.66600 07	0.11350 08	0.0473	88.59
20.	19613.	0.85320 07	0.12770 08	0.0613	99.62
30.	29420.	0.97430 07	0.14860 08	0.0712	115.91
40.	39227.	0.10810 08	0.16870 08	0.0793	131.63
50.	49033.	0.11790 08	0.18730 08	0.0861	146.11
60.	58840.	0.12590 08	0.20600 08	0.0922	160.73
70.	68647.	0.13330 08	0.22360 08	0.0976	174.45
80.	78453.	0.14080 08	0.23940 08	0.1026	186.79
90.	88260.	0.14850 08	0.25350 08	0.1072	197.79

EXPERIMENTAL EMPIRICAL CONSTANTS

$$C = M * (P ** N)$$

WHERE...

$$M = 0.15500-02$$

$$N = 0.3720$$

$$P = 80 + B1*(T**EXPM) + B2*(T**EXPN)$$

WHERE...

$$B0 = -0.789060 06$$

$$B1 = 0.753910 06$$

$$B2 = 0.124530 00$$

$$EXPM = 0.999680-02$$

$$EXPN = 0.199820 01$$

AVERAGE VALUES FOR SPECIFIC VOLUME AND SURFACE

$$\text{AVERAGE SPECIFIC VOLUME, (V)} = 2.47$$

$$\text{AVERAGE SPECIFIC SURFACE, (SW)} = 4372.$$

$$\text{AVERAGE SPECIFIC SURFACE, (SV)} = 1769.$$

Appendix VI (Continued)

 *
 * WHOLE PULP RETAINED ON 10 MESH FIBER LENGTH = 3.88 MM. *
 *

ORIGINAL DATA

FILTRATION EXPERIMENT			COMPRESSIBILITY EXPERIMENT		SOLIDS CONC. G./CC.
PRESSURE CM. H ₂ O	CHART READING	TIME SEC.	PRESSURE DYNES/SQCM.	PAD THICK. INCHES	
10.	8.00	240.00	8150.	3.4449	0.0450
20.	13.40	402.00	13100.	2.8874	0.0537
30.	17.75	532.50	22900.	2.3457	0.0661
40.	21.77	653.10	37700.	1.9486	0.0796
50.	25.33	759.90	62300.	1.6165	0.0959
60.	28.72	861.60	96400.	1.3742	0.1128
70.	31.95	958.50	145800.	1.1782	0.1316
80.	34.86	1045.80			
90.	37.65	1129.50			

FILT. PAD WT. = 24.8004 G. EQ. VOL. = 90146.69 CC. CONSISTENCY = 0.028 PERCENT
 FLOW RATE = 77.3 CC./SEC. H₂O VISC. = 0.009709 POISE COMP. PAD WT. = 17.9365 G.

FILTRATION RESISTANCE AND MAT SOLIDS CONCENTRATION AS FUNCTIONS OF PRESSURE

PRESSURE		FILTRATION RESISTANCE		MAT DENSITY C G./CC.	DP/DT
P CM. H ₂ O	DYNES/SQCM.	AVERAGE (R) CM./G.	LOCAL R CM./G.		
10.	9807.	0.5302D 07	0.7184D 07	0.0482	55.36
20.	19613.	0.6331D 07	0.8824D 07	0.0624	68.00
30.	29420.	0.7159D 07	0.1012D 08	0.0726	78.00
40.	39227.	0.7794D 07	0.1126D 08	0.0808	86.77
50.	49033.	0.8373D 07	0.1222D 08	0.0877	94.17
60.	58840.	0.8862D 07	0.1310D 08	0.0939	100.92
70.	68647.	0.9294D 07	0.1390D 08	0.0994	107.13
80.	78453.	0.9735D 07	0.1460D 08	0.1045	112.54
90.	88260.	0.1014D 08	0.1526D 08	0.1092	117.58

EXPERIMENTAL EMPIRICAL CONSTANTS

$$C = M * (P ** N)$$

WHERE...

$$M = 0.1579D-02$$

$$N = 0.3720$$

$$P = B0 + B1*(T**EXPM) + B2*(T**EXPN)$$

WHERE...

$$B0 = -0.23048D 06$$

$$B1 = 0.22094D 06$$

$$B2 = 0.10664D 01$$

$$EXPM = 0.10019D-01$$

$$EXPN = 0.15996D 01$$

AVERAGE VALUES FOR SPECIFIC VOLUME AND SURFACE

$$\text{AVERAGE SPECIFIC VOLUME, (V)} = 2.08$$

$$\text{AVERAGE SPECIFIC SURFACE, (SW)} = 3608.$$

$$\text{AVERAGE SPECIFIC SURFACE, (SV)} = 1732.$$

ORIGINAL DATA

FILTRATION RESISTANCE AND MAT SOLIDS CONCENTRATION AS FUNCTIONS OF PRESSURE

EXPERIMENTAL EMPIRICAL CONSTANTS

62 = 0.378690 00

999

APPENDIX VII

HISTORICAL PROGRAM AND OUTPUT FOR CALCULATION OF $\langle S_w \rangle$
AND $\langle v \rangle$ AS FUNCTIONS OF PRESSURE FROM FILTRATION
RESISTANCE AND COMPRESSIBILITY DATA

```

/JOB GO,TIME=50
/FILE DISK=(1,IOUT,NREC=5000),RSIZ=80,VOL=SYSFL1,DISP=(NEW,DELETE)
/FILE DISK=(2,JOUT,NREC=5000),RSIZ=80,VOL=SYSFL1,DISP=(NEW,DELETE)
/FILE DISK=(3,KOUT,NREC=5000),RSIZ=80,VOL=SYSFL1,DISP=(NEW,DELETE)

CRFILP === CONSTANT RATE FILTRATION (PRESSURE)

ANTHONY P. BINOTTO
NOVEMBER 13,1974

THIS PROGRAM IS DESIGNED TO CALCULATE THE AVERAGE FIBER
SPECIFIC VOLUME, V, AND SPECIFIC SURFACE, SW, FROM CONSTANT
RATE FILTRATION EXPERIMENTS AND COMPRESSIBILITY EXPERIMENTS.
THE SPECIFIC VOLUME AND SPECIFIC SURFACE ARE ALSO
CALCULATED AS FUNCTIONS OF WET MAT PRESSURE BY EMPLOYING
THE FOLLOWING TECHNIQUE...
VALUES OF CP**3 VS. DP/(T*SQRT(CP)) ARE PLOTTED. THE CURVED
PLOT WHICH USUALLY RESULTS IS FITTED EXACTLY WITH AN EQUATION
OF THE FORM... Y = B0 + B1*(X**M) + B2*(X**N). THIS EQUATION
IS USED TO GENERATE A LARGE NUMBER OF DATA POINTS. THE DATA
POINTS ARE THEN TAKEN THREE AT A TIME AND FITTED WITH A BEST
STRAIGHT LINE USING LINEAR REGRESSION. THE SLOPE AND INTERCEP
OF THE STRAIGHT LINE ARE USED TO CALCULATE V AND SW FROM THE
MODIFIED DARCY RELATIONSHIP...
DP/(T*SQRT(CP)) = A*((SW**2)/SQRT(V)) * (1 + B*(V**3)*CP**3))
WHERE...
A = (3.5*(1-N/2)*(W/EQVOL)*UO*MU)
B = 57.0*((1-N/2)**6)

OFF-LINE PLOTS OF ....
1. CP**3 VS. DP/(T*SQRT(CP))
2. V VS. PRESSURE
3. SW VS. PRESSURE
MAY BE OBTAINED BY KEEPING DATA FILES AND USING PLOTTING
PROGRAM 'ABPLOT'.

THE USER MUST SUPPLY THE FOLLOWING DATA
1. DATA CARD 1 -- ANY TITLE. CENTERING ON THE CARD
WILL ENSURE CENTERING ON OUTPUT.
2. DATA CARD 2 -- CHART READINGS FROM THE CONSTANT
RATE FILTRATION EXPERIMENT. CHART SPEED SHOULD BE
2 INCHES PER MINUTE. FORMAT (9F8.0).
3. DATA CARD 3 -- THE FOLLOWING INFORMATION IN ORDER
USING FORMAT (9F8.0).
A. PAD WT. FROM FILTRATION EXPERIMENT IN GRAMS
B. FILTRATION FLOW RATE IN CC./SEC.
C. WATER TEMPERATURE IN DEG. C
D. FILTRATION EQUIVALENT VOLUME IN CC.
4. DATA CARD 4 -- PAD WT. FROM THE COMPRESSIBILITY
EXPERIMENT IN GRAMS, AND PAD THICKNESSES IN INCHES FROM
FOR THE RESPECTIVE INCREMENTS IN PRESSURE. FORMAT(9F8.0)

THE USERS CARD DECK SHOULD CONTAIN THE FOLLOWING CARDS
/ID XXXXXXXXX,XXX
/INCLUDE CRFILP
/INCLUDE CMPRSS
/INCLUDE PRESSR
/INCLUDE SUBCRV
/INCLUDE LINREG
/INCLUDE PLOTVS
/DATA
*****
USERS DATA DECK
*****
9999999999999999
/END

DIMENSION DP(20),CP(20),CP2(20),CP3(20),T(20),Y(20),CHTRD(20)
DIMENSION R(20),DP2(20),SCONC(20),PDTHCK(20),DPTCP(20)
DIMENSION WPRESS(20),ITITLE(20),V(20),SW(20),SV(20)
DOUBLE PRECISION DP,CP,CP2,CP3,T,Y,V,SW,SV,DP2,SCONC,PDTHCK
DOUBLE PRECISION M,N,MU,WR,UO,TEMP,EQVOL,A
COMMON ITITLE,NPTS,IOUT,JOUT,KOUT
COMMON M,N,MU,UO,A,WR,EQVOL
IOUT = 1
JOUT = 2
KOUT = 3
LOUT = 1
CHTSPD = 2.
NPTS = 9
PTS = NPTS

```

Appendix I (Continued)

```

A = 45.43
AC = 45.54
DP2(3) = 9036.78
DP2(4) = 13998.48
DP2(5) = 23805.57
DP2(6) = 38506.50
DP2(7) = 63033.89
DP2(8) = 97014.77
DP2(9) = 146112.62
WRITE (IOUT,30)
WRITE (IOUT,31)
WRITE (JOUT,45)
WRITE (KOUT,45)
WRITE (JOUT,46)
WRITE (KOUT,47)
1 READ (5,2) ITITLE
  IF (ICOMP(ITITLE,1,249,4,1)) 3,99,3
2 FORMAT (20A4)
3 READ (5,4) (CHTRD(I),I=1,9)
  READ (5,4) WR,UO,TEMP,EQVOL
  READ (5,4) WCP,(PDTHCK(I),I=3,9)
4 FORMAT (9F8.0)
  IF (TEMP - 20.) 5,5,6
5 ETA=(1301./(998.333+8.1855*(TEMP-20.)+.00585*((TEMP-20.)**2)))
  MU = (10. ** ETA) * .01
  GO TO 7
6 ETA=(1.3272*(20.-TEMP)-.001053*((TEMP-20.)**2))/(TEMP+105.)
  MU = (10. ** ETA) * .01002
7 WRITE (6,8)
8 FORMAT (1H1,16X,'*****')
  *****
  WRITE (6,9)
  WRITE (6,9)
  WRITE (6,10) ITITLE
  WRITE (6,9)
  WRITE (6,9)
9 FORMAT (' ',16X,'*',85X,'*')
10 FORMAT (' ',16X,'*',3X,20A4,2X,'*')
  WRITE (6,11)
11 FORMAT (' ',16X,'*****')
  *****
  WRITE (6,12)
  WRITE (6,13)
12 FORMAT ('0','ORIGINAL DATA')
13 FORMAT (' ','-----',//)
  WRITE (6,14)
14 FORMAT ('0',10X,'FILTRATION EXPERIMENT',31X,'COMPRESSIBILITY EXPE
  1RIMENT',/)
  WRITE (6,15)
  WRITE (6,16)
15 FORMAT (' ',10X,'PRESSURE',7X,'CHART',9X,'TIME',20X,'PRESSURE',10X
  1'PAD THICK.',8X,'SOLIDS CONC. ')
16 FORMAT (' ',10X,'CM. H2O',8X,'READING',7X,'SEC.',20X,'DYNES/SQCM.'
  1,7X,'INCHES',12X,'G./CC.',//)
  C1 = WR / EQVOL
  CIP = C1 * 100.
  DO 17 I=3,9
17 SCONC(I) = WCP / (AC* PDTHCK(I) * 2.54)
  DO 18 I=1,9
  Y(I) = (CHTRD(I) * 60.) / CHTSPD
  WPRESS(I) = I * 10
  DP(I) = WPRESS(I) * 980.665
  R(I) = (DP(I) * A**2)/(MU * T(I) * (UO**2) * C1)
18 WRITE (6,19) WPRESS(I),CHTRD(I),T(I),DP2(I),PDTHCK(I),SCONC(I)
19 FORMAT ('0',12X,F4.0,8X,F6.2,7X,F8.2,16X,F10.0,10X,F8.4,11X,F6.4)
  WRITE (6,20) WR,EQVOL,C1P
  WRITE (6,21) UO,MU,WCP
20 FORMAT ('0','FILT. PAD WT. =',F7.4,' G.',5X,'EQ. VOL. =',F9.2,
  1' CC.',7X,'CONSISTENCY =',F5.3,' PERCENT')
21 FORMAT ('0','FLOW RATE =',F5.1,' CC./SEC.',5X,'H2O VISC. =',F8.6,
  1' POISE',5X,'COMP. PAD WT. =',F7.4,' G.',//)
C***** LEAST SQUARES APPROACH TO CALCULATING COMPRESSIBILITY
  CALL CMPRSS (WCP,PDTHCK,AC,N,M,CP,CP2,CP3,Y,DP2,DP,T)
  WRITE (6,22)
  WRITE (6,23)
22 FORMAT ('0','FILTRATION RESISTANCE AND MAT SOLIDS CONCENTRATION AS
  1 FUNCTIONS OF PRESSURE')
23 FORMAT (' ',1'-----',//)
  1
  WRITE (6,24)
  WRITE (6,25)
  WRITE (6,26)
24 FORMAT ('0',36X,'FILTRATION',5X,'MAT SOLIDS')
25 FORMAT (' ',15X,'PRESSURE',13X,'RESISTANCE',5X,'CONCENTRATION',
  15X,'DP/(T*SQRT(CP))',5X,'CP**3',/)
26 FORMAT ('0',10X,'CM. H2O',4X,'DYNES/SQCM.',6X,'CM./G.',10X,
  1'G./CC.',//)
  DO 27 I=1,9

```

00850
 00860
 00870
 00880
 00890
 00900
 00910
 00920
 00930
 00940
 00950
 00960
 00970
 00980
 00990
 01000
 01010
 01020
 01030
 01040
 01050
 01060
 01070
 01080
 01090
 01100
 01110
 01120
 01130
 01140
 01150
 01160
 01170
 01180
 01190
 01200
 01210
 01220
 01230
 01240
 01250
 01260
 01270
 01280
 01290
 01300
 01310
 01320
 01330
 01340
 01350
 01360
 01370
 01380
 01390
 01400
 01410
 01420
 01430
 01440
 01450
 01460
 01470
 01480
 01490
 01500
 01510
 01520
 01530
 01540
 01550
 01560
 01570
 01580
 01590
 01610
 01620
 01630
 01640
 01650
 01660
 01670
 01680
 01690
 01700
 01710
 01720

[illegible]

Appendix VII (Continued)

```

SUMY2 = 0.
SUMX = 0.
SUMX2 = 0.
SUMXY = 0.
SUMM = 0.
DO 1 I=3,9
  MATCON(I) = W / (AREA * PDTHCK(I) * 2.54)
  LMC(I) = DLOG(MATCON(I))
  LDP2(I) = DLOG(DP2(I))
  SUMY = SUMY + LMC(I)
  SUMY2 = SUMY2 + (LMC(I) ** 2)
  SUMX = SUMX + LDP2(I)
  SUMX2 = SUMX2 + (LDP2(I) ** 2)
  SUMXY = SUMXY + (LMC(I) * LDP2(I))
  Q1 = (PTS * SUMXY) - (SUMX * SUMY)
  Q2 = (PTS * SUMX2) - (SUMX ** 2)
  N = Q1 / Q2
DO 2 I=3,9
  SUMM = SUMM + (MATCON(I) / (DP2(I) ** N))
M = SUMM / NPTS
DO 3 I=1,9
  CP(I) = M * DP(I) ** N
  CP2(I) = M * DP2(I) ** N
  CP3(I) = CP(I) ** 3
  DPTCP(I) = DP(I) / (T(I) * SQRT(CP(I)))
RETURN
END

```

02610
02620
02630
02640
02650
02660
02670
02680
02690
02700
02710
02720
02730
02740
02750
02760
02770
02780
02790
02800
02810
02820
02830
02840
02850
02860
02870

C
C
C
C
C
C
C
C
C
C
C

```

SUBROUTINE PRESSR == V,SW,SV AS FUNCTIONS OF PRESSURE
      ANTHONY P. BINOTTO
      JUNE 17,1975

```

02880
02890
02900
02910
02920
02930
02940
02950
02960
02970
02980
02990
03000
03010
03020
03030
03040
03050
03060
03070
03080
03090
03100
03110
03120
03130
03140
03150
03160
03170
03180
03190
03200
03210
03220
03230
03240
03250
03260
03270
03280
03290
03300
03310
03320
03330
03340
03350
03360
03370
03380
03390
03400
03410
03420
03430
03440
03450
03460

```

THIS SUBROUTINE CALCULATES VALUES OF V, SW, AND SV AS FUNCTION
OF PRESSURE FROM FILTRATION RESISTANCE AND COMPRESSIBILITY
DATA.
THE PROCEDURE INVOLVES FITTING THE BEST SMOOTH CURVE USING
NON-LINEAR REGRESSION (NLREG) TO ANALYSE THE PLOT OF CP**3 VS.
DP/(T*SQRT(CP)). THE DERIVATIVES (SLOPES) AND INTERCEPT
ARE CALCULATED FROM THE REGRESSION EQUATIONS AND ARE USED TO
SOLVE THE MODIFIED DARCY EQUATION.

```

```

SUBROUTINE PRESSR (CP3,DPTCP,V,SW,SV)
  DIMENSION CP3(20),DPTCP(20),V(20),SW(20),SV(20),ITITLE(20)
  DIMENSION X1(3),Y1(3),X(500),Y(500),DP(500),WPRESS(500)
  DOUBLE PRECISION CP3,DPTCP,SLOPE,INTCPT,CONST1,CONST2,EQ1
  DOUBLE PRECISION EQ2,V,SW,SV,N,CONSIS,MU,UO,A,WR,EQVOL,M
  DOUBLE PRECISION B0,B1,B2,EXPM,EXPN,X,Y,DP,X1,Y1
  COMMON ITITLE,NPTS,IOUT,JOUT,KOUT
  COMMON M,V,MU,UO,A,WR,EQVOL
  DPTS = 300.0
  DO 1 I=1,NPTS
    X(I) = CP3(I)
    Y(I) = DPTCP(I)
    CONSIS = WR / EQVOL
    CONST1 = ((1 - N/2.)* 3.5 * CONSIS * UO * MU) / (A**2)
    CONST2 = 57. * ((1 - N/2.))**6
    CALL CRVFIT (X,Y,B0,B1,B2,EXPM,EXPN,DPTS)
    XFIRST = CP3(1)
    XLAST = CP3(NPTS)
    XINCR = (XLAST - XFIRST) / DPTS
    DO 3 I=1,NPTS
      X1(I) = CP3(I) - XINCR
      X1(2) = CP3(I)
      X1(3) = CP3(I) + XINCR
    DO 2 J=1,3
      Y1(J) = B0 + B1*(X1(J)**EXPM) + B2*(X1(J)**EXPJ)
    CALL LINREG (X1,Y1,3,INTCPT,SLOPE)
    EQ1 = INTCPT / CONST1
    EQ2 = DABS(SLOPE) / (CONST1 * CONST2)
    V(I) = (EQ2/EQ1) ** .333333
    SW(I) = DSQRT((INTCPT * DSQRT(V(I))) / (CONST1 * UO))
    SV(I) = SW(I) / V(I)
    DP(I) = ((X1(2)**.333333)/M)**(1/N)
    WPRESS(I) = DP(I) / 980.665
    WRITE (JOUT,4) ITITLE
    WRITE (KOUT,4) ITITLE
    WRITE (JOUT,5) NPTS
    WRITE (KOUT,5) NPTS
    WRITE (JOUT,6) (WPRESS(I),V(I),I=1,NPTS)
    WRITE (KOUT,6) (WPRESS(I),SW(I),I=1,NPTS)
  FORMAT (20A4)
  FORMAT (I3,' 2 2 -1 3')
  FORMAT (2E15.7)
  CALL PLOTVS (X,Y,DPTS,CONST1,CONST2)
RETURN
END

```

1
2
3
4
5
6

Appendix VII (Continued)

```

C          CRVFIT === CURVE FITTING                                03470
C          ANTHONY P. BINOTTO                                       03480
C          AUGUST 25, 1975                                           03490
C          THIS PROGRAM IS DESIGNED TO CALCULATE THE BEST EQUATION  03500
C          OF THE FORM...  $Y = B0 + B1*(X**M) + B2*(X**N)$            03510
C          TO ANY SET OF DATA. THE PROCEDURE INVOLVES MINIMIZING THE 03520
C          SUM OF SQUARES.  $Y = B0 + B1*(X**M) + B2*(X**N)$          03530
C          *** WARNING *** THE RESULTING EQUATION WILL ONLY BE ONE OF 03540
C          MANY COMBINATIONS OF B0,B1,B2,M,N WHICH GIVE A 'BEST'    03550
C          FIT TO THE DATA. THE FINAL EQUATION IS THEREFORE DEPENDENT 03560
C          ON THE INITIAL ESTIMATE OF M AND N.                       03570
C          SUBROUTINE CRVFIT (X,Y,B0,B1,B2,M,N,DPTS)                03580
C          DIMENSION ITITLE(20),A(5,6),X(500),Y(500)               03590
C          DOUBLE PRECISION X,Y,B0,B1,B2,M,N,A                     03600
C          DOUBLE PRECISION DELB0,DELB1,DELB2,DELM,DELN             03610
C          COMMON ITITLE,NPTS,IOUT,JOUT,KOUT                        03620
C****      IOUT == OUTPUT STORED ON DISK OR TAPE FOR PLOTTING.     03630
C          NCOUNT = 0.0                                           03640
C          WRITE (IOUT,1) ITITLE                                    03650
C          WRITE (IOUT,2) NPTS                                       03660
C          WRITE (IOUT,3) (X(I),Y(I),I=1,NPTS)                     03670
C          FORMAT (20A4)                                           03680
C          FORMAT (I3,' 1 1 -1 3')                                  03690
C          FORMAT (2E15.7)                                           03700
C****      ESTIMATE VALUES OF B0,B1,B2,M,N                        03710
C          B0 = 200.0                                               03720
C          B1 = 1000.0                                              03730
C          B2 = 1000.0                                              03740
C          M = 0.120                                                03750
C          N = 0.500                                                03760
C          TEST1 = 0.0                                              03770
C          CALL SUM (X,Y,NPTS,B0,B1,B2,M,N,A)                      03780
C          CALL SIMEQN (A,5,6)                                       03790
C          DELB0 = A(1,6) / A(1,1)                                   03800
C          DELB1 = A(2,6) / A(2,2)                                   03810
C          DELB2 = A(3,6) / A(3,3)                                   03820
C          DELM = A(4,6) / A(4,4)                                    03830
C          DELN = A(5,6) / A(5,5)                                    03840
C****      DATA FIT MAY BE IMPROVED AT THE EXPENSE OF CALCULATION TIME 03850
C****      BY REDUCING THE VALUE OF 'TEST'.                        03860
C          TEST = 10.                                               03870
C          TEST2 = DELB0 + DELB1 + DELB2 + DELM + DELN             03880
C          DIFF = TEST2 - TEST1                                       03890
C          IF (ABS(DIFF)-TEST) 7,7,5                                03900
C          TEST1 = TEST2                                             03910
C          NCOUNT = NCOUNT + 1                                    03920
C          B0 = B0 + DELB0                                           03930
C          B1 = B1 + DELB1                                           03940
C          B2 = B2 + DELB2                                           03950
C          IF (NCOUNT-100) 4,4,6                                     03960
C          NCOUNT = 0                                              03970
C          M = M + DELM                                              03980
C          N = N + DELN                                              03990
C          GO TO 5                                                    04000
C          CALL EQN (B0,B1,B2,M,N,IOUT,X,Y,DPTS)                  04010
C          RETURN                                                    04020
C          END                                                        04030
C          SUBROUTINE EQN (B0,B1,B2,M,N,IOUT,X,Y,DPTS)             04040
C          THIS SUBROUTINE GENERATES DATA POINTS FROM THE CALCULATED 04050
C          EQUATION TO BE USED IN PLOTTING PROGRAM 'ABPLOT'.        04060
C          DIMENSION X(500),Y(500)                                  04070
C          DOUBLE PRECISION X,Y,DPTS,XFIRST,XLAST,XINCR,B0,B1,B2,M,N 04080
C          LPTS = DPTS                                              04090
C          XFIRST = X(1)                                             04100
C          XLAST = X(9)                                              04110
C          DPTS = LPTS                                               04120
C          XINCR = (XLAST - XFIRST) / DPTS                           04130
C          WRITE (IOUT,1)                                           04140
C          WRITE (IOUT,2) LPTS                                       04150
C          FORMAT ('Y = B0 + B1*(X**M) + B2*(X**N)')                04160
C          FORMAT (I3,' -1 -1 0')                                   04170
C          X(1) = XFIRST                                             04180
C          DO 3 I=1,LPTS                                             04190
C          Y(I) = B0 + B1*(X(I)**M) + B2*(X(I)**N)                  04200
C          X(I+1) = X(I) + XINCR                                     04210
C          WRITE (IOUT,4) X(I),Y(I)                                  04220
C          FORMAT (2E15.7)                                           04230
C          RETURN                                                    04240
C          END                                                        04250
C          SUBROUTINE SUM (X,Y,NPTS,B0,B1,B2,M,N,A)                04260
C          DIMENSION A(5,6),X(500),Y(500)                         04270
C          DOUBLE PRECISION X,Y,B0,B1,B2,M,N,A,PTS,SXMYR2           04280
C          DOUBLE PRECISION SY,SXM,SXN,SXMY,SX2M,SXMXN,SXNY,SX2N,SXMYR,SXMR 04290

```

Appendix VII (Continued)

```

DOUBLE PRECISION SX2MR, SXMxNR, SXNYR, SXNR, SXMR2, SX2MR2, SXMNR2
DOUBLE PRECISION SXNR2, SX2NR2, SXNYR2, SX2NR, XN, XM, X2M, X2N, R, R2
PTS = NPTS
SY = 0.0
SXM = 0.0
SXN = 0.0
SXY = 0.0
SX2M = 0.0
SXMxN = 0.0
SXNY = 0.0
SX2N = 0.0
SXYR = 0.0
SxMR = 0.0
SX2MR = 0.0
SXMxNR = 0.0
SXNYR = 0.0
SXNR = 0.0
SX2NR = 0.0
SxMR2 = 0.0
SX2MR2 = 0.0
SXMNR2 = 0.0
SXYR2 = 0.0
SXNR2 = 0.0
SX2NR2 = 0.0
SXNYR2 = 0.0
DO 1 I=1, NPTS
  XM = X(I) ** M
  XN = X(I) ** N
  X2M = XM ** 2
  X2N = XN ** 2
  R = DLOG(X(I))
  R2 = R ** 2
  SY = SY + Y(I)
  SXM = SXM + XM
  SXN = SXN + XN
  SXY = SXY + (XM * Y(I))
  SX2M = SX2M + X2M
  SXMxN = SXMxN + (XM * XN)
  SXNY = SXNY + (XN * Y(I))
  SX2N = SX2N + X2N
  SXYR = SXYR + (XM * Y(I) * R)
  SxMR = SxMR + (XM * R)
  SX2MR = SX2MR + (X2M * R)
  SXMxNR = SXMxNR + (XM * XN * R)
  SXNYR = SXNYR + (XN * Y(I) * R)
  SXNR = SXNR + (XN * R)
  SX2NR = SX2NR + (X2N * R)
  SxMR2 = SxMR2 + (XM * R2)
  SX2MR2 = SX2MR2 + (X2M * R2)
  SXMNR2 = SXMNR2 + (XM * XN * R2)
  SXYR2 = SXYR2 + (XM * Y(I) * R2)
  SXNR2 = SXNR2 + (XN * R2)
  SX2NR2 = SX2NR2 + (X2N * R2)
  SXNYR2 = SXNYR2 + (XN * Y(I) * R2)
A(1,1) = PTS
A(1,2) = SXM
A(1,3) = SXN
A(1,4) = B1 * SxMR
A(1,5) = B2 * SXNR
A(1,6) = -(PTS*B0 + B1*SXM + B2*SXN - SY)
A(2,1) = SX2M
A(2,2) = SXMxN
A(2,3) = B0*SxMR + 2.0*B1*SX2MR + B2*SXMxNR - SXYR
A(2,4) = B0*SXMxNR
A(2,5) = -(B0*SXM + B1*SX2M + B2*SXMxN - SXY)
A(3,1) = SXN
A(3,2) = SXMxN
A(3,3) = SX2N
A(3,4) = SXMxNR
A(3,5) = B0*SXNR + B1*SXMxNR + 2.0*B2*SX2NR - SXNYR
A(3,6) = -(B0*SXN + B1*SXMxN + B2*SX2N - SXNY)
A(4,1) = SxMR
A(4,2) = SX2MR
A(4,3) = SXMxNR
A(4,4) = B0*SxMR2 + 2.0*B1*SX2MR2 + B2*SXMNR2 - SXYR2
A(4,5) = B2*SXMNR2
A(4,6) = -(B0*SxMR + B1*SX2MR + B2*SXMxNR - SXYR)
A(5,1) = SXNR
A(5,2) = SXMxNR
A(5,3) = SX2NR
A(5,4) = B1*SXMNR2
A(5,5) = B0*SXNR2 + B1*SXMNR2 + 2.0*B2*SX2NR2 - SXNYR2
A(5,6) = -(B0*SXNR + B1*SXMxNR + B2*SX2NR - SXNYR)
RETURN
END

```

04340
 04350
 04360
 04370
 04380
 04390
 04400
 04410
 04420
 04430
 04440
 04450
 04460
 04470
 04480
 04490
 04500
 04510
 04520
 04530
 04540
 04550
 04560
 04570
 04580
 04590
 04600
 04610
 04620
 04630
 04640
 04650
 04660
 04670
 04680
 04690
 04700
 04710
 04720
 04730
 04740
 04750
 04760
 04770
 04780
 04790
 04800
 04810
 04820
 04830
 04840
 04850
 04860
 04870
 04880
 04890
 04900
 04910
 04920
 04930
 04940
 04950
 04960
 04970
 04980
 04990
 05000
 05010
 05020
 05030
 05040
 05050
 05060
 05070
 05080
 05090
 05100
 05110
 05120
 05130
 05140
 05150
 05160
 05170
 05180
 05190

Appendix VII (Continued)

```

C      SUBROUTINE SIMEQN (A,NR,NC)
C*****      SOLUTION OF SIMULTANEOUS LINEAR EQUATIONS
C*****      MATRIX OF COEFFICIENTS = A
C*****      NR = NUMBER OF ROWS IN A
C*****      NC = NUMBER OF COLUMNS IN A
C*****      DIMENSION A(5,6),R(100)
C*****      DOUBLE PRECISION A,R,D,T
C*****      IF(NR - NC) 4,4,3
C*****      3 NCT = NC
C*****      GO TO 5
C*****      4 NCT = NR
C*****      5 K = 1
C*****      D = 1.
C*****      7 IF(A(K,K)) 12,8,12
C*****      DIAGONAL=0, FIND A ROW WITH A NON-ZERO ELEMENT
C*****      AND INTERCHANGE THE ROWS
C*****      8 DO 9 I = K,NR
C*****      IF(A(I,K)) 10,9,10
C*****      9 CONTINUE
C*****      IF THERE IS NO NON-ZERO ELEMENT, PROBLEM IS COMPLETE
C*****      GO TO 17
C*****      INTERCHANGE ROW I AND ROW K
C*****      10 DO 11 J = 1,NC
C*****      T = A(I,J)
C*****      A(I,J) = A(K,J)
C*****      11 A(K,J) = T
C*****      CORRECT THE SYSTEM OF EQUATIONS FOR ROW K
C*****      12 DO 16 I = 1,NR
C*****      IF(I - K) 13,16,13
C*****      13 DO 14 J = 1,NC
C*****      R(J) = (A(I,J)*A(K,K) - A(I,K)*A(K,J))/D
C*****      DO 15 J = 1,NC
C*****      15 A(I,J) = R(J)
C*****      16 CONTINUE
C*****      D = A(K,K)
C*****      K = K + 1
C*****      IF(K - NCT) 7,7,17
C*****      17 RETURN
C*****      END
C
C      LINREG === LINEAR REGRESSION
C      ANTHONY P. BINOTTO
C      JUNE 16, 1975
C
C      THIS SUBROUTINE IS USED TO CALCULATE THE STRAIGHT LINE
C      RELATIONSHIP BETWEEN PAIRS OF X,Y-DATA
C
C      SUBROUTINE LINREG (X,Y,NPTS,INTCPT,SLOPE)
C*****      DIMENSION X(10),Y(10)
C*****      DOUBLE PRECISION X,Y,LY,SUMX,SUMX2,SUMY,SUMY2,SUMXY,SLOPE,INTCPT
C*****      DOUBLE PRECISION Q1,Q2,PTS
C*****      PTS = NPTS
C*****      SUMY = 0.
C*****      SUMX = 0.
C*****      SUMX2 = 0.
C*****      SUMXY = 0.
C*****      SUMINT = 0.
C*****      DO 1 I=1,NPTS
C*****      SUMY = SUMY + Y(I)
C*****      SUMX = SUMX + X(I)
C*****      SUMX2 = SUMX2 + (X(I) ** 2)
C*****      SUMXY = SUMXY + (X(I) * Y(I))
C*****      Q1 = SUMXY - (SUMX * SUMY)/PTS
C*****      Q2 = SUMX2 - (SUMX ** 2)/PTS
C*****      SLOPE = Q1/Q2
C*****      INTCPT = (SUMY - SLOPE * SUMX) / PTS
C*****      RETURN
C*****      END
C
C      PLOTVS === PLOTTING POINTS FOR V AND SW
C
C      SUBROUTINE PLOTVS (X,Y,DPTS,CONST1,CONST2)
C*****      DIMENSION ITITLE(20),X(500),Y(500),X1(3),Y1(3)
C*****      DIMENSION V(300),SW(300),SV(300),DP(500),WPRESS(500)
C*****      DOUBLE PRECISION M,N,MU,UO,A,WR,EQVOL,X,Y,X1,Y1,V,SW,SV,DP
C*****      DOUBLE PRECISION WPRESS,CONST1,CONST2,SLOPE,INTCPT
C*****      COMMON ITITLE,NPTS,IOUT,JOUT,KOUT
C*****      COMMON M,N,MU,UO,A,WR,EQVOL
C*****      NCDUNT = 0
C*****      LPTS = DPTS/3.0
C*****      WRITE (JOUT,1)
C*****      WRITE (KOUT,1)
C*****      WRITE (JOUT,2) LPTS
C*****      WRITE (KOUT,2) LPTS
C*****      FORMAT (' ',1)
C*****      FORMAT ('I3,' -2 -2 ' 0')

```


Appendix VII (Continued)

*
* FIELD FRACTION RETAINED ON 65 MESH FIBER LENGTH = 1.63 MM. *
*

ORIGINAL DATA

FILTRATION EXPERIMENT			COMPRESSIBILITY EXPERIMENT		
PRESSURE CM. H ₂ O	CHART READING	TIME SEC.	PRESSURE DYNES/SQCM.	PAD THICK. INCHES	SOLIDS CONC. G./CC.
10.	7.46	223.90	0.	0.0	0.0
20.	11.68	350.50	0.	0.0	0.0
30.	14.91	447.30	9037.	1.0338	0.0517
40.	17.55	526.50	13998.	0.8665	0.0616
50.	19.80	594.00	23806.	0.7039	0.0759
60.	21.87	656.00	38507.	0.5848	0.0913
70.	23.70	710.90	63034.	0.4851	0.1101
80.	25.29	758.70	97015.	0.4124	0.1295
90.	26.76	802.90	146113.	0.3536	0.1510

FILT. PAD WT. = 6.7979 G. EQ. VOL. = 65132.20 CC. CONSISTENCY = 0.010 PERCENT
FLOW RATE = 78.6 CC./SEC. H₂O VISC. = 0.008705 POISE COMP. PAD WT. = 6.1767 G.

FILTRATION RESISTANCE AND MAT SOLIDS CONCENTRATION AS FUNCTIONS OF PRESSURE

PRESSURE		FILTRATION RESISTANCE	MAT SOLIDS CONCENTRATION	DP/(T*SQRT(CP))	CP**3
CM. H ₂ O	DYNES/SQCM.	CM./G.	G./CC.		
10.	9807.	.1612E 08	0.0537	189.05	0.1547D-03
20.	19613.	.2059E 08	0.0701	211.38	0.3442D-03
30.	29420.	.2420E 08	0.0819	229.80	0.5497D-03
40.	39227.	.2742E 08	0.0915	246.30	0.7662D-03
50.	49033.	.3038E 08	0.0997	261.42	0.9913D-03
60.	58840.	.3301E 08	0.1070	274.26	0.1223D-02
70.	68647.	.3553E 08	0.1135	286.64	0.1462D-02
80.	78453.	.3805E 08	0.1195	299.16	0.1705D-02
90.	88260.	.4045E 08	0.1250	310.90	0.1954D-02

M = 0.1563D-02 N = 0.3848

HYDRODYNAMIC SPECIFIC VOLUME AND SURFACE AS FUNCTIONS OF PRESSURE

PRESSURE CM. H ₂ O	V CC./G.	SW SQCM./G.	SV SQCM./CC.
10.	3.80	6502.79	1712.43
20.	3.30	6467.64	1958.15
30.	3.03	6478.16	2140.98
40.	2.84	6502.60	2293.49
50.	2.69	6532.48	2427.39
60.	2.58	6564.57	2548.41
70.	2.48	6597.43	2659.87
80.	2.40	6630.34	2763.86
90.	2.33	6662.94	2861.80

AVERAGE VALUES FOR SPECIFIC VOLUME AND SURFACE

AVERAGE SPECIFIC VOLUME = 2.83 CC./G.
AVERAGE SPECIFIC SURFACE, SW = 6548.77 SQCM./G.
AVERAGE SPECIFIC SURFACE, SV = 2374.04 SQCM./CC.

Appendix VII (Continued)

*
* FIELD FRACTION RETAINED ON 20 MESH FIBER LENGTH = 3.05 MM.
*
*

ORIGINAL DATA

FILTRATION EXPERIMENT			COMPRESSIBILITY EXPERIMENT		
PRESSURE CM. H2O	CHART READING	TIME SEC.	PRESSURE DYNES/SQCM.	PAD THICK. INCHES	SOLIDS CONC. G./CC.
10.	7.15	214.42	0.	0.0	0.0
20.	11.12	333.52	0.	0.0	0.0
30.	14.13	423.82	9037.	1.2830	0.0491
40.	16.67	500.17	13998.	1.0754	0.0586
50.	18.94	568.13	23806.	0.8736	0.0721
60.	20.81	624.30	38507.	0.7258	0.0868
70.	22.58	677.32	63034.	0.6021	0.1047
80.	24.20	726.15	97015.	0.5118	0.1231
90.	25.68	770.47	146113.	0.4388	0.1436

FILT. PAD WT. = 9.7035 G. EQ. VOL. = 62375.00 CC. CONSISTENCY = 0.016 PERCENT
FLOW RATE = 78.2 CC./SEC. H2O VISC. = 0.009299 POISE COMP. PAD WT. = 7.2896 G.

FILTRATION RESISTANCE AND MAT SOLIDS CONCENTRATION AS FUNCTIONS OF PRESSURE

PRESSURE		FILTRATION RESISTANCE	MAT SOLIDS CONCENTRATION	DP/(T*SQRT(CP))	CP**3
CM. H2O	DYNES/SQCM.	CM./G.	G./CC.		
10.	9807.	.1066E 08	0.0510	202.43	0.1330D-03
20.	19613.	.1370E 08	0.0666	227.79	0.2960D-03
30.	29420.	.1617E 08	0.0779	248.71	0.4727D-03
40.	39227.	.1827E 08	0.0870	265.87	0.6588D-03
50.	49033.	.2011E 08	0.0948	280.29	0.8524D-03
60.	58840.	.2196E 08	0.1017	295.53	0.1052D-02
70.	68647.	.2362E 08	0.1079	308.51	0.1257D-02
80.	78453.	.2517E 08	0.1136	320.53	0.1466D-02
90.	88260.	.2669E 08	0.1189	332.24	0.1680D-02

M = 0.1486D-02 N = 0.3848

HYDRODYNAMIC SPECIFIC VOLUME AND SURFACE AS FUNCTIONS OF PRESSURE

PRESSURE CM. H2O	V CC./G.	SW SQCM./G.	SV SQCM./CC.
10.	4.14	5435.06	1312.66
20.	3.52	5412.05	1538.66
30.	3.18	5424.29	1703.87
40.	2.96	5446.19	1840.14
50.	2.79	5471.41	1958.76
60.	2.66	5497.68	2065.24
70.	2.55	5524.06	2162.72
80.	2.46	5550.12	2253.19
90.	2.38	5575.64	2338.02

AVERAGE VALUES FOR SPECIFIC VOLUME AND SURFACE

AVERAGE SPECIFIC VOLUME = 2.96 CC./G.
AVERAGE SPECIFIC SURFACE, SW = 5481.83 SQCM./G.
AVERAGE SPECIFIC SURFACE, SV = 1908.14 SQCM./CC.

Appendix VII. (Continued)

 * FIELD FRACTION RETAINED ON 10 MESH FIBER LENGTH = 3.94 MM. *
 * *****

ORIGINAL DATA

FILTRATION EXPERIMENT			COMPRESSIBILITY EXPERIMENT		
PRESSURE CM. H2O	CHART READING	TIME SEC.	PRESSURE DYNES/SQCM.	PAD THICK. INCHES	SOLIDS CONC. G./CC.
10.	9.27	278.10	0.	0.0	0.0
20.	14.90	447.00	0.	0.0	0.0
30.	19.51	585.20	9037.	2.0327	0.0479
40.	23.48	704.40	13998.	1.7037	0.0571
50.	27.11	813.30	23806.	1.3841	0.0703
60.	30.42	912.70	38507.	1.1498	0.0846
70.	33.36	1000.80	63034.	0.9538	0.1020
80.	36.12	1083.50	97015.	0.8109	0.1200
90.	38.68	1160.40	146113.	0.6952	0.1399

FILT. PAD WT. = 16.8514 G. EQ. VOL. = 97743.30 CC. CONSISTENCY = 0.017 PERCENT
 FLOW RATE = 81.1 CC./SEC. H2O VISC. = 0.009028 POISE COMP. PAD WT. = 11.2539 G.

FILTRATION RESISTANCE AND MAT SOLIDS CONCENTRATION AS FUNCTIONS OF PRESSURE

PRESSURE		FILTRATION RESISTANCE	MAT SOLIDS CONCENTRATION	DP/(T*SQRT(CP))	CP**3
CM. H2O	DYNES/SQCM.	CM./G.	G./CC.		
10.	9807.	.7109E 07	0.0497	158.11	0.12300-03
20.	19613.	.8846E 07	0.0649	172.18	0.27390-03
30.	29420.	.1014E 08	0.0759	182.47	0.43740-03
40.	39227.	.1123E 08	0.0848	191.24	0.60960-03
50.	49033.	.1215E 08	0.0924	198.34	0.78880-03
60.	58840.	.1300E 08	0.0991	204.78	0.97350-03
70.	68647.	.1383E 08	0.1052	211.51	0.11630-02
80.	78453.	.1460E 08	0.1107	217.61	0.13570-02
90.	88260.	.1533E 08	0.1158	223.47	0.15550-02

M = 0.1448D-02 N = 0.3848

HYDRODYNAMIC SPECIFIC VOLUME AND SURFACE AS FUNCTIONS OF PRESSURE

PRESSURE CM. H2O	V CC./G.	SW SQCM./G.	SV SQCM./CC.
10.	3.74	4451.23	1189.68
20.	3.12	4376.03	1401.97
30.	2.81	4347.00	1547.32
40.	2.61	4333.72	1662.24
50.	2.46	4327.91	1759.22
60.	2.35	4326.22	1844.20
70.	2.25	4327.04	1920.47
80.	2.18	4329.48	1990.12
90.	2.11	4333.01	2054.51

AVERAGE VALUES FOR SPECIFIC VOLUME AND SURFACE

AVERAGE SPECIFIC VOLUME = 2.62 CC./G.
 AVERAGE SPECIFIC SURFACE, SW = 4350.18 SQCM./G.
 AVERAGE SPECIFIC SURFACE, SV = 1707.75 SQCM./CC.

Appendix VII (Continued)

 * FLOC FRACTION RETAINED ON 65 MESH FIBER LENGTH = 1.74 MM. *

ORIGINAL DATA

FILTRATION EXPERIMENT			COMPRESSIBILITY EXPERIMENT		
PRESSURE CM. H ₂ O	CHART READING	TIME SEC.	PRESSURE DYNES/SQCM.	PAD THICK. INCHES	SOLIDS CONC. G./CC.
10.	6.68	200.30	0.	0.0	0.0
20.	10.86	325.90	0.	0.0	0.0
30.	14.36	430.80	9037.	1.6190	0.0475
40.	17.44	523.20	13998.	1.3570	0.0567
50.	20.07	602.20	23806.	1.1024	0.0697
60.	22.52	675.70	38507.	0.9158	0.0840
70.	24.77	743.00	63034.	0.7597	0.1012
80.	26.86	805.90	97015.	0.6458	0.1191
90.	28.83	864.80	146113.	0.5537	0.1389

FILT. PAD WT. = 11.2212 G. EQ. VOL. = 75825.40 CC. CONSISTENCY = 0.015 PERCENT
 FLOW RATE = 84.9 CC./SEC. H₂O VISC. = 0.009979 POISE COMP. PAD WT. = 8.8940 G.

FILTRATION RESISTANCE AND MAT SOLIDS CONCENTRATION AS FUNCTIONS OF PRESSURE

PRESSURE		FILTRATION RESISTANCE	MAT SOLIDS CONCENTRATION	DP/(T*SQRT(CP))	CP**3
CM. H ₂ O	DYNES/SQCM.	CM./G.	G./CC.		
10.	9807.	.9493E 07	0.0494	220.39	0.12020-03
20.	19613.	.1167E 08	0.0644	237.08	0.26760-03
30.	29420.	.1324E 08	0.0753	248.84	0.42730-03
40.	39227.	.1454E 08	0.0841	258.48	0.59560-03
50.	49033.	.1579E 08	0.0917	268.91	0.77060-03
60.	58840.	.1688E 08	0.0983	277.68	0.95110-03
70.	68647.	.1791E 08	0.1044	286.01	0.11360-02
80.	78453.	.1887E 08	0.1099	293.71	0.13260-02
90.	88260.	.1979E 08	0.1149	301.02	0.15190-02

M = 0.14370-02 N = 0.3848

HYDRODYNAMIC SPECIFIC VOLUME AND SURFACE AS FUNCTIONS OF PRESSURE

PRESSURE CM. H ₂ O	V CC./G.	SW SQCM./G.	SV SQCM./CC.
10.	3.45	5106.59	1482.25
20.	2.97	5014.75	1689.16
30.	2.72	4976.48	1832.29
40.	2.55	4957.42	1946.43
50.	2.42	4947.78	2043.47
60.	2.32	4943.51	2129.04
70.	2.24	4942.61	2206.27
80.	2.17	4943.93	2277.14
90.	2.11	4946.80	2342.96

AVERAGE VALUES FOR SPECIFIC VOLUME AND SURFACE

AVERAGE SPECIFIC VOLUME = 2.55 CC./G.
 AVERAGE SPECIFIC SURFACE, SW = 4975.54 SQCM./G.
 AVERAGE SPECIFIC SURFACE, SV = 1994.33 SQCM./CC.

Appendix VII (Continued)

 * FLOC FRACTION RETAINED ON 65 MESH FIBER LENGTH = 2.07 MM. *
 * *****

ORIGINAL DATA

FILTRATION EXPERIMENT			COMPRESSIBILITY EXPERIMENT		
PRESSURE CM. H2O	CHART READING	TIME SEC.	PRESSURE DYNES/SQCM.	PAD THICK. INCHES	SOLIDS CONC. G./CC.
10.	6.13	183.84	0.	0.0	0.0
20.	10.20	305.88	0.	0.0	0.0
30.	13.56	406.80	9037.	2.0490	0.0462
40.	16.51	495.36	13998.	1.7174	0.0551
50.	19.13	573.90	23806.	1.3952	0.0678
60.	21.57	647.10	38507.	1.1590	0.0816
70.	23.84	715.14	63034.	0.9615	0.0984
80.	26.00	780.06	97015.	0.8174	0.1158
90.	27.91	837.18	146113.	0.7008	0.1350

FILT. PAD WT. = 15.3695 G. EQ. VOL. = 74956.90 CC. CONSISTENCY = 0.021 PERCENT
 FLOW RATE = 87.4 CC./SEC. H2O VISC. = 0.009218 POISE COMP. PAD WT. = 10.9453 G.

FILTRATION RESISTANCE AND MAT SOLIDS CONCENTRATION AS FUNCTIONS OF PRESSURE

PRESSURE		FILTRATION RESISTANCE	MAT SOLIDS CONCENTRATION	DP/(T*SQRT(CP))	CP**3
CM. H2O	DYNES/SQCM.	CM./G.	G./CC.		
10.	9807.	.7629E 07	0.0480	243.50	0.11050-03
20.	19613.	.9171E 07	0.0627	256.16	0.24600-03
30.	29420.	.1034E 08	0.0732	267.24	0.39280-03
40.	39227.	.1133E 08	0.0818	276.86	0.54760-03
50.	49033.	.1222E 08	0.0891	286.16	0.70840-03
60.	58840.	.1300E 08	0.0956	294.05	0.87440-03
70.	68647.	.1373E 08	0.1015	301.35	0.10450-02
80.	78453.	.1438E 08	0.1068	307.73	0.12190-02
90.	88260.	.1508E 08	0.1118	315.34	0.13960-02

M = 0.13970-02 N = 0.3848

HYDRODYNAMIC SPECIFIC VOLUME AND SURFACE AS FUNCTIONS OF PRESSURE

PRESSURE CM. H2O	V CC./G.	SW SQCM./G.	SV SQCM./CC.
10.	3.18	4560.27	1432.07
20.	2.81	4474.97	1592.44
30.	2.60	4434.63	1705.33
40.	2.46	4411.70	1796.01
50.	2.35	4397.75	1873.42
60.	2.26	4389.13	1941.86
70.	2.19	4383.98	2003.75
80.	2.13	4381.20	2060.63
90.	2.07	4380.12	2113.52

AVERAGE VALUES FOR SPECIFIC VOLUME AND SURFACE

AVERAGE SPECIFIC VOLUME = 2.45 CC./G.
 AVERAGE SPECIFIC SURFACE, SW = 4423.75 SQCM./G.
 AVERAGE SPECIFIC SURFACE, SV = 1835.45 SQCM./CC.

Appendix VII (Continued)

 * FLOC FRACTION RETAINED ON 20 MESH FIBER LENGTH = 2.98 MM. *
 * *****

ORIGINAL DATA

FILTRATION EXPERIMENT			COMPRESSIBILITY EXPERIMENT		
PRESSURE CM. H2O	CHART READING	TIME SEC.	PRESSURE DYNES/SQCM.	PAD THICK. INCHES	SOLIDS CONC. G./CC.
10.	8.64	259.12	0.	0.0	0.0
20.	14.49	434.70	0.	0.0	0.0
30.	19.37	581.17	9037.	2.5497	0.0451
40.	23.79	713.77	13998.	2.1370	0.0538
50.	27.81	834.30	23806.	1.7361	0.0662
60.	31.55	946.57	38507.	1.4422	0.0797
70.	35.09	1052.62	63034.	1.1964	0.0961
80.	38.32	1149.67	97015.	1.0171	0.1131
90.	41.16	1234.80	146113.	0.8720	0.1319

FILT. PAD WT. = 20.8284 G. EQ. VOL. = 110658.80 CC. CONSISTENCY = 0.019 PERCENT
 FLOW RATE = 87.6 CC./SEC. H2O VISC. = 0.009175 POISE COMP. PAD WT. = 13.3006 G.

FILTRATION RESISTANCE AND MAT SOLIDS CONCENTRATION AS FUNCTIONS OF PRESSURE

PRESSURE		FILTRATION RESISTANCE	MAT SOLIDS CONCENTRATION	DP/(T*SQRT(CP))	CP**3
CM. H2O	DYNES/SQCM.	CM./G.	G./CC.		
10.	9807.	.5894E 07	0.0469	174.82	0.10290-03
20.	19613.	.7027E 07	0.0612	182.40	0.22910-03
30.	29420.	.7884E 07	0.0715	189.28	0.36590-03
40.	39227.	.8559E 07	0.0799	194.43	0.51000-03
50.	49033.	.9153E 07	0.0871	199.19	0.65980-03
60.	58840.	.9681E 07	0.0934	203.41	0.81440-03
70.	68647.	.1016E 08	0.0991	207.17	0.97300-03
80.	78453.	.1063E 08	0.1043	211.28	0.11350-02
90.	88260.	.1113E 08	0.1092	216.35	0.13000-02

M = 0.13640-02 N = 0.3848

HYDRODYNAMIC SPECIFIC VOLUME AND SURFACE AS FUNCTIONS OF PRESSURE

PRESSURE CM. H2O	V CC./G.	SW SQCM./G.	SV SQCM./CC.
10.	3.07	4014.35	1309.66
20.	2.67	3922.46	1468.05
30.	2.46	3876.80	1575.46
40.	2.32	3848.76	1659.86
50.	2.21	3829.84	1730.78
60.	2.13	3816.39	1792.71
70.	2.06	3806.53	1848.16
80.	2.00	3799.18	1898.68
90.	1.95	3793.67	1945.31

AVERAGE VALUES FOR SPECIFIC VOLUME AND SURFACE

AVERAGE SPECIFIC VOLUME = 2.32 CC./G.
 AVERAGE SPECIFIC SURFACE, SW = 3856.44 SQCM./G.
 AVERAGE SPECIFIC SURFACE, SV = 1692.07 SQCM./CC.

Appendix VII (Continued)

 * FLOC FRACTION RETAINED ON 10 MESH FIBER LENGTH = 4.13 MM. *

ORIGINAL DATA

FILTRATION EXPERIMENT			COMPRESSIBILITY EXPERIMENT		
PRESSURE CM. H ₂ O	CHART READING	TIME SEC.	PRESSURE DYNES/SQCM.	PAD THICK. INCHES	SOLIDS CONC. G./CC.
10.	8.11	243.30	0.	0.0	0.0
20.	13.51	405.30	0.	0.0	0.0
30.	18.14	544.30	9037.	2.2036	0.0452
40.	22.51	675.40	13998.	1.8469	0.0540
50.	26.39	791.60	23806.	1.5004	0.0664
60.	30.17	905.10	38507.	1.2465	0.0800
70.	33.80	1014.10	63034.	1.0340	0.0964
80.	37.29	1118.80	97015.	0.8790	0.1134
90.	40.71	1221.40	146113.	0.7536	0.1323

FILT. PAD WT. = 30.3815 G. EQ. VOL. = 111436.70 CC. CONSISTENCY = 0.027 PERCENT
 FLOW RATE = 90.0 CC./SEC. H₂O VISC. = 0.008551 POISE COMP. PAD WT. = 11.5314 G.

FILTRATION RESISTANCE AND MAT SOLIDS CONCENTRATION AS FUNCTIONS OF PRESSURE

PRESSURE		FILTRATION RESISTANCE	MAT SOLIDS CONCENTRATION	DP/(T*SQRT(CP))	CP**3
CM. H ₂ O	DYNES/SQCM.	CM./G.	G./CC.		
10.	9807.	.4409E 07	0.0470	185.90	0.10390-03
20.	19613.	.5293E 07	0.0614	195.32	0.23130-03
30.	29420.	.5912E 07	0.0717	201.79	0.36940-03
40.	39227.	.6352E 07	0.0801	205.15	0.51480-03
50.	49033.	.6775E 07	0.0873	209.60	0.66610-03
60.	58840.	.7110E 07	0.0937	212.40	0.82220-03
70.	68647.	.7404E 07	0.0994	214.70	0.98230-03
80.	78453.	.7670E 07	0.1046	216.77	0.11460-02
90.	88260.	.7904E 07	0.1095	218.37	0.13130-02

M = 0.1369D-02 N = 0.3848

HYDRODYNAMIC SPECIFIC VOLUME AND SURFACE AS FUNCTIONS OF PRESSURE

PRESSURE CM. H ₂ O	V CC./G.	SW SQCM./G.	SV SQCM./CC.
10.	3.44	3535.82	1027.34
20.	2.65	3396.39	1279.68
30.	2.28	3317.14	1457.44
40.	2.04	3261.71	1599.67
50.	1.87	3219.07	1720.40
60.	1.74	3184.41	1826.46
70.	1.64	3155.20	1921.76
80.	1.56	3129.94	2008.78
90.	1.49	3107.67	2089.17

AVERAGE VALUES FOR SPECIFIC VOLUME AND SURFACE

AVERAGE SPECIFIC VOLUME = 2.08 CC./G.
 AVERAGE SPECIFIC SURFACE, SW = 3256.37 SQCM./G.
 AVERAGE SPECIFIC SURFACE, SV = 1658.97 SQCM./CC.

Appendix VII (Continued)

 * WHOLE PULP RETAINED ON 65 MESH FIBER LENGTH = 1.49 MM. *
 * *****

----- ORIGINAL DATA -----

FILTRATION EXPERIMENT			COMPRESSIBILITY EXPERIMENT		
PRESSURE CM. H2O	CHART READING	TIME SEC.	PRESSURE DYNES/SQCM.	PAD THICK. INCHES	SOLIDS CONC. G./CC.
10.	6.71	201.30	0.	0.0	0.0
20.	10.93	327.90	0.	0.0	0.0
30.	14.28	428.40	9037.	1.5735	0.0468
40.	17.08	512.40	13998.	1.3188	0.0559
50.	19.62	588.60	23806.	1.0714	0.0688
60.	21.73	651.90	38507.	0.8900	0.0828
70.	23.84	715.20	63034.	0.7383	0.0998
80.	25.77	773.10	97015.	0.6277	0.1174
90.	27.42	822.60	146113.	0.5381	0.1370

FILT. PAD WT. = 9.8641 G. EQ. VOL. = 66882.94 CC. CONSISTENCY = 0.015 PERCENT
 FLOW RATE = 77.3 CC./SEC. H2O VISC. = 0.009571 POISE COMP. PAD WT. = 8.5246 G.

----- FILTRATION RESISTANCE AND MAT SOLIDS CONCENTRATION AS FUNCTIONS OF PRESSURE -----

PRESSURE		FILTRATION RESISTANCE	MAT SOLIDS CONCENTRATION	DP/(T*SQRT(CP))	CP**3
CM. H2O	DYNES/SQCM.	CM./G.	G./CC.		
10.	9807.	.1192E 08	0.0487	220.82	0.1153D-03
20.	19613.	.1464E 08	0.0635	237.28	0.2566D-03
30.	29420.	.1680E 08	0.0743	251.97	0.4098D-03
40.	39227.	.1873E 08	0.0830	265.76	0.5713D-03
50.	49033.	.2038E 08	0.0904	277.04	0.7391D-03
60.	58840.	.2209E 08	0.0970	289.82	0.9123D-03
70.	68647.	.2349E 08	0.1029	299.19	0.1090D-02
80.	78453.	.2483E 08	0.1083	308.30	0.1272D-02
90.	88260.	.2625E 08	0.1134	318.67	0.1457D-02
		M = 0.1417D-02	N = 0.3848		

----- HYDRODYNAMIC SPECIFIC VOLUME AND SURFACE AS FUNCTIONS OF PRESSURE -----

PRESSURE CM. H2O	V CC./G.	SW SQCM./G.	SV SQCM./CC.
10.	3.53	5763.89	1630.83
20.	3.16	5694.86	1799.60
30.	2.94	5670.55	1927.92
40.	2.78	5663.76	2035.35
50.	2.66	5665.67	2129.70
60.	2.56	5672.48	2214.94
70.	2.48	5682.27	2293.37
80.	2.41	5693.93	2366.47
90.	2.34	5706.82	2435.28

----- AVERAGE VALUES FOR SPECIFIC VOLUME AND SURFACE -----

AVERAGE SPECIFIC VOLUME = 2.76 CC./G.
 AVERAGE SPECIFIC SURFACE, SW = 5690.46 SQCM./G.
 AVERAGE SPECIFIC SURFACE, SV = 2092.60 SQCM./CC.

Appendix VII (Continued)

 *
 * WHOLE PULP RETAINED ON 20 MESH FIBER LENGTH = 2.76 MM.
 *
 *

ORIGINAL DATA

FILTRATION EXPERIMENT			COMPRESSIBILITY EXPERIMENT		
PRESSURE CM. H ₂ O	CHART READING	TIME SEC.	PRESSURE DYNES/SQCM.	PAD THICK. INCHES	SOLIDS CONC. G./CC.
10.	6.29	188.70	0.	0.0	0.0
20.	9.82	294.60	0.	0.0	0.0
30.	12.90	387.00	9037.	2.7308	0.0442
40.	15.50	465.00	13998.	2.2888	0.0527
50.	17.76	532.80	23806.	1.8594	0.0649
60.	19.97	599.10	38507.	1.5447	0.0781
70.	22.00	660.00	63034.	1.2814	0.0942
80.	23.80	714.00	97015.	1.0893	0.1108
90.	25.39	761.70	146113.	0.9339	0.1292

FILT. PAD WT. = 17.1414 G. EQ. VOL. = 61389.57 CC. CONSISTENCY = 0.028 PERCENT
 FLOW RATE = 77.3 CC./SEC. H₂O VISC. = 0.009686 POISE COMP. PAD WT. = 13.9570 G.

FILTRATION RESISTANCE AND MAT SOLIDS CONCENTRATION AS FUNCTIONS OF PRESSURE

PRESSURE		FILTRATION RESISTANCE	MAT SOLIDS CONCENTRATION	DP/(T*SQRT(CP))	CP**3
CM. H ₂ O	DYNES/SQCM.	CM./G.	G./CC.		
10.	9807.	.6637E 07	0.0459	242.53	0.9680D-04
20.	19613.	.8502E 07	0.0600	271.91	0.2155D-03
30.	29420.	.9709E 07	0.0701	287.18	0.3441D-03
40.	39227.	.1077E 08	0.0783	301.51	0.4796D-03
50.	49033.	.1175E 08	0.0853	315.11	0.6206D-03
60.	58840.	.1254E 08	0.0915	324.69	0.7660D-03
70.	68647.	.1328E 08	0.0971	333.81	0.9151D-03
80.	78453.	.1403E 08	0.1022	343.69	0.1068D-02
90.	88260.	.1480E 08	0.1069	354.32	0.1223D-02

M = 0.1337D-02 N = 0.3848

HYDRODYNAMIC SPECIFIC VOLUME AND SURFACE AS FUNCTIONS OF PRESSURE

PRESSURE CM. H ₂ O	V CC./G.	SW SQCM./G.	SV SQCM./CC.
10.	4.45	4509.75	1013.47
20.	3.56	4448.18	1250.23
30.	3.13	4423.50	1413.98
40.	2.86	4411.48	1543.45
50.	2.67	4405.47	1652.39
60.	2.52	4402.81	1747.45
70.	2.40	4402.19	1832.38
80.	2.31	4402.90	1909.56
90.	2.22	4404.52	1980.58

AVERAGE VALUES FOR SPECIFIC VOLUME AND SURFACE

AVERAGE SPECIFIC VOLUME = 2.90 CC./G.
 AVERAGE SPECIFIC SURFACE, SW = 4423.42 SQCM./G.
 AVERAGE SPECIFIC SURFACE, SV = 1593.72 SQCM./CC.

Appendix VII (Continued)

 *
 * WHOLE PULP RETAINED ON 10 MESH FIBER LENGTH = 3.88 MM. *
 *

ORIGINAL DATA

FILTRATION EXPERIMENT			COMPRESSIBILITY EXPERIMENT		
PRESSURE CM. H2O	CHART READING	TIME SEC.	PRESSURE DYNES/SQCM.	PAD THICK. INCHES	SOLIDS CONC. G./CC.
10.	8.00	240.00	0.	0.0	0.0
20.	13.40	402.00	0.	0.0	0.0
30.	17.75	532.50	9037.	3.4449	0.0450
40.	21.77	653.10	13998.	2.8874	0.0537
50.	25.33	759.90	23806.	2.3457	0.0661
60.	28.72	861.60	38507.	1.9486	0.0796
70.	31.95	958.50	63034.	1.6165	0.0959
80.	34.86	1045.80	97015.	1.3742	0.1128
90.	37.65	1129.50	146113.	1.1782	0.1316

FILT. PAD WT. = 24.8004 G. EQ. VOL. = 90146.69 CC. CONSISTENCY = 0.028 PERCENT
 FLOW RATE = 77.3 CC./SEC. H2O VISC. = 0.009709 POISE COMP. PAD WT. = 17.9365 G.

FILTRATION RESISTANCE AND MAT SOLIDS CONCENTRATION AS FUNCTIONS OF PRESSURE

PRESSURE		FILTRATION RESISTANCE	MAT SOLIDS CONCENTRATION	DP/(T*SQRT(CP))	CP**3
CM. H2O	DYNES/SQCM.	CM./G.	G./CC.		
10.	9807.	.5284E 07	0.0468	188.93	0.10230-03
20.	19613.	.6309E 07	0.0611	197.42	0.22780-03
30.	29420.	.7144E 07	0.0714	206.78	0.36380-03
40.	39227.	.7767E 07	0.0797	212.69	0.50710-03
50.	49033.	.8344E 07	0.0869	218.90	0.65600-03
60.	58840.	.8831E 07	0.0932	223.69	0.80970-03
70.	68647.	.9261E 07	0.0989	227.73	0.96740-03
80.	78453.	.9700E 07	0.1041	232.49	0.11290-02
90.	88260.	.1010E 08	0.1089	236.74	0.12930-02

M = 0.1362D-02 N = 0.3848

HYDRODYNAMIC SPECIFIC VOLUME AND SURFACE AS FUNCTIONS OF PRESSURE

PRESSURE CM. H2O	V CC./G.	SW SQCM./G.	SV SQCM./CC.
10.	3.38	3860.99	1142.04
20.	2.83	3759.68	1328.08
30.	2.56	3710.86	1451.94
40.	2.38	3681.19	1547.97
50.	2.25	3661.16	1627.80
60.	2.15	3646.82	1696.89
70.	2.07	3636.16	1758.28
80.	2.00	3628.06	1813.83
90.	1.94	3621.82	1864.79

AVERAGE VALUES FOR SPECIFIC VOLUME AND SURFACE

AVERAGE SPECIFIC VOLUME = 2.39 CC./G.
 AVERAGE SPECIFIC SURFACE, SW = 3689.64 SQCM./G.
 AVERAGE SPECIFIC SURFACE, SV = 1581.29 SQCM./CC.

Appendix VII (Continued)

*
* WHOLE PULP -- NOT CLASSIFIED *
*

ORIGINAL DATA

FILTRATION EXPERIMENT			COMPRESSIBILITY EXPERIMENT		
PRESSURE CM. H2O	CHART READING	TIME SEC.	PRESSURE DYNES/SQCM.	PAD THICK. INCHES	SOLIDS CONC. G./CC.
10.	6.07	182.10	0.	0.0	0.0
20.	9.50	285.00	0.	0.0	0.0
30.	12.30	369.00	9037.	2.1378	0.0443
40.	14.69	440.70	13998.	1.7918	0.0528
50.	16.83	504.90	23806.	1.4557	0.0650
60.	18.80	564.00	38507.	1.2093	0.0783
70.	20.65	619.50	63034.	1.0032	0.0943
80.	22.37	671.10	97015.	0.8528	0.1110
90.	23.88	716.40	146113.	0.7311	0.1295

FILT. PAD WT. = 13.5742 G. EQ. VOL. = 58602.66 CC. CONSISTENCY = 0.023 PERCENT
FLOW RATE = 77.3 CC./SEC. H2O VISC. = 0.009436 POISE COMP. PAD WT. = 10.9475 G.

FILTRATION RESISTANCE AND MAT SOLIDS CONCENTRATION AS FUNCTIONS OF PRESSURE

PRESSURE		FILTRATION RESISTANCE	MAT SOLIDS CONCENTRATION	DP/(T*SQRT(CP))	CP**3
CM. H2O	DYNES/SQCM.	CM./G.	G./CC.		
10.	9807.	.8510E 07	0.0460	251.08	0.97360-04
20.	19613.	.1088E 08	0.0601	280.79	0.21670-03
30.	29420.	.1260E 08	0.0702	300.90	0.34610-03
40.	39227.	.1407E 08	0.0784	317.83	0.48240-03
50.	49033.	.1535E 08	0.0855	332.20	0.62420-03
60.	58840.	.1649E 08	0.0917	344.57	0.77040-03
70.	68647.	.1751E 08	0.0973	355.29	0.92040-03
80.	78453.	.1847E 08	0.1024	365.32	0.10740-02
90.	88260.	.1947E 08	0.1072	376.37	0.12300-02

M = 0.13390-02 N = 0.3848

HYDRODYNAMIC SPECIFIC VOLUME AND SURFACE AS FUNCTIONS OF PRESSURE

PRESSURE CM. H2O	V CC./G.	SW SQCM./G.	SV SQCM./CC.
10.	4.60	5116.50	1111.73
20.	3.68	5067.98	1375.69
30.	3.24	5053.32	1559.10
40.	2.96	5049.62	1704.65
50.	2.76	5050.81	1827.50
60.	2.61	5054.55	1934.96
70.	2.49	5059.72	2031.21
80.	2.39	5065.75	2118.84
90.	2.31	5072.29	2199.63

AVERAGE VALUES FOR SPECIFIC VOLUME AND SURFACE

AVERAGE SPECIFIC VOLUME = 3.01 CC./G.
AVERAGE SPECIFIC SURFACE, SW = 5065.61 SQCM./G.
AVERAGE SPECIFIC SURFACE, SV = 1762.59 SQCM./CC.

```

/JOB GO,TIME=99
/FILE DISK=(1,NREC=20000),R SIZ=128
/FILE DISK=(2,IDUT,NREC=4000),R SIZ=80,VOL=SYSFL1,DISP=(NEW,DELETE)
/FILE DISK=(3,KOUT,NREC=4000),R SIZ=80,VOL=SYSFL1,DISP=(NEW,DELETE)
/FILE DISK=(4,MOUT,NREC=5000),R SIZ=128,VOL=SYSFL1,DISP=(NEW,DELETE)

```

ANTHONY P. BINOTTO
JANUARY 16, 1975

THE PROGRAM IS DIVIDED INTO SEVERAL SUBROUTINES WHICH CALCULATE THE VARIOUS PARAMETERS NEEDED TO SOLVE THE EQUATION. THE FUNCTIONS OF EACH SUBROUTINE ARE EXPLAINED IN THEIR RESPECTIVE COMMENT STATEMENTS.

```

/ID XXXXXXXXXX,XXX
/INCLUDE PRMEAT
/INCLUDE SOLCON
/INCLUDE DATFIT
/INCLUDE FVSX
/INCLUDE CURVE
/DATA

```

```

DATA CARD 1 -- ANY TITLE, CENTERING ON THE CARD WILL
                ENSURE CENTERING ON OUTPUT.
DATA CARD 2 -- THE FOLLOWING DATA IN 8F10.0 FORMAT.
                1ST. O.D. WT. OF MAT, G.
                2ND. WET MAT THICKNESS, CM.
                3RD. PERMEATION VELOCITY, CM./SEC.
                4TH. WATER TEMP., DEG. C.
DATA CARD 3 -- PRESSURE DROPS FOR TAPS 1 THRU 8
DATA CARD 4 -- PRESSURE DROPS FOR TAPS 9 THRU 12
DATA CARD 5 -- MAT THICK. FROM COMPRESSIBILITY EXP.
DATA CARD 6 -- INITIAL WATER LEVEL FOR COMP. EXPERIMENT
                /END

```

```

DIMENSION DPZ(12),PDTHCK(12),DP2(8),MATCON(8),V(12),SW(12),SV(12)
DIMENSION CMH2O(8),Z(12),H2ODPZ(12),TTITLE(20),OH2ODP(12)
DIMENSION ODPZ(12)
DOUBLE PRECISION N,M,MATCON,EXPM,EXPN,V,DPL,DPZ,L,Z,A,B,C,H2OLVL
DOUBLE PRECISION MU,U,H2ODPZ,H2ODPL,BZ,W,PDTHCK,AREA,DP2,B0,B1
DOUBLE PRECISION SW,SV
COMMON MU,U,M,N,L,DPL,A,B,C,B0,B1,B2,EXPM,EXPN

```

```
C***      COMMON /UOCTHAPLTOPC/A,B,C,YB6701,YB2,EXP,H,XAPN  
K = 12, LAST TAP TO BE ANALYZED  
K = 12  
C***      SAVE FILE ''IOUT'' TO OBTAIN PLOTS OF ''CP**3 VS. F''  
IOUT = 2  
C***      SAVE FILE ''JOUT'' TO OBTAIN PUNCHED OUTPUT OF ''P,V,SW,SV''  
JOUT = 1  
C***      SAVE FILE ''KOUT'' TO OBTAIN PLOTS OF ''DPZ/DPL VS. Z/L''  
KOUT = 3  
C***      SAVE FILE ''LOUT'' TO OBTAIN PLOTS OF ''SOLIDS CONC. VS. PRESS.'''  
LOUT = 1  
C***      SAVE FILE ''MOUT'' TO OBTAIN PRINTED OUTPUT OF DATA AND RESULTS  
MOUT = 6
```

```

WRITE (IOUT,9008)
WRITE (IOUT,9009)
WRITE (JOUT,9006)
WRITE (JOUT,9007)
WRITE (KOUT,9014)
WRITE (KOUT,9015)
WRITE (LOUT,9011)
WRITE (LOUT,9012)
1 READ(5,9019) ITITLE
  IF (ICOMP(ITITLE,1,249,4,1)) 2,7,2
2 READ(5,9120) W,L,U,T,J,LIN,EXP,N,INIT
  NPTS = K - J + 1
  READ(5,9020) (H2QDPL(I),I=1,12)
  READ(5,9020) (PDTHCK(I), I=1,8)
  WRITE (JOUT,9019) ITITLE
  WRITE (JOUT,9005) NPTS
  WRITE (IOUT,9019) ITITLE
  WRITE (KOUT,9019) ITITLE
  WRITE (KOUT,9016)
  WRITE (LOUT,9019) ITITLE
  WRITE (LOUT,9013)
  READ (5,9020) H2DLVL,DPLQ
  H2QDPL = 60.
  DPL = H2QDPL * 980.638

```

Appendix VIII (Continued)

```

DO 3 I=1,12
  ODPZ(I) = OH2ODP(I) * 980.638
3  DPZ(I) = OH2ODP(I) * 980.638
  AREA = 45.58
  BW = W / (L * AREA)
  IF (T-20) 4,4,5
4  ETA = (1301.7 / (998.333 + 8.1855 * (T-20.) + .00585 * ((T-20.)**2)))
  MU = 10. ** (ETA - 3.30233)
  GO TO 6
5  ETA = (1.3272 * (20.-T) - .001053 * ((T-20.)**2)) / (T+105.)
  MU = (10. ** ETA) * .01002
6  CALL SOLCON (W,PDTHCK,AREA,N,M,MATCON,DP2,CMH2O,H2OLVL,LOUT,DPZ,
  *L,DPL0)
  CALL DATFIT (DPZ,Z,INIT,K,KOUT)
  CALL FVSX (DPZ,Z,V,SW,SV,J,LIN,K,IOUT,DPL0,80,82)
DO 8 I=1,12
8  H2ODPZ(I) = DPZ(I) / 980.638
  WRITE (MOUT,9042)
  WRITE (MOUT,9021)
  WRITE (MOUT,9022)
  WRITE (MOUT,9022)
  WRITE (MOUT,9023) ITITLE
  WRITE (MOUT,9022)
  WRITE (MOUT,9022)
  WRITE (MOUT,9024)
  WRITE (MOUT,9025)
  WRITE (MOUT,9026)
  WRITE (MOUT,9027) BW
  WRITE (MOUT,9028) W
  WRITE (MOUT,9029) L
  WRITE (MOUT,9030) H2ODPL
  WRITE (MOUT,9031) U
  WRITE (MOUT,9032) T
  WRITE (MOUT,9033) MU
  WRITE (MOUT,9034)
  WRITE (MOUT,9035)
  WRITE (MOUT,9036)
  WRITE (MOUT,9037)
  WRITE (MOUT,9038)
  WRITE (MOUT,9039)
  WRITE (MOUT,9040) (I,Z(I),OH2ODP(I),ODPZ(I),CMH2O(I),DP2(I),
  * PDTHCK(I),MATCON(I),I=1,8)
  WRITE (MOUT,9041) (I,Z(I),OH2ODP(I),ODPZ(I),I=9,12)
  WRITE (MOUT,9042)
  WRITE (MOUT,9043)
  WRITE (MOUT,9044)
  WRITE (MOUT,9045) M
  WRITE (MOUT,9046) N
  WRITE (MOUT,9042)
  WRITE (MOUT,9047)
  WRITE (MOUT,9048)
  WRITE (MOUT,9049)
  WRITE (MOUT,9050)
  WRITE (MOUT,9051) A,80,EXPM
  WRITE (MOUT,9052) B,81,EXPB
  WRITE (MOUT,9053) C,82
  WRITE (MOUT,9042)
  IF (LIN-12) 10,9,7
9  WRITE (MOUT,9059)
  WRITE (MOUT,9060)
  WRITE (MOUT,9061) DPL0,H2ODPL
  WRITE (MOUT,9062) V(K)
  WRITE (MOUT,9063) SW(K)
  WRITE (MOUT,9064) SV(K)
  WRITE (MOUT,9042)
  GO TO 1
10 WRITE (MOUT,9054)
  WRITE (MOUT,9055)
  WRITE (MOUT,9056)
  WRITE (MOUT,9057)
  WRITE (MOUT,9058) (H2ODPZ(I),V(I),SW(I),SV(I),I=J,K)
  WRITE (MOUT,9042)
  WRITE (JOUT,9018) (H2ODPZ(I),V(I),SW(I),SV(I),I=J,K)
  GO TO 1
7  WRITE (IOUT,9017)
  WRITE (JOUT,9017)
  WRITE (KOUT,9017)
  WRITE (LOUT,9017)
  WRITE (MOUT,9017)
  END FILE IOUT
  END FILE JOUT
  END FILE KOUT
  END FILE LOUT
  END FILE MOUT
STOP

```

Appendix VIII (Continued)

```

9005 FORMAT (I3,' 2 2 -1 3')
9006 FORMAT ('PRESSURE, CM. H2O')
9007 FORMAT ('SPEC. VOLUME, CC./G.')
9008 FORMAT ('(CL*(DPZ/DPL)**N)**3')
9009 FORMAT ('F')
9011 FORMAT ('PRESSURE, DYNES/SQCM.')
9012 FORMAT ('SOLIDS CONC., G./CC.')
9013 FORMAT (' 7 2 2 -1 3')
9014 FORMAT ('Z/L')
9015 FORMAT ('DPZ/DPL')
9016 FORMAT (' 12 1 1 -1 3')
9017 FORMAT ('999999999999999')
9018 FORMAT (4E15.7)
9019 FORMAT (20A4)
9020 FORMAT (8F10.0)
9021 FORMAT (4F10.0,I2,8X,I2,8X,F10.0,I2)
9021 FORMAT (1H1,16X,'*****')
9022 FORMAT (' 16X, 85X, ')
9023 FORMAT (' 16X, 3X, 20A4, 2X, ')
9024 FORMAT (' 16X, '*****')
9025 FORMAT ('0', 'ORIGINAL DATA')
9026 FORMAT ('0', '-----', '/')
9027 FORMAT ('0', 10X, 'MAT SOLIDS CONC. ', 12X, '=', F10.4, ' G./CC.')
9028 FORMAT ('0', 10X, 'O.D. MAT WT. ', 14X, '=', F10.4, ' G.')
9029 FORMAT ('0', 10X, 'MAT THICKNESS, L', 13X, '=', F8.2, ' CM.')
9030 FORMAT ('0', 10X, 'TOTAL PRESSURE DROP, DPL', 5X, '=', F8.2,
* ' CM. H2O')
9031 FORMAT ('0', 10X, 'PERMEATION VELOCITY, U', 7X, '=', F12.6,
* ' CM./SEC.')
9032 FORMAT ('0', 10X, 'WATER TEMPERATURE, T', 9X, '=', F7.1, ' DEG. C.')
9033 FORMAT ('0', 10X, 'WATER VISCOSITY, MU', 10X, '=', F12.6, ' POISES', '/')
9034 FORMAT ('0', 10X, 'PERMEATION EXPERIMENT', 35X, 'COMPRESSIBILITY EXPE
* RIMENT')
9035 FORMAT ('0', 26X, 'Z', 19X, 'DPZ')
9036 FORMAT ('0', 10X, 'PRESSURE DISTANCE', 62X, 'MAT MAT SOLIDS')
9037 FORMAT ('0', 12X, 'TAP', 8X, 'FROM TOP', 6X, 'PRESSURE TAP READING', 14X,
* 'PRESSURE', 11X, 'THICKNESS CONCENTRATION')
9038 FORMAT ('0', 11X, 'NUMBER', 7X, 'OF MAT')
9039 FORMAT ('0', 25X, 'CM.', 8X, 'CM. H2O', 4X, 'DYNES/SQCM.', 8X, 'CM. H2O',
* 3X, 'DYNES/SQCM.', 6X, 'CM.', 7X, 'G./CC.', '/')
9040 FORMAT ('0', 13X, I2, 8X, F7.4, 7X, F6.2, 4X, F9.2, 10X, F6.2, 6X, F7.0, 6X,
* F6.4, 6X, F6.4)
9041 FORMAT ('0', 13X, I2, 8X, F7.4, 7X, F6.2, 4X, F9.2)
9042 FORMAT ('0', '/')
9043 FORMAT ('0', 'COMPRESSIBILITY CONSTANTS')
9044 FORMAT ('0', '-----', '/')
9045 FORMAT ('0', 10X, 'M = ', E11.4)
9046 FORMAT ('0', 10X, 'N = ', F7.4)
9047 FORMAT ('0', 'EXPERIMENTAL EMPIRICAL CONSTANTS')
9048 FORMAT ('0', '-----', '/')
9049 FORMAT ('0', 10X, 'DPZ/DPL = A * ((Z/L)**B) * EXP(C*Z/L)', 5X, 'F = B
* 0 + B1*(X**EXPM) + B2*(X**EXPN)')
9050 FORMAT ('0', 10X, 'WHERE...', 34X, 'WHERE...')
9051 FORMAT ('0', 15X, 'A = ', F9.5, 29X, 'B0 = ', E12.5, 5X, 'EXPM = ', E12.5)
9052 FORMAT ('0', 15X, 'B = ', F9.5, 29X, 'B1 = ', E12.5, 5X, 'EXPN = ', E12.5)
9053 FORMAT ('0', 15X, 'C = ', F9.5, 29X, 'B2 = ', E12.5)
9054 FORMAT ('0', 'HYDRODYNAMIC SPECIFIC VOLUME AND SURFACE AS FUNCTION
* S OF PRESSURE')
9055 FORMAT ('0', '-----')
9056 FORMAT ('0', 15X, 'PRESSURE', 11X, 'V', 13X, 'SW', 16X, 'SV')
9057 FORMAT ('0', 15X, 'CM. H2O', 10X, 'CC./G.', 8X, 'SQCM./G.', 9X,
* 'SQCM./CC.', '/')
9058 FORMAT ('0', 15X, F6.2, 11X, F5.2, 7X, F10.2, 7X, F10.2)
9059 FORMAT ('0', 'HYDRODYNAMIC SPECIFIC VOLUME AND SURFACE')
9060 FORMAT ('0', '-----', '/')
9061 FORMAT ('0', 10X, 'STATIC LOAD = ', F6.2, ' CM. H2O', 5X,
* 'FLUID PRESSURE DROP = ', F5.2, ' CM. H2O')
9062 FORMAT ('0', 10X, 'AVERAGE SPECIFIC VOLUME, V = ', F4.2, ' CC./G.')
9063 FORMAT ('0', 10X, 'AVERAGE SPECIFIC SURFACE, SW = ', F7.2,
* ' SQCM./G.')
9064 FORMAT ('0', 10X, 'AVERAGE SPECIFIC SURFACE, SV = ', F7.2,
* ' SQCM./CC.')
END

```

Appendix VIII (Continued)

DATFIT === DATA FITTING

C
C
C
C
C
C
C

```

THIS SUBROUTINE IS USED TO FIT EXPERIMENTAL VALUES OF DPZ/DPL
VS. Z/L TO THE EXPRESSION.
DPZ/DPL = A * (Z/L)**B * EXP(C * (Z/L))
THE COEFFICIENTS A,B,AND C ARE DETERMINED BY MULTIPLE REGRESSION.

SUBROUTINE DATFIT (DPZ,Z,J,K,KOUT)
DIMENSION DPZ(12),Z(12),A1(3,4),X2(12),Y(12),DLNY(12)
DOUBLE PRECISION Y,SUMY,X1,SUMX1,SSQX1,X2,SUMX2,SSQX2,SX1X2,A1
DOUBLE PRECISION SUMX1Y,SUMX2Y,DLNY,DPZ,DPL,Z,L,A,B,C,MU,U,N,M
COMMON MU,U,M,N,L,DPL,A,B,C
SUMY = 0.
SUMX1 = 0.
SSQX1 = 0.
SUMX2 = 0.
SSQX2 = 0.
SX1X2 = 0.
SUMX1Y = 0.
SUMX2Y = 0.
COUNT = 0.0
DO 3 I=1,12
  Z(I) = L - (.3084 + (12 - I) * .3810)
  X2(I) = Z(I)/L
  IF (Z(I)) 1,1,2
1  DPZ(I) = 0.0
2  Y(I) = DPZ(I)/DPL
  WRITE (KOUT,9005) X2(I),Y(I)
  DO 5 J=J,K
    IF (Z(I)) 5,5,4
4  DLNY(I) = DLOG(Y(I))
    SUMY = SUMY + DLNY(I)
    X1 = DLOG(X2(I))
    SUMX1 = SUMX1 + X1
    SSQX1 = SSQX1 + (X1**2)
    SUMX2 = SUMX2 + X2(I)
    SSQX2 = SSQX2 + (X2(I)**2)
    SX1X2 = SX1X2 + (X1 * X2(I))
    SUMX1Y = SUMX1Y + (X1 * DLNY(I))
    SUMX2Y = SUMX2Y + (X2(I) * DLNY(I))
    COUNT = COUNT + 1.
5  CONTINUE
  A1(1,1) = COUNT
  A1(1,2) = SUMX1
  A1(1,3) = SUMX2
  A1(1,4) = SUMY
  A1(2,1) = A1(1,2)
  A1(2,2) = SSQX1
  A1(2,3) = SX1X2
  A1(2,4) = SUMX1Y
  A1(3,1) = A1(1,3)
  A1(3,2) = A1(2,3)
  A1(3,3) = SSQX2
  A1(3,4) = SUMX2Y
  CALL SIMEQN (A1,3,4)
  A = DEXP(A1(1,4)/A1(1,1))
  B = A1(2,4) / A1(2,2)
  C = A1(3,4) / A1(3,3)
C*** PLOTTING DATA FOR 'DPZ/DPL VS. Z/L'
  WRITE (KOUT,9006)
  WRITE (KOUT,9007)
  ZL = X2(J)
  ZLINCR = (X2(K) - X2(J)) / 200.
  DO 6 I=1,200
    DPZDPL = A * (ZL**B) * EXP(C*ZL)
    WRITE (KOUT,9005) ZL,DPZDPL
6  ZL = ZL + ZLINCR
C*** DATA SMOOTHING
  DO 7 I=J,K
    DPZ(I) = DPL * ((A * (Z(I)/L)**B) * DEXP(C*Z(I)/L))
  RETURN
9005 FORMAT (2E15,7)
9006 FORMAT ('DPZ/DPL = A * ((Z/L)**B) * EXP(C*Z/L)')
9007 FORMAT ('200 -1 -1 0')
END

```

C
C

SIMEQN === SOLUTION OF SIMULTANEOUS LINEAR EQUATIONS

```

SUBROUTINE SIMEQN (A,NR,NC)
DIMENSION A(3,4),R(100)
DOUBLE PRECISION A,R,D,T
IF(NR - NC) 2,2,1
1 NCT = NC
  GO TO 3
2 NCT = NR
  K = 1
  D = 1.
4 IF(A(K,K)) 9,5,9
5 DO 6 I = K,NR
  IF(A(I,K)) 7,6,7
6 CONTINUE
  GO TO 14
7 DO 8 J = 1,NC
  T = A(I,J)
  A(I,J) = A(K,J)
8 A(K,J) = T
9 DO 13 I = 1,NR
  IF(I - K) 10,13,10
10 DO 11 J = 1,NC
  R(J) = (A(I,J)*A(K,K) - A(I,K)*A(K,J))/D
11 DO 12 J = 1,NC
  A(I,J) = R(J)
12 CONTINUE
  D = A(K,K)
  K = K + 1
  IF(K - NCT) 4,4,14
14 RETURN
END

```

Appendix VIII (Continued)

SOLCON === SOLIDS CONCENTRATION

THIS SUBROUTINE IS USED TO CALCULATE THE MAT SOLIDS CONCENTRATION FROM MEASUREMENTS OF PAD THICKNESS AND THE O.D. WT. OF THE MAT. THE PROCEDURE INVOLVES A LEAST SQUARES APPROACH TO COMPUTING COMPRESSIBILITY CONSTANTS M AND N.

C
C
C
C
C
C
C
C

```

SUBROUTINE SOLCON (W,PDTHCK,AREA,N,M,MATCON,DP2,CMH2O,H2OLVL,
*LOUT,DPZ,L)
  DIMENSION PDTHCK(12),DP2(8),MATCON(8),LMC(8),LDP2(8),CMH2O(8)
  DIMENSION DPZ(12)
  DOUBLE PRECISION MATCON,LMC,LDP2,SUMY,SUMY2,SUMX,SUMX2,SUMXY,Q1,L
  DOUBLE PRECISION Q2,N,M,SUMM,W,PDTHCK,AREA,DP2,H2OLVL,DPZ,CO,DPZO
  PTS = 7.0
  NPTS = 8
  CALL PISTON (H2OLVL,PDTHCK,DP2)
  SUMY = 0.
  SUMY2 = 0.
  SUMX = 0.
  SUMX2 = 0.
  SUMXY = 0.
  SUMM = 0.
  MATCON(1) = W / (PDTHCK(1) * AREA)
  DO 1 I=2,NPTS
    CMH2O(I) = DP2(I) / 980.638
    MATCON(I) = W / (PDTHCK(I) * AREA)
    LMC(I) = DLOG(MATCON(I))
    LDP2(I) = DLOG(DP2(I))
    SUMY = SUMY + LMC(I)
    SUMY2 = SUMY2 + (LMC(I) ** 2)
    SUMX = SUMX + LDP2(I)
    SUMX2 = SUMX2 + (LDP2(I) ** 2)
    SUMXY = SUMXY + (LMC(I) * LDP2(I))
  1 Q1 = (PTS * SUMXY) - (SUMX * SUMY)
  Q2 = (PTS * SUMX2) - (SUMX ** 2)
  N = Q1/Q2
  DO 2 I=2,NPTS
  2 SUMM = SUMM + (MATCON(I) / (DP2(I) ** N))
  M = SUMM / PTS
C*** GENERATION OF PLOTTING DATA FOR 'SOLIDS CONC. VS. PRESSURE'
  WRITE (LOUT,9006) (DP2(I),MATCON(I),I=2,NPTS)
  WRITE (LOUT,9007)
  WRITE (LOUT,9008)
  XINCR = (DP2(8) - DP2(2))/100.
  X = DP2(2)
  DO 5 I=1,100
    Y = M * X ** N
    WRITE (LOUT,9006) X,Y
  5 X = X + XINCR
  RETURN
9006 FORMAT (2E15.7)
9007 FORMAT ('C = M * DELTAP ** N')
9008 FORMAT ('100 -2 -2 0')
END
SUBROUTINE PISTON (H2OLVL,PDTHCK,DP2)
  DIMENSION DP2(8),DISSUB(8),VOLDIS(8),PDTHCK(12)
  DOUBLE PRECISION H2OLVL,DP2,PDTHCK
C*** CUMULATIVE WEIGHT IN GRAMS
  DP2(2) = 345.90
  DP2(3) = 572.58
  DP2(4) = 1027.99
  DP2(5) = 1710.66
  DP2(6) = 2849.66
  DP2(7) = 4428.66
  DP2(8) = 6708.66
C*** CONVERT WEIGHT INTO PRESSURE
  DO 1 I=2,8
  1 DISSUB(I) = H2OLVL - PDTHCK(I)
  VOLDIS(I) = 10.**(0.025164 * DISSUB(I) + 1.47138)
  DP2(I) = ((DP2(1) - VOLDIS(I)) / 45.58) * 980.665
  DP2(1) = 0.0
  RETURN
END

```


Appendix VIII (Continued)

```

C      FVSX == FITS BEST CURVES TO PLOTS OF **CP**3 VS. F**
C
SUBROUTINE FVSX (DPZ,Z,V,SW,SV,J,LIN,K,IOUT,DPLO)
DIMENSION DPZ(12),Z(12),F(12),X(12),SV(12),F1(12),V(12),SW(12)
DOUBLE PRECISION DPL,DPZ,L,Z,B,C,N,MU,U,F,X,K1,K2,A,M,Q,CL
DOUBLE PRECISION B0,B1,B2,EXPM,EXPX,F1,SLOPE,INTCPT,V,SW,SV
COMMON MU,U,M,N,L,DPL,A,B,C,B0,B1,B2,EXPM,EXPX
K1 = 3.5
K2 = 57.
LPTS = LIN - J + 1
NPTS = K - J + 1
WRITE (IOUT,9017) NPTS
IF (DPLO) 3,3,1
1  BOYNCY = 10.**(0.025164 * (28. - L) + 1.47138)
DPLO = ((DPL - BOYNCY)/45.58)*980.665
3  CL = M * (DPL + DPLO) ** N
Q = DPL/(MU * L * U * K1 * (CL**1.5))
DO 4 I=J,K
X(I) = (CL**3) * ((DPZ(I)/DPL)**(3*N))
F(I) = Q * (C + (B*L/Z(I)))*((DPZ(I)/DPL)**(1-1.5*N))
4  WRITE (IOUT,9018) X(I),F(I)
DPLO = DPLO/980.638
IF (LPTS - 1) 9,9,5
C*** CALCULATION OF SLOPE AND INTERCEPT FOR THE INITIAL PORTION OF THE
C*** **CP**3 VS. F** PLOT. THIS PORTION IS USUALLY LINEAR AT LOW DPZ.
5  CALL LINREG (X,F,LPTS,INTCPT,SLOPE,J,LIN)
B0 = INTCPT
B2 = SLOPE
WRITE (IOUT,9019) INTCPT,SLOPE
WRITE (IOUT,9020)
XLINCR = (X(LIN) - X(J))/10.
XL = X(J)
DO 7 I=1,2
FL = INTCPT + SLOPE * XL
WRITE (IOUT,9018) XL,FL
7  XL = X(LIN) + XLINCR
DO 8 I=J,LIN
V(I) = (SLOPE/(INTCPT*K2)) ** .333333
SW(I) = DSQRT(INTCPT * DSQRT(V(I)))
8  SV(I) = SW(I) / V(I)
IF (K - LIN) 15,15,9
9  CALL CRVFIT (X,F,B0,B1,B2,EXPM,EXPX,LIN,K,IOUT)
C*** CALCULATION OF SLOPE AND INTERCEPT USING PLOT OF **CP**3 VS. F**
IF (LPTS - 1) 11,11,10
10 LIN = LIN + 1
DO 14 I=LIN,K
F1(I) = B0 + B1*(X(I)**EXPM) + B2*(X(I)**EXPX)
SLOPE = EXPX*B1*(X(I)**(EXPX-1.)) + EXPX*B2*(X(I)**(EXPX-1.))
INTCPT = F1(I) - SLOPE * X(I)
IF (INTCPT) 14,14,12
IF (SLOPE) 14,14,13
12 V(I) = (SLOPE/(INTCPT*K2)) ** 0.333333
SW(I) = DSQRT(INTCPT * DSQRT(V(I)))
SV(I) = SW(I) / V(I)
14 CONTINUE
15 WRITE (I,9016) (I,V(I),SW(I),I=J,K)
RETURN
9016 FORMAT (' ',15,5X,F6.2,5X,F10.2)
9017 FORMAT ('1 1 -1 3')
9018 FORMAT ('2E15.7')
9019 FORMAT ('F = ',E7.2,' + ',E7.2,' * CP3')
9020 FORMAT (' 2 -1 -1 0')
END

```

LINREG == LINEAR REGRESSION
ANTHONY P. BINOTTO
JUNE 16, 1975

THIS SUBROUTINE IS USED TO CALCULATE THE STRAIGHT LINE
RELATIONSHIP BETWEEN PAIRS OF X,Y-DATA

```

C      SUBROUTINE LINREG (X,Y,NPTS,INTCPT,SLOPE,J,LIN)
C      DIMENSION X(12),Y(12)
C      DOUBLE PRECISION X,Y,SUMX,SUMX2,SUMY,SUMXY,SLOPE,INTCPT,Q1,Q2,PTS
C      PTS = NPTS
C      SUMY = 0.
C      SUMX = 0.
C      SUMX2 = 0.
C      SUMXY = 0.
C      DO 1 I=J,LIN
C      SUMY = SUMY + Y(I)
C      SUMX = SUMX + X(I)
C      SUMX2 = SUMX2 + (X(I) ** 2)
C      SUMXY = SUMXY + (X(I) * Y(I))
1  Q1 = SUMXY - (SUMX * SUMY)/PTS
Q2 = SUMX2 - (SUMX ** 2)/PTS
SLOPE = Q1/Q2
INTCPT = (SUMY - SLOPE * SUMX) / PTS
RETURN
END

```

Appendix VIII (Continued)

CURVE ==== CURVE FITTING

```

SUBROUTINE CRVFIT(X,Y,B0,B1,B2,M,N,J,K,IOUT)
  DIMENSION X(12),Y(12),A(5,6)
  DOUBLE PRECISION X,Y,B0,B1,B2,M,N,A,ORIGN,ORIGN
  DOUBLE PRECISION DELB0,DELB1,DELB2,DELM,DELN
  NPTS = K - J + 1
C**** INITIAL VALUES OF B0, B1, AND M ESTIMATED BY 'SUBROUTINE XM'
  CALL EXPDMM(X,Y,NPTS,B0,B1,M,J,K)
  B2 = 1000.
  N = 0.48
C*** DATA FIT MAY BE IMPROVED AT THE EXPENSE OF CALCULATION TIME
C*** BY DECREASING THE VALUE OF 'TEST'.
  TEST = .10E06
  1 MCOUNT = 0
    NCOUNT = 0
    ORIGN = M
    ORIGN = N
    TEST1 = 0.0
  2 CALL SUM(X,Y,NPTS,B0,B1,B2,M,N,A,J,K)
    CALL SIMEQ(A,5,6)
    DELB0 = A(1,6) / A(1,1)
    DELB1 = A(2,6) / A(2,2)
    DELB2 = A(3,6) / A(3,3)
    DELM = A(4,6) / A(4,4)
    DELN = A(5,6) / A(5,5)
    TEST2 = DELB0 + DELB1 + DELB2 + DELM + DELN
    DIFF = TEST2 - TEST1
    IF (ABS(DIFF) - TEST) 6,6,3
  3 TEST1 = TEST2
    NCOUNT = NCOUNT + 1
    B0 = B0 + DELB0
    B1 = B1 + DELB1
    B2 = B2 + DELB2
    IF (NCOUNT-100) 2,2,4
  4 NCOUNT = 0
    M = M + DELM
    N = N + DELN
    MCOUNT = MCOUNT + 1
    IF (MCOUNT - 04) 2,2,5
  5 M = ORIGN
    N = ORIGN + 0.01
    GO TO 1
  6 CALL EQN(B0,B1,B2,M,N,IOUT,X,J,K)
  RETURN
END

```

SUBROUTINE EQN === GENERATION OF PLOTTING POINTS

```

C
C
C
THIS SUBROUTINE GENERATES DATA POINTS FROM THE CALCULATED
EQUATION TO BE USED IN PLOTTING PROGRAM 'ABPLOT'.
SUBROUTINE EQN(B0,B1,B2,M,N,IOUT,X,J,K)
  DIMENSION X(12)
  DOUBLE PRECISION X,DPTS,XINCR,B0,B1,B2,M,N,P,R
  NPTS = 200
  DPTS = NPTS
  XINCR = (X(K) - X(J)) / DPTS
  WRITE(IOUT,9002) M,N
  WRITE(IOUT,9003) NPTS
  P = X(J)
  DO 1 I=1,NPTS
    R = B0 + B1 * (P ** M) + B2 * (P ** N)
    WRITE(IOUT,9004) P,R
  1 P = P + XINCR
  RETURN
9002 FORMAT ('F = B0 + B1*(CP3**',F4.2,' ) + B2*(CP3**',F4.2,' )')
9003 FORMAT (I3,' -1 -1 0')
9004 FORMAT (2D15.7)
END

```

SUBROUTINE SUM === CALCULATION OF SUM OF SQUARES

```

C
C
SUBROUTINE SUM(X,Y,NPTS,B0,B1,B2,M,N,A,J,K)
  DIMENSION X(12),Y(12),A(5,6)
  DOUBLE PRECISION X,Y,B0,B1,B2,M,N,A,PTS,SXMYR2
  DOUBLE PRECISION SY,SXM,SXN,SXMY,SX2M,SXMXN,SXNY,SX2N,SXMYR,SXMR
  DOUBLE PRECISION SX2MR,SXMXNR,SXNYR,SXNR,SXMR2,SX2MR2,SXMXNR2
  DOUBLE PRECISION SXNR2,SX2NR2,SXNYR2,SX2NR,XN,XM,X2M,X2N,R,R2
  PTS = NPTS
  SY = 0.0
  SXM = 0.0
  SXN = 0.0
  SXMY = 0.0
  SX2M = 0.0
  SXMXN = 0.0
  SXNY = 0.0
  SX2N = 0.0
  SXMYR = 0.0
  SXMR = 0.0
  SX2MR = 0.0
  SXMXNR = 0.0
  SXNYR = 0.0

```

Appendix VIII (Continued)

```

SXNR = 0.0
SX2NR = 0.0
SXMR2 = 0.0
SX2MR2 = 0.0
SXMNR2 = 0.0
SXYR2 = 0.0
SXNR2 = 0.0
SX2NR2 = 0.0
SXNYR2 = 0.0
DO 1 I=J,K
  XM = X(I) ** M
  XN = X(I) ** N
  X2M = XM ** 2
  X2N = XN ** 2
  R = DLOG(X(I))
  R2 = R ** 2
  SY = SY + Y(I)
  SXM = SXM + XM
  SXN = SXN + XN
  SXY = SXY + (XM * Y(I))
  SX2M = SX2M + X2M
  SXMN = SXMN + (XM * XN)
  SXNY = SXNY + (XN * Y(I))
  SX2N = SX2N + X2N
  SXYR = SXYR + (XM * Y(I) * R)
  SXMR = SXMR + (XM * R)
  SX2MR = SX2MR + (X2M * R)
  SXMNR = SXMNR + (XM * XN * R)
  SXNYR = SXNYR + (XN * Y(I) * R)
  SXNR = SXNR + (XN * R)
  SX2NR = SX2NR + (X2N * R)
  SXMR2 = SXMR2 + (XM * R2)
  SX2MR2 = SX2MR2 + (X2M * R2)
  SXMNR2 = SXMNR2 + (XM * XN * R2)
  SXYR2 = SXYR2 + (XM * Y(I) * R2)
  SXNR2 = SXNR2 + (XN * R2)
  SX2NR2 = SX2NR2 + (X2N * R2)
  SXNYR2 = SXNYR2 + (XN * Y(I) * R2)
1 A(1,1) = PTS
  A(1,2) = SXM
  A(1,3) = SXN
  A(1,4) = B1 * SXM
  A(1,5) = B2 * SXN
  A(1,6) = -(PTS*B0 + B1*SXM + B2*SXN - SY)
  A(2,1) = SXM
  A(2,2) = SX2M
  A(2,3) = SXMN
  A(2,4) = B0*SXM + 2.0*B1*SX2M + B2*SXMN - SXYR
  A(2,5) = B2*SXMN
  A(2,6) = -(B0*SXM + B1*SX2M + B2*SXMN - SXYR)
  A(3,1) = SXN
  A(3,2) = SXMN
  A(3,3) = SX2N
  A(3,4) = B0*SXN + B1*SXMN + 2.0*B2*SX2N - SXNYR
  A(3,5) = B2*SX2N
  A(3,6) = -(B0*SXN + B1*SXMN + B2*SX2N - SXNYR)
  A(4,1) = SXMR
  A(4,2) = SX2MR
  A(4,3) = SXMNR
  A(4,4) = B0*SXMR + 2.0*B1*SX2MR + B2*SXMNR - SXYR2
  A(4,5) = B2*SXMNR
  A(4,6) = -(B0*SXMR + B1*SX2MR + B2*SXMNR - SXYR2)
  A(5,1) = SXNR
  A(5,2) = SXMNR
  A(5,3) = SX2NR
  A(5,4) = B1*SXMNR
  A(5,5) = B0*SXNR + B1*SXMNR + 2.0*B2*SX2NR - SXNYR2
  A(5,6) = -(B0*SXNR + B1*SXMNR + B2*SX2NR - SXNYR2)
RETURN
END

```

C
C
C

SUBROUTINE SIMEQN === SOLUTION OF SIMULTANEOUS LINEAR EQUATIONS

```

SUBROUTINE SIMEQ (A,NR,NC)
  DIMENSION A(5,6),R(100)
  DOUBLE PRECISION A,R,D,T
  IF(NR - NC) 2,2,1
1  NCT = NC
  GO TO 3
2  NCT = NR
3  K = 1
  D = 1.
4  IF(A(K,K)) 9,5,9
5  DO 6 I = K,NR
  IF(A(I,K)) 7,6,7
6  CONTINUE
  GO TO 14
7  DO 8 J = 1,NC
  T = A(I,J)
  A(I,J) = A(K,J)
8  A(K,J) = T
9  DO 13 I = 1,NR
  IF(I - K) 10,13,10
10 DO 11 J = 1,NC
11 R(J) = (A(I,J)*A(K,K) - A(I,K)*A(K,J))/D
  DO 12 J = 1,NC
12 A(I,J) = R(J)
13 CONTINUE
  D = A(K,K)
  K = K + 1
14 IF(K - NCT) 4,4,14
RETURN
END

```

Appendix VIII (Continued)

```

C SUBROUTINE EXPONM = ESTIMATION OF INITIAL VALUE OF EXPONENT **M**
C
SUBROUTINE EXPONM (X,Y,NPTS,BOMIN,B1MIN,MMIN,G,H)
DIMENSION X(12),Y(12)
DOUBLE PRECISION X,XM,Y,M,PTS,SUMXM,SUMX2M,SUMY,SUMXMY,SMIN
DOUBLE PRECISION S,B0,B1,MMIN,BOMIN,B1MIN,MAXM
INTEGER G,H
PTS = NPTS
M = 0.10
MAXM = 0.2
UNIT = .0001
SMIN = 16.0D70
J = 1
6 SUMXM = 0.
SUMX2M = 0.
SUMY = 0.
SUMXMY = 0.
DO 7 I=G,H
XM = X(I) ** M
SUMXM = SUMXM + XM
SUMX2M = SUMX2M + (XM**2)
SUMY = SUMY + Y(I)
7 SUMXMY = SUMXMY + (XM * Y(I))
Q1 = SUMXMY - (SUMXM * SUMY) / PTS
Q2 = SUMX2M - (SUMXM ** 2) / PTS
B1 = Q1 / Q2
B0 = (SUMY - B1 * SUMXM) / PTS
S = DSQRT(B0**2 + B1**2)
8 IF (S - SMIN) 8,9,9
SMIN = S
BOMIN = B0
B1MIN = B1
MMIN = M
9 J = J + 1
M = M + UNIT
IF (M - MAXM) 6,6,11
11 RETURN
END

```

Appendix VIII (Continued)

```
*****
*
*   FIELD CN 65 MESH, RUN 1
*
*****
```

ORIGINAL DATA

```
MAT SOLIDS CONC.      = 0.0666 G./CC.
O.D. MAT WT., W       = 12.1858 G.
MAT THICKNESS, L      = 4.01 CM.
TOTAL PRESSURE DROP, DPL = 60.00 CM. H2O
PERMEATION VELOCITY, U = 0.577000 CM./SEC.
WATER TEMPERATURE, T  = 29.0 DEG. C.
WATER VISCOSITY, MU   = 0.008149 POISES
```

PERMEATION EXPERIMENT

COMPRESSIBILITY EXPERIMENT

PRESSURE TAP NUMBER	DISTANCE FROM TOP OF MAT CM.	DPZ		PRESSURE		MAT THICKNESS CM.	MAT SOLIDS CONCENTRATION G./CC.
		CM. H2O	DYNES/SQCM.	CM. H2O	DYNES/SQCM.		
1	-0.4844	0.0	0.0	0.0	0.	6.6000	0.0405
2	-0.1034	0.0	0.0	6.24	6116.	4.2450	0.0630
3	0.2776	0.25	245.16	11.17	10956.	3.7750	0.0708
4	0.6586	1.05	1029.67	21.12	20713.	3.2600	0.0820
5	1.0396	2.40	2353.53	36.06	35366.	2.8400	0.0941
6	1.4206	4.70	4609.00	61.02	59839.	2.4450	0.1093
7	1.8016	7.60	7452.85	95.64	93784.	2.1200	0.1261
8	2.1826	11.60	11375.40	145.63	142813.	1.8350	0.1457
9	2.5636	17.00	16670.84				
10	2.9446	24.20	23731.43				
11	3.3256	34.00	33341.69				
12	3.7066	46.00	45109.34				

COMPRESSIBILITY CONSTANTS

```
M = 0.6001D-02
N = 0.2657
```

EXPERIMENTAL EMPIRICAL CONSTANTS

```
DPZ/DPL = A * ((Z/L)**B) * EXP(C*Z/L)    F = B0 + B1*(X**EXPM) + B2*(X**EXPNI)
WHERE...                                   WHERE...
A = 0.21597                               B0 = 0.22525D 09    EXPM = 0.13540D 00
B = 1.51946                               B1 = -0.18538D 10    EXPN = 0.27807D 00
C = 1.50437                               B2 = 0.27234D 10
```

HYDRODYNAMIC SPECIFIC VOLUME AND SURFACE AS FUNCTIONS OF PRESSURE

PRESSURE CM. H2O	V CC./G.	SW SQCM./G.	SV SQCM./CC.
1.06	3.73	6171.22	1655.23
2.46	3.73	6171.22	1655.23
4.55	3.45	6232.32	1805.10
7.53	3.41	6254.89	1834.55
11.63	3.26	6352.42	1946.98
17.13	3.07	6509.63	2117.54
24.38	2.87	6710.52	2336.10
33.84	2.67	6942.40	2547.83
46.02	2.48	7195.85	2900.40

Appendix VIII (Continued)

*
* FIELD CN 65 MESH, RUN 2
*

ORIGINAL DATA

MAT SOLIDS CONC. = 0.0660 G./CC.
O.D. MAT WT., W = 12.7468 G.
MAT THICKNESS, L = 4.24 CM.
TOTAL PRESSURE DROP, DPL = 60.00 CM. H2O
PERMEATION VELOCITY, U = 0.657800 CM./SEC.
WATER TEMPERATURE, T = 30.5 DEG. C.
WATER VISCOSITY, MU = 0.007892 POISES

PERMEATION EXPERIMENT

PRESSURE TAP NUMBER	DISTANCE FROM TOP OF MAT CM.	DPZ	
		PRESSURE CM. H2O	TAP READING DYNES/SQCM.
1	-0.2594	0.0	0.0
2	0.1216	0.20	196.13
3	0.5026	0.95	931.61
4	0.8836	2.00	1961.28
5	1.2646	3.50	3432.23
6	1.6456	5.80	5687.70
7	2.0266	8.85	8678.64
8	2.4076	13.10	12846.36
9	2.7886	18.40	18534.05
10	3.1696	25.70	25202.39
11	3.5506	35.00	34322.32
12	3.9316	48.00	47070.62

COMPRESSIBILITY EXPERIMENT

PRESSURE		MAT THICKNESS	MAT SOLIDS CONCENTRATION
CM. H2O	DYNES/SQCM.	CM.	G./CC.
0.0	0.	7.1700	0.0390
6.32	6200.	4.5800	0.0611
11.25	11037.	4.0350	0.0693
21.20	20791.	3.4500	0.0811
36.14	35444.	3.0000	0.0932
61.10	59914.	2.5550	0.1095
95.71	93858.	2.2100	0.1265
145.71	142887.	1.9050	0.1468

COMPRESSIBILITY CONSTANTS

M = 0.51790-02
N = 0.2789

EXPERIMENTAL EMPIRICAL CONSTANTS

DPZ/DPL = A * ((Z/L)**B) * EXP(C*Z/L) F = B0 + B1*(X**EXPM) + B2*(X**EXPN)

WHERE...

A = 0.09231
B = 0.95777
C = 2.42722

WHERE...

B0 = 0.318880 09 EXPM = 0.141300 00
B1 = -0.388260 10 EXPN = 0.149250 00
B2 = 0.476470 10

HYDRODYNAMIC SPECIFIC VOLUME AND SURFACE AS FUNCTIONS OF PRESSURE

PRESSURE CM. H2O	V CC./G.	SV SQCM./G.	SV SQCM./CC.
2.05	3.78	5631.70	1491.72
3.59	3.78	5631.70	1491.72
5.74	3.78	5631.70	1491.72
8.71	3.66	5701.94	1555.82
12.78	3.58	5763.63	1610.02
18.30	3.40	5918.38	1739.24
25.73	3.18	6151.47	1936.19
35.67	2.93	6445.86	2198.40
48.92	2.69	6785.97	2525.78

Appendix VIII (Continued)

```
*****
*
* FIELD ON 20 MESH, RUN 1
*
*****
```

ORIGINAL DATA

```
MAT SOLIDS CONC.      = 0.0643 G./CC.
O.D. MAT WT., W       = 11.9946 G.
MAT THICKNESS, L      = 4.09 CM.
TOTAL PRESSURE DROP, DPL = 60.00 CM. H2O
PERMEATION VELOCITY, U = 0.678000 CM./SEC.
WATER TEMPERATURE, T  = 30.7 DEG. C.
WATER VISCOSITY, MU   = 0.007858 POISES
```

PERMEATION EXPERIMENT

PRESSURE TAP NUMBER	Z DISTANCE FROM TOP OF MAT CM.	DPZ	
		PRESSURE CM. H2O	TAP READING DYNES/SQCM.
1	-0.4094	0.0	0.0
2	-0.0284	0.0	0.0
3	0.3526	0.20	196.13
4	0.7336	0.85	833.54
5	1.1146	1.95	1912.24
6	1.4956	3.60	3530.30
7	1.8766	6.20	6079.95
8	2.2576	8.84	8668.84
9	2.6386	14.00	13728.93
10	3.0196	22.00	21574.03
11	3.4006	31.50	30890.09
12	3.7816	47.25	46335.14

COMPRESSIBILITY EXPERIMENT

PRESSURE CM. H2O	DYNES/SQCM.	MAT THICKNESS CM.	MAT SOLIDS CONCENTRATION G./CC.
0.0	0.	6.7050	0.0392
6.50	6373.	4.0450	0.0651
11.44	11221.	3.5850	0.0734
21.40	20986.	3.0700	0.0857
36.35	35647.	2.6700	0.0986
61.31	60127.	2.2900	0.1149
95.94	94079.	1.9850	0.1326
145.94	143115.	1.7250	0.1526

COMPRESSIBILITY CONSTANTS

```
M = 0.57170-02
N = 0.2741
```

EXPERIMENTAL EMPIRICAL CONSTANTS

```
DPZ/DPL = A * ((Z/L)**B) * EXP(C*Z/L)      F = B0 + B1*(X**EXPM) + B2*(X**EXPN)
WHERE...                                     WHERE...
A = 0.14953                                B0 = 0.124030 09    EXPM = 0.129600 00
B = 1.59952                                B1 = -0.809450 09    EXPN = 0.264580 00
C = 1.86714                                B2 = 0.161580 10
```

HYDRODYNAMIC SPECIFIC VOLUME AND SURFACE AS FUNCTIONS OF PRESSURE

PRESSURE CM. H2O	V CC./G.	SM SQCM./G.	SV SQCM./CC.
1.87	4.07	5392.15	1324.78
3.55	4.01	5415.08	1350.56
6.08	3.77	5531.47	1467.93
9.72	3.47	5719.77	1647.09
14.84	3.17	5957.17	1878.25
21.92	2.89	6226.88	2157.66
31.54	2.62	6517.37	2484.29
44.48	2.39	6820.89	2858.60

Appendix VIII (Continued)

```
*****
*
*   FIELD CN 20 MESH, RUN 2
*
*****
```

ORIGINAL DATA

```
MAT SOLIDS CONC.      = 0.0596 G./CC.
O.D. MAT WT., W       = 14.8896 G.
MAT THICKNESS, L      = 5.48 CM.
TOTAL PRESSURE DROP, DPL = 60.00 CM. H2O
PERMEATION VELOCITY, U = 0.748700 CM./SEC.
WATER TEMPERATURE, T  = 28.5 DEG. C.
WATER VISCOSITY, MU   = 0.008237 POISES
```

PERMEATION EXPERIMENT

PRESSURE TAP NUMBER	Z DISTANCE FROM TOP OF MAT CM.	DPZ	
		PRESSURE CM. H2O	TAP READING DYNES/SQCM.
1	0.9856	0.85	833.54
2	1.3666	1.70	1667.08
3	1.7476	2.80	2745.79
4	2.1286	4.30	4216.74
5	2.5096	6.30	6178.02
6	2.8906	9.00	8825.74
7	3.2716	12.80	12552.16
8	3.6526	17.00	16670.84
9	4.0336	22.90	22456.60
10	4.4146	29.30	28732.68
11	4.7956	38.50	37754.56
12	5.1766	49.00	48051.26

COMPRESSIBILITY EXPERIMENT

PRESSURE CM. H2O	DYNES/SQCM.	MAT THICKNESS CM.	MAT SOLIDS CONCENTRATION G./CC.
6.48	6350.	5.6150	0.0582
11.40	11140.	4.8800	0.0669
21.34	20928.	4.1350	0.0790
36.28	35577.	3.5750	0.0914
61.23	60046.	3.0650	0.1066
95.84	93987.	2.6500	0.1233
145.84	143016.	2.3050	0.1417

COMPRESSIBILITY CONSTANTS

```
M = 0.4698D-02
N = 0.2H5C
```

EXPERIMENTAL EMPIRICAL CONSTANTS

```
DPZ/DPL = A * ((Z/L)**B) * EXP(C*Z/L)      F = B0 + B1*(X**EXPM) + B2*(X**EXPN)
WHERE...                                     WHERE...
A = 0.16667                                B0 = 0.11232D 09      EXPM = 0.13030D 00
B = 1.61452                                B1 = -0.89447D 09    EXPN = 0.22766D 00
C = 1.78421                                B2 = 0.14177D 10
```

HYDRODYNAMIC SPECIFIC VOLUME AND SURFACE AS FUNCTIONS OF PRESSURE

PRESSURE CM. H2O	V CC./G.	SW SQCM./G.	SV SQCM./CC.
2.79	3.99	5007.86	1255.44
4.34	3.94	5019.81	1273.56
6.40	3.79	5070.69	1336.68
9.11	3.60	5156.75	1432.07
12.59	3.39	5271.04	1554.36
17.03	3.18	5407.06	1700.99
22.62	2.97	5559.48	1870.68
29.62	2.77	5724.07	2062.88
38.33	2.59	5897.58	2277.52
49.09	2.42	6077.50	2514.82

Appendix VIII (Continued)

```
*****
* FIELD ON 10 MESH, RUN 1
*
*****
```

ORIGINAL DATA

MAT. SOLIDS CONC. = 0.0616 G./CC.
 O.D. MAT WT., W = 14.0474 G.
 MAT THICKNESS, L = 5.00 CM.
 TOTAL PRESSURE DROP, DPL = 60.00 CM. H2O
 PERMEATION VELOCITY, U = 1.546900 CM./SEC.
 WATER TEMPERATURE, T = 30.0 DEG. C.
 WATER VISCOSITY, MU = 0.007976 POISES

PERMEATION EXPERIMENT

PRESSURE TAP NUMBER	Z DISTANCE FROM TOP OF MAT CM.	DPZ	
		PRESSURE CM. H2O	TAP READING DYNES/SQCM.
1	0.5056	1.10	1078.70
2	0.8866	2.10	2059.34
3	1.2676	3.20	3138.04
4	1.6486	4.95	4854.16
5	2.0296	7.10	6962.53
6	2.4106	10.00	9806.38
7	2.7916	14.10	13826.99
8	3.1726	18.80	18435.98
9	3.5536	24.20	23731.43
10	3.9346	31.50	30890.09
11	4.3156	40.00	39225.52
12	4.6966	51.00	50012.53

COMPRESSIBILITY EXPERIMENT

PRESSURE CM. H2O	PRESSURE DYNES/SQCM.	MAT THICKNESS CM.	MAT SOLIDS CONCENTRATION G./CC.
0.0	0.	8.9750	0.0343
6.12	5997.	5.5950	0.0551
11.02	10811.	4.8550	0.0635
20.95	20545.	4.1300	0.0746
35.88	35183.	3.5950	0.0857
60.82	59642.	3.1000	0.0994
95.42	93574.	2.6850	0.1148
145.41	142593.	2.3350	0.1320

COMPRESSIBILITY CONSTANTS

M = 0.49860-02
 N = 0.2738

EXPERIMENTAL EMPIRICAL CONSTANTS

DPZ/DPL = A * ((Z/L)**B) * EXP(C*Z/L) F = B0 + B1*(X**EXPM) + B2*(X**EXPN)
 WHERE... WHERE...
 A = 0.09581 B0 = 0.174580 09 EXPM = 0.139000 00
 B = 0.83485 B1 = -0.273090 10 EXPN = 0.179530 00
 C = 2.41167 B2 = 0.310400 10

HYDRODYNAMIC SPECIFIC VOLUME AND SURFACE AS FUNCTIONS OF PRESSURE

PRESSURE CM. H2O	V CC./G.	SM SQCM./G.	SV SQCM./CC.
3.36	4.01	3623.44	903.85
5.03	4.01	3623.44	903.85
7.19	4.01	3623.44	903.85
9.98	3.94	3656.44	929.14
13.55	3.91	3666.70	936.92
18.12	3.80	3723.66	978.71
23.93	3.64	3823.06	1050.78
31.31	3.44	3958.47	1151.36
40.64	3.22	4123.04	1279.68
52.40	3.00	4310.38	1435.60

Appendix VIII (Continued)

```
*****
*
*   FIELD ON 10 MESH, RUN 2
*
*****
```

ORIGINAL DATA

```
MAT SOLIDS CONC.      = 0.0603 G./CC.
O.D. MAT WT., W       = 14.7078 G.
MAT THICKNESS, L      = 5.35 CM.
TOTAL PRESSURE DROP, DPL = 60.00 CM. H2O
PERMEATION VELOCITY, U = 1.385200 CM./SEC.
WATER TEMPERATURE, T  = 27.0 DEG. C.
WATER VISCOSITY, MU   = 0.008513 POISES
```

PERMEATION EXPERIMENT

PRESSURE TAP NUMBER	Z DISTANCE FROM TOP OF MAT CM.	DPZ	
		PRESSURE CM. H2O	TAP READING DYNES/SQCM.
1	0.8506	2.00	1961.28
2	1.2316	3.10	3039.98
3	1.6126	4.50	4412.87
4	1.9936	6.19	6070.14
5	2.3746	8.40	8237.36
6	2.7556	11.50	11277.34
7	3.1366	15.00	14709.57
8	3.5176	19.20	18828.24
9	3.8986	24.30	23829.49
10	4.2796	31.50	30890.09
11	4.6606	40.00	39225.52
12	5.0416	51.00	50012.53

COMPRESSIBILITY EXPERIMENT

PRESSURE CM. H2O	DYNES/SQCM.	MAT THICKNESS CM.	MAT SOLIDS CONCENTRATION G./CC.
0.0	0.	9.4100	0.0343
6.31	6184.	5.7800	0.0558
11.22	11003.	5.0050	0.0645
21.15	20741.	4.2250	0.0764
36.08	35386.	3.7000	0.0872
61.03	59848.	3.1800	0.1015
95.64	93785.	2.7650	0.1167
145.63	142809.	2.4050	0.1342

COMPRESSIBILITY CONSTANTS

```
M = 0.4859D-02
N = 0.2769
```

EXPERIMENTAL EMPIRICAL CONSTANTS

```
DPZ/DPL = A * ((Z/L)**B) * EXP(C*Z/L)      F = B0 + B1*(X**EXPM) + B2*(X**EXPN)
WHERE...                                     WHERE...
A = 0.08271                                B0 = 0.16405D 09      EXPM = 0.14070D 00
B = 0.71294                                B1 = -0.27029D 10    EXPN = 0.17955D 00
C = 2.51176                                B2 = 0.30543D 10
```

HYDRODYNAMIC SPECIFIC VOLUME AND SURFACE AS FUNCTIONS OF PRESSURE

PRESSURE CM. H2O	V CC./G.	SW SQCM./G.	SV SQCM./CC.
4.50	4.05	3446.34	850.43
6.26	4.05	3446.34	850.43
8.48	4.05	3446.34	850.43
11.28	3.92	3500.03	892.98
14.79	3.87	3521.22	908.92
19.19	3.76	3580.96	952.10
24.69	3.60	3675.90	1020.53
31.56	3.41	3801.23	1113.31
40.11	3.21	3951.75	1230.11
50.73	3.01	4122.49	1371.02

Appendix VIII (Continued)

```
*****
*
* FIELD ON 10 MESH, RUN 3
*
*****
```

ORIGINAL DATA

```
MAT SOLIDS CONC.      = 0.0613 G./CC.
O.D. MAT WT., W       = 14.2630 G.
MAT THICKNESS, L      = 5.10 CM.
TOTAL PRESSURE DROP, DPL = 60.00 CM. H2O
PERMEATION VELOCITY, U = 1.607500 CM./SEC.
WATER TEMPERATURE, T  = 30.0 DEG. C.
WATER VISCOSITY, MU   = 0.007976 POISES
```

PERMEATION EXPERIMENT

PRESSURE TAP NUMBER	Z DISTANCE FROM TOP OF MAT CM.	DPZ	
		PRESSURE, CM. H2O	TAP READING DYNES/SQCM.
1	0.6056	1.20	1176.77
2	0.9866	2.10	2059.34
3	1.3676	3.60	3530.30
4	1.7486	5.35	5246.41
5	2.1296	8.65	8482.52
6	2.5106	10.90	10688.95
7	2.8916	14.20	13925.05
8	3.2726	18.90	18534.05
9	3.6536	24.50	24025.63
10	4.0346	32.00	31380.41
11	4.4156	40.00	39225.52
12	4.7966	51.00	50012.53

COMPRESSIBILITY EXPERIMENT

PRESSURE		MAT THICKNESS CM.	MAT SOLIDS CONCENTRATION G./CC.
CM. H2O	DYNES/SQCM.		
0.0	0.	9.4350	0.0332
6.56	6436.	5.7600	0.0543
11.49	11268.	5.0150	0.0624
21.43	21015.	4.1900	0.0747
36.37	35667.	3.6400	0.0860
61.33	60138.	3.1150	0.1005
95.94	94082.	2.7000	0.1159
145.94	143111.	2.3300	0.1343

COMPRESSIBILITY CONSTANTS

```
M = 0.4181D-02
N = 0.2902
```

EXPERIMENTAL EMPIRICAL CONSTANTS

```
DPZ/DPL = A * ((Z/L)**B) * EXP(C*Z/L)      F = B0 + B1*(X**EXPM) + B2*(X**EXPN)
WHERE...                                     WHERE...
A = 0.14870                                B0 = 0.11947D 09      EXPM = 0.13790D 00
B = 1.06670                                B1 = -0.17846D 10    EXPN = 0.17951D 00
C = 1.92432                                B2 = 0.20468D 10
```

HYDRODYNAMIC SPECIFIC VOLUME AND SURFACE AS FUNCTIONS OF PRESSURE

PRESSURE CM. H2O	V CC./G.	SM SQCM./G.	SV SQCM./CC.
3.67	3.46	3854.32	1115.33
5.50	3.46	3854.32	1115.33
7.84	3.46	3854.32	1115.33
10.78	3.38	3875.91	1145.11
14.47	3.33	3895.52	1170.18
19.06	3.23	3939.75	1221.06
24.75	3.10	4006.39	1294.20
31.77	2.95	4092.42	1387.89
40.38	2.79	4194.74	1501.32
50.91	2.64	4310.49	1634.22

Appendix VIII (Continued)

```
*****
*
* FLOC ON 65 MESH -- II, RUN 2
*
*****
```

ORIGINAL DATA

```
MAT SOLIDS CONC.      = 0.0662 G./CC.
O.D. MAT WT., W       = 15.0664 G.
MAT THICKNESS, L      = 4.99 CM.
TOTAL PRESSURE DROP, DPL = 60.00 CM. H2O
PERMEATION VELOCITY, U = 1.102300 CM./SEC.
WATER TEMPERATURE, T  = 28.5 DEG. C.
WATER VISCOSITY, MU   = 0.008237 POISES
```

PERMEATION EXPERIMENT

PRESSURE TAP NUMBER	L DISTANCE FROM TOP OF MAT CM.	DPZ	
		PRESSURE CM. H2O	TAP READING DYNES/SQCM.
1	0.4906	1.45	1421.92
2	0.8716	2.60	2549.66
3	1.2526	4.30	4216.74
4	1.6336	6.30	6178.02
5	2.0146	8.90	8727.68
6	2.3956	12.80	12552.16
7	2.7766	16.50	16180.52
8	3.1576	21.30	20887.57
9	3.5386	27.10	26575.28
10	3.9196	34.00	33341.69
11	4.3006	42.50	41677.11
12	4.6816	52.00	50993.17

COMPRESSIBILITY EXPERIMENT

PRESSURE		MAT THICKNESS CM.	MAT SOLIDS CONCENTRATION G./CC.
CM. H2O	DYNES/SQCM.		
0.0	0.	7.8400	0.0422
6.33	6205.	5.4150	0.0610
11.26	11041.	4.8500	0.0682
21.20	20792.	4.2200	0.0783
36.14	35440.	3.7150	0.0890
61.09	59906.	3.2150	0.1028
95.70	93846.	2.8150	0.1174
145.69	142869.	2.4450	0.1352

COMPRESSIBILITY CONSTANTS

```
M = 0.6515D-02
N = 0.2524
```

EXPERIMENTAL EMPIRICAL CONSTANTS

```
DPZ/DPL = A * ((L/L)**B) * EXP(C*Z/L)    F = B0 + B1*(X**EXPM) + B2*(X**EXPN)
WHERE...                                WHERE...
A = 0.16012                            B0 = 0.29920D 09    EXPM = 0.15020D 00
B = 0.91156                            B1 = -0.64203D 10    EXPN = 0.17964D 00
C = 1.89057                            B2 = 0.69346D 10
```

HYDRODYNAMIC SPECIFIC VOLUME AND SURFACE AS FUNCTIONS OF PRESSURE

PRESSURE CM. H2O	V CC./G.	SW SQCM./G.	SV SQCM./CC.
4.38	3.45	4018.66	1165.80
6.45	3.45	4018.66	1165.80
9.02	3.45	4018.66	1165.80
12.20	3.45	4018.66	1165.80
16.12	3.45	4018.66	1165.80
20.94	3.45	4018.66	1165.80
26.84	3.42	4042.17	1181.55
34.04	3.36	4088.00	1215.73
42.79	3.26	4174.05	1279.42
53.41	3.13	4295.21	1370.65

Appendix VIII (Continued)

```
*****
*
* FLOC ON 65 MESH -- I, RUN I
*
*****
```

ORIGINAL DATA

```
MAT SOLIDS CONC.      = 0.0645 G./CC.
O.D. MAT WT., W       = 15.3764 G.
MAT THICKNESS, L      = 5.23 CM.
TOTAL PRESSURE DROP, DPL = 60.00 CM. H2O
PERMEATION VELOCITY, U = 1.455900 CM./SEC.
WATER TEMPERATURE, T  = 29.0 DEG. C.
WATER VISCOSITY, MU   = 0.008149 POISES
```

PERMEATION EXPERIMENT

PRESSURE TAP NUMBER	Z DISTANCE FROM TOP OF MAT CM.	DPZ	
		PRESSURE CM. H2O	TAP READING DYNES/SQCM.
1	0.7306	1.70	1667.08
2	1.1116	2.95	2892.88
3	1.4926	4.60	4510.93
4	1.8736	6.85	6717.37
5	2.2546	9.55	9365.09
6	2.6356	13.00	12748.29
7	3.0166	17.10	16768.90
8	3.3976	22.00	21574.03
9	3.7786	27.80	27261.72
10	4.1596	35.00	34322.32
11	4.5406	43.00	42167.43
12	4.9216	52.00	50993.17

COMPRESSIBILITY EXPERIMENT

PRESSURE		MAT THICKNESS CM.	MAT SOLIDS CONCENTRATION G./CC.
CM. H2O	DYNES/SQCM.		
0.0	0.	8.3300	0.0405
6.40	6280.	5.8250	0.0579
11.34	11116.	5.2250	0.0646
21.28	20864.	4.5250	0.0746
36.21	35512.	3.9800	0.0848
61.16	59977.	3.4500	0.0978
95.77	93916.	3.0250	0.1115
145.76	142940.	2.6300	0.1283

COMPRESSIBILITY CONSTANTS

```
M = 0.61010-02
N = 0.2537
```

EXPERIMENTAL EMPIRICAL CONSTANTS

```
DPZ/DPL = A * ((Z/L)**B) * EXP(C*Z/L)    F = B0 + B1*(X**EXPM) + B2*(X**EXPN)
WHERE...
A = 0.20397                                B0 = 0.199620 09    EXPM = 0.1431CD C0
B = 1.13078                                B1 = -0.33888D 10   EXPN = 0.17959D C0
C = 1.63461                                B2 = 0.37553D 10
```

HYDRODYNAMIC SPECIFIC VOLUME AND SURFACE AS FUNCTIONS OF PRESSURE

PRESSURE CM. H2O	V CC./G.	SW SQCM./G.	SV SQCM./CC.
4.73	3.49	3749.18	1075.37
6.89	3.49	3749.18	1075.37
9.56	3.49	3749.18	1075.37
12.85	3.49	3749.18	1075.37
16.86	3.45	3765.31	1090.35
21.73	3.44	3771.32	1095.50
27.60	3.38	3806.41	1124.68
34.66	3.29	3867.70	1174.54
43.11	3.18	3951.67	1243.06
53.20	3.05	4054.74	1328.91

Appendix VIII (Continued)

```
*****
* FLOC ON 65 MESH -- 1, RUN 2
*
*****
```

ORIGINAL DATA

```
MAT SOLIDS CONC.      = 0.0637 G./CC.
O.D. MAT WT., W       = 14.7122 G.
MAT THICKNESS, L      = 5.06 CM.
TOTAL PRESSURE DROP, DPL = 60.00 CM. H2O
PERMEATION VELOCITY, U = 1.516600 CM./SEC.
WATER TEMPERATURE, T  = 27.0 DEG. C.
WATER VISCOSITY, MU   = 0.008513 POISES
```

PERMEATION EXPERIMENT

PRESSURE TAP NUMBER	DISTANCE FROM TOP OF MAT CM.	DPZ	
		PRESSURE CM. H2O	TAP READING DYNES/SQCM.
1	0.5656	3.45	3383.20
2	0.9466	4.75	4658.03
3	1.3276	6.55	6423.18
4	1.7086	8.60	8433.48
5	2.0896	11.40	11179.27
6	2.4706	15.00	14709.57
7	2.8516	18.90	18534.05
8	3.2326	23.20	22750.80
9	3.6136	28.70	28144.30
10	3.9946	35.00	34322.32
11	4.3756	43.00	42167.43
12	4.7566	52.00	50993.17

COMPRESSIBILITY EXPERIMENT

PRESSURE CM. H2O	DYNES/SQCM.	MAT THICKNESS CM.	MAT SOLIDS CONCENTRATION G./CC.
0.0	0.	8.3700	0.0366
6.36	6237.	5.7000	0.0566
11.29	11067.	5.0450	0.0640
21.23	20816.	4.3750	0.0738
36.16	35462.	3.8300	0.0843
61.11	59928.	3.3200	0.0972
95.72	93864.	2.8800	0.1121
145.71	142889.	2.5150	0.1283

COMPRESSIBILITY CONSTANTS

```
M = 0.56710-02
N = 0.2601
```

EXPERIMENTAL EMPIRICAL CONSTANTS

```
DPZ/DPL = A * ((L/L)**B) * EXP(C*Z/L)      F = H0 + B1*(X**EXPM) + B2*(X**EXPN)
WHERE...                                     WHERE...
A = 0.10827                                H0 = 0.221730 09      EXPM = 0.145900 00
B = 0.41938                                B1 = -0.417810 10     EXPN = 0.179630 00
C = 2.26711                                B2 = 0.458650 10
```

HYDRODYNAMIC SPECIFIC VOLUME AND SURFACE AS FUNCTIONS OF PRESSURE

PRESSURE CM. H2O	V CC./G.	SV SQCM./G.	SV SQCM./CC.
8.85	4.01	3175.58	791.86
11.42	4.01	3175.58	791.86
14.53	4.01	3175.58	791.86
18.30	4.01	3175.58	791.86
22.87	4.01	3176.75	791.58
28.42	3.96	3204.76	808.38
35.15	3.86	3270.50	847.59
43.31	3.71	3370.73	908.44
53.19	3.53	3500.95	940.50

Appendix VIII (Continued)

```
*****
*
*   FLUC ON 20 MESH, RUN 1
*
*****
```

ORIGINAL DATA

```
MAT SOLIDS CONC.      = 0.0793 G./CC.
O.D. MAT WT., W       = 14.7360 G.
MAT THICKNESS, L      = 4.07 CM.
TOTAL PRESSURE DROP, DPL = 60.00 CM. H2O
PERMEATION VELOCITY, U = 1.789300 CM./SEC.
WATER TEMPERATURE, T  = 30.0 DEG. C.
WATER VISCOSITY, MU   = 0.007976 POISES
```

PERMEATION EXPERIMENT

PRESSURE TAP NUMBER	Z DISTANCE FROM TOP OF MAT CM.	DPZ	
		PRESSURE CM. H2O	TAP READING DYNES/SQCM.
1	-0.4244	0.20	196.13
2	-0.0434	0.60	588.38
3	0.3376	4.20	4118.68
4	0.7186	7.25	7109.63
5	1.0996	10.40	10198.63
6	1.4806	14.60	14317.31
7	1.8616	19.00	18632.12
8	2.2426	24.00	23535.31
9	2.6236	30.50	29909.46
10	3.0046	37.00	36283.60
11	3.3856	44.50	43638.39
12	3.7666	53.00	51973.81

COMPRESSIBILITY EXPERIMENT

PRESSURE CM. H2O	DYNES/SQCM.	MAT THICKNESS CM.	MAT SOLIDS CONCENTRATION G./CC.
6.33	6203.	5.3200	0.0608
11.26	11042.	4.7950	0.0674
21.21	20797.	4.2300	0.0764
36.15	35449.	3.7650	0.0859
61.10	59918.	3.3050	0.0978
95.71	93856.	2.8850	0.1121
145.70	142880.	2.5100	0.1288

COMPRESSIBILITY CONSTANTS

```
M = 0.74400-02
N = 0.2366
```

EXPERIMENTAL EMPIRICAL CONSTANTS

```
DPZ/DPL = A * ((Z/L)**B) * EXP(C*Z/L)   F = B0 + B1*(X**EXPM) + B2*(X**EXPN)
WHERE...                                WHERE...
A = 0.26628                            B0 = 0.568480 07   EXPM = 0.0
B = 0.58727                            B1 = 0.0           EXPN = 0.200000 00
C = 1.36890                            B2 = 0.851280 10
```

HYDRODYNAMIC SPECIFIC VOLUME AND SURFACE

```
STATIC LOAD = 19.96 CM. H2O   FLUID PRESSURE DROP = 60.00 CM. H2O
AVERAGE SPECIFIC VOLUME, V = 2.97 CC./G.
AVERAGE SPECIFIC SURFACE, SW = 3130.75 SQCM./G.
AVERAGE SPECIFIC SURFACE, SV = 1053.15 SQCM./CC.
```

Appendix VIII (Continued)

```
*****
*
* FLOC UN 20 MESH, RUN 2
*
*****
```

ORIGINAL DATA

```

MAT SOLIDS CONC.      = 0.0812 G./CC.
U.D. MAT WT., W      = 16.0273 G.
MAT THICKNESS, L      = 4.33 CM.
TOTAL PRESSURE DROP, DPL = 60.00 CM. H2O
PERMEATION VELOCITY, U = 1.556900 CM./SEC.
WATER TEMPERATURE, T = 30.0 DEG. C.
WATER VISCOSITY, MU   = 0.007976 POISES
    
```

PERMEATION EXPERIMENT

PRESSURE TAP NUMBER	Z DISTANCE FROM TOP OF MAT CM.	DPZ	
		PRESSURE CM. H2O	TAP READING DYNES/SQCM.
1	-0.1694	0.15	147.10
2	0.2116	3.10	3039.98
3	0.5426	6.20	6079.95
4	0.9736	9.42	9237.61
5	1.3546	13.40	13140.55
6	1.7356	17.90	17553.41
7	2.1166	22.10	21672.09
8	2.4976	27.20	26673.35
9	2.8786	33.50	32851.37
10	3.2596	39.00	38244.88
11	3.6406	46.50	45599.66
12	4.0216	54.00	52954.45

COMPRESSIBILITY EXPERIMENT

PRESSURE CM. H2O	DYNES/SQCM.	MAT THICKNESS CM.	MAT SOLIDS CONCENTRATION G./CC.
6.41	6283.	5.7800	0.0608
11.35	11128.	5.3100	0.0662
21.30	20883.	4.7000	0.0748
36.24	35535.	4.2000	0.0837
61.19	60001.	3.6700	0.0958
95.79	93939.	3.2200	0.1092
145.78	142960.	2.8000	0.1256

COMPRESSIBILITY CONSTANTS

```

M = 0.77360-02
N = 0.2309
    
```

EXPERIMENTAL EMPIRICAL CONSTANTS

```

DPZ/DPL = A * ((Z/L)**H) * EXP(C*Z/L)      F = B0 + B1*(X**EXPM) + B2*(X**EXPV)
WHERE...                                     WHERE...
A = 0.31888                                B0 = 0.669820 07      EXPM = 0.0
B = 0.63027                                B1 = 0.0              EXPV = 0.200000 00
C = 1.19225                                B2 = 0.897010 10
    
```

HYDRODYNAMIC SPECIFIC VOLUME AND SURFACE

```

STATIC LOAD = 14.99 CM. H2O      FLUID PRESSURE DROP = 60.00 CM. H2O
AVERAGE SPECIFIC VOLUME, V = 2.86 CC./G.
AVERAGE SPECIFIC SURFACE, SW = 3366.86 SQCM./G.
AVERAGE SPECIFIC SURFACE, SV = 1175.54 SQCM./CC.
    
```


Appendix VIII (Continued)

```
*****
*
* FLOC ON 10 MESH, RUN 1
*
*****
```

ORIGINAL DATA

```
MAT SOLIDS CONC.      = 0.0963 G./CC.
O.D. MAT WT., W       = 16.5439 G.
MAT THICKNESS, L      = 3.77 CM.
TOTAL PRESSURE DROP, DPL = 60.00 CM. H2O
PERMEATION VELOCITY, L = 1.870200 CM./SEC.
WATER TEMPERATURE, T  = 30.0 DEG. C.
WATER VISCOSITY, MU   = 0.007976 POISES
```

PERMEATION EXPERIMENT

PRESSURE TAP NUMBER	Z DISTANCE FROM TOP OF MAT CM.	DPZ	
		PRESSURE CM. H2O	TAP READING DYNES/SQCM.
1	~0.7294	0.40	392.26
2	~0.3484	1.00	980.64
3	0.0326	2.50	2451.59
4	0.4136	6.85	6717.37
5	0.7946	12.00	11767.65
6	1.1756	17.20	16866.97
7	1.5566	22.00	21574.03
8	1.9376	27.50	26967.54
9	2.3186	34.00	33341.69
10	2.6996	40.00	39225.52
11	3.0806	47.50	46580.30
12	3.4616	54.50	53444.77

COMPRESSIBILITY EXPERIMENT

PRESSURE CM. H2O	DYNES/SQCM.	MAT THICKNESS CM.	MAT SOLIDS CONCENTRATION G./CC.
0.0	0.	8.2200	0.0442
6.39	6268.	6.1650	0.0595
11.31	11086.	5.2650	0.0589
21.25	20842.	4.6650	0.0775
36.20	35495.	4.2150	0.0861
61.15	59966.	3.7650	0.0964
95.76	93906.	3.3500	0.1083
145.75	142929.	2.9600	0.1226

COMPRESSIBILITY CONSTANTS

```
M = 0.84580-02
N = 0.2231
```

EXPERIMENTAL EMPIRICAL CONSTANTS

```
DPZ/DPL = A * ((Z/L)**B) * EXP(C*Z/L)      F = B0 + B1*(X**EXPM) + B2*(X**EXPN)
WHERE...                                     WHERE...
A = 0.56425                                B0 = 0.78651D 07      EXPM = 0.0
B = 0.75014                                B1 = 0.0              EXPN = 0.10000D 01
C = 0.58976                                B2 = 0.18065D 10
```

HYDRODYNAMIC SPECIFIC VOLUME AND SURFACE

```
STATIC LOAD = 54.55 CM. H2O      FLUID PRESSURE DROP = 60.00 CM. H2O
AVERAGE SPECIFIC VOLUME, V = 1.59 CC./G.
AVERAGE SPECIFIC SURFACE, SW = 3149.86 SQCM./G.
AVERAGE SPECIFIC SURFACE, SV = 1479.41 SQCM./CC.
```

Appendix VIII (Continued)

```
*****
*
*   FLUC ON 10 MESH, RUN 2
*
*****
```

ORIGINAL DATA

```
MAT SOLIDS CONC.      = 0.0897 G./CC.
O.D. MAT WT., W      = 18.3970 G.
MAT THICKNESS, L      = 4.50 CM.
TOTAL PRESSURE DROP, DPL = 60.00 CM. H2O
PERMEATION VELOCITY, U = 1.839900 CM./SEC.
WATER TEMPERATURE, T = 32.0 DEG. C.
WATER VISCOSITY, MU   = 0.007647 POISES
```

PERMEATION EXPERIMENT

PRESSURE TAP NUMBER	DISTANCE FROM TOP OF MAT CM.	DPZ	
		PRESSURE CM. H2O	TAP READING DYNES/SQCM.
1	0.0006	2.50	2451.59
2	0.3816	5.95	5834.79
3	0.7626	9.60	9414.12
4	1.1436	14.00	13728.93
5	1.5246	17.60	17259.22
6	1.9056	23.20	22750.80
7	2.2866	27.60	27065.60
8	2.6676	33.00	32361.05
9	3.0486	38.00	37264.24
10	3.4296	43.50	42657.75
11	3.8106	50.00	49031.89
12	4.1916	56.00	54915.72

COMPRESSIBILITY EXPERIMENT

PRESSURE CM. H2O	DYNES/SQCM.	MAT THICKNESS CM.	MAT SOLIDS CONCENTRATION G./CC.
6.43	6304.	6.9450	0.0581
11.33	11113.	5.9550	0.0678
21.28	20868.	5.3450	0.0755
36.22	35517.	4.8100	0.0839
61.16	59980.	4.2450	0.0951
95.77	93914.	3.7550	0.1075
145.75	142929.	3.2650	0.1236

COMPRESSIBILITY CONSTANTS

```
M = 0.76460-02
N = 0.2313
```

EXPERIMENTAL EMPIRICAL CONSTANTS

```
DPZ/DPL = A * ((Z/L)**B) * EXP(C*Z/L)      F = B0 + B1*(X**EXPM) + B2*(X**EXPN)
WHERE...                                     WHERE...
A = 0.48837                                B0 = 0.676840 07      EXPM = 0.0
B = 0.68145                                B1 = 0.0              EXPN = 0.200000 00
C = 0.76601                                B2 = 0.306050 10
```

HYDRODYNAMIC SPECIFIC VOLUME AND SURFACE

```
STATIC LOAD = 40.04 CM. H2O      FLUID PRESSURE DROP = 60.00 CM. H2O
AVERAGE SPECIFIC VOLUME, V = 1.99 CC./G.
AVERAGE SPECIFIC SURFACE, SW = 3091.69 SQCM./G.
AVERAGE SPECIFIC SURFACE, SV = 1550.19 SQCM./CC.
```

Appendix VIII (Continued)

```
*****
*
*   WHOLE PULP CN 65 MESH, RUN 1
*
*****
```

ORIGINAL DATA

```
MAT SOLIDS CONC.      = 0.0642 G./CC.
O.D. MAT WT., W       = 13.0303 G.
MAT THICKNESS, L      = 4.45 CM.
TOTAL PRESSURE DROP, DPL = 60.00 CM. H2O
PERMEATION VELOCITY, L = 1.011400 CM./SEC.
WATER TEMPERATURE, T  = 29.0 DEG. C.
WATER VISCOSITY, MU   = 0.008149 POISES
```

PERMEATION EXPERIMENT

PRESSURE TAP NUMBER	L DISTANCE FROM TOP OF MAT CM.	DPZ	
		PRESSURE CM. H2O	TAP READING DYNES/SQCM.
1	-0.6494	0.20	196.13
2	0.3316	0.80	784.51
3	0.7126	1.80	1765.15
4	1.6936	3.30	3236.10
5	1.4746	5.30	5197.38
6	1.8556	8.10	7943.16
7	2.2366	11.80	11571.52
8	2.6176	16.50	16180.52
9	2.9986	22.00	21574.03
10	3.3796	29.00	28438.50
11	3.7606	38.50	37754.56
12	4.1416	49.50	48541.57

COMPRESSIBILITY EXPERIMENT

PRESSURE		MAT THICKNESS	MAT SOLIDS CONCENTRATION
CM. H2O	DYNES/SQCM.	CM.	G./CC.
0.0	0.	7.2350	0.0395
6.28	6156.	4.7950	0.0596
11.21	10991.	4.2400	0.0674
21.15	20743.	3.6600	0.0781
36.09	35394.	3.1950	0.0895
61.05	59863.	2.7550	0.1038
95.66	93805.	2.3400	0.1196
145.65	142832.	2.0750	0.1378

COMPRESSIBILITY CONSTANTS

```
M = 0.5714D-02
N = 0.2653
```

EXPERIMENTAL EMPIRICAL CONSTANTS

```
DPZ/DPL = A * ((Z/L)**B) * EXP(C*Z/L)      F = B0 + B1*(X**EXPM) + B2*(X**EXPN)
WHERE...                                     WHERE...
A = 0.12232                                B0 = 0.29737D 09      EXPM = 0.14510D 00
B = 0.92842                                B1 = -0.54785D 10    EXPN = 0.17962D 00
C = 2.15303                                B2 = 0.60558D 10
```

HYDRODYNAMIC SPECIFIC VOLUME AND SURFACE AS FUNCTIONS OF PRESSURE

PRESSURE CM. H2O	V CC./G.	SW SQCM./G.	SV SQCM./CC.
3.39	3.66	4494.34	1228.17
5.37	3.66	4494.34	1228.17
8.00	3.66	4494.34	1228.17
11.43	3.66	4494.34	1228.17
15.91	3.57	4551.36	1275.76
21.70	3.49	4607.00	1319.63
29.16	3.35	4725.42	1411.07
38.72	3.17	4846.97	1546.20
50.93	2.97	5111.00	1723.08

Appendix VIII (Continued)

```

*****
*
*   WHOLE PULP CN 65 MESH, RUN 2
*
*****

```

ORIGINAL DATA

```

MAT SOLIDS CONC.      = 0.0647 G./CC.
O.D. MAT WT., W       = 12.9967 G.
MAT THICKNESS, L      = 4.40 CM.
TOTAL PRESSURE DROP, DPL = 60.00 CM. H2O
PERMEATION VELOCITY, L = 1.131500 CM./SEC.
WATER TEMPERATURE, T  = 34.0 DEG. C.
WATER VISCOSITY, MU   = 0.007340 POISES

```

PERMEATION EXPERIMENT

PRESSURE TAP NUMBER	Z DISTANCE FROM TOP OF MAT CM.	DPZ	
		PRESSURE CM. H2O	TAP READING DYNES/SQCM.
1	-0.0944	0.50	490.32
2	0.2866	1.15	1127.73
3	0.6676	2.30	2255.47
4	1.0486	3.80	3726.42
5	1.4296	5.90	5785.76
6	1.8106	8.75	8580.58
7	2.1916	12.00	11767.65
8	2.5726	16.80	16474.70
9	2.9536	22.30	21868.21
10	3.3346	29.50	28928.82
11	3.7156	39.00	38244.88
12	4.0966	50.00	49031.89

COMPRESSIBILITY EXPERIMENT

PRESSURE CM. H2O	DYNES/SQCM.	MAT THICKNESS CM.	MAT SOLIDS CONCENTRATION G./CC.
0.0	0.	7.1650	0.0398
6.38	6259.	4.7750	0.0597
11.32	11098.	4.2300	0.0674
21.27	20856.	3.6600	0.0779
36.21	35508.	3.1850	0.0895
61.16	59979.	2.7250	0.1046
95.78	93922.	2.3500	0.1213
145.77	142951.	2.0250	0.1408

COMPRESSIBILITY CONSTANTS

```

M = 0.92920-02
N = 0.2732

```

EXPERIMENTAL EMPIRICAL CONSTANTS

```

DPZ/DPL = A * ((Z/L)**B) * EXP(C*Z/L)      F = B0 + B1*(X**EXPM) + B2*(X**EXPN)
WHERE...                                     WHERE...
A = 0.09132                                B0 = 0.287510 09      EXPM = 0.145700 00
B = 0.63930                                B1 = -0.545210 10     EXPN = 0.179620 00
C = 2.45745                                B2 = 0.602460 10

```

HYDRODYNAMIC SPECIFIC VOLUME AND SURFACE AS FUNCTIONS OF PRESSURE

PRESSURE CM. H2O	V CC./G.	SV SQCM./G.	SV SQCM./CC.
3.93	3.72	4359.78	1173.39
5.92	3.72	4359.78	1173.39
8.52	3.72	4359.78	1173.39
11.91	3.72	4359.78	1173.39
16.32	3.66	4398.83	1200.59
22.05	3.57	4469.58	1253.19
29.47	3.40	4605.93	1353.84
39.06	3.20	4798.34	1500.51
51.42	2.98	5035.90	1642.60

Appendix VIII (Continued)

```
*****
*
* WHOLE PULP ON 20 MESH, RUN 1
*
*****
```

ORIGINAL DATA

```
MAT SOLIDS CONC.      = 0.0745 G./CC.
O.D. MAT WT., W       = 13.2351 G.
MAT THICKNESS, L       = 3.90 CM.
TOTAL PRESSURE DROP, DPL = 60.00 CM. H2O
PERMEATION VELOCITY, U = 1.567100 CM./SEC.
WATER TEMPERATURE, T  = 32.0 DEG. C.
WATER VISCOSITY, MU    = 0.007647 POISES
```

PERMEATION EXPERIMENT

PRESSURE TAP NUMBER	Z DISTANCE FROM TOP OF MAT CM.	DPZ	
		PRESSURE CM. H2O	TAP READING DYNES/SQCM.
1	-0.5994	0.0	0.0
2	-0.2184	0.0	0.0
3	0.1626	2.30	2255.47
4	0.5436	4.65	4559.96
5	0.9246	7.60	7452.85
6	1.3056	11.50	11277.34
7	1.6866	15.50	15199.89
8	2.0676	20.50	20103.07
9	2.4486	26.00	25496.59
10	2.8296	33.00	32361.05
11	3.2106	42.00	41186.79
12	3.5916	51.50	50502.85

COMPRESSIBILITY EXPERIMENT

PRESSURE		MAT THICKNESS CM.	MAT SOLIDS CONCENTRATION G./CC.
CM. H2O	DYNES/SQCM.		
0.0	0.	7.1250	0.0408
6.30	6173.	4.9200	0.0590
11.23	11013.	4.4250	0.0656
21.18	20771.	3.9600	0.0745
36.12	35423.	3.4400	0.0844
61.07	59892.	2.9900	0.0971
95.69	93833.	2.6050	0.1115
145.68	142859.	2.2750	0.1276

COMPRESSIBILITY CONSTANTS

```
M = 0.6729D-02
N = 0.2447
```

EXPERIMENTAL EMPIRICAL CONSTANTS

```
DPZ/DPL = A * ((Z/L)**B) * EXP(C*Z/L)
WHERE...
A = 0.18217
B = 0.52321
C = 1.75961
```

```
F = 80 + B1*(X**EXPM) + B2*(X**EXPN)
WHERE...
B0 = 0.65434D 07
B1 = 0.0
B2 = 0.14564D 11
EXPM = 0.0
EXPN = 0.20000D 00
```

HYDRODYNAMIC SPECIFIC VOLUME AND SURFACE

```
STATIC LOAD = 19.93 CM. H2O    FLUID PRESSURE DROP = 60.00 CM. H2O
AVERAGE SPECIFIC VOLUME, V = 3.39 CC./G.
AVERAGE SPECIFIC SURFACE, SW = 3471.66 SQCM./G.
AVERAGE SPECIFIC SURFACE, SV = 1023.29 SQCM./CC.
```

Appendix VIII (Continued)

 *
 * WHOLE PULP ON 20 MESH, RUN 2
 *

ORIGINAL DATA

MAT SOLIDS CONC. = 0.0758 G./CC.
 O.D. MAT WT., W = 13.5194 G.
 MAT THICKNESS, L = 3.91 CM.
 TOTAL PRESSURE DROP, DPL = 60.00 CM. H2O
 PERMEATION VELOCITY, U = 1.425600 CM./SEC.
 WATER TEMPERATURE, T = 29.0 DEG. C.
 WATER VISCOSITY, MU = 0.008149 POISES

PERMEATION EXPERIMENT

PRESSURE TAP NUMBER	Z DISTANCE FROM TOP OF MAT CM.	DPZ	
		PRESSURE CM. H2O	TAP READING DYNES/SQCM.
1	-0.5844	0.10	98.06
2	-0.2034	0.35	343.22
3	0.1776	2.85	2794.82
4	0.5586	5.20	5099.32
5	0.9396	8.20	8041.23
6	1.3206	12.10	11865.71
7	1.7016	16.20	15886.33
8	2.0826	21.40	20985.64
9	2.4636	26.90	26379.15
10	2.8446	34.00	33341.69
11	3.2256	42.00	41186.79
12	3.6066	52.00	50993.17

COMPRESSIBILITY EXPERIMENT

PRESSURE		MAT THICKNESS	MAT SOLIDS CONCENTRATION
CM. H2O	DYNES/SQCM.	CM.	G./CC.
0.0	0.	7.5700	0.0392
6.33	6211.	5.1150	0.0580
11.27	11051.	4.6000	0.0645
21.22	20805.	4.0150	0.0739
36.16	35457.	3.5450	0.0837
61.11	59925.	3.0700	0.0966
95.72	93866.	2.6750	0.1109
145.71	142890.	2.3150	0.1281

COMPRESSIBILITY CONSTANTS

M = 0.62260-02
 N = 0.2513

EXPERIMENTAL EMPIRICAL CONSTANTS

$$DPZ/DPL = A * ((Z/L)**B) * EXP(C*Z/L)$$

WHERE...

A = 0.17763
 B = 0.46357
 C = 1.79133

$$F = B0 + B1*(X**EXPM) + B2*(X**EXPN)$$

WHERE...

B0 = 0.71134D 07 EXPM = 0.0
 B1 = 0.0 EXPN = 0.200000 00
 B2 = 0.15913D 11

HYDRODYNAMIC SPECIFIC VOLUME AND SURFACE

STATIC LOAD = 14.96 CM. H2O FLUID PRESSURE DROP = 60.00 CM. H2O
 AVERAGE SPECIFIC VOLUME, V = 3.40 CC./G.
 AVERAGE SPECIFIC SURFACE, SW = 3621.22 SQCM./G.
 AVERAGE SPECIFIC SURFACE, SV = 1065.60 SQCM./CC.

Appendix VIII (Continued)

```
*****
*
*   WHOLE PULP ON 10 MESH, RUN 1
*
*****
```

ORIGINAL DATA

```

MAT SOLIDS CONC.      = 0.0838 G./CC.
O.D. MAT WT., W      = 14.3837 G.
MAT THICKNESS, L      = 3.76 CM.
TOTAL PRESSURE DROP, DPL = 60.00 CM. H2O
PERMEATION VELOCITY, L = 1.880300 CM./SEC.
WATER TEMPERATURE, T = 29.0 DEG. C.
WATER VISCOSITY, MU   = 0.008149 POISES
    
```

PERMEATION EXPERIMENT

PRESSURE TAP NUMBER	Z DISTANCE FROM TOP OF MAT CM.	UPZ	
		PRESSURE CM. H2O	TAP READING DYNES/SQCM.
1	-0.7344	0.0	0.0
2	-0.3534	0.0	0.0
3	0.0276	1.60	1569.02
4	0.4086	6.20	6079.95
5	0.7896	10.00	9806.38
6	1.1706	14.90	14611.50
7	1.5516	19.00	18632.12
8	1.9326	24.50	24025.63
9	2.3136	31.00	30399.77
10	2.6946	37.00	36283.60
11	3.0756	44.00	43148.07
12	3.4566	53.00	51973.81

COMPRESSIBILITY EXPERIMENT

PRESSURE CM. H2O	DYNES/SQCM.	MAT THICKNESS CM.	MAT SOLIDS CONCENTRATION G./CC.
6.38	6259.	5.2650	0.0599
11.32	11104.	4.8100	0.0656
21.28	20864.	4.2650	0.0740
36.22	35518.	3.8150	0.0827
61.17	55989.	3.3450	0.0943
95.79	93931.	2.9500	0.1070
145.79	142962.	2.6600	0.1186

COMPRESSIBILITY CONSTANTS

```

M = 0.8416D-02
N = 0.2209
    
```

EXPERIMENTAL EMPIRICAL CONSTANTS

```

DPZ/DPL = A * ((Z/L)**B) * EXP(C*Z/L)
WHERE...
A = 0.37018
B = 0.62821
C = 1.00625
    
```

```

F = B0 + B1*(X**EXPM) + B2*(X**EXPN)
WHERE...
B0 = 0.62169D 07    EXPM = 0.0
B1 = 0.0             EXPN = 0.20000D 00
B2 = 0.69349D 10
    
```

HYDRODYNAMIC SPECIFIC VOLUME AND SURFACE

```

STATIC LOAD = 29.91 CM. H2O    FLUID PRESSURE DROP = 60.00 CM. H2O
AVERAGE SPECIFIC VOLUME, V = 2.69 CC./G.
AVERAGE SPECIFIC SURFACE, SW = 3194.62 SQCM./G.
AVERAGE SPECIFIC SURFACE, SV = 1185.47 SQCM./CC.
    
```

Appendix VIII (Continued)

```
*****
*
*   WHOLE PULP UN 10 MESH, RUN 2
*
*****
```

ORIGINAL DATA

MAT SOLIDS CONC. = 0.0818 G./CC.
O.D. MAT WT., W = 17.9218 G.
MAT THICKNESS, L = 4.80 CM.
TOTAL PRESSURE DROP, DPL = 60.00 CM. H2O
PERMEATION VELOCITY, U = 1.486200 CM./SEC.
WATER TEMPERATURE, T = 28.0 DEG. C.
WATER VISCOSITY, MU = 0.008328 POISES

PERMEATION EXPERIMENT

PRESSURE TAP NUMBER	Z DISTANCE FROM TOP OF MAT CM.	DPZ	
		PRESSURE CM. H2O	TAP READING DYNES/SQCM.
1	0.3056	4.00	3922.55
2	0.6866	6.95	6815.43
3	1.0676	11.80	11571.52
4	1.4486	15.80	15494.08
5	1.8296	19.20	18828.24
6	2.2106	23.20	22750.80
7	2.5916	27.60	27065.60
8	2.9726	32.00	31380.41
9	3.3536	37.00	36283.60
10	3.7346	42.00	41186.79
11	4.1156	48.00	47070.62
12	4.4966	55.00	53935.09

COMPRESSIBILITY EXPERIMENT

PRESSURE CM. H2O	DYNES/SQCM.	MAT THICKNESS CM.	MAT SOLIDS CONCENTRATION G./CC.
0.0	0.	8.7000	0.0452
6.44	6314.	6.5300	0.0602
11.38	11162.	6.0850	0.0646
21.33	20920.	5.4550	0.0716
36.27	35568.	4.9300	0.0798
61.21	60029.	4.3250	0.0909
95.82	93961.	3.7850	0.1039
145.80	142977.	3.2800	0.1199

COMPRESSIBILITY CONSTANTS

M = 0.8383D-02
N = 0.2194

EXPERIMENTAL EMPIRICAL CONSTANTS

DPZ/DPL = A * ((Z/L)**B) * EXP(C*Z/L)
WHERE...

A = 0.53488
B = 0.78143
C = 0.61615

F = B0 + B1*(X**EXPM) + B2*(X**EXPN)
WHERE...

B0 = 0.82792D 07 EXPM = 0.0
B1 = 0.0 EXPN = 0.20000D 00
B2 = 0.42856D 10

HYDRODYNAMIC SPECIFIC VOLUME AND SURFACE

STATIC LOAD = 20.06 CM. H2O FLUID PRESSURE DROP = 60.00 CM. H2O
AVERAGE SPECIFIC VOLUME, V = 2.09 CC./G.
AVERAGE SPECIFIC SURFACE, SW = 3458.12 SQCM./G.
AVERAGE SPECIFIC SURFACE, SV = 1657.52 SQCM./CC.

Appendix VIII (Continued)

```
*****
*
*   WHOLE PULP -- NOT CLASSIFIED, RUN 1
*
*****
```

ORIGINAL DATA

```
MAT SOLIDS CONC.           = 0.0762 G./CC.
O.D. MAT WT., W           = 16.7617 G.
MAT THICKNESS, L          = 4.82 CM.
TOTAL PRESSURE DROP, DPL  = 60.00 CM. H2O
PERMEATION VELOCITY, U    = 1.223600 CM./SEC.
WATER TEMPERATURE, T     = 37.5 DEG. C.
WATER VISCOSITY, MU       = 0.006849 POISES
```

PERMEATION EXPERIMENT

PRESSURE TAP NUMBER	Z DISTANCE FROM TOP OF MAT CM.	DPZ	
		PRESSURE CM. H2O	TAP READING DYNES/SQCM.
1	0.3256	3.60	3530.30
2	0.7066	6.00	5883.82
3	1.0876	8.70	8531.55
4	1.4686	11.80	11571.52
5	1.8496	15.50	15199.89
6	2.2306	19.40	19024.37
7	2.6116	23.50	23044.99
8	2.9926	27.50	26967.54
9	3.3736	33.00	32361.05
10	3.7546	39.50	38735.20
11	4.1356	47.00	46089.98
12	4.5166	54.00	52954.45

COMPRESSIBILITY EXPERIMENT

PRESSURE CM. H2O	DYNES/SQCM.	MAT THICKNESS CM.	MAT SOLIDS CONCENTRATION G./CC.
0.0	0.	8.5200	0.0432
6.40	6280.	6.2000	0.0593
11.34	11125.	5.7250	0.0642
21.29	20880.	5.1100	0.0720
36.22	35524.	4.5100	0.0815
61.17	59984.	3.9100	0.0941
95.77	93916.	3.3900	0.1085
145.75	142933.	2.9150	0.1267

COMPRESSIBILITY CONSTANTS

```
M = 0.6820D-02
N = 0.2411
```

EXPERIMENTAL EMPIRICAL CONSTANTS

```
DPZ/DPL = A * ((Z/L)**B) * EXP(C*Z/L)
WHERE...
```

```
A = 0.26383
B = 0.59202
C = 1.36708
```

```
F = B0 + B1*(X**EXPM) + B2*(X**EXPN)
WHERE...
```

```
B0 = 0.873420 07
B1 = 0.0
B2 = 0.143730 11
EXPM = 0.0
EXPN = 0.200000 00
```

HYDRODYNAMIC SPECIFIC VOLUME AND SURFACE

```
STATIC LOAD = 20.07 CM. H2O    FLUID PRESSURE DROP = 60.00 CM. H2O
AVERAGE SPECIFIC VOLUME, V = 3.07 CC./G.
AVERAGE SPECIFIC SURFACE, SW = 3911.25 SQCM./G.
AVERAGE SPECIFIC SURFACE, SV = 1274.98 SQCM./CC.
```

Appendix VIII (Continued)

```
*****
*
*   WHOLE PULP -- NOT CLASSIFIED , RUN 2
*
* *****
```

ORIGINAL DATA

```
MAT SOLIDS CONC.      = 0.0737 G./CC.
D.D. MAT WT., W       = 16.5539 G.
MAT THICKNESS, L      = 4.92 CM.
TOTAL PRESSURE DROP, DPL = 60.00 CM. H2O
PERMEATION VELOCITY, L = 1.102500 CM./SEC.
WATER TEMPERATURE, T  = 32.0 DEG. C.
WATER VISCOSITY, MU   = 0.007647 POISES
```

PERMEATION EXPERIMENT

PRESSURE TAP NUMBER	L DISTANCE FROM TOP OF MAT CM.	DPZ	
		PRESSURE CM. H2O	TAP READING DYNES/SQCM.
1	0.4256	3.45	3383.20
2	0.8066	5.90	5785.76
3	1.1876	8.82	8649.22
4	1.5686	12.00	11767.65
5	1.9496	15.10	14807.63
6	2.3306	18.50	18141.80
7	2.7116	22.20	21770.16
8	3.0926	27.10	26575.28
9	3.4736	33.00	32361.05
10	3.8546	38.00	37264.24
11	4.2356	46.00	45109.34
12	4.6166	53.00	51973.81

COMPRESSIBILITY EXPERIMENT

PRESSURE		MAT THICKNESS CM.	MAT SOLIDS CONCENTRATION G./CC.
CM. H2O	DYNES/SQCM.		
0.0	0.	8.6950	0.0418
6.43	6302.	6.3050	0.0576
11.37	11146.	5.8100	0.0625
21.31	20897.	5.1400	0.0707
36.24	35539.	4.4950	0.0808
61.18	59999.	3.8800	0.0936
95.79	93931.	3.3550	0.1083
145.77	142948.	2.8900	0.1257

COMPRESSIBILITY CONSTANTS

```
M = 0.60660-02
N = 0.2511
```

EXPERIMENTAL EMPIRICAL CONSTANTS

```
DPZ/DPL = A * ((L/L)**B) * EXP(C*Z/L)
WHERE...
```

```
A = 0.30793
B = 0.72668
C = 1.16871
```

```
F = B0 + B1*(X**EXPM) + B2*(X**EXPN)
WHERE...
```

```
B0 = 0.106060 00    EXPM = 0.0
B1 = 0.0             EXPN = 0.200000 00
B2 = 0.115610 11
```

HYDRODYNAMIC SPECIFIC VOLUME AND SURFACE

```
STATIC LOAD = 20.08 CM. H2O    FLUID PRESSURE DROP = 60.00 CM. H2O
AVERAGE SPECIFIC VOLUME, V = 2.67 CC./G.
AVERAGE SPECIFIC SURFACE, SW = 4164.54 SQCM./G.
AVERAGE SPECIFIC SURFACE, SV = 1557.31 SQCM./CC.
```

APPENDIX IX

ANALYSIS OF INHERENT ASSUMPTION IN DETERMINING \underline{S}_W AND \underline{v} AS FUNCTIONS OF PRESSURE SIMULTANEOUSLY

During the analysis of average specific surface, $\langle \underline{S}_W \rangle$, and average specific volume, $\langle \underline{v} \rangle$, from constant rate filtration and wet mat compressibility data, Equations (29) and (46) are used; these are of the general form:

$$Y = k_1 \langle \underline{S}_W \rangle^2 \langle \underline{v} \rangle^{-1/2} + k_2 \langle \underline{S}_W \rangle^2 \langle \underline{v} \rangle^{2.5} X \quad (48)$$

where $\langle \underline{S}_W \rangle = \underline{S}_W$ and $\langle \underline{v} \rangle = \underline{v}$ in Equation (46) and where:

<p>Equation (29)</p> $\underline{k}_1 = 3.5(1-N/2)$ $\underline{k}_2 = \underline{k}_1 57(1-N/2)^6$ $\underline{X} = \underline{c}^3$ $\underline{Y} = \frac{\underline{\Delta P}}{\underline{c}^{1/2} \underline{t}}$	<p>Equation (46)</p> 1 57 $[\underline{c}_L (\underline{\Delta P}_Z / \underline{\Delta P}_L)^N]^3$ $\frac{\underline{\Delta P}_L (\underline{C} + \underline{BL}/\underline{z})}{3.5 \underline{\mu L U c}_L^{1.5}} (\underline{\Delta P}_Z / \underline{\Delta P}_L)^{1-1.5N}$
--	--

Equation (31) is in the form of a straight line; therefore, a plot of \underline{Y} vs. \underline{X} should be linear assuming $\langle \underline{S}_W \rangle$ and $\langle \underline{v} \rangle$ independent of \underline{X} . That is:

$$\text{slope} = \frac{dY}{dX} = k_2 \langle \underline{S}_W \rangle^2 \langle \underline{v} \rangle^{2.5} \quad (49)$$

$$\text{intercept} = Y - X \frac{dY}{dX} = k_1 \langle \underline{S}_W \rangle^2 \langle \underline{v} \rangle^{-1/2} \quad (50)$$

In actuality, a plot of \underline{Y} vs. \underline{X} is not linear, and the nonlinearity has been attributed to the dependence of $\langle \underline{S}_W \rangle$ and $\langle \underline{v} \rangle$ on \underline{X} (41); such that:

$$\frac{dY}{dX} = Q + k_2 \langle \underline{S}_W \rangle^2 \langle \underline{v} \rangle^{2.5} \quad (51)$$

$$Y - X \frac{dY}{dX} = k_1 \langle S_W \rangle^2 \langle v \rangle^{-1/2} - X Q \quad (52)$$

where Q represents those terms containing $d\langle S_W \rangle/dX$ and $d\langle v \rangle/dX$. Previously it was believed that if Q was assumed negligible then $\langle S_W \rangle$ and $\langle v \rangle$ may be determined as functions of X , and subsequently pressure, by dividing a plot of Y vs. X into segments and applying Equations (51) and (52) to each segment. This procedure was further improved by direct calculation of dY/dX using the numerical procedure discussed in the text.

But, Grace (61) and Nelson (53) have demonstrated this method of analysis is valid only if Q is exactly equal to zero. Furthermore, Nelson (53) has shown by analysis of this method of data reduction for Equation (29) that it is equivalent to a further (and unstated) assumption represented by Equation (53).

$$\frac{k_1}{k_2 \langle v \rangle^3} = c^3 \left[\frac{\frac{\Delta P_f}{c^3} \frac{dc^3}{d\Delta P_f}}{1 - \frac{\Delta P_f}{6c^3} \frac{dc^3}{d\Delta P_f} - \frac{\Delta P_f}{t} \frac{dt}{d\Delta P_f}} \right] \quad (53)$$

Equation (53) represents the implied definition of $\langle v \rangle$. Since Equation (53) presently has no physical significance, it must be rejected as a plausible assumption; and therefore Equation (29) may only be solved for a singular value of $\langle S_W \rangle$ and $\langle v \rangle$. The argument pertaining to Equation (46) is believed similar.